AFRL-RQ-WP-TR-2020-0069

AIRCRAFT STRUCTURAL RELIABILITY AND RISK ANALYSIS HANDBOOK

Volume 2: Structural Fatigue Degradation and Probability of Failure Examples

Eric J. Tuegel

Structures Technology Branch
Aerospace Vehicles Division

OCTOBER 2020
Final Report

AIR FORCE RESEARCH LABORATORY
AEROSPACE SYSTEMS DIRECTORATE
WRIGHT-PATTERSON AIR FORCE BASE, OH 45433-7542
AIR FORCE MATERIEL COMMAND
UNITED STATES AIR FORCE

NOTICE AND SIGNATURE PAGE

This report was cleared for public release by the USAF 88th Air Base Wing (88 ABW) Public Affairs Office (PAO) and is available to the general public, including foreign nationals.

Copies may be obtained from the Defense Technical Information Center (DTIC) (https://discover.dtic.mil/).

AFRL-RQ-WP-TR-2020-0069 HAS BEEN REVIEWED AND IS APPROVED FOR PUBLICATION IN ACCORDANCE WITH ASSIGNED DISTRIBUTION STATEMENT.

REPORT DOCUMENTATION PAGE

Form Approved
OMB No. 0704-0188

1. REPORT DATE *(DD-MM-YY)*	2. REPORT TYPE	3. DATES COVERED *(From - To)*
October 2020	Final	1 June 2013 – 1 October 2020

4. TITLE AND SUBTITLE
AIRCRAFT STRUCTURAL RELIABILITY AND RISK ANALYSIS HANDBOOK
Volume 2: Structural Fatigue Degradation and Probability of Failure Examples

5a. CONTRACT NUMBER
In-house

5b. GRANT NUMBER

5c. PROGRAM ELEMENT NUMBER
62201F

6. AUTHOR(S)
Eric J. Tuegel

5d. PROJECT NUMBER
3048

5e. TASK NUMBER

5f. WORK UNIT NUMBER
Q0S6

7. PERFORMING ORGANIZATION NAME(S) AND ADDRESS(ES)
Structures Technology Branch (AFRL/RQVS)
Aerospace Vehicles Division
Air Force Research Laboratory Aerospace Systems Directorate
Wright-Patterson Air Force Base, OH 45433-7542
Air Force Materiel Command, United States Air Force

8. PERFORMING ORGANIZATION REPORT NUMBER
AFRL-RQ-WP-TR-2020-0069

9. SPONSORING/MONITORING AGENCY NAME(S) AND ADDRESS(ES)
Air Force Research Laboratory
Aerospace Systems Directorate
Wright-Patterson Air Force Base, OH 45433-7542
Air Force Materiel Command
United States Air Force

10. SPONSORING/MONITORING AGENCY ACRONYM(S)
AFRL/RQVS

11. SPONSORING/MONITORING AGENCY REPORT NUMBER(S)
AFRL-RQ-WP-TR-2020-0069

12. DISTRIBUTION/AVAILABILITY STATEMENT
DISTRIBUTION STATEMENT A. Approved for public release. Distribution is unlimited.

13. SUPPLEMENTARY NOTES
PA Clearance Number: 88ABW-2020-3043; Clearance Date: 30 September 2020.

This material is declared a work of the U.S. Government and is not subject to copyright protection in the United States.

This handbook is a follow on volume to AFRL-RQ-WP-TR-2013-0132.

14. ABSTRACT
This handbook provides examples of how to calculate single flight probability of failure (SFPOF) as a result of fatigue degradation of a structure. The examples begin with one random variable (fracture toughness) and increase in complexity to three random variables (fracture toughness, equivalent initial damage size (EIDS), and maximum stress during a flight). A final example demonstrates how to model the effect of nondestructive inspections on the SFPOF using the probability of detecting a fatigue crack of a given size.

All examples are worked using Monte Carlo simulation. The algorithms used were written as macros within Microsoft Excel®, and are provided in appendices. Procedures for determining the probability distributions for the EIDS and the maximum stress during a flight are presented. Uncertainty about the probability distributions for the random variables and in the resulting SFPOF are also discussed.

15. SUBJECT TERMS
probabilistic risk assessment, structural reliability assessment, single flight probability of failure (SFPOF), equivalent initial damage size (EIDS), probability of detection (POD)

16. SECURITY CLASSIFICATION OF:			17. LIMITATION OF ABSTRACT:	18. NUMBER OF PAGES	19a. NAME OF RESPONSIBLE PERSON (Monitor)
a. REPORT	b. ABSTRACT	c. THIS PAGE			Eric J. Tuegel
Unclassified	Unclassified	Unclassified	SAR	207	19b. TELEPHONE NUMBER (Include Area Code) N/A

Table of Contents

List of Figures

List of Tables

1 INTRODUCTION

This second volume of the Aircraft Structural Reliability and Risk Analysis Handbook provides the reader with an introduction to structural reliability analysis when there are random variables with distributions that change over time. For example, the distribution of possible fatigue crack sizes in a part changes with continued loading of the part. The mean crack size and the dispersion of possible crack sizes both increase with continued loading. The type of probability distribution, Gaussian, Lognormal, Weibull, etc., may also change. All of these changes must be considered when assessing the structural reliability.

The aim of this volume is to help the engineer performing a reliability analysis develop some understanding and comfort with probabilistic reliability analysis. Thus, simple analysis methods are used throughout this volume to perform some typical reliability analyses. This handbook does not provide a compilation of the various methods available for assessing structural reliability. The reader who wants to develop greater fluency with probabilistic structural reliability analysis is encourage to explore the many texts and references on the subject.

This volume is structured so that the complexity of the examples increases with each subsequent one. Section 2 reviews some fundamental concepts, commonly used probability distributions, and the calculation methods used throughout this handbook. Section 3 contains examples of time-dependent reliability calculations without considering inspections and subsequent repair of cracks. Section 3 begins with an example with a single random variable, fracture toughness. An example with two random variables, fracture toughness and crack size, is next. The last example in Section 3 has three random variables, fracture toughness, crack size, and the maximum stress during a flight. An example of an inspection and repair is worked in Section 4.

2 STRUCTURAL RELIABILITY FUNDAMENTALS

This section presents a brief description of the fundamental concepts of structural reliability analysis. It is the same as Section 3.0 of Volume 1 of the Aircraft Structural Reliability and Risk Analysis Handbook [1], and is repeated here for ease of reference. The reader in need of refresher on the basics of statistics and probability should consult the *NIST/SEMATECH e-Handbook of Statistical Methods*, [2] online at http://www.itl.nist.gov/div898/handbook/.

This section begins by defining important terms and concepts used in structural reliability analysis. Then, common probability distributions used in structural reliability analysis are reviewed. The section ends with the description of calculation methods that are used throughout this handbook.

2.1 Definitions

The following terms are important for structural reliability analysis.

2.1.1 Risk

Risk is the potential for losses and rewards as a result of a failure event. Risk is a characteristic of an uncertain future, and not of either the present or past. When uncertainties are resolved, or the future becomes the present, risk becomes nonexistent. Risk does not exist for historical events or events that are currently happening. Risk is evaluated in terms of both the probability of occurrence and the impact of the occurrence. The USAF Airworthiness process uses a matrix to determine the risk in terms of a Risk Assessment Code (RAC). The RAC is determined from the matrix shown in Figure 1. The Severity Categories are defined in Table 1.

USAF Airworthiness Risk Assessment Matrix			Severity Category			
Probability Level	Probability per FH or Sortie	Freq per 100K FH or 100K Sorties	Catastrophic (1)	Critical (2)	Marginal (3)	Negligible (4)
Frequent (A)	$10^{-3} \leq$ Prob	100 ≤ Freq	1	3	7	13
Probable (B)	$10^{-4} \leq$ Prob $< 10^{-3}$	10 ≤ Freq < 100	2	5	9	16
Occasional (C)	$10^{-5} \leq$ Prob $< 10^{-4}$	1 ≤ Freq < 10	4	6	11	18
Remote (D)	$10^{-6} \leq$ Prob $< 10^{-5}$	0.1 ≤ Freq < 1	8	10	14	19
Improbable (E)	0 < Prob $< 10^{-6}$	0 < Freq < 0.1	12	15	17	20
Eliminated (F)	Prob = 0	Freq = 0	Eliminated			

High	CAE Risk Acceptance RAC = 1 - 5	Medium	PM Risk Acceptance RAC = 10 - 17
Serious	PEO Risk Acceptance RAC = 6 - 9	Low	Risk Acceptance as Directed RAC = 18 - 20

Figure 1. USAF Airworthiness Risk Acceptance Matrix [3]

Table 1. Severity Category Definitions [3]

SEVERITY CATEGORIES		
Description	**Severity Category**	**Mishap Result Criteria**
Catastrophic	**1**	Could result in one or more of the following: death, permanent total disability, irreversible significant environmental impact, or monetary loss equal to or exceeding $10M.
Critical	**2**	Could result in one or more of the following: permanent partial disability, injuries or occupational illness that may result in hospitalization of at least three personnel, reversible significant environmental impact, or monetary loss equal to or exceeding $1M but less than $10M.
Marginal	**3**	Could result in one or more of the following: injury or occupational illness resulting in one or more lost work day(s), reversible moderate environmental impact, or monetary loss equal to or exceeding $100K but less than $1M.
Negligible	**4**	Could result in one or more of the following: injury or occupational illness not resulting in a lost work day, minimal environmental impact, or monetary loss less than $100K.

2.1.2 Reliability

Reliability is the probability that a system or component will survive, i.e., function as intended, under designated operating or environmental conditions for a specified time period. Reliability is the complement to the probability of failure,

$$\text{Reliability} = 1 - \text{Failure Probability}.$$

2.1.3 Lifetime Distribution

A lifetime distribution describes how a nonrepairable population fails over time. The lifetime distribution can be any probability density function (PDF), $f_T(t)$, defined over the range of time from $t = 0$ to $t =$ infinity. The corresponding cumulative distribution function (CDF), $F_T(t)$, gives the probability that a randomly selected unit will fail before time t.

2.1.4 PDF

A PDF, $f_X(y)$, defines the probability that a continuous random variable will take a particular value. The probability that the random variable X will have a value within the interval from x_1 to x_2 is:

$$Pr(x_1 \leq X \leq x_2) = \int_{x_1}^{x_2} f_X(y)dy\,. \tag{1}$$

A PDF must be nonnegative and the total area under the PDF curve must be equal to one.

2.1.5 Cumulative Distribution Function (CDF)

A CDF, $F_X(y)$, gives the probability that a continuous random variable, X, will take a value less than or equal to a specified value, x_1,

$$F_X(x_1) = Pr(X \leq x_1) = \int_{-\infty}^{x_1} f_X(y)\, dy. \quad (2)$$

The value of the CDF must be greater than or equal to 0, and less than or equal to 1. The CDF is a non-decreasing function.

2.1.6 Exceedance Distribution Function (EDF)

An EDF, $D_X(y)$, gives the probability that a continuous random variable, X, will take a value greater than a specified value, x_1. The sum of the CDF, $F_X(y)$, and the EDF is equal to one since the total probability is equal to one, and the CDF and EDF cover all the possibilities for the random variable X. Hence,

$$\begin{aligned} D_X(x_1) &= Pr(X > x_1) = 1 - F_X(x_1) \\ &= 1 - \int_{-\infty}^{x_1} f_X(y)\, dy = \int_{x_1}^{\infty} f_X(y)\, dy. \end{aligned} \quad (3)$$

The value of the EDF must be greater than or equal to 0, and less than or equal to 1. The EDF is a non-increasing function.

2.1.7 Hazard Rate Function (HRF)

The HRF is defined from the probability of failure of an item in the time interval t to $t+\Delta t$ with the condition that the item is functioning at time t, for small Δt. The probability that the failure time T is between t and $t+\Delta t$ with the condition that T is greater than t is given by

$$Pr(t < T \leq t + \Delta t | T > t) = \frac{f_T(t)}{1-F_T(t)} \Delta t \quad (4)$$

where $f_T(t)$ is the PDF and $F_T(t)$ is the CDF of the lifetime distribution for the item, respectively. The HRF, $h_T(t)$, is defined as

$$h_T(t) = \frac{f_T(t)}{1-F_T(t)}. \quad (5)$$

The HRF is a measure of the proneness to failure as a function of age. The expected proportion of items of age t that fail in a short time Δt is equal to $\Delta t \cdot h_T(t)$. $\Delta t \cdot h_T(t)$ is known as the failure rate function, the instantaneous failure rate, or force of mortality.

The HRF is strictly not a probability. A cumulative hazard rate function, $H_T(t)$, can be defined as

$$H_T(t) = \int_0^t h_T(x) dx. \quad (6)$$

The relationship between $H_T(t)$ and the CDF of the lifetime distribution, $F_T(t)$, is

$$F_T(t) = 1 - e^{-H_T(t)}. \quad (7)$$

When t equals ∞, $F_T(\infty)$ equals 1 and $H_T(\infty)$ equals ∞. Therefore, the cumulative hazard rate function cannot be a CDF since it has values greater than 1, and $h_T(t)$ cannot be a PDF.

2.1.8 Single Flight Probability of Failure (SFPOF)

SFPOF is the probability of a failure during one flight with the condition that there has not been a failure in any of the previous flights. The SFPOF can be calculated as the product of the HRF at a specified flight, $h_T(t)$, and a time increment Δt of one flight.

2.2 Common Probability Distributions

This section introduces four probability distributions that are commonly used in structural reliability analysis. These include the normal, lognormal, exponential, and Weibull distributions. (The *NIST/SEMATECH e-Handbook of Statistical Methods* [2] has additional details on these and other distributions.) The descriptions of these four probability distributions is repeated from [1] and are included for ease of reference. New material on the Gumbel extreme value distribution that is used to describe the probability of a maximum stress value occurring in a flight is added in Section 2.2.5.

Like many of the widely used statistical distributions, these are location-scale distributions. The scale parameter prescribes the spread of the distribution (wide, skewed). Examples of scale parameters are the standard deviation (σ) for normal and lognormal distributions and shape parameter (α) for Weibull. The location parameter specifies the location of a central point of the distribution. Examples of location parameters are the mean (μ) for the normal, the median (e^{μ}) for the lognormal, and the scale parameter (β) for Weibull. (Note the paradox: the Weibull scale parameter is a location parameter because about 63 percent of a population is always less than the scale parameter.)

2.2.1 Normal Distribution

The normal distribution is perhaps the best-known distribution. For a mean μ and standard deviation σ, the PDF of the normal distribution is given by

$$f(t) = \frac{1}{\sigma\sqrt{2\pi}} exp\left\{-0.5\left[\frac{t-\mu}{\sigma}\right]^2\right\}. \quad (8)$$

Figure 2 shows plots of the PDF and CDF of the normal distribution for a mean of 5 and three different values of standard deviation. A normal distribution with a mean of 0 and a standard deviation of 1 is known as the standard normal distribution. The CDF for the standard normal, usually represented by $\Phi(t)$, is tabulated in the back of most probability textbooks. Any normal distribution can be mapped into the standard normal distribution through the standard normal random variable,

$$z = \frac{t-\mu}{\sigma}. \quad (9)$$

The normal distribution has several convenient properties, including:

- Central limit theorem: The distribution of the sum of independent random variables usually tends to a normal distribution as the number of elements in the sum increases. Since scatter in real world observations can often be thought of as the sum of many random effects, the normal distribution has been found to fit many data sets over a wide range of disciplines.
- Additive property: A random variable is normally distributed if it is the sum of 2 or more independent random variables, each of which is normally distributed. Its mean is the sum of the means, and its variance (the square of standard deviation) is the sum of the variances.

Since the normal distribution extends over negative values, it is sometimes inappropriate for representing data that can only be positive. Such would be the case when the standard deviation is relatively large compared to the mean so that the normal distribution would predict a reasonably large chance of an impossible negative observation. For example, distributions of structural crack sizes typically have standard deviations that are greater than the mean, so that a normal distribution would indicate a large percentage of negative crack sizes. On the other hand, when observations that can only be positive are all far separated from zero relative to their scatter, the normal distribution can still provide a useful model. For example, a normal distribution is often fit to observations of tensile strength and fracture toughness.

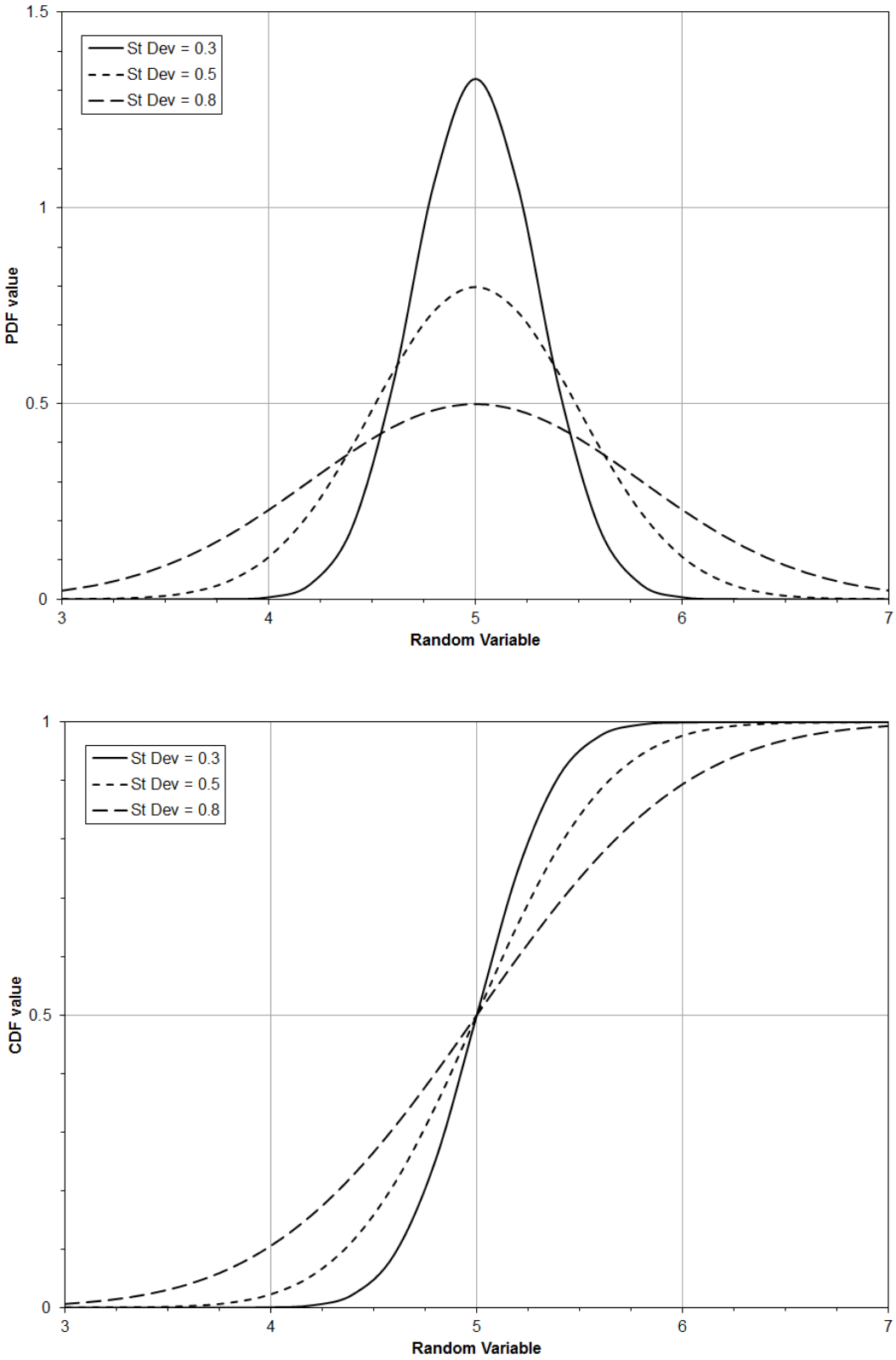

Figure 2. Normal Probability Density and CDFs

2.2.2 Lognormal Distribution

The lognormal distribution for *t* is simply a normal distribution of the natural log, *ln(t)*. The PDF of the lognormal distribution is given by

$$f(t) = \frac{1}{t\sigma\sqrt{2\pi}} exp\left\{-0.5\left[\frac{ln(t) - \mu}{\sigma}\right]^2\right\}. \quad (10)$$

In Equation (10), μ and σ are the mean and standard deviations of *ln(t)*. The median (CDF = 0.5) of the distribution of *t* is given by e^{μ}. Figure 3 shows graphs of the PDF and CDF for the Lognormal distribution for a log mean of 0 (i.e., *ln*(1.0)) and three different values of standard deviation.

The lognormal distribution has been commonly used for decades to represent the distribution of structural integrity variables such as fatigue life, strength, fracture toughness, crack growth rate, and crack sizes. It shares convenient features of the normal distribution. For example, consider this corollary to the additive property of the normal distribution: A random variable is lognormally distributed if it is the product of two or more independent random variables, each of which is lognormally distributed.

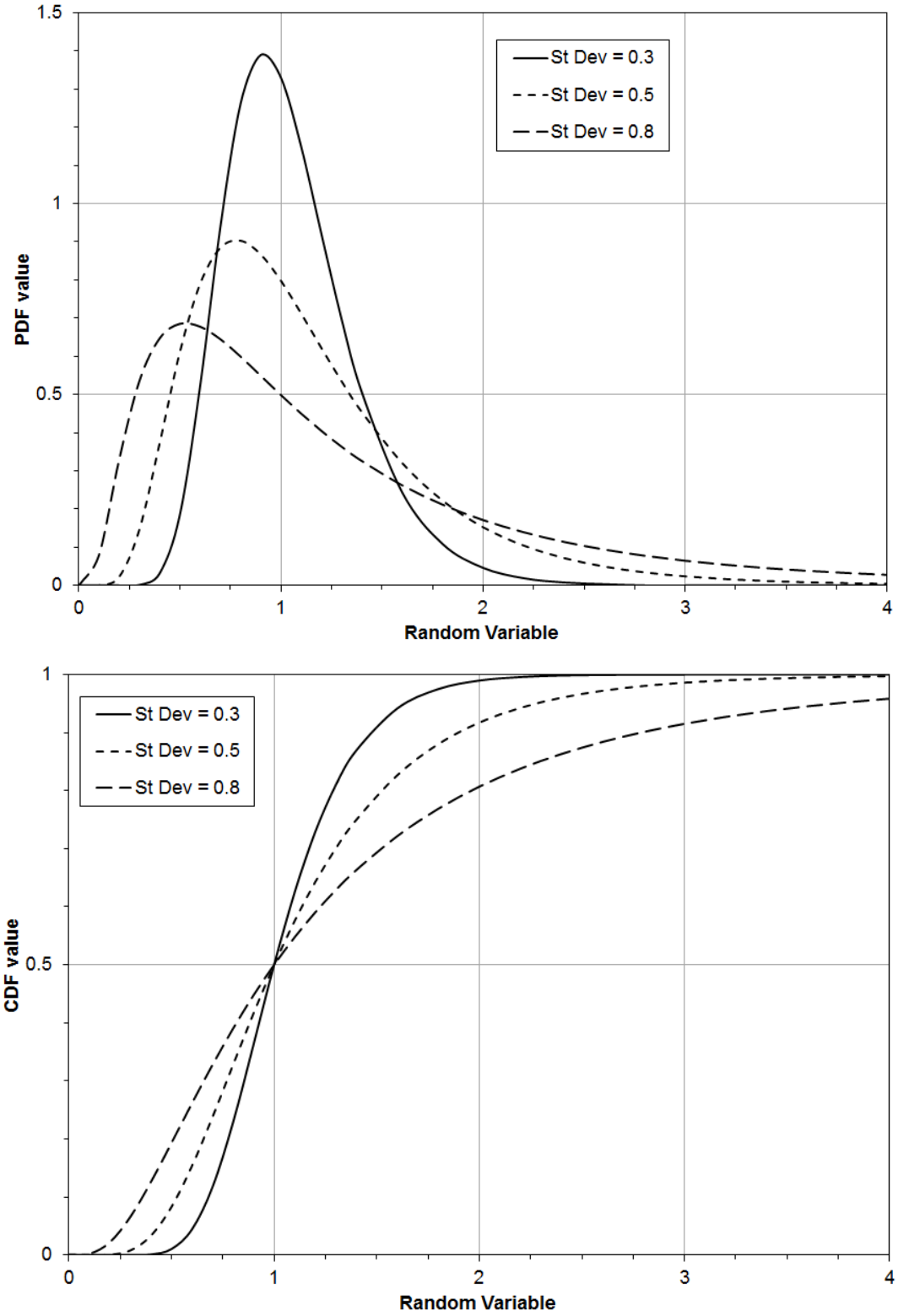

Figure 3. Lognormal Probability Functions

2.2.3 Weibull Distribution

Waloddi Weibull is credited with the introduction of the Weibull probability distribution in 1937. It was found to work well with extremely few data samples (even as few as 2 or 3). The Weibull distribution is now routinely used in reliability applications involving aircraft and propulsion system service life. Examples include:

- Fatigue life scatter in metallic alloys,
- Equivalent initial flaw size distributions,
- Crack growth rate scatter in metallic alloys.

The Weibull distribution can be a three-parameter or two-parameter distribution. The three-parameter Weibull distribution has a shape parameter α, scale parameter β, and a location parameter t_0. The Weibull distribution starts at the value of the location parameter. Thus, t_0 provides an estimate of the smallest value in the domain of the distribution. The location parameter is frequently set equal to zero for structural reliability applications; reducing to the two-parameter Weibull distribution. The PDF and CDF for the Weibull distribution are, respectively:

$$f(t) = \frac{\alpha}{\beta}\left(\frac{t-t_0}{\beta}\right)^{\alpha-1} exp\left\{-\left[\frac{t-t_0}{\beta}\right]^{\alpha}\right\}, \tag{11}$$

$$F(t) = 1 - exp\left\{-\left[\frac{t-t_0}{\beta}\right]^{\alpha}\right\}. \tag{12}$$

The mean and standard deviation of the Weibull distribution are, respectively

$$\mu = \beta\,\Gamma(1+1/\alpha) + t_0, \tag{13}$$

$$\sigma = \beta\sqrt{\Gamma\left(1+\frac{2}{\alpha}\right) - \left[\Gamma\left(1+\frac{1}{\alpha}\right)\right]^2}, \tag{14}$$

where $\Gamma(x)$ is the gamma function,

$$\Gamma(x) = \int_0^{\infty} e^{-y} y^{x-1}\, dy. \tag{15}$$

Figure 4 shows graphs of the PDF and CDF for the Weibull distribution for scale parameter (β) of 1 and three different values of shape parameter (α). (When using any program, make sure which variable is the scale parameter and which is the shape parameter.)

The two-parameter Weibull distribution is simply the case where $t_0 = 0$. When $t - t_0$ equals β, the value of the Weibull CDF is

$$F(\beta + t_0) = 1 - exp\left\{-\left(\frac{\beta}{\beta}\right)^{\alpha}\right\} = 1 - e^{-1} = 0.632. \tag{16}$$

Thus, the two-parameter Weibull CDF at t equal to β is 0.632 regardless of the value of shape parameter α. Therefore in life calculations involving the Weibull distribution, the scale parameter β is sometimes called the characteristic life.

When the shape parameter is equal to 1, the Weibull distribution becomes equal to the exponential distribution. For a shape parameter of 2, the Weibull distribution is the Rayleigh distribution which is commonly used in dynamics. For shape parameter values between 3 and 4, the shape of the Weibull distribution is close to that of the normal distribution.

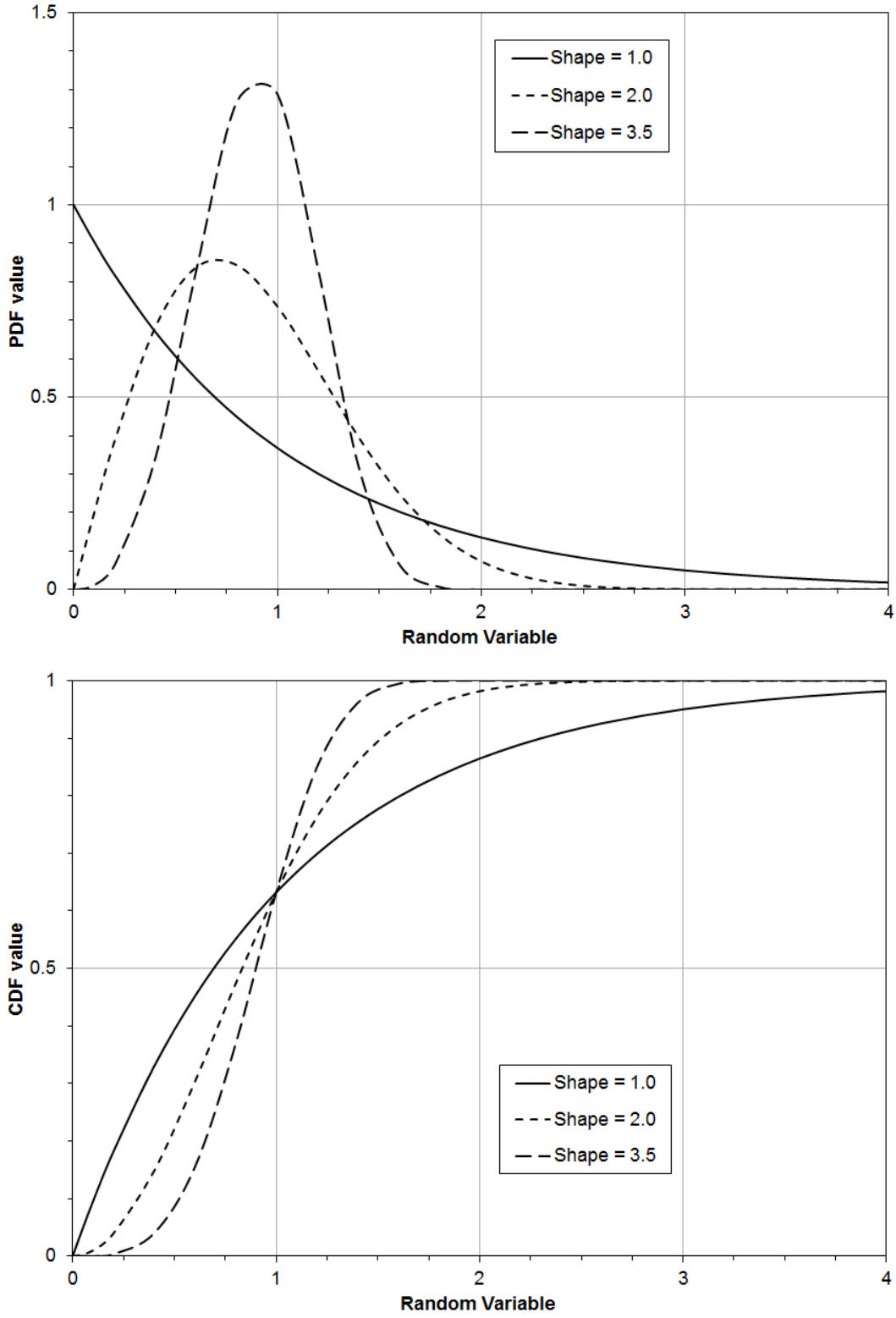

Figure 4. Weibull Probability Functions

2.2.4 Exponential Distribution

As mentioned above, the exponential distribution is the limiting case of the two- parameter Weibull Distribution with Weibull shape parameter equal to one. As a result, the exponential distribution has a single parameter, λ, sometimes called the rate parameter. The PDF and CDF of the exponential distribution are given by

$$f(t) = (1/\lambda)\, exp(-t/\lambda) \tag{17}$$

$$F(t) = 1 - exp(-t/\lambda) \tag{18}$$

The HRF for the exponential distribution is constant and equal to $1/\lambda$.

Figure 5 shows graphs of the PDF and CDF for the exponential distribution for three different values of the rate parameter λ.

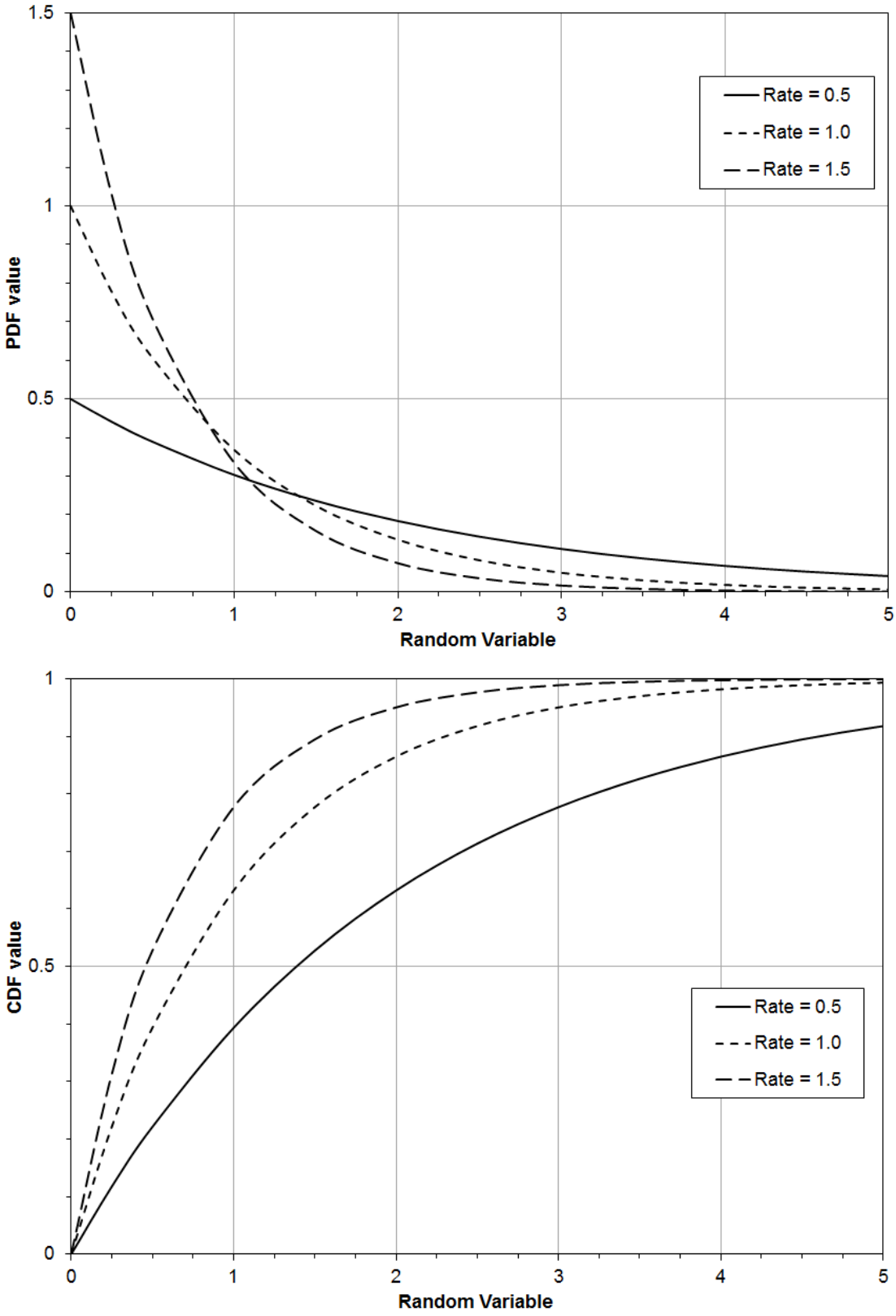

Figure 5. Exponential Probability Functions

2.2.5 Gumbel Distribution

The Gumbel distribution is the common name for the extreme value Type 1 distribution. It has two forms: one based on the smallest extreme value, and the other based on the largest extreme value. The Gumbel distribution for the largest extreme value has been used to model the distribution of maximum stresses in a sequence of flights, and thus, the probability of a maximum stress of a given value occurring in a flight. Hence, Gumbel distribution will refer to the Gumbel distribution for the largest extreme in this handbook.

The Gumbel distribution is described by two parameters: the location parameter, α, and the scale parameter, β. The PDF and CDF for the Gumbel distribution are, respectively,

$$f(x) = \frac{1}{\beta} e^{-\frac{x-\alpha}{\beta}} exp\left[-e^{-\frac{x-\alpha}{\beta}}\right] \tag{19}$$

$$F(x) = exp\left[-e^{-\frac{x-\alpha}{\beta}}\right] \tag{20}$$

Graphs of the PDF and CDF for select values of α and β are shown in Figure 6.

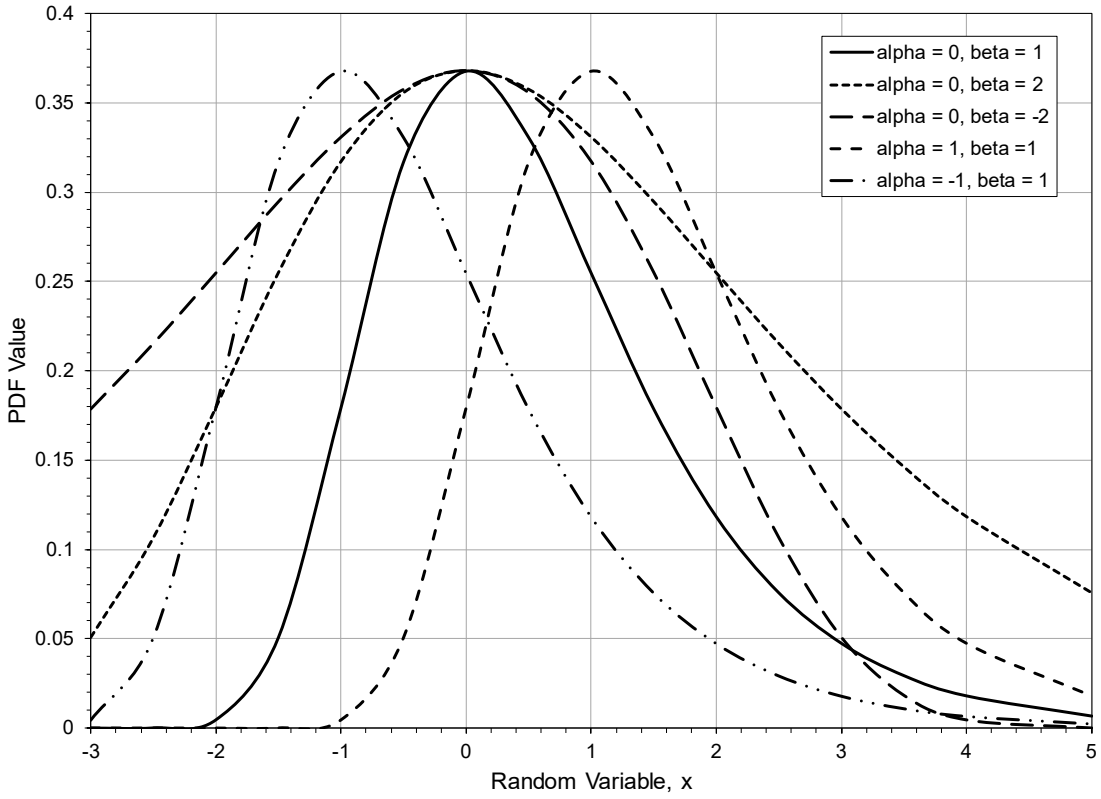

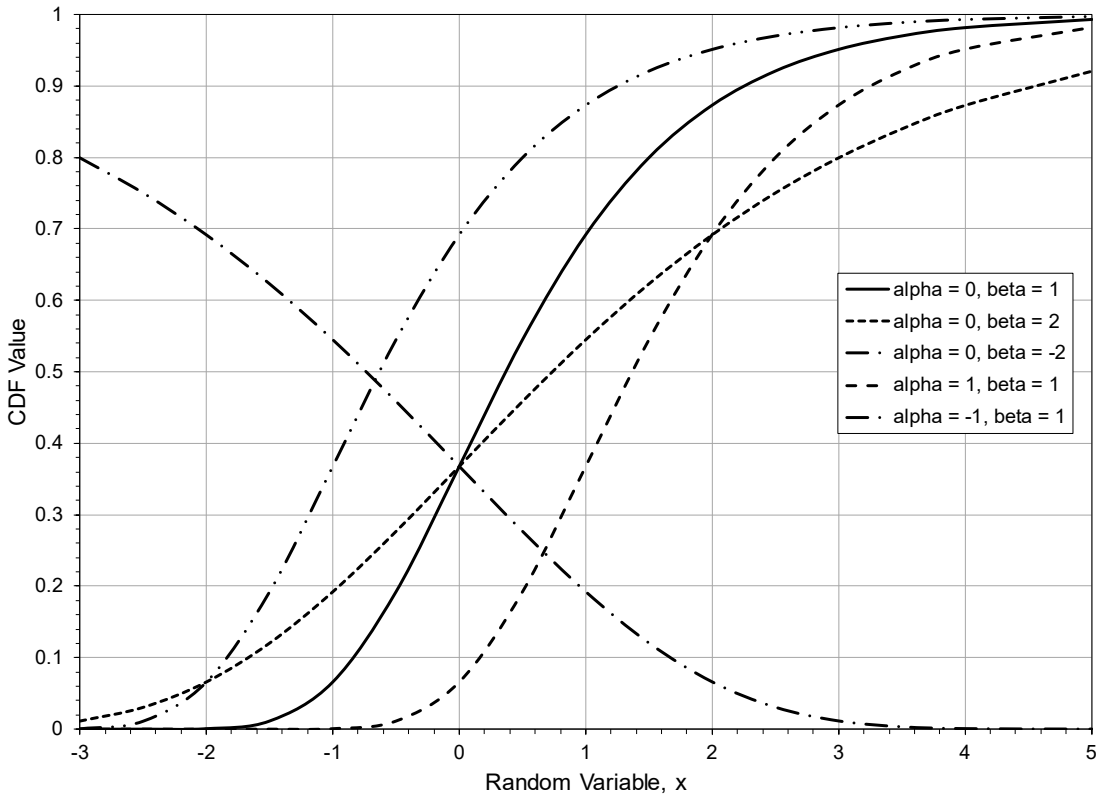

Figure 6. Gumbel Probability Functions

2.3 Calculation Methods

This section introduces some calculations methods that will be used throughout this handbook.

2.3.1 Benard Median Rank Approximation

Median rank is recommended for rank ordering skewed datasets. Mean rank, the other method of ranking data samples, will assign a probability that is too high to the lowest ranked members of the dataset and is too low for the highest ranked members [4]. Thus, median rank ordering is preferred.

The median rank is somewhat difficult to calculate directly. Therefore, Benard's approximation of the median rank is often used. The median rank, *r*, of the *j*th smallest member of a dataset with *n* members is

$$r = \frac{j - 0.3}{n + 0.4} \tag{21}$$

2.3.2 Monte Carlo Simulation

Monte Carlo Simulation (MCS) will be used throughout this handbook to calculate POF because

- it is easy to understand the process,
- there is no limit on the number of random variables, and
- it is the standard against which other reliability calculation methods are validated.

The basic idea of MCS is to randomly choose a sample from the known distribution for each random variable in the problem at hand [5]. For example, choose a value of ultimate tensile strength (UTS) from the distribution for UTS, and a value for the applied stress from the distribution for the applied stress. Then, with this pair of values, determine if this instance would have survived or failed. This process of choosing samples and determining whether the instance would have failed is repeated over and over until a large number of instances have been generated keeping track of the total number of instances and the number that failed. The fraction of the total number of instances that failed is an estimate of the POF given the distributions of the random variables.

Mathematically, MCS solves the integral

$$POF = \int_{-\infty}^{\infty} h(x) f_T(x) dx \tag{22}$$

where *f(x)* is the joint pdf for the random variable in the problem, and *h(x)* is a function that is equal to 1 if the part has failed and 0 otherwise. This integral gives the expected value of *h(x)*, $E_f[h(x)]$. For samples $X_1, \ldots, X_N$, the POF estimate is

$$POF = E_f[h(x)] = \frac{1}{N}\sum_{1}^{N} h(X_i) = \frac{\#\ of\ failures}{N}. \tag{23}$$

Physically, MCS can be thought of as fabricating a large number of parts from random pieces of material drawn from the population of all material of that type and processed with all the variation seen in typical manufacturing processes. Then each of the parts is subjected to some of

the many uses that it could expect to see during its life. The fraction of these parts that fail under these range of uses is the POF for that part.

2.3.3 Importance Sampling

When the POF is very small, millions of MCS samples are required to get a reasonable estimate of the POF. This is not always practical.

An alternate approach to a regular MCS is to do importance sampling (IS) [5]. Instead of drawing samples from the original distribution of the random variable, another distribution *g(x)* is introduced with characteristics that make the integral easier to estimate:

$$POF = \int_{-\infty}^{\infty} h(x) f_T(x) dx = \int_{-\infty}^{\infty} \left[\frac{h(x) f_T(x)}{g(x)}\right] g(x) dx = E_g\left[\frac{h(x) f_T(x)}{g(x)}\right] \quad (24)$$

Thus, the POF can be estimated from the expected value of the function $\frac{h(x)f_T(x)}{g(x)}$.

The accuracy of the POF estimate can be gauged by calculating the variance of the POF estimate since it is also a random value. The variance (square of the standard deviation) of the POF estimate is

$$Var(POF) = E\left[\left(\frac{h(x) f_T(x)}{g(x)}\right)^2\right] - E\left[\frac{h(x) f_T(x)}{g(x)}\right] \quad (25)$$

The alternate sampling distribution is selected to cover the region most likely to cause failure so that fewer samples are required to obtain a good estimate of the POF. The functional form of the sampling distributions should be chosen to make sampling easy and to ensure that $f_T(x_i)/g(x_i)$ does not get large. If $f_T(x_i)/g(x_i)$ gets large, the error in the estimate of POF can get large as will be shown later. A uniform distribution is one possible choice for the sampling distribution. The value of $g(x_i)$ is then constant for all x_i and equal to

$$g(x) = \frac{1}{UB - LB} \quad (26)$$

where *UB* and *LB* are the upper and lower bounds, respectively, of the uniform distribution.

3 RELIABILITY WITHOUT INSPECTION OR REPAIR

In this section, the calculation of the POF in situations where either the resistance to failure or the applied force changes over time is demonstrated.

The MCS algorithms were implemented as VBS macros in a Microsoft Excel® workbook. These routines are not the fastest way to perform MCS, but they allowed intermediate values in the simulation to be easily captured for illustration purposes of this handbook. For solving real life problems, it is recommended that MCS be performed in Matlab, Python, or some other computer language.

The examples in this section are presented in order of increasing complexity; the number of random variables increases with each example. The first example is a specimen with a known crack size under constant amplitude loading. The only random variable is the fracture toughness. The second example is a specimen with a hole under constant amplitude loading. The random variables are the fracture toughness and the equivalent initial damage size (EIDS). The last example is a part with a hole under spectrum loading. The random variables are the fracture toughness, EIDS, and the maximum stress during a flight.

A sensitivity study should be performed as part of every risk and reliability analysis because of the uncertainty inherent in the random variables. In the examples of this section, a structured process for performing a sensitivity study is demonstrated. Though not as rigorous as other approaches to assessing sensitivity, the method demonstrated here minimizes the number of additional reliability assessments that need to be performed while providing a reasonable assessment of the sensitivity of the reliability results to each random variable.

Inspection and subsequent repair of cracks are not considered in any of the examples in this section. The additional complexity of simulating an inspection and repair of cracks is addressed in Section 4.

3.1 Middle Tension Specimen, M(T), under Constant Amplitude Loading

This example is a center cracked panel, also called a middle tension or M(T) specimen, in a crack growth test under constant amplitude loading. The questions to be answered are: When is the specimen likely to fail? How much crack growth data is likely to be obtained from the experiment? These answers to these questions are not important for typical tests, but for illustration purposes these questions provide a goal for the reliability calculation.

This example contains one random variable: fracture toughness, K_c. First, the reliability of the specimen as a function of crack size and load cycles will be determined. Then the POF function is found. Finally, the HRF will calculated.

3.1.1 Test Conditions

The specimen (Figure 7) is cut from 0.063-inch-thick 7475-T61 aluminum sheet. The specimen is loaded in the longitudinal grain orientation to a maximum stress of 12 ksi at a stress ratio of 0.1. The crack grows in the long transverse grain orientation.

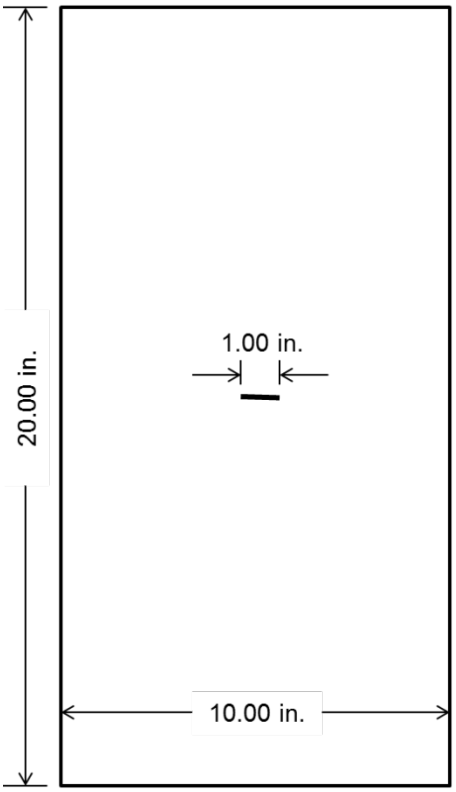

Figure 7. Middle Tension Specimen Geometry

The stress intensity range, ΔK, for this arrangement is found using the following equation from ASTM Standard E647 [6],

$$\Delta K = \Delta\sigma \sqrt{\frac{\pi a}{cos\left(\frac{\pi a}{W}\right)}} \tag{27}$$

where $\Delta\sigma$ is 10.8 ksi, a is 0.5 inch and W is 10 inches. Note that for the middle tension specimen, the total crack length is $2a$.

3.1.2 Material Properties

Fracture toughness and crack growth rate properties were found in Volume 5 of the Damage Tolerant Design Handbook [7]. The fracture toughness values for 0.063-inch-thick 7475-T61 aluminum sheet in the L-T orientation are listed in median rank order in Table 2. A two-parameter Weibull distribution with a shape factor of 12.49 and a scale of 88.89 ksi√in provided a better fit to the data than either a normal or lognormal distribution. The Weibull probability plot of the data and the least squares estimated (LSE) fit to the data are shown in Figure 8.

Table 2. Fracture Toughness, K_c, Values for 7475-T61 Aluminum Sheet 0.63 inch, L-T Orientation

Index	Median Rank	Fracture Toughness, K_c
1	0.0673	70.72
2	0.1635	81.11
3	0.2596	82.76
4	0.3558	83.44
5	0.4519	83.82
6	0.5481	85.10
7	0.6442	88.95
8	0.7404	89.05
9	0.8365	94.77
10	0.9327	95.56

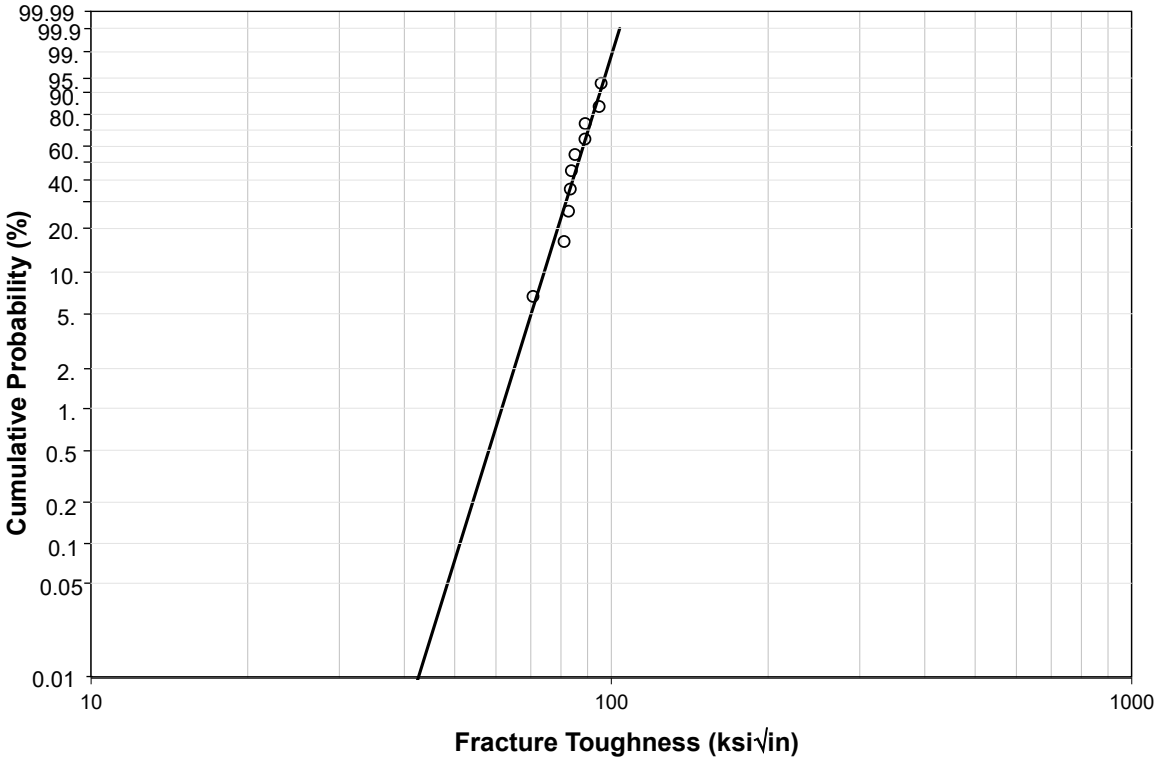

Figure 8. Weibull Distribution of Fracture Toughness Values for 7475-T61 Aluminum Sheet (0.63 inch, L-T)

(Shape parameter of 12.49 and scale parameter of 88.89 ksi √in)

Fatigue crack growth rate data from the Damage Tolerant Design Handbook databook [7] are plotted in Figure 9. The data are described by the following relationship:

$$\frac{\mathrm{da}}{\mathrm{dN}} = 1.01 \times 10^{-10}\Delta\mathrm{K}^{4.7} \quad \text{for } \Delta K \leq 11.56 \text{ ksi}\sqrt{\text{inch}} \quad (28a)$$

$$\frac{da}{dN} = 1.36 \times 10^{-8}\Delta K^{2.7} \quad \text{for } 11.56 \text{ ksi}\sqrt{\text{inch}} \leq \Delta K \leq 25 \text{ ksi}\sqrt{\text{inch}} \quad (28b)$$

$$\mathbf{\frac{da}{dN} = 6.74 \times 10^{-6}\, exp(0.099 * \Delta K)} \quad \text{for } \Delta K \geq 25 \text{ ksi}\sqrt{\text{inch}} \quad (28c)$$

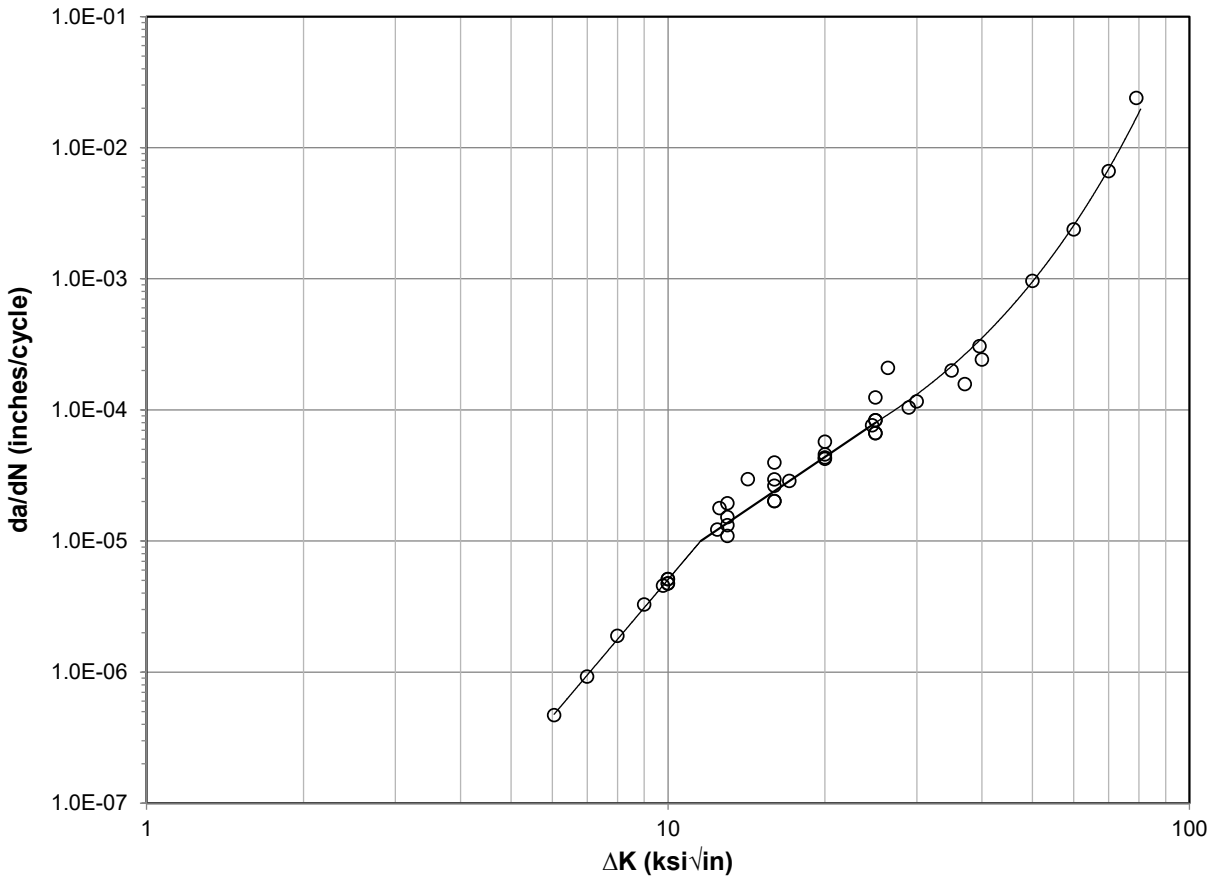

Figure 9. Crack Growth Rate Curve for 7475-T61 Aluminum sheet (0.63 inch, L-T)

3.1.3 Reliability Calculation

Determining the reliability requires the calculation of crack size as a function of load cycles. Equation (27) is only valid for this test configuration to 2*a*/W equal to 0.8, or a crack size of 4 inches, though the calculations can be performed to a crack size of 4.95. The crack size at the start of the (*i*+1) cycle is calculated with the following recursive algorithm.

$$a_{i+1} = a_i + \Delta a_i \quad \text{for } i = 1 \text{ to } N \qquad (29)$$

where Δa_i is found using equation (28), and

$$\Delta K_i = 10.8\ ksi\sqrt{\frac{\pi a_i}{cos(0.1\pi a_i)}} \qquad (30)$$

The crack growth calculation starts with a_i equal to 0.5 inch. The resulting crack size versus load cycle curve is presented in Figure 10. A partial listing of the crack sizes as a function of load cycles is given in Table 3.

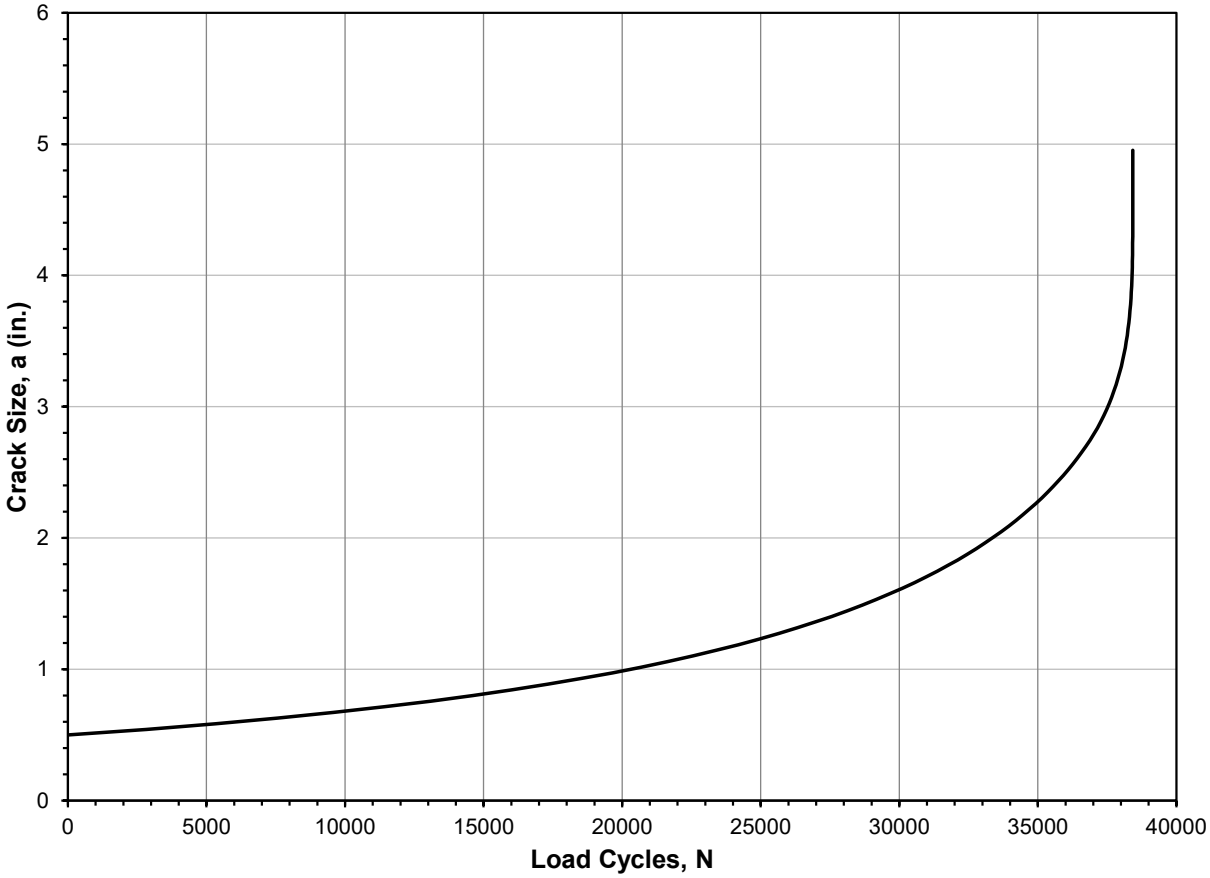

Figure 10. Predicted Crack Growth Curve for Experiment

The *POF* of the specimen as a function of loading cycle can be calculated two different ways. MCS can be used. Then, since standard distributions are used for fracture toughness and yield strength, the CDF can be directly used. The CDF calculations will be used to instill confidence in MCS. The CDF calculations will be performed first because it is known to be correct.

3.1.3.1 CDF Calculation

Step 1. Using the crack size in Column 2 of Table 3, calculate the maximum stress intensity during the *i*th loading cycle, $K_{max}(i)$, using equation (31). Some of the values are shown in Column 3 of Table 3.

$$K_{max}(i) = 12\ ksi\sqrt{\frac{\pi a_i}{cos(0.1\pi a_i)}} \qquad (31)$$

Table 3. Representative Cycles in Calculation of POF for Experiment

Cycle, i	Crack size, a_i	Max. Stress Intensity, K_{max}(i) (ksi√in)	Cumulative POF, $CDF_f(i)$	$PDF(i)$	Hazard Rate, $h(i)$
1	0.5000	15.13	2.49E-10		
2	0.5000	15.13	2.49E-10	5.00E-14	5.00E-14
3	0.5000	15.13	2.49E-10	5.00E-14	5.00E-14
29	0.5004	15.14	2.50E-10	5.03E-14	5.03E-14
30	0.5005	15.14	2.50E-10	5.03E-14	5.03E-14
31	0.5005	15.14	2.50E-10	5.03E-14	5.03E-14
64	0.50099	15.15	2.52E-10	5.06E-14	5.06E-14
65	0.50101	15.15	2.52E-10	5.06E-14	5.06E-14
66	0.50102	15.15	2.52E-10	5.07E-14	5.07E-14
67	0.50104	15.15	2.52E-10	5.07E-14	5.07E-14
68	0.50105	15.15	2.52E-10	5.07E-14	5.07E-14
69	0.50107	15.15	2.52E-10	5.07E-14	5.07E-14
70	0.50108	15.15	2.52E-10	5.07E-14	5.07E-14
71	0.50110	15.15	2.52E-10	5.07E-14	5.07E-14
72	0.50112	15.15	2.52E-10	5.07E-14	5.07E-14
73	0.50113	15.15	2.52E-10	5.07E-14	5.07E-14
74	0.50115	15.15	2.52E-10	5.07E-14	5.07E-14
75	0.50116	15.15	2.52E-10	5.08E-14	5.08E-14
76	0.50118	15.15	2.52E-10	5.08E-14	5.08E-14
77	0.50119	15.15	2.52E-10	5.08E-14	5.08E-14
78	0.50121	15.15	2.53E-10	5.08E-14	5.08E-14
79	0.50123	15.15	2.53E-10	5.08E-14	5.08E-14
80	0.50124	15.15	2.53E-10	5.08E-14	5.08E-14
81	0.50126	15.15	2.53E-10	5.08E-14	5.08E-14
82	0.50127	15.15	2.53E-10	5.08E-14	5.08E-14
83	0.50129	15.15	2.53E-10	5.08E-14	5.08E-14
84	0.50131	15.15	2.53E-10	5.09E-14	5.09E-14
85	0.50132	15.15	2.53E-10	5.09E-14	5.09E-14
86	0.50134	15.15	2.53E-10	5.09E-14	5.09E-14
87	0.50135	15.15	2.53E-10	5.09E-14	5.09E-14
88	0.50137	15.15	2.53E-10	5.09E-14	5.09E-14
89	0.50138	15.15	2.53E-10	5.09E-14	5.09E-14
90	0.50140	15.15	2.53E-10	5.09E-14	5.09E-14
91	0.50142	15.16	2.53E-10	5.09E-14	5.09E-14
92	0.50143	15.16	2.53E-10	5.09E-14	5.09E-14
93	0.50145	15.16	2.53E-10	5.10E-14	5.10E-14
94	0.50146	15.16	2.53E-10	5.10E-14	5.10E-14
95	0.50148	15.16	2.53E-10	5.10E-14	5.10E-14
96	0.50149	15.16	2.53E-10	5.10E-14	5.10E-14
97	0.50151	15.16	2.53E-10	5.10E-14	5.10E-14
98	0.50153	15.16	2.54E-10	5.10E-14	5.10E-14
99	0.50154	15.16	2.54E-10	5.10E-14	5.10E-14
100	0.50156	15.16	2.54E-10	5.10E-14	5.10E-14
101	0.50157	15.16	2.54E-10	5.10E-14	5.10E-14
102	0.50159	15.16	2.54E-10	5.11E-14	5.11E-14
103	0.50160	15.16	2.54E-10	5.11E-14	5.11E-14

Step 2. Calculate the probability that the specimen will fracture on or before the *i*th load cycle, $F_T(i)$, i.e., the probability that the fracture toughness is less than or equal to $K_{max}(i)$ using the Weibull distribution for fracture toughness equation (30). The load and fracture toughness do not change from cycle to cycle. Thus, $F_T(i)$is the cumulative POF through cycle *i*. Some of the values are shown in Column 4 of Table 3.

$$F_T(i) = 1 - exp\left[-\left(\frac{K_{max}(i)}{88.89}\right)^{12.49}\right] \tag{32}$$

Step 3. Calculate the PDF of the failure distribution on the *i*th load cycle, $f_T(i)$, in Column 5. The PDF is the derivative of the CDF so a two-point centered difference (equation 33) is used to approximate the derivative. [8]

$$f_T(i) = \frac{F_T(i+1) - F_T(i-1)}{(i+1) - (i-1)} \tag{33}$$

Step 4. Calculate the HRF on the *i*th load cycle, $h_T(i)$, in Column 6. $F_T\ (i\text{-}1)$ is used in the denominator since the HRF is based on the condition that the specimen has survived to the i^{th} cycle, or through the $(i\text{-}1)^{th}$ cycle.

$$h_T(i) = \frac{f_T(i)}{1 - F_T(i-1)} \tag{34}$$

$F_T(i)$, $f_T(i)$, and $h_T(i)$ are plotted as a function of loading cycle in Figure 11. The $f_T(i)$ and $h_T(i)$ curves plot on top of one another. As described, this specimen has less than one in a million chance of failing before 30,000 cycles and less than one in a thousand chance of failing before 37,500 cycles. After 37,500 cycles, the POF increases rapidly with each load cycle.

$h_T(i)$ is approximately equal to $f_T(i)$ until 38,150 cycles. In this example, a HRF of 10^{-7} is associated with a cumulative POF of less than 8×10^{-5} and a HRF of 10^{-5} is associated with a cumulative POF of less than 0.002.

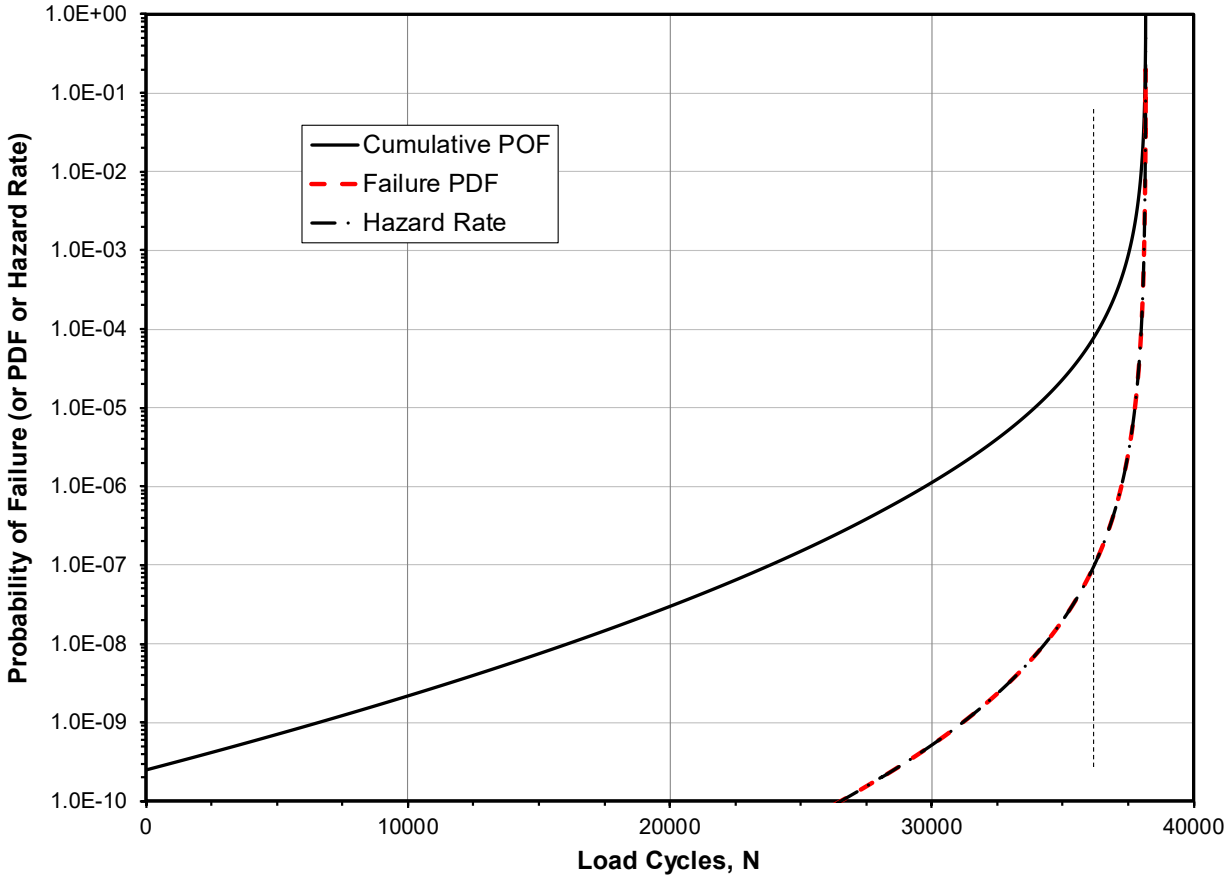

Figure 11. $F_T(i)$, $f_T(i)$, and $h_T(i)$ as Function of Cycles for Example 1

3.1.3.2 Monte Carlo Simulation

The POF can also be determined with MCS. The calculations of crack size and maximum stress intensity as a function cycle number from Section 3.1.3.1 will be used in the MCS.

Step 1. Generate a collection of random fracture toughness values, K_{crit}, from the fracture toughness CDF. This is done by generating random numbers between 0 and 1 using a (pseudo-) random number generator. These random numbers are CDF values, P, for the fracture toughness distribution. The random numbers are plugged into the inverse CDF,

$$K_{crit} = 88.89 \left[ln\left(\frac{1}{1-P}\right)\right]^{\frac{1}{12.49}} \tag{35}$$

to obtain values of K_{crit}. Two thousand samples of K_{crit} were generated.

Step 2. Calculate the probability that the specimen will fracture by the end of the ith cycle, $F_T(i)$, by determining the number of samples, $N_f(i)$, that would have fractured out of the total number of samples, N_T,

$$F_T(i) = \frac{N_f(i)}{N_T} \tag{36}$$

Figure 12 compares $F_T(i)$ from the MCS to the direct integration for cycles greater than 37,000. With 2,000 samples, the MCS is not significantly different from the direct integration. The accuracy of MCS is improved by increasing the number of samples. Thus, if the results in Figure 12 were not accurate enough, more samples would have been generated.

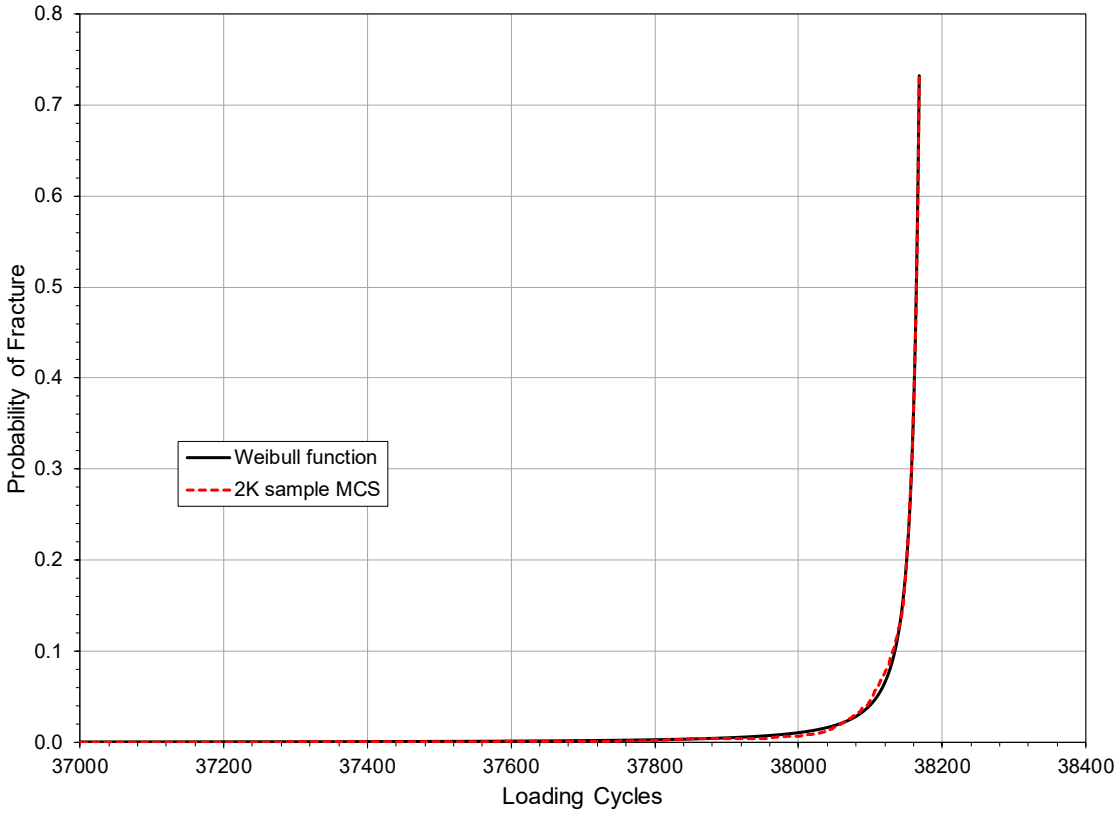

Figure 12. Comparison of $F_T(i)$ from MCS and Weibull Function for Example 1

3.1.4 Sensitivity Study

The results obtained here are dependent upon the fracture toughness distribution used in the analysis. There are only ten fracture toughness values with which to estimate the distribution. This is not nearly enough data to establish the distribution with much certainty. Therefore, a sensitivity study is performed to determine how sensitive the reliability results are to the definition of the fracture toughness distribution. In general, a sensitivity study provides information as to whether additional data should be obtained to reduce the uncertainty in some of the random variables. In this section, a structured procedure for performing a sensitivity analysis will be described.

A sensitivity analysis apportions uncertainty in the output to different sources of uncertainty in the input [9]. The random variable for this examples is the fracture toughness. The variation, or uncertainty, in this random variable is fully described by variation in the shape and scale parameters of the fracture toughness distribution.

There are several different statistical methods for performing a sensitivity analysis [9]. All of these would require tens to hundreds of analyses of the problem to be performed with different combinations of values for the shape and scale parameters of the fracture toughness distribution.

And as the number of random variables in a problem increases, the number of analyses needed increases dramatically. This is a limitation on these methods.

In this example, the method of Robust Design and analysis of variance (ANOVA) was employed to perform the sensitivity analysis [10]. The reason for using these methods is that a relatively small number of additional analyses with different combinations of inputs are required to explore a portion of the space surrounding the analysis point. Orthogonal arrays are utilized to reduce the number of analyses required as the number of random inputs increases.

Robust Design uses an additive model to approximate the effect of input parameters on the output, i.e., the effect of the shape and scale parameters of the fracture toughness distribution on the POF. An additive model is also referred to as a *superposition model* or a *variables separable model*. The additive model requires that the factors in the sensitivity analysis (i.e., the shape and scale parameters) have an equal number of levels at which the result of interest is evaluated, in this case POF or HRF. Furthermore, each value must be used in the same number of POF evaluations, and at least once with every value of the other factors.

Generally, two to three factor levels are recommended. Two factor levels allow only linear trends to be observed. Three factor levels allow quadratic behavior to be discovered. In this example, three factor levels were used. The values for the shape factor are 14.5, 12.49, and 10.5. The values for the scale factor are 93.9, 88.89, and 83.9. These values were chosen to generate fracture toughness distributions that were at the 95% confidence bounds of the distribution fit and still gave reasonable values for the lowest toughness values. The extremes of the distributions that result from combinations of these values are compared to the 95% confidence bounds for the LSE fracture toughness distribution in Figure 13. The shape parameter and scale parameter combinations that were used in the sensitivity analysis are presented in Table 4. A total of nine additional analyses (3x3 = 9) are required for the sensitivity analysis. This is a full factorial array because only two variables are considered. Every combination of the shape and scale parameters is considered.

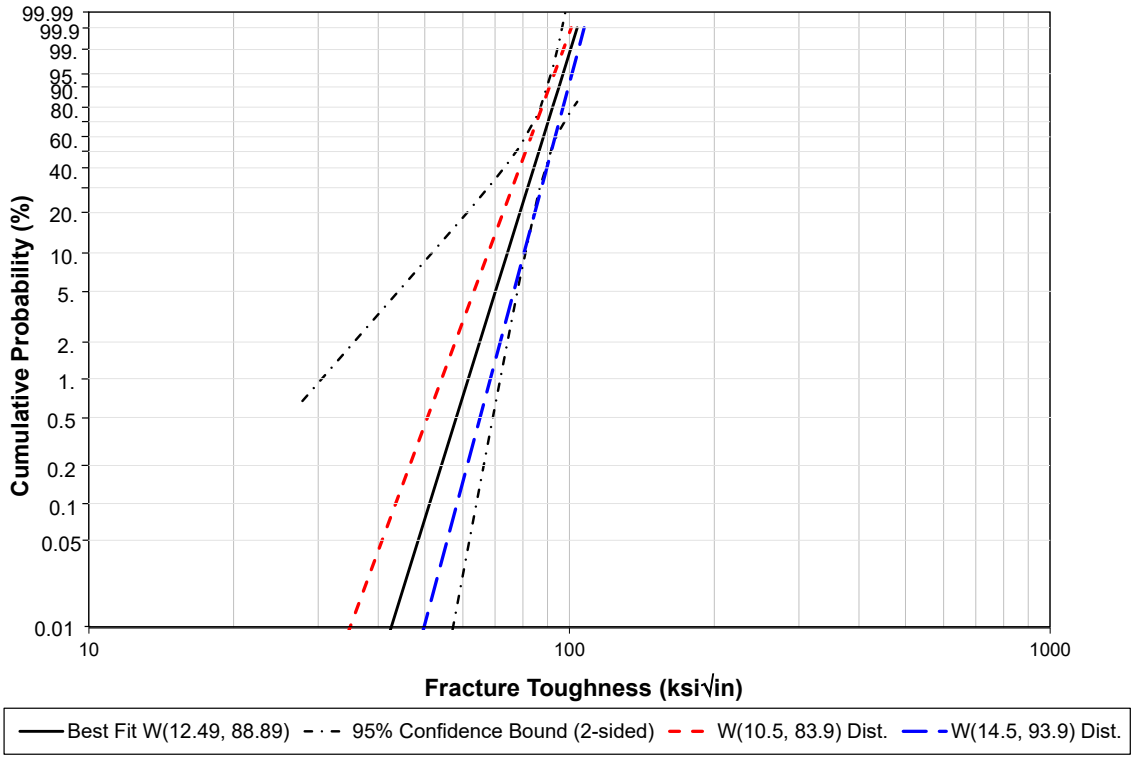

Figure 13. Fracture Toughness Distributions Range for Sensitivity Study

Table 4. Shape and Scale Factor Combinations for Sensitivity ANOVA

Run	Shape Factor	Scale Factor
1	14.5	93.9
2	14.5	88.89
3	14.5	83.9
4	12.49	93.9
5	12.49	88.89
6	12.49	83.9
7	10.5	93.9
8	10.5	88.89
9	10.5	83.9

The cumulative POF and HRF curves for the nine shape and scale parameter combinations in Table 4 are presented in Figure 14 and Figure 15. It is apparent from these graphs that the Weibull shape factor affects both the cumulative POF and the HRF more than the scale factor. The POF and HRF curves lie in distinct bands determined by the shape factor.

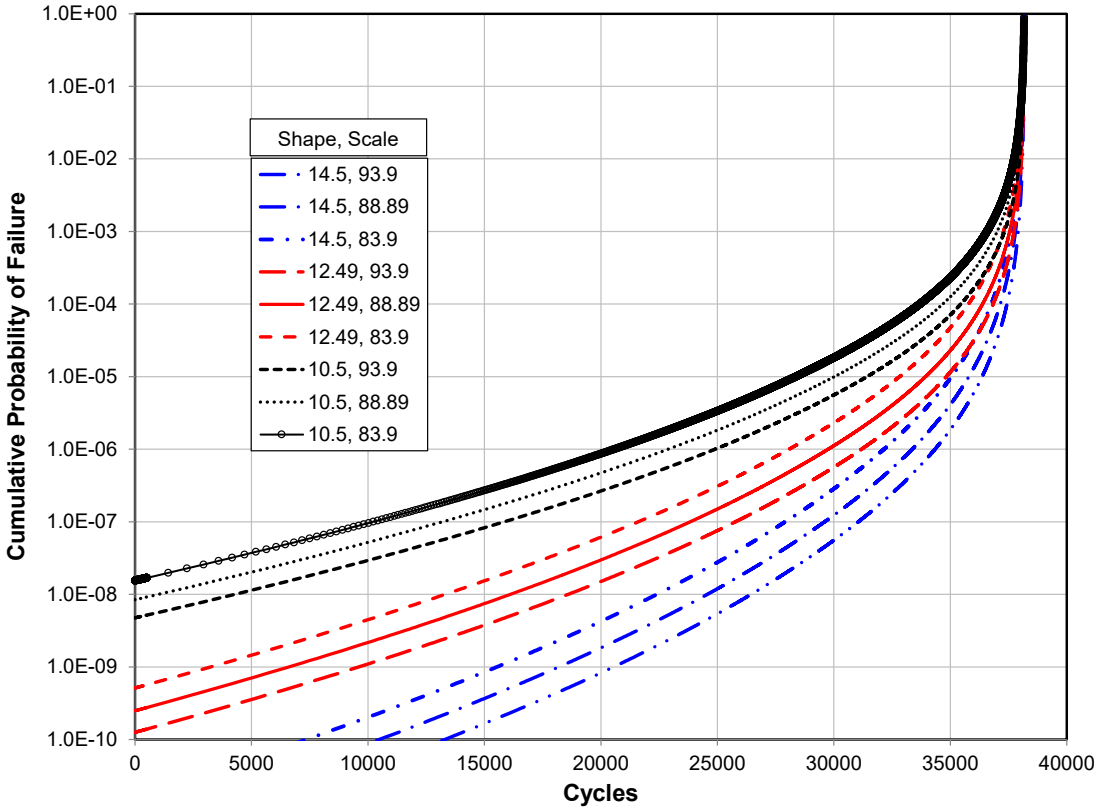

Figure 14. Cumulative POF vs. Cycles Curves for Nine Analyses Used in ANOVA

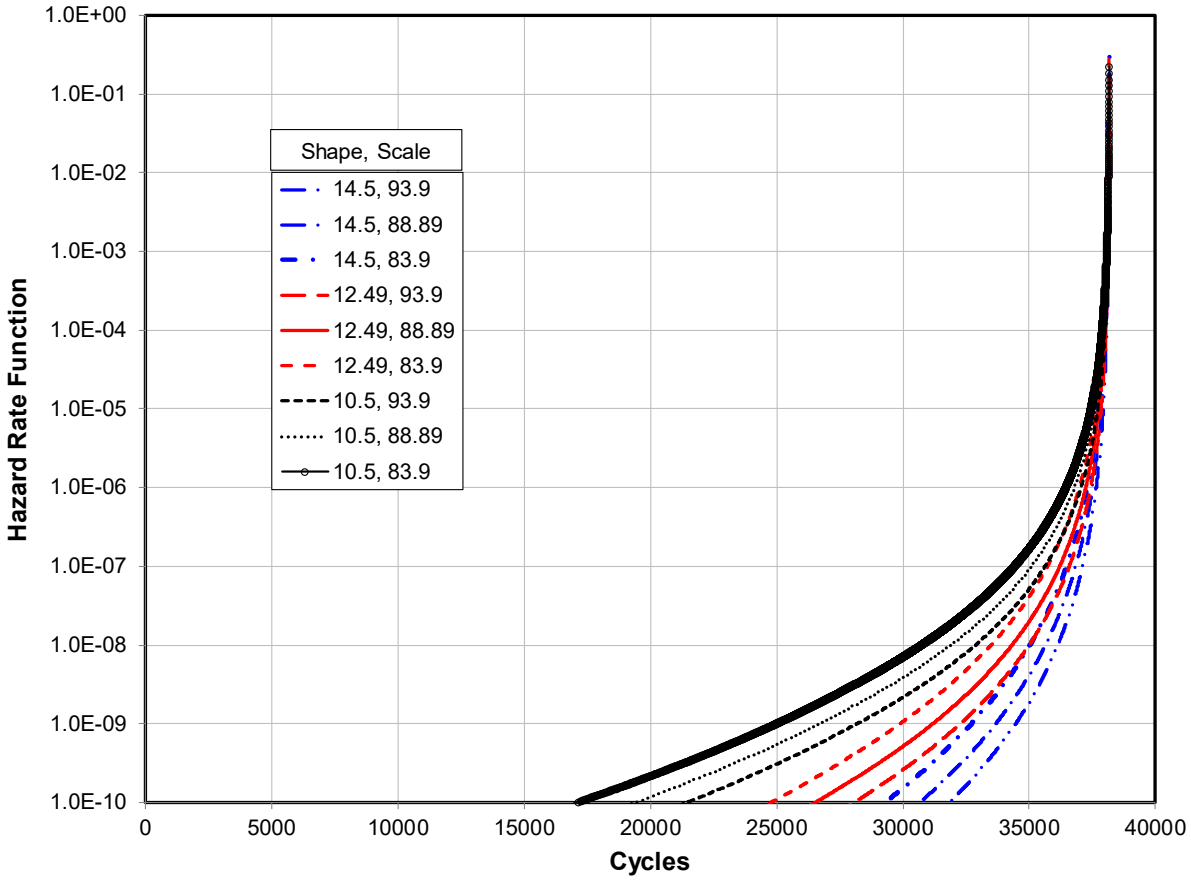

Figure 15. HRF vs. Cycles Curves for Nine Analyses Used in ANOVA

A more quantitative analysis of the sensitivity study is possible. Since current USAF risk criteria are expressed in terms of SFPOF (HRF x 1 flight), the focus of the sensitivity analysis will be on the HRF. Based on the current USAF risk criteria, it was decided to look at the cycles at which a HRF of 10^{-7} and 10^{-5} are reached (Figure 15). Other values of the HRF or POF can be used depending upon the application.

The logarithm of cycles is easier to work with than cycles and improves the additivity of the factor effects [10]. The logarithm of cycles to a HRF of 10^{-7} and 10^{-5} for each combination of Weibull parameters are given in Table 5 and Table 6, respectively. The average logarithm of cycles to a HRF of 10^{-7} and 10^{-5} for each value of the scale factor and shape factor, that is, the averages of each row and column, are calculated in the tables. The row and column averages provide an indication of the main effect of the scale or shape factor at that specific value. Each row and column mean is compared to the overall average (Total Mean) of all nine analyses as part of the sensitivity study. The row or column averages versus the value of the shape or scale factor are plotted in Figure 16.

Table 5. Common Logarithm of Cycles to HRF of 10^{-7}

	Shape			
Scale	**14.5**	**12.49**	**10.5**	**Row Means**
93.9	4.5695	4.5633	4.5517	4.5615
88.89	4.5663	4.5588	4.5451	4.5567
83.9	4.562	4.553	4.5368	4.5506
Column Means	4.566	4.5584	4.5445	
Total Mean	4.5563			

Table 6. Common Logarithm of Cycles to HRF of 10^{-5}

	Shape			
Scale	**14.5**	**12.49**	**10.5**	**Row Means**
93.9	4.579	4.5781	4.5765	4.5779
88.89	4.5782	4.577	4.5752	4.5768
83.9	4.577	4.5756	4.5734	4.5753
Column Means	4.5780	4.5769	4.575	
Total Mean	4.5766			

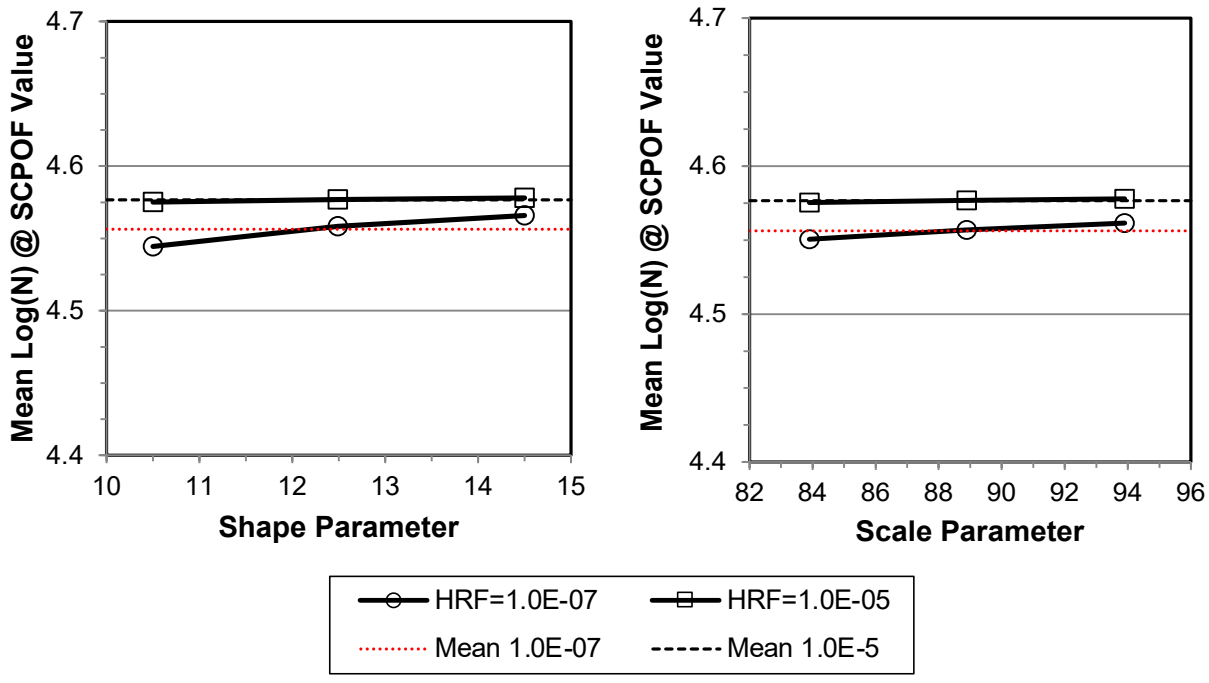

Figure 16. Mean Log(Cycles) to HRF Value versus Factor Level

The almost horizontal line segments for HRF equal 10^{-5} in Figure 16 shows that the cycles to a HRF of 10^{-5} is not very sensitive to values of the shape and scale parameters within the chosen range. The means of the logarithm of the cycles to reach a HRF of 10^{-5} differ by 0.003 for the

shape parameter and 0.0026 for the scale parameter. This is a difference of one cycle in the mean which is not significant compared to the more than 37,000 cycles applied before a HRF of 10^{-5} is reached.

The cycles to a HRF of 10^{-7} are a slightly more sensitive to the values of the shape and scale parameters. The difference in the mean logarithm cycles to a HRF of 10^{-7} is .0215 for the shape factor and 0.0109 for the scale factor. This is also a difference of about one cycle in the mean which again is not significant compared to the more than 35,000 cycles applied before a HRF of 10^{-7} is reached.

Within the ranges of shape and scale factor values investigated, the predicted load cycles at which a HRF of 10^{-7} or 10^{-5} is reached is not very sensitive to the fracture toughness distribution. Wider shape and scale factor ranges could have been chosen and different results may have been obtained. The ranges chosen here just seemed to be reasonable ones for this example. More quantitative analysis of the sensitivity study is possible. It seemed to be unnecessary for this example in light of the lack of sensitivity found. The quantitative analysis will be demonstrated in the next example.

3.2 Hole Specimen under Constant Amplitude Loading

This example is of a panel with a central hole under constant amplitude cyclic loading. The questions again is: When is the specimen likely to fail? The answer to this question is not important for typical tests, but for illustration purposes this question provides a goal for the reliability calculation.

This example contains two random variables: fracture toughness, K_c, and the equivalent initial damage size (EIDS), a_o. The EIDS determines how quickly a crack will grow to a size that can cause fracture. First, the reliability of the specimen as a function of crack size and load cycles is determined. Then the POF function is found. Finally, the HRF is calculated.

3.2.1 Test Conditions

The specimen (Figure 17) is made from 0.063-inch-thick 7475-T61 aluminum sheet. The test will be conducted at room temperature in laboratory air. The specimen is loaded in the longitudinal grain orientation to a maximum stress of 12 ksi at a stress ratio of 0.1. The crack grows in the long transverse grain orientation.

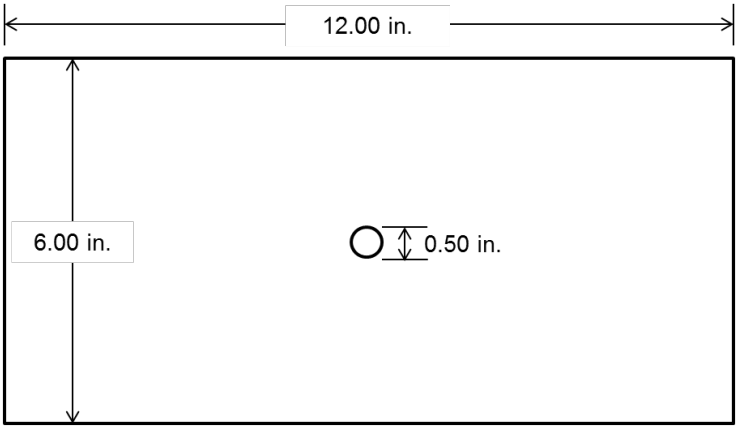

Figure 17. Hole Specimen Geometry

3.2.2 Material Properties

Fracture toughness and crack growth rate properties are the same as in the previous example, Section 3.1.2. They are summarized again here for reference. The fracture toughness is described by a two-parameter Weibull distribution with a shape factor of 12.49 and a scale of 88.89 ksi√inch.

Fatigue crack growth rate data are described by equation (28), which is repeated here for convenience:

$$\frac{\mathrm{da}}{\mathrm{dN}} = 1.01 \times 10^{-10} \Delta \mathrm{K}^{4.7} \quad \text{for } \Delta K \leq 11.56 \text{ ksi}\sqrt{\text{inch}} \quad (28a)$$

$$\frac{da}{dN} = 1.36 \times 10^{-8} \Delta K^{2.7} \quad \text{for } 11.56 \text{ ksi}\sqrt{\text{inch}} \leq \Delta K \leq 25 \text{ ksi}\sqrt{\text{inch}} \quad (28b)$$

$$\frac{\mathrm{da}}{\mathrm{dN}} = 6.74 \times 10^{-6} \exp(0.099 * \Delta \mathrm{K}) \quad \text{for } 25 \text{ ksi}\sqrt{\text{inch}} \leq \Delta K \quad (28c)$$

3.2.3 Equivalent Initial Damage Size

The EIDS is the theoretical size for a single crack at the location of interest that when used in a specified fatigue crack growth computation results in the observed fatigue crack growth at that location [11]. The EIDS lumps all the variables that affect fatigue crack formation and growth such as local grain size, the number and size of cracked constituent particles, scratches in the bore of the hole, link-up of microcracks, etc., into a single parameter, the crack size. The EIDS as a model of the crack size at a location is a clear example of the adage that all models are wrong, but some are useful.

When the same location in a number of nominally similar parts are considered, they invariably have different fatigue lives, i.e., load cycles or service hours to a specified crack size. Each part will have a different EIDS. Parts with longer lives will have smaller EIDSs and parts with shorter lives will have larger EIDSs. Rank ordering this collection of EIDSs generates a probability distribution for the EIDS for that location on that part. This distribution gives the probability that the EIDS at that location on any of the nominally similar parts will be less than a specified size, or alternatively that the EIDS is greater than a specified size. Since the EIDS is related to the fatigue life, this distribution can be used to determine the probability that the location of interest has a fatigue life longer (or shorter) than a given value.

The EIDS is frequently found from multiple trials using different initial crack sizes in a fatigue crack growth model consisting of a particular software package, load spectrum, and stress intensity model in order to replicate the observed fatigue life of a test specimen, part on a full scale test article, or part from an in-service aircraft. Because the EIDS developed in this manner is intimately tied to the software package, load spectrum, and part geometry, this EIDS distribution cannot be readily used for different model aircraft or in another software package. Sometimes, however, there is no other choice but to use an EIDS distribution developed for a different detail.

There have been efforts to develop physically based initial flaw size distributions [12, 13, 14, 15]. These efforts have considered only the basic material character so far. They have not yet addressed the effect of part fabrication, hole drilling, and assembly on the flaw size distribution as a part enters service.

3.2.3.1 Determining the EIDS Distribution

If there are some instances of fatigue cracking in the detail of interest, either in service or during a full scale durability test, the sizes of the cracks, the flight hours or cycles associated with each crack size, and the loading history for each instance can be used to estimate an EIDS using a fatigue crack growth code. Estimation of the EIDS should be done with the same fatigue crack growth code that will be used in subsequent analyses of the structure. The crack size versus FH (or cycles) curve that results from an EIDS determination is only guaranteed to match the observed crack size and FH at the single observation used to estimate the EIDS. Since there are typically no other crack size history data, there is no way of knowing how well the crack growth curve from the EIDS represents the actual crack growth history for the detail.

An alternate approach of determining the EIDS from a full scale durability test, or a number of representative coupon tests, is to insert marker bands into the load history and then perform fractography to determine multiple crack sizes at various times during each individual test. Fitting a curve to the crack size and FH pairs for each specimen and extrapolating back to time zero yields an EIDS estimate for each specimen. This approach is more time consuming and expensive than the analytical method above. It is also difficult to ensure that laboratory specimens are representative of actual manufacturing quality. However, the EIDSs found by curve fitting to fractographic data are slightly more physical and less sensitive to the loading spectrum used, especially if the curve fit is limited to a power law as recommended in [11, 15]. Thus, EIDSs from fractographic data can used for other details and other load spectra with less uncertainty, though still not complete confidence.

For this example, the fractographic determination of EIDS is demonstrated. Fractographic data from volume 8 of [11] will be used. The material is aluminum alloy 7475-T7351 plate which is a different temper than the –T61 temper of this example. However, work on developing a physical initial flaw sizes [12] in 7075-T6 sheet has shown that the origin of fatigue cracks are cracked iron-bearing constituent particles. The size of these constituent particles are not changed by the temper of the alloy. The only other contributor to the fatigue process is the quality of the hole drilling. A number of different specimen geometries were used in [11]. Data from specimens with fasteners in holes but no load transfer is used here as this is most similar to the example.

3.2.3.2 Fractographic Determination of EIDS

Fifty-three specimens with no load transfer were tested using an F-16 400-hour load spectrum [11]. The specimens had different hole diameters, fasteners, and reference stresses as shown in Table 7. Each specimen had two holes as shown in Figure 18 for a total of 106 possible EIDS values.

Table 7. Specimen Information

Hole Diameter (in.)	Fastener	Reference Stress (ksi)	No. of Specimens
0.25	MS-90353	32	7
0.188	MS-90353	32	5
0.25	MS-90353	34	12
0.25	NAS 1580	38	10
0.25	MS-90353	38	19

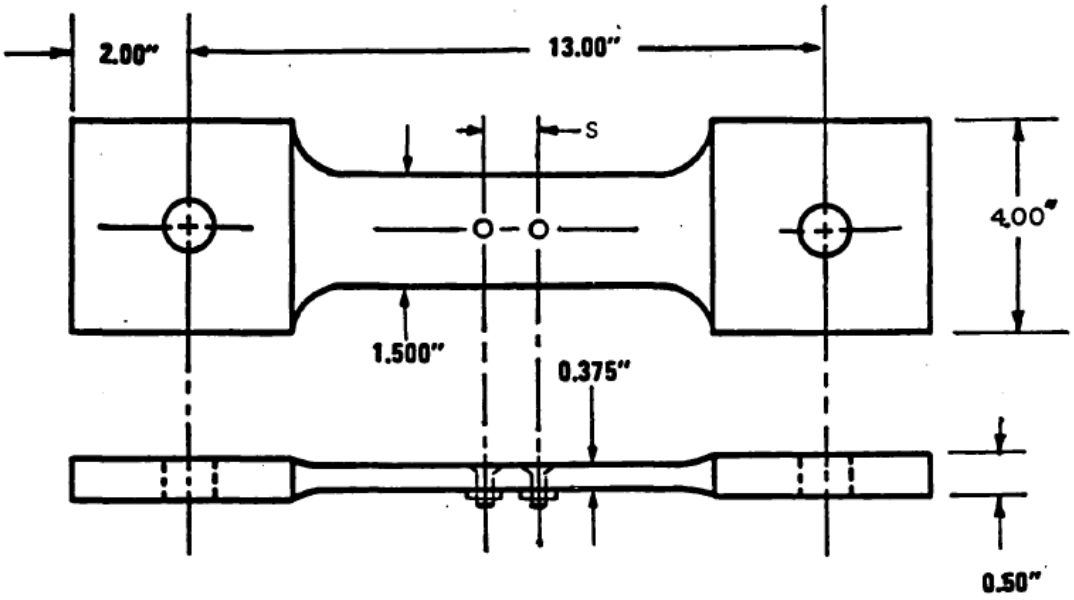

Figure 18. No Load Transfer Specimen for EIDS Tests [11]
Two different hole spacings used: S=1.00 inch and S=3.00 inches.

This particular load spectrum created marker bands on the fracture surface, so it was possible to relate various crack sizes during each test to a specific time expressed in terms of spectrum FH. At the small crack sizes used in determining the EIDS, the crack is either a corner crack or surface crack. A single number for the crack size does not adequately describe the shape of the crack. The dimension into the depth of the specimen and along the surface are needed. Unfortunately, only the depth of the crack into the specimen was recorded in [11].

The crack size measurements less than 1 mm (0.0394 inch) were used to estimate the EIDS following the recommendations in [15]. This reduces impact of the various effects that develop as the crack gets longer making the resulting EIDS more physical and transferable to other

situations. For crack sizes less than 1 mm, it was found that a power equation fits the crack growth reasonably well. Thus, the crack size as a function of time, *a(t)*, is

$$a(t) = \beta t^{\theta} \tag{37}$$

where β is the EIDS for that specimen. An example of the curve fitting procedure for determining the EIDS is provided in Figure 19. The complete listing of the fractographic data for all 53 specimens is in Appendix A along with plots of the curve fit to the crack sizes less than 1 mm.

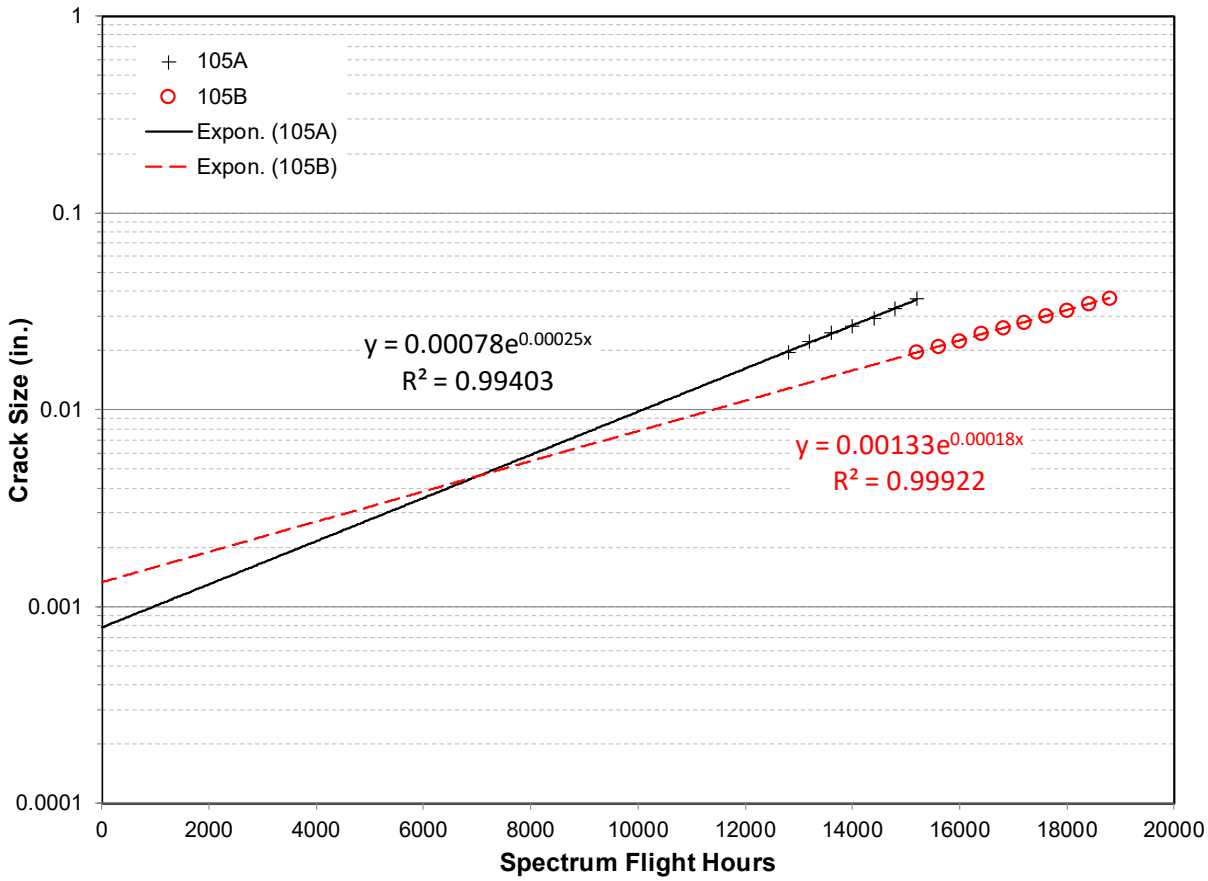

Figure 19. Determination of EIDS for Both Holes on One Specimen

The EIDSs that could be determined are listed in Table 8. The EIDS could not be determined for a number of holes. One specimen was destroyed in the fixture. Another specimen had a crack that could not be read back to a size less than 1 mm (0.0394 inch). And there were numerous holes that did not crack within the maximum number of spectrum FH. The holes that did not crack are treated as censored data. The EIDSs for the uncracked holes must be smaller than the EIDS for any of the cracked holes. So, the uncracked holes are placed in the rank ordering below the lowest EIDS value and the number of uncracked holes, 45, added to the rank of the lowest EIDS. The specimen that was destroyed was not considered part of the sample reducing the total number of holes sampled by 2 to 104.

It is not obvious how the cracked hole that could not be read back to a crack size less than 1 mm should be handled. It should not be discarded from the sample because it did crack. And it should not be placed into the small crack portion of the sample with the uncracked holes because the

smallest crack size that could be read, 0.2163 inch at 10,800 SFH, is significant when compared to the crack sizes at other holes on similarly loaded specimens at 10,800 SFH. Trials putting this hole in as an unknown value at different ranks at the high end of the rankings did not change the resulting distribution at all, so it was treated as an unknown value in the 104^{th} rank.

The rank order and median rank for the EIDS values are provided in Table 9. The EIDS values are plotted against their median rank on a Weibull probability plot in Figure 20. The line in Figure 20 was fit to the data using LSE. The correlation coefficient for the fit, R^2, was 94.2%. The resulting Weibull distribution has a shape parameter of 0.372 and a scale parameter of 0.00062.

Table 8. EIDS Values Found for No Load Transfer Specimens

Specimen & Hole ID	EIDS (inch)	Reference Stress (ksi)	Hole Diameter (inch)	Fastener
99A	0.00025	32	0.188	MS-90353
99B	0.00037			
100A	0.002			
101A	0.00147			
621A	0.00039			
623A	0.00181			
102A	0.00169	32	0.25	MS-90353
103B	0.00134			
104B	0.00145			
105A	0.00078			
105B	0.00133			
106A	0.0015			
106B	0.00016			
107A	0.00014			
107B	0.00187			
108B	0.0004			
109A	0.00175	34	0.25	MS-90353
109B	0.00248			
111A	0.00022			
111B	0.0002			
112A	0.00012			
112B	0.00128			
113A	0.00115			
114A	0.00009			
114B	0.00011			
115A	0.00049			
115B	0.00017			
116A	0.0006			
117A	0.00074			
117B	0.00075			
383A	0.00152	38	0.25	MS-90353
384A	0.00123			
385B	0.00091			
386B	0.00113			
387A	0.0007			
581A	0.01072			
582B	0.00166			
583B	0.0049			
584B	0.00124			
585B	0.00277			
654B	0.00324			
655A	0.00225			
656A	0.00417			
657A	0.00213			
658B	0.00097			
660B	0.00025			
661B	0.00448			
662B	0.00216			
696A	0.00024			
697A	0.00059			
699B	0.00145			
700A	0.00128			
700B	0.00125			
467A	0.00229	38	0.25	NAS 1580
468A	0.00286			
469B	0.00106			
470B	0.0024			
471B	0.00072			
472A	0.00014			
473A	0.00237			
474A	0.00022			
475A	0.00388			
476B	0.00033			

Table 9. Rank Order of EIDS Values

Rank	Median Rank (Benard)	EIFS (in.)
46	0.4177	0.00009
47	0.4269	0.00011
48	0.4360	0.00012
49	0.4452	0.00014
50	0.4543	0.00014
51	0.4634	0.00016
52	0.4726	0.00017
53	0.4817	0.00020
54	0.4909	0.00022
55	0.5000	0.00022
56	0.5091	0.00024
57	0.5183	0.00025
58	0.5274	0.00025
59	0.5366	0.00033
60	0.5457	0.00037
61	0.5548	0.00039
62	0.5640	0.00040
63	0.5731	0.00049
64	0.5823	0.00059
65	0.5914	0.00060
66	0.6005	0.00070
67	0.6097	0.00072
68	0.6188	0.00074
69	0.6280	0.00075
70	0.6371	0.00078
71	0.6463	0.00091
72	0.6554	0.00097
73	0.6645	0.00098
74	0.6737	0.00106
75	0.6828	0.00113
76	0.6920	0.00115
77	0.7011	0.00123
78	0.7102	0.00124
79	0.7194	0.00125
80	0.7285	0.00128
81	0.7377	0.00128
82	0.7468	0.00133
83	0.7559	0.00134
84	0.7651	0.00145
85	0.7742	0.00145
86	0.7834	0.00147
87	0.7925	0.00150
88	0.8016	0.00152
89	0.8108	0.00166
90	0.8199	0.00169
91	0.8291	0.00175
92	0.8382	0.00181
93	0.8473	0.00187
94	0.8565	0.00200
95	0.8656	0.00213
96	0.8748	0.00225
97	0.8839	0.00229
98	0.8931	0.00237
99	0.9022	0.00240
100	0.9113	0.00248
101	0.9205	0.00277
102	0.9296	0.00286
103	0.9388	0.00324
104	0.9479	0.00388
105	0.9570	0.00417
106	0.9662	0.00448
107	0.9753	0.00490
108	0.9845	0.01072

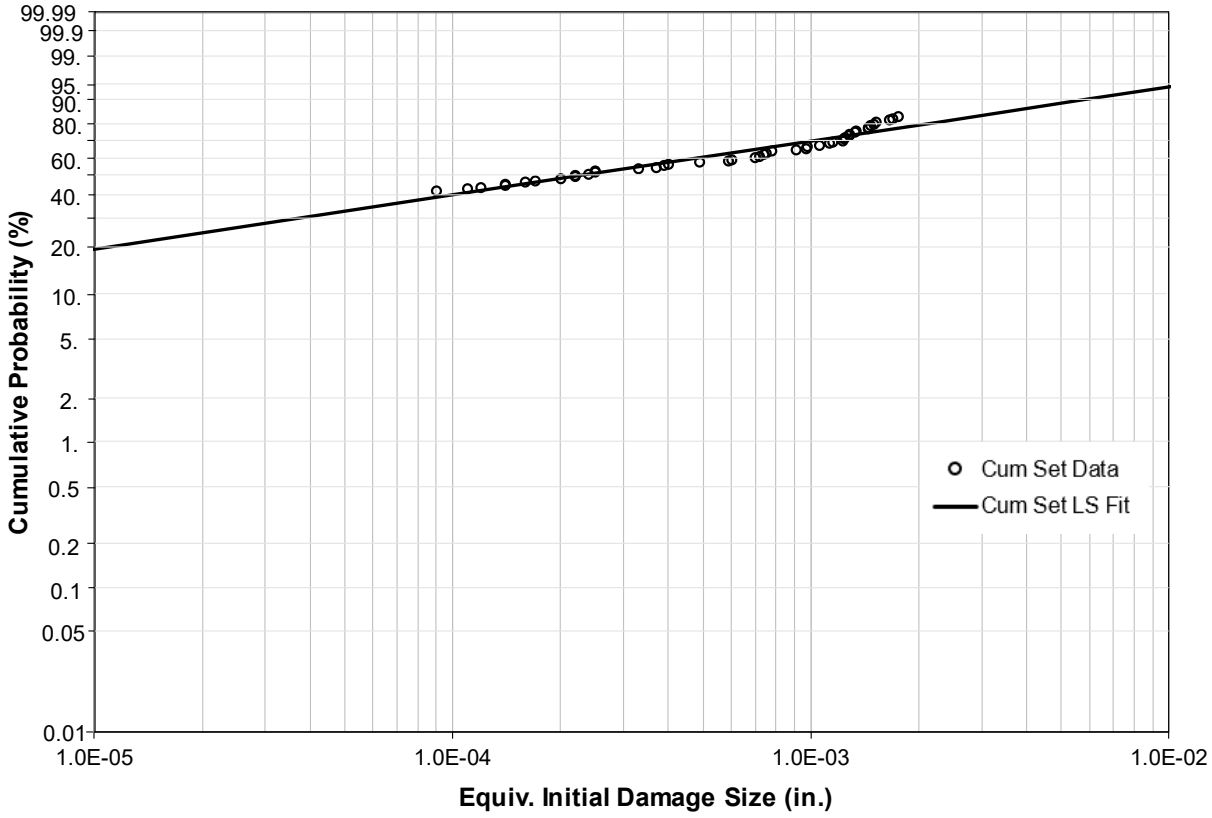

Figure 20. Weibull Probability Plot of EIDS Values

3.2.4 Stress Intensity Calculation

The assumed cracking scenario is a corner crack growing from one side of the hole. A one-to-one aspect ratio is assumed until both dimensions equal the thickness of the specimen, 0.063 inch, in order to keep this example simple. Then a through crack is assumed beginning at a length of 0.063 inch. In a real problem, the aspect ratio of the part-through crack should be allowed to vary as the crack growth dictates.

The stress intensity factor, *K*, for the corner crack along the surface is [16]

$$K = \beta_c \sigma \sqrt{\pi c} \tag{38}$$

$$\beta_c = G_0 G_w \tag{39}$$

$$G_0 = \frac{0.7071 + 0.7548 z_0 + 0.3415 z_0^2 + 0.642 z_0^3 + 0.9196 z_0^4}{1 + 0.13 z_0^2} \tag{40}$$

$$z_0 = \frac{1}{1 + 2\left(\frac{a}{D}\right) cos(0.85\varphi)} \tag{41}$$

$$G_w = M_0 g_1 g_3 g_4 f_w f_\varphi f_x \tag{42}$$

$$M_0 = 1.13 - 0.09\frac{a}{c} + m_2\left(\frac{a}{t}\right)^2 + m_3\left(\frac{a}{t}\right)^4 \quad (43)$$

$$m_2 = -0.54 + \frac{0.89}{0.2 + (a/c)} \quad (44)$$

$$m_3 = 0.5 - \frac{1}{0.65 + (a/c)} + 14\left(1 - \frac{a}{c}\right)^{24} \quad (45)$$

$$g_1 = 1 + \left[0.1 + 0.35\left(\frac{a}{t}\right)^2\right](1 - sin\,\varphi)^2 \quad (46)$$

$$g_3 = \left[1 + 0.04\left(\frac{a}{c}\right)\right][1 + 0.1(1 - cos\,\varphi)^2]\left[0.85 + 0.15\left(\frac{a}{t}\right)^{0.25}\right] \quad (47)$$

$$g_4 = 1 - 0.7\left[1 - \frac{a}{t}\right]\left[\frac{a}{c} - 0.2\right]\left[1 - \frac{a}{c}\right] \quad (48)$$

$$f_w = \sqrt{sec\left(\frac{\pi c}{W}\sqrt{\frac{a}{t}}\right)} \quad (49)$$

$$f_\varphi = \left[\left(\frac{a}{c}cos\,\varphi\right)^2 + sin^2\varphi\right]^{0.25} \quad (50)$$

$$f_x = \frac{1}{\sqrt{1 + 1.464\left(\frac{a}{c}\right)^{1.65}}} \quad (51)$$

where φ equals 10°, *a/c* equals 1, *t* equals 0.63 inch, *D* equals 0.50 inch, and *W* equals 6.00 inch.

The stress intensity once the crack becomes a through crack, i.e., *a* greater than or equal to the thickness, 0.063 inch, is [16]

$$K = \beta_t \sigma\sqrt{\pi c} \quad (52)$$

$$\beta_t = G_t G_{w*} \quad (53)$$

$$G_t = 0.7071 + 0.7548z_0 + 0.3415z_0^2 + 0.642z_0^3 - 0.9196z_0^4 \quad (54)$$

$$z_0 = \frac{1}{1 + (2a/D)} \quad (55)$$

$$G_{w*} = \frac{1}{\sqrt{\frac{(sec\,\lambda\,sin\,\delta)}{\delta}}} \quad (56)$$

$$\lambda = \frac{\pi}{2}\left(\frac{D + a}{2B - a}\right) \quad (57)$$

$$\delta = \frac{D}{B} - \frac{2D}{W} \tag{58}$$

where D equals 0.50 inch, W equals 6.00 inch, and B, the shortest distance from the center of the hole to a free edge, equals half of W in this example.

The results of equations (38 through 51) and (52 through 58) are plotted against the crack dimension on the surface of the specimen, c, in Figure 21. A small peak in the curve is observed at c equals 0.063 inch, where the crack transitions to a through crack. The through crack stress intensity decreases slightly as the crack grows out of the stress concentration around the hole before starting to increase at a crack size around 0.175 inch.

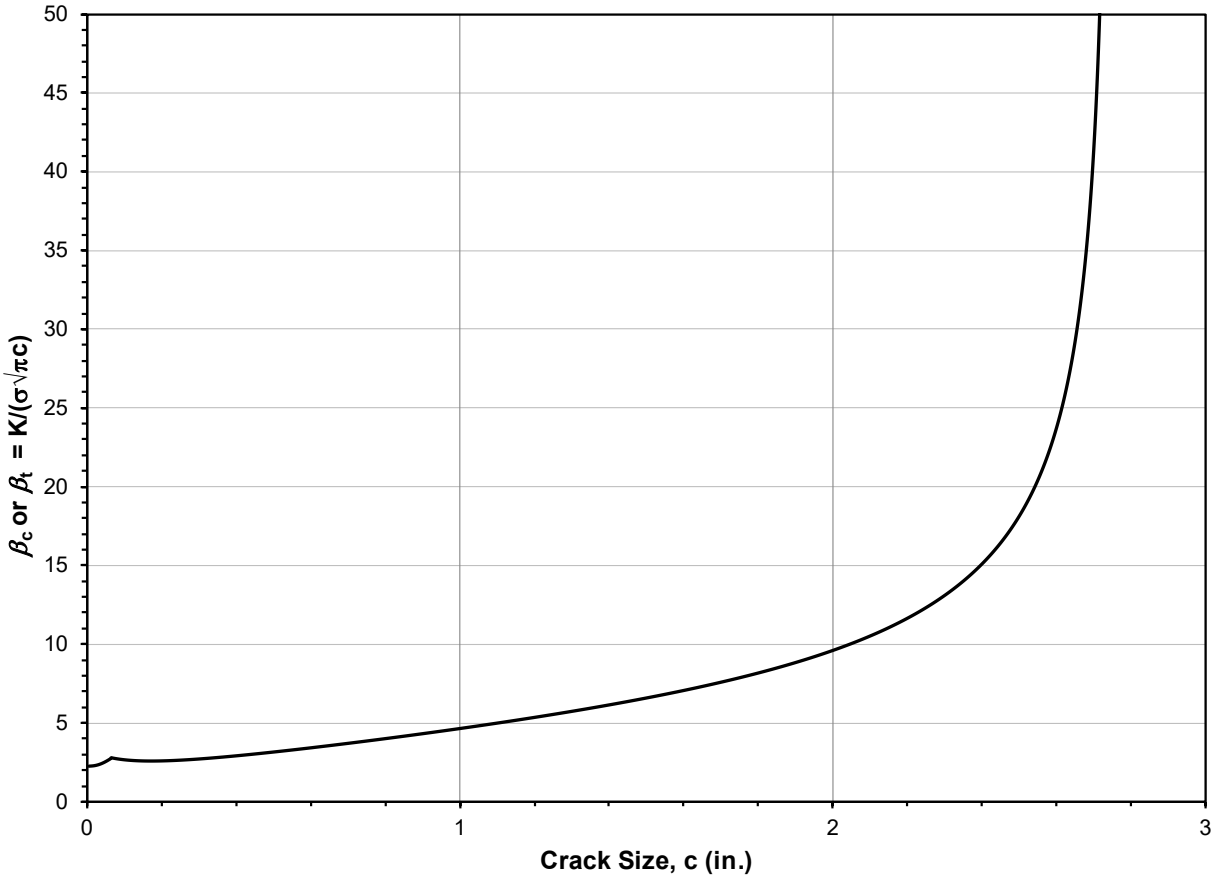

Figure 21. Geometry Factor β_c (Corner Crack) or β_t (Through Crack) for Example Hole Specimen

3.2.5 POF Calculation

MCS will be used to calculate the determine the failure CDF as a function cycles, $F_T(n)$. The failure PDF as a function of cycles, $f_T(n)$, is determined from $F_T(n)$. Finally, the HRF as a function of cycles, $h_T(n)$, is found.

3.2.5.1 Reliability by Monte Carlo Simulation

The basic idea of MCS is to randomly choose the starting conditions (i.e., K_C and EIDS) for a sample that is representative of a physical specimen. Then simulate the repeated loading of this sample until it fails, i.e., the applied stress intensity equals or exceeds K_C. Record the number of load cycles when this sample fails. Repeat this process of creating samples and modeling the

fatigue degradation until a sufficiently large number of samples have been generated that the POF can be estimated with acceptable confidence.

Mathematically, to estimate POFs in the 10^{-7} tail region of the failure distribution, a very large number of samples are needed because the tails of the input distributions are where the samples with early failures arise. Numbers of a billion or more samples are quoted. For the typical structural reliability problem, the data supporting the fracture toughness and EIDS distributions are limited. There is seldom data in the tails of the fracture toughness or EIDS distributions. The tails are extrapolations using standard probability distributions fit to data clustered around the mean. In reality, generating several billion samples gives an accurate POF values based on extrapolations of uncertain validity. This important aspect of the results often gets lost in the accuracy of the theoretical mathematics.

Estimates of the mean and standard deviation of the reliability distribution require only a few thousand samples. The low POF tail can be estimated by fitting a function to the central part of the reliability distribution and extrapolating to the lower POF values. The extrapolation aspects of this approach is then obvious to all.

The steps in performing a MCS for this example problem are discussed in the following paragraphs. The MCS was performed in Excel using a VBA macro and the inputs developed in the preceding sections.

Step 1. Randomly select K_C for MCS sample. Use a (pseudo-) random number generator to randomly generate a number between 0 and 1. Recall that the CDF has a range of 0 to 1. The random number is the CDF value, P, of K_C. Plug the random number into the inverse CDF determine K_C. Save the random number and K_C in columns B and C of a worksheet. The inverse CDF for the Weibull distribution is

$$K_C = \beta \left[LN\left(\frac{1}{1-P}\right)\right]^{1/\alpha} \tag{59}$$

where α is the shape parameter and β is scale parameter. The routine for randomly generating K_C is listed in Appendix B.2.

Step 2. Randomly select EIDS for MCS sample. Use a (pseudo-) random number generator to randomly generate a number between 0 and 1. Plug the random number into inverse CDF determine EIDS. Save the random number and EIDS in columns D and E of a worksheet. A Weibull distribution was also fit to the EIDS data for this example. The routine for randomly generating EIDS is also listed in Appendix B.2.

Step 3. Simulate the growth of the EIDS under the prescribed cyclic loading. This can be done with a master crack growth curve developed with a crack growth code such as AFGROW or NASGRO. Or each sample can be simulated individually as was done for this example. Individual simulation of each sample takes longer to run the MCS.

A simple crack growth algorithm was written for this example. It calculates the increment of crack growth for each load cycle assuming a corner crack with a constant aspect ratio of 1 when the crack size is less than the specimen thickness. The crack transitions to a through crack once the crack size is equal to or greater than the thickness. The simulation is stopped when the maximum stress intensity during a cycle

equals or exceeds K_C for the sample. The cycles to failure and maximum stress intensity during the last cycle are recorded.

The cycles to failure can be very large for very small EIDS values. The crack growth simulation for such a sample takes a long time. When an EIDS less than 0.0001 inch was generated, the crack growth simulation was skipped to speed up the MCS since samples with long lives are not of much interest. The cycles to failure was set to 50,000,000 and the maximum stress intensity was set to -1.

Step 4. Rank order the cycles to failure. The cycles to failure from all samples are sorted from shortest to longest. The samples with 50,000,000 cycles to failure count in the total number of samples, but they are all at the high end of the ranking. Median rank is assigned to each sample using Benard's approximation, Section 2.3.1. Recall that the median rank is an estimate of the CDF value for the sample.

Step 5. Fit a function the low life tail of the cumulative failure distribution. It is unlikely that the reliability function will readily fit any of the well-known distributions. However, many probability distributions are exponential functions such as the normal, lognormal, and Weibull distributions. A few are double exponential functions such as the Gumbel distribution. Thus, a good place to start when trying to fit a function to the MCS results is to look at:

1. LN(CDF) vs. Load Cycle, (Figure 22)
2. LN(CDF) vs. LN (Load Cycle), (Figure 23)
3. LN(-LN(CDF)) vs. Load Cycle, (Figure 24)
4. LN(-LN(CDF)) vs. LN (Load Cycle). (Figure 25)

The trendline options in Microsoft Excel® were used to find the best fit function in each of the four cases. A quadratic polynomial fit to LN(-LN(CDF)) vs. LN(Load Cycle) had the best correlation coefficient. The fit in the short life tail is not real good, but remember there is a small number of samples in the tail and we are extrapolating outside the range for which we have supporting input data. Rearranging the equation in Figure 25 gives a CDF of

$$F_T(n) = Pr\left(N_f \leq n\right) = exp\left\{-exp\left[\left(\frac{LN(n) - 21.58}{8.03}\right)^2 - 0.57\right]\right\} \quad (60)$$

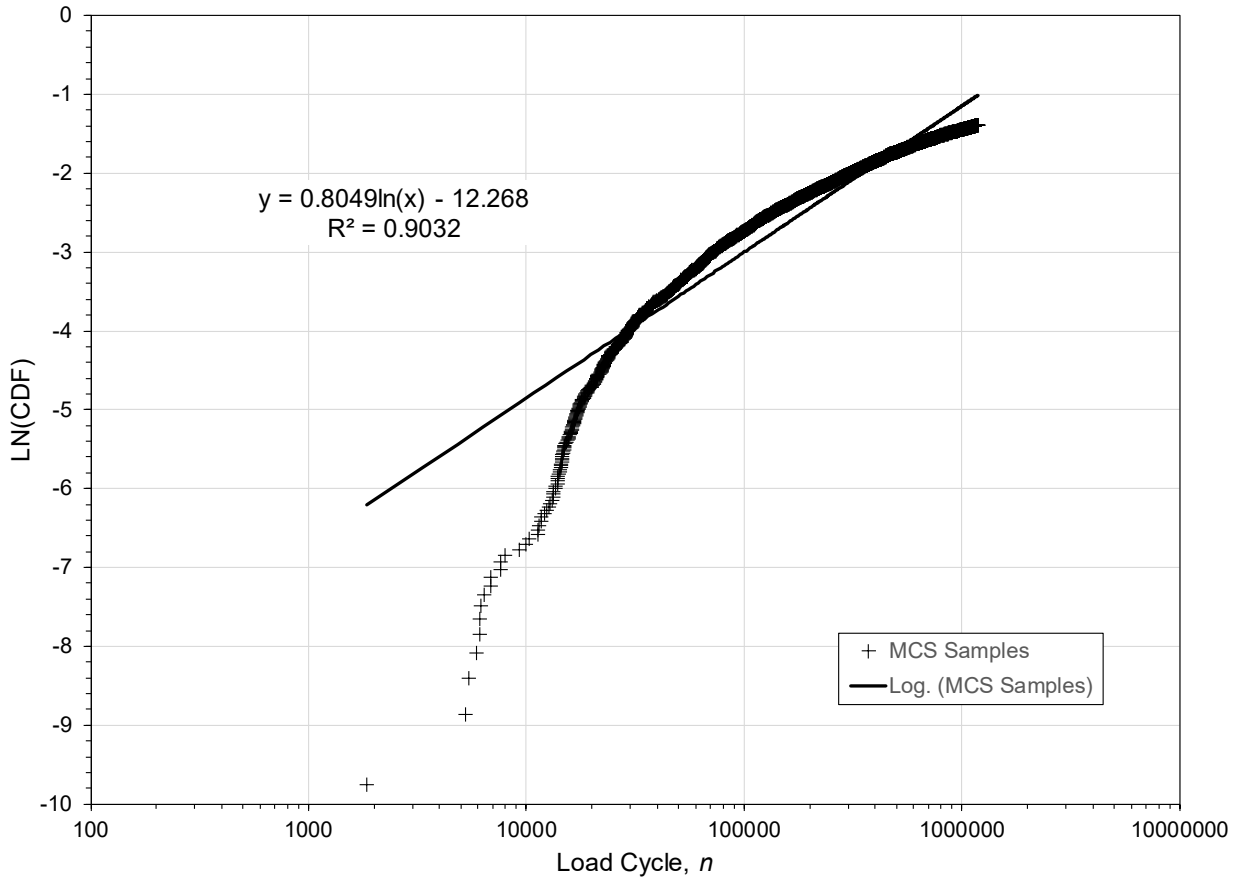

Figure 22. Plot of LN(CDF) vs. Load Cycle, *n*

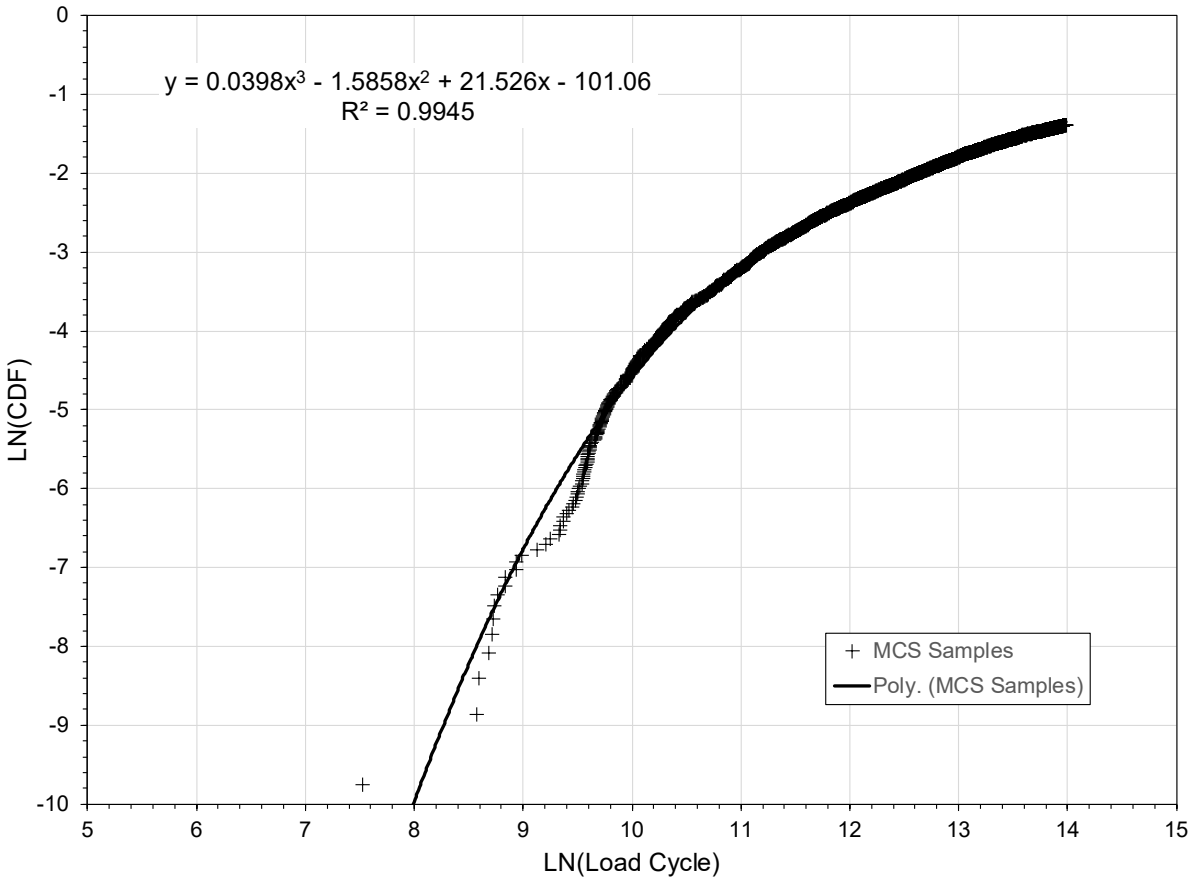

Figure 23. Plot of LN(CDF) vs. LN(*n*)

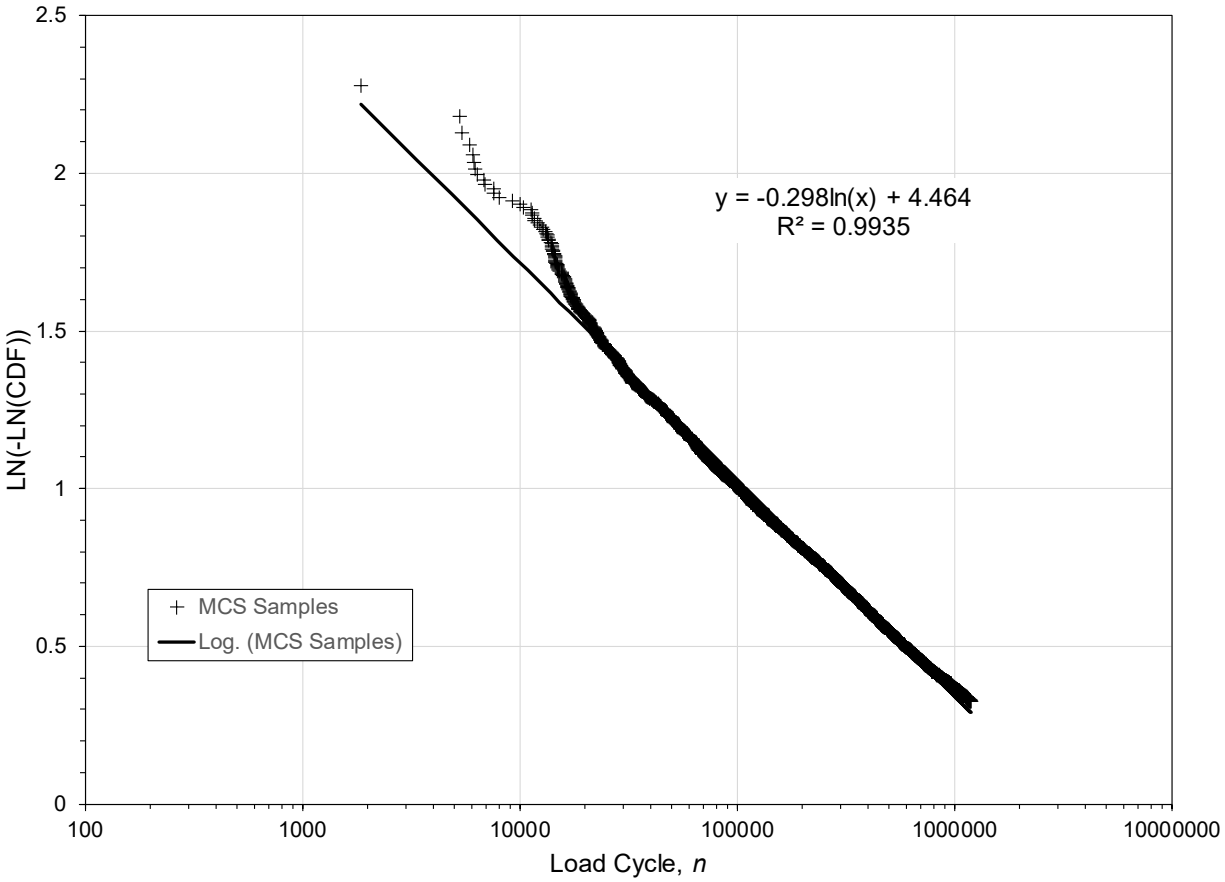

Figure 24. Plot of LN(-LN(CDF)) vs. Load Cycle, *n*

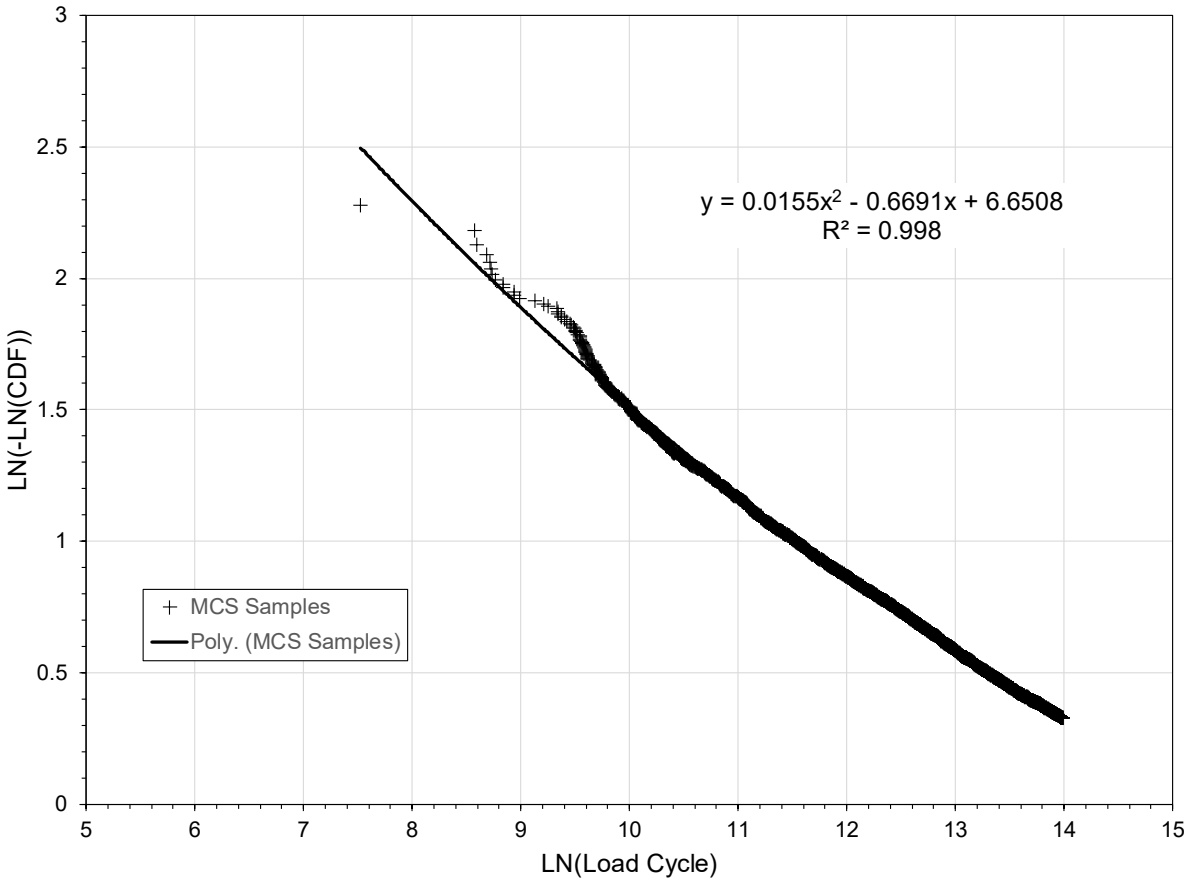

Figure 25. Plot of LN(-LN(CDF)) vs. LN(*n*)

3.2.5.2 PDF Determination

The HRF, $h_T(n)$, is defined as

$$h_T(n) = \frac{f_T(n)}{(1 - F_T(n))} \tag{62}$$

The PDF, $f_T(n)$, is found by differentiating $F_T(n)$, equation (60). This can be done either mathematically or numerically. Numerical differentiation is easier because of the complexity of the function, and is less prone to error. Using the two-point centered difference method [8], numerical differentiation is accomplished with the equation

$$f_T(n) = \frac{exp\left\{-exp\left[\left(\frac{LN(n+1)-21.58}{8.03}\right)^2 - 0.57\right]\right\} - exp\left\{-exp\left[\left(\frac{LN(n-1)-21.58}{8.03}\right)^2 - 0.57\right]\right\}}{2} \tag{62}$$

The PDF was numerically calculated at 500 cycle increments from 500 to 200,000 cycles (CDF values from 2.8 x 10^{-10} to 0.11). The results of the calculations for 500 to 11,000 cycles are shown in Table 10. A plot of LN(-LN($f_T(n)$)) vs. LN(n) with a cubic polynomial trendline fit in Figure 26 yields the PDF for the short life tail of

$$f_T(n) = exp\left\{-exp\left[\begin{matrix}-0.0036LN(n)^3 + 0.133LN(n)^2 \\ -1.606LN(n) + 8.923\end{matrix}\right]\right\} \tag{63}$$

Table 10. Calculation of PDF

Load Cycle, *n*	PDF
500	5.7967E-12
1000	8.70065E-10
1500	6.66399E-09
2000	2.0813E-08
2500	4.34754E-08
3000	7.30022E-08
3500	1.07324E-07
4000	1.44573E-07
4500	1.83259E-07
5000	2.2227E-07
5500	2.60812E-07
6000	2.98339E-07
6500	3.34488E-07
7000	3.69035E-07
7500	4.01852E-07
8000	4.32882E-07
8500	4.62117E-07
9000	4.89584E-07
9500	5.15331E-07
10000	5.39421E-07
10500	5.61927E-07
11000	5.82927E-07

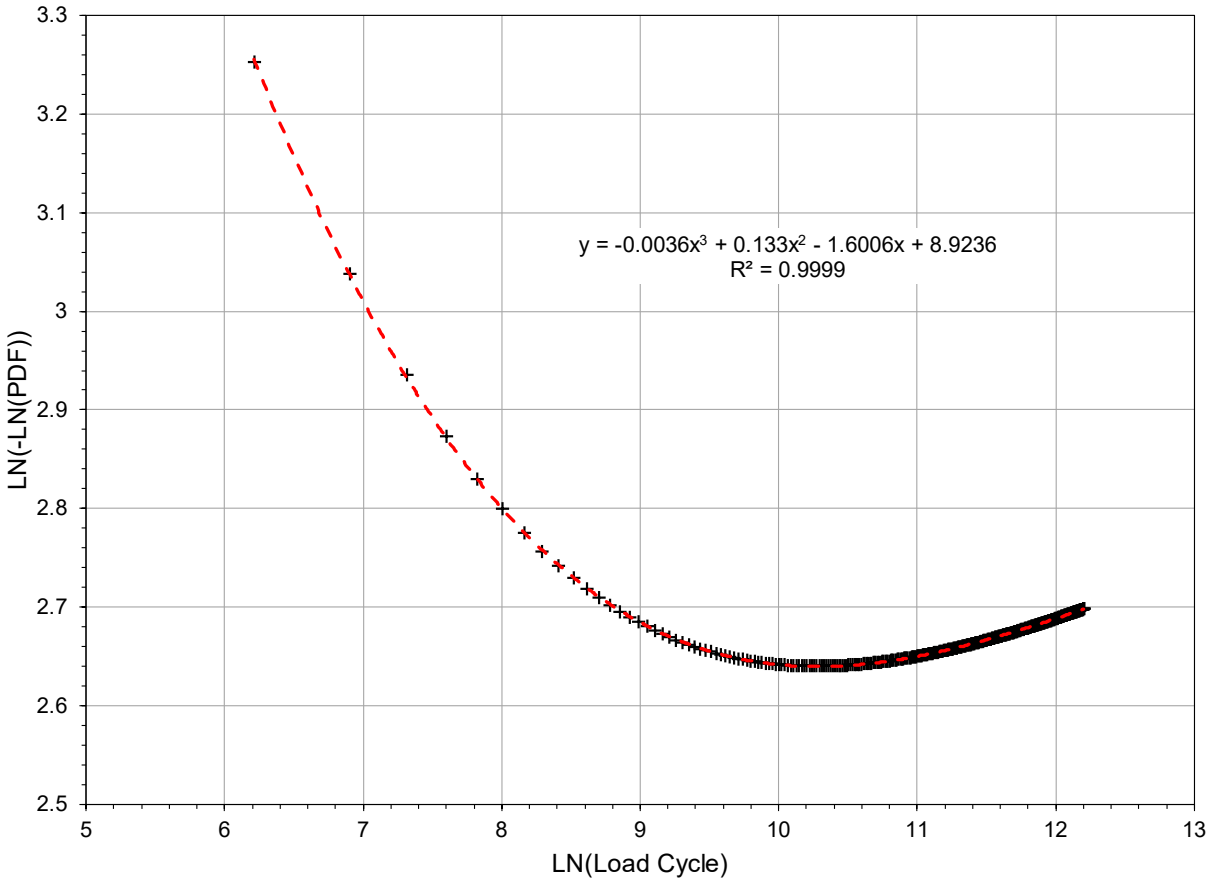

Figure 26. LN(-LN($f_T(n)$)) vs. LN(n) Plot

3.2.5.3 Hazard Rate Calculation

The HRF is found using the PDF in equation (63) and the CDF in equation (60) in the HRF equation of equation (61). The HRF was calculated at 500 cycles increments from 500 to 200,000 cycles as illustrated in Table 11 for 500 to 11,000 cycles. The plot of LN(-LN($h_T(n)$)) versus LN(n) in Figure 27 shows a HRF of 10^{-7} (the dashed red line) is reached shortly after LN(N) equals 8 (n equals 2980 cycles). Table 11 shows that the HRF equals 10^{-7} shortly before 3500 cycles. Subsequent fitting of a cubic polynomial to the points in Figure 27 yields a HR equation of

$$h_T(n) = exp\left\{-exp\left[\frac{(LN(n)-21.6573)((LN(n))^2-15.295*LN(n)+112.0194)}{-265.8443}\right]\right\} \quad (64)$$

Table 11. Hazard Rate Calculation

Load Cycle, *n*	PDF	CDF	HRF
500	5.7967E-12	2.76298E-10	5.7967E-12
1000	8.70065E-10	1.19971E-07	8.70065E-10
1500	6.66399E-09	1.7004E-06	6.664E-09
2000	2.0813E-08	8.19719E-06	2.08131E-08
2500	4.34754E-08	2.39418E-05	4.34764E-08
3000	7.30022E-08	5.28184E-05	7.3006E-08
3500	1.07324E-07	9.77418E-05	1.07335E-07
4000	1.44573E-07	0.000160628	1.44596E-07
4500	1.83259E-07	0.000242552	1.83303E-07
5000	2.2227E-07	0.000343939	2.22346E-07
5500	2.60812E-07	0.000464742	2.60934E-07
6000	2.98339E-07	0.000604581	2.98519E-07
6500	3.34488E-07	0.000762851	3.34744E-07
7000	3.69035E-07	0.000938802	3.69382E-07
7500	4.01852E-07	0.001131597	4.02307E-07
8000	4.32882E-07	0.001340356	4.33463E-07
8500	4.62117E-07	0.00156418	4.62841E-07
9000	4.89584E-07	0.001802178	4.90468E-07
9500	5.15331E-07	0.002053477	5.16391E-07
10000	5.39421E-07	0.002317232	5.40674E-07
10500	5.61927E-07	0.002592634	5.63388E-07
11000	5.82927E-07	0.002878908	5.8461E-07

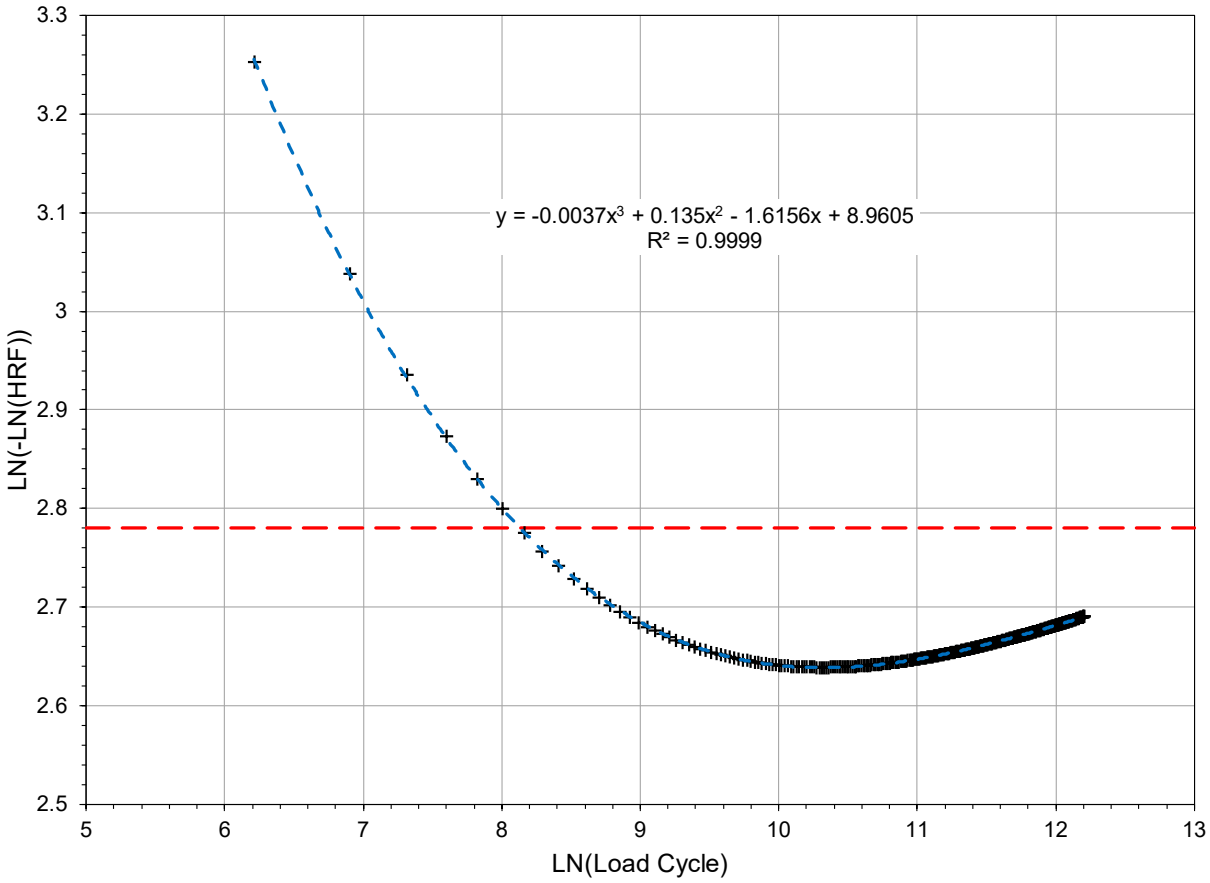

Figure 27. LN[-LN($h_T(n)$)] vs. LN(n) Plot

A HRF of 10^{-7} occurs at 3,400 cycles which corresponds to a cumulative POF of 8.74 x 10^{-5}. Remember this problem is considering only the crack growth during a single load cycle. Considering SFPOF where there is a number of load cycles in each flight, an SFPOF of 10^{-7} may be associated with a higher cumulative POF.

3.2.6 Sensitivity Study

As in Section 3.1.4, the methods of Robust Design and ANOVA were employed to perform the sensitivity analysis [10]. Three factor levels were used for each of the shape and scale factors for the fracture toughness and EIDS distributions to allow quadratic behavior to be discovered. The values for the shape factor of the fracture toughness distribution used previously were used here. These are 14.5, 12.49, and 10.5, and the scale factor values are 93.9, 88.89, and 83.9. The values for the shape factor of the EIDS distribution are 0.424, 0.374, and 0.324, and the scale factor values are 0.00064, 0.00054, and 0.00044. The resulting range of distributions considered are compared to the 95% confidence bounds for the EIDS distribution in Figure 28. Note that the middle value in each set of parameters is the value used in the analysis above.

Eighty-one additional analyses (3·3·3·3 = 81) would be required to investigate every variable combination. Using an $L_9(3^4)$ orthogonal array as shown in Table 12 reduces the number of analyses to nine. Each of the entries in the table represents one of the values selected above for the sensitivity study. For example, variable A can be the shape factor for the fracture toughness distribution and A1, A2, and A3 are one of the three values chosen above. Each value of a

parameter only occurs three times in the array. The array is orthogonal because the values B1, B2, and B3 occur the same number of times for each A value, once. A similar relation holds for the C and D values.

Selecting the shape and scale factor values used in the baseline analysis as the first value for each variable allows the baseline analysis to be used for Trial 1. Only eight more analyses are then needed. The shape parameter and scale parameter combinations that were used in the sensitivity analysis are given in Table 13. The random numbers generated for the baseline analysis was re-used for the sensitivity study. The parameters of the EIDS and fracture toughness distributions were changed which changed the EIDS and fracture toughness for each MCS sample. The cycles to failure for each sample were determined from the master crack growth curve in Figure 29.

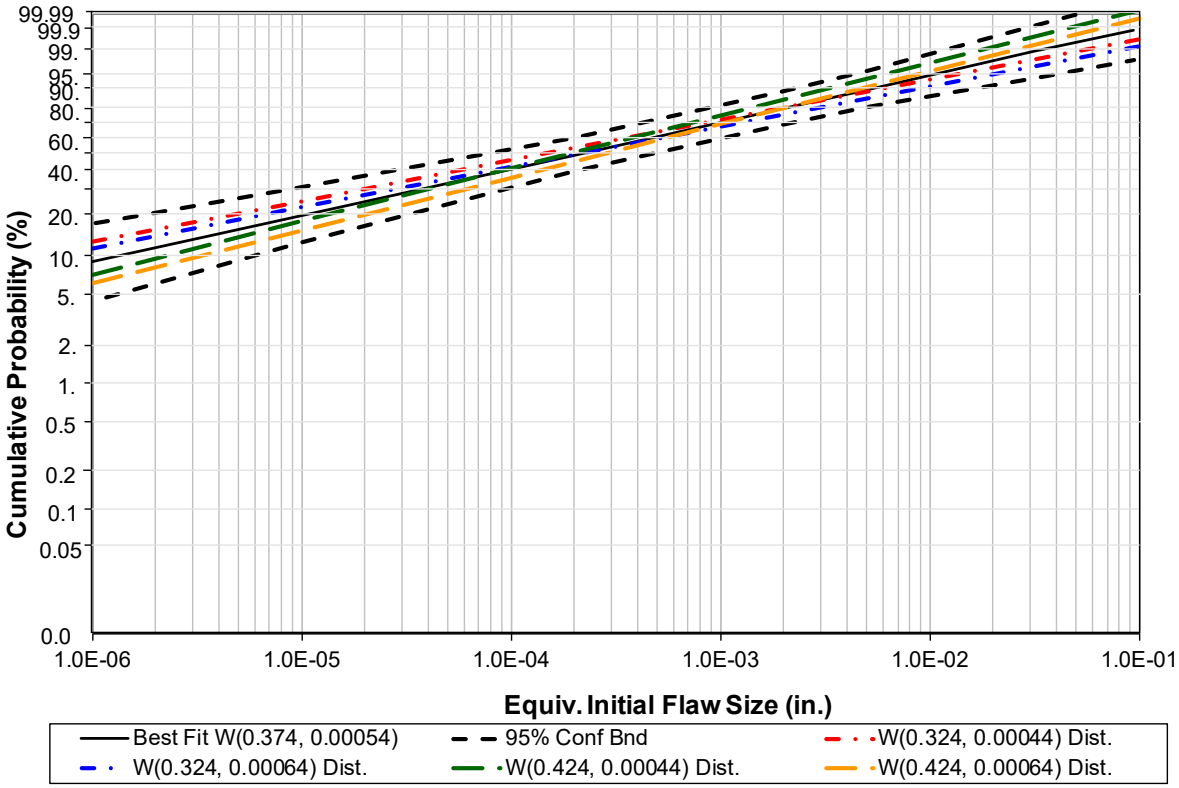

Figure 28. EIDS Distributions Range for Sensitivity Study

Table 12. $L_9(3^4)$ Orthogonal Array Layout

	Variable Name			
Trial No.	A	B	C	D
1	A1	B1	C1	D1
2	A1	B2	C2	D2
3	A1	B3	C3	D3
4	A2	B1	C2	D3
5	A2	B2	C3	D1
6	A2	B3	C1	D2
7	A3	B1	C3	D2
8	A3	B2	C1	D3
9	A3	B3	C2	D1

Table 13. Shape and Scale Factor Combinations for Sensitivity ANOVA

	Variable			
Trial No.	Shape(K_C)	Scale(K_C)	Shape(EIDS)	Scale(EIDS)
1	12.49	88.89	0.374	0.00054
2	12.49	83.9	0.324	0.00044
3	12.49	93.9	0.424	0.00064
4	10.5	88.89	0.324	0.00064
5	10.5	83.9	0.424	0.00054
6	10.5	93.9	0.374	0.00044
7	14.5	88.89	0.424	0.00044
8	14.5	83.9	0.374	0.00064
9	14.5	93.9	0.324	0.00054

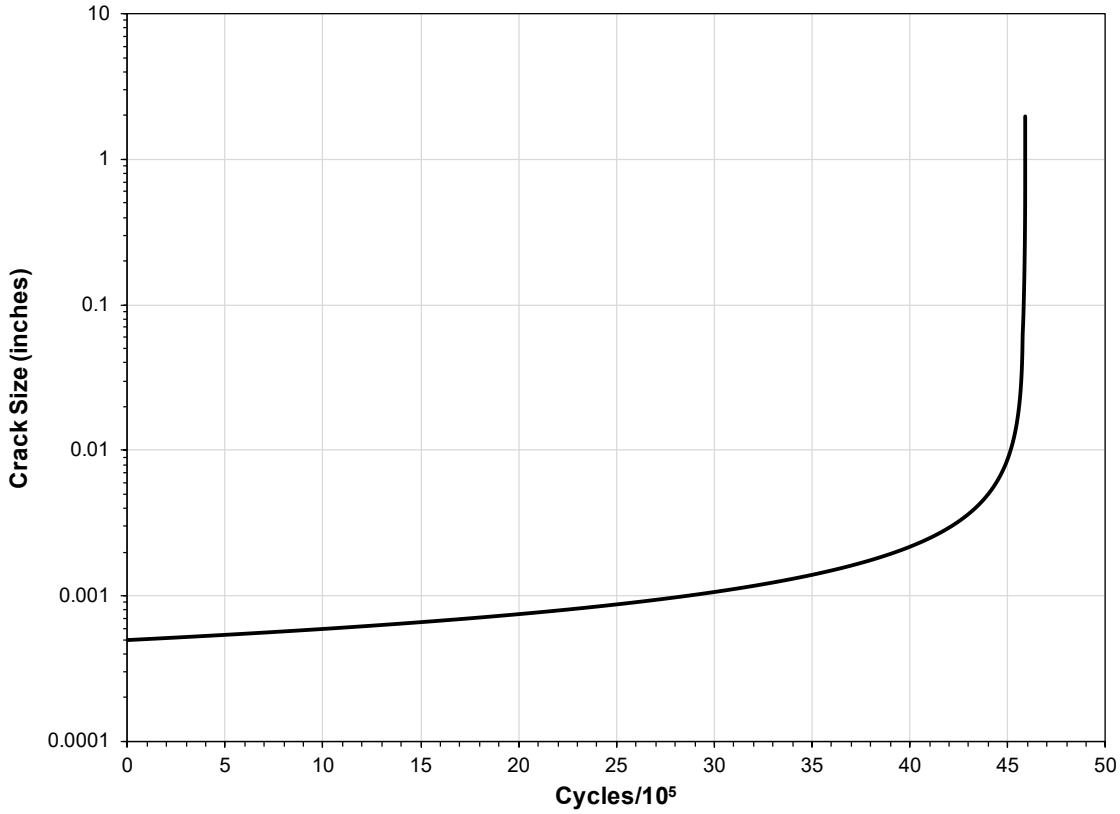

Figure 29. Master Crack Growth Curve for Sensitivity Study

The CDF for each trial was determined as for the baseline case. Then the PDF and HRF were determined. The cycles to a HRF value of 10^{-7} are listed in Table 14 for each trial.

Table 14. Results from Sensitivity Trials

	Variable				Cycles at HR = 10^{-7}
Trial No.	Shape(K_C)	Scale(K_C)	Shape(EIDS)	Scale(EIDS)	
1	12.49	88.89	0.374	0.00054	2604
2	12.49	83.9	0.324	0.00044	994
3	12.49	93.9	0.424	0.00064	5835
4	10.5	88.89	0.324	0.00064	362
5	10.5	83.9	0.424	0.00054	6921
6	10.5	93.9	0.374	0.00044	4117
7	14.5	88.89	0.424	0.00044	8482
8	14.5	83.9	0.374	0.00064	2878
9	14.5	93.9	0.324	0.00054	604

The effect of each variable is determined by averaging the results (the cycles to an HR of 10^{-7}) for all trials with the same parameter value. It is easier to compare results by first taking the common logarithm of the cycles to a HR of 10^{-7}. As an example, for the fracture toughness shape

parameter value of 12.49, compute the average of $\log_{10}(2604)$, $\log_{10}(994)$, and $\log_{10}(5835)$. The averages of the logarithm of the results for each parameter value are listed in Table 15.

Table 15. Average of Common Logarithm of Cycles to HR of 10^{-7}

Shape (K_C)	Avg. Log_{10}
10.5	3.34
12.49	3.39
14.5	3.39

Shape (EIDS)	Avg. Log_{10}
0.324	2.78
0.374	3.50
0.424	3.84

Scale (K_C)	Avg. Log_{10}
83.9	3.43
88.89	3.30
93.9	3.39

Scale (EIDS)	Avg. Log_{10}
0.00044	3.51
0.00054	3.35
0.00064	3.26

The affect of each parameter is most easily seen in the graphs in Figure 30 to Figure 33. The vertical scale on all the graphs is the same. It is easy to see that the shape parameter of the EIDS distribution has the most effect on the cycles to a HRF value of 10^{-7}. The scale parameter of the EIDS distribution has the second highest effect indicating that the EIDS distribution has the most effect on the cycles to a HRF value of 10^{-7}. More data regarding the EIDS distribution will have the most effect on the risk analysis.

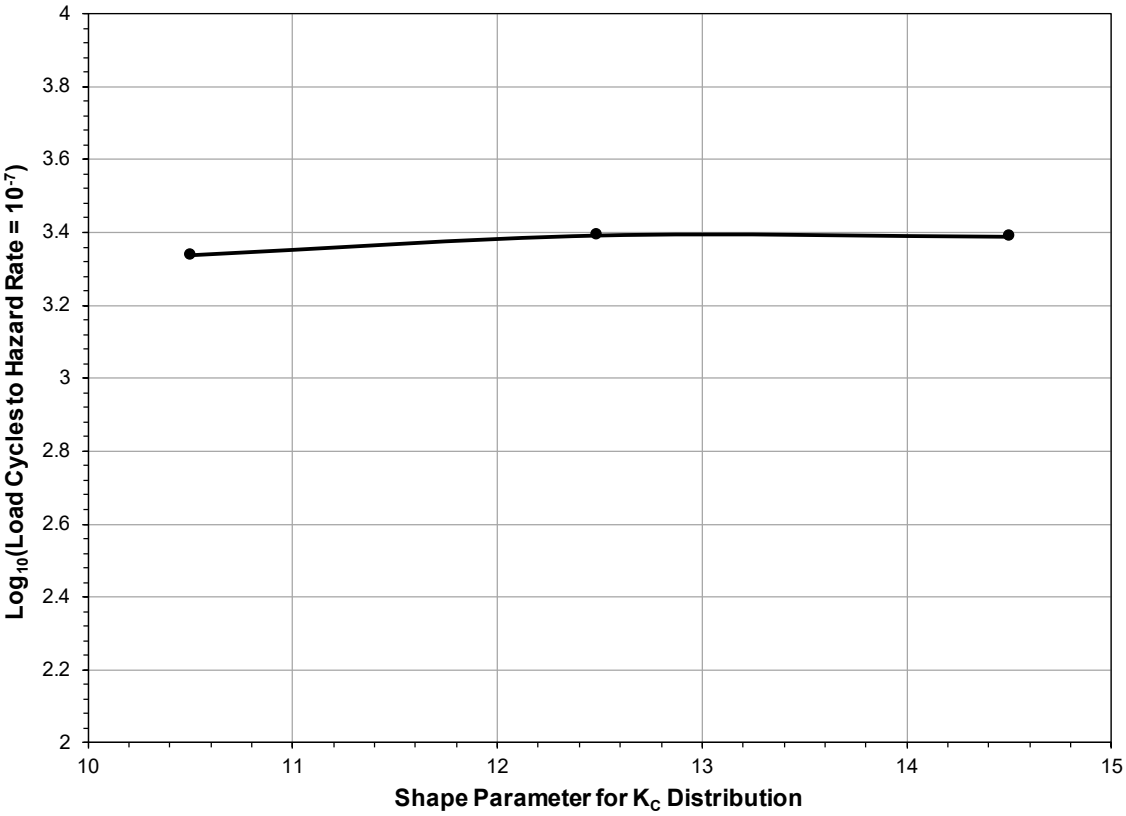

Figure 30. Sensitivity to the Shape Parameter of the K_C Distribution

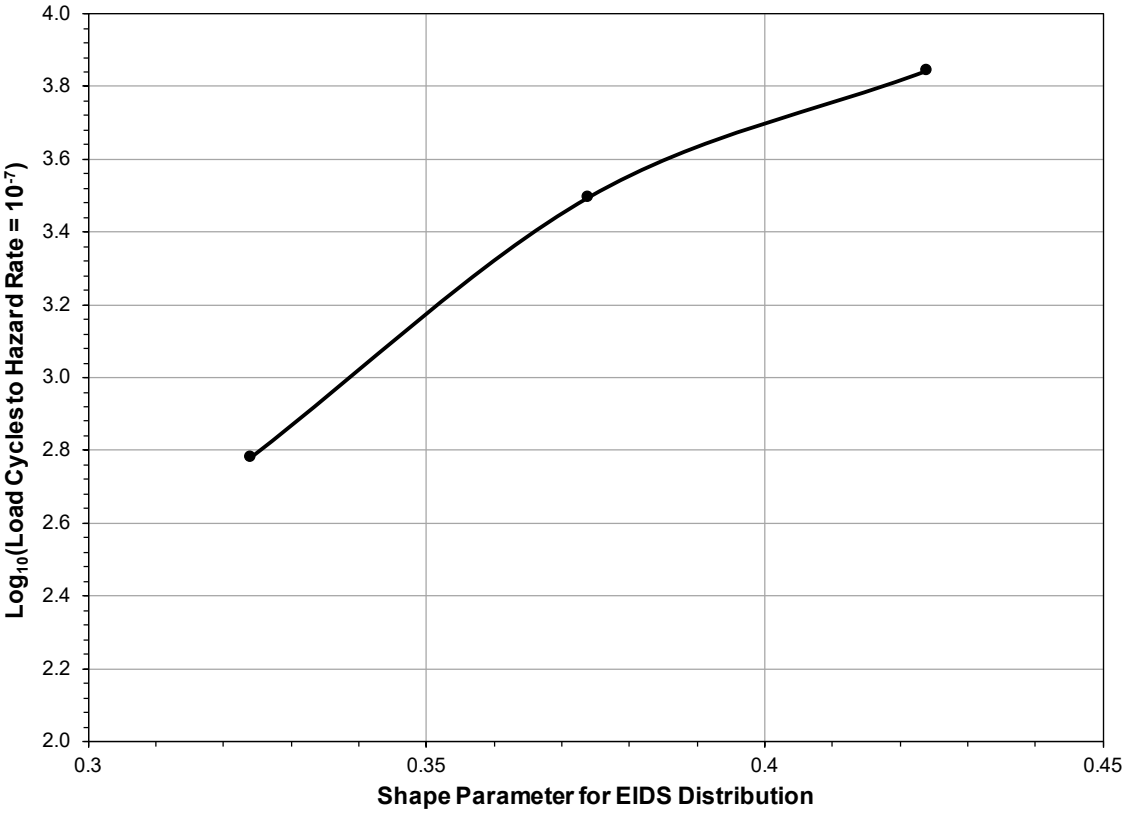

Figure 31. Sensitivity to the Shape Parameter of the EIDS Distribution

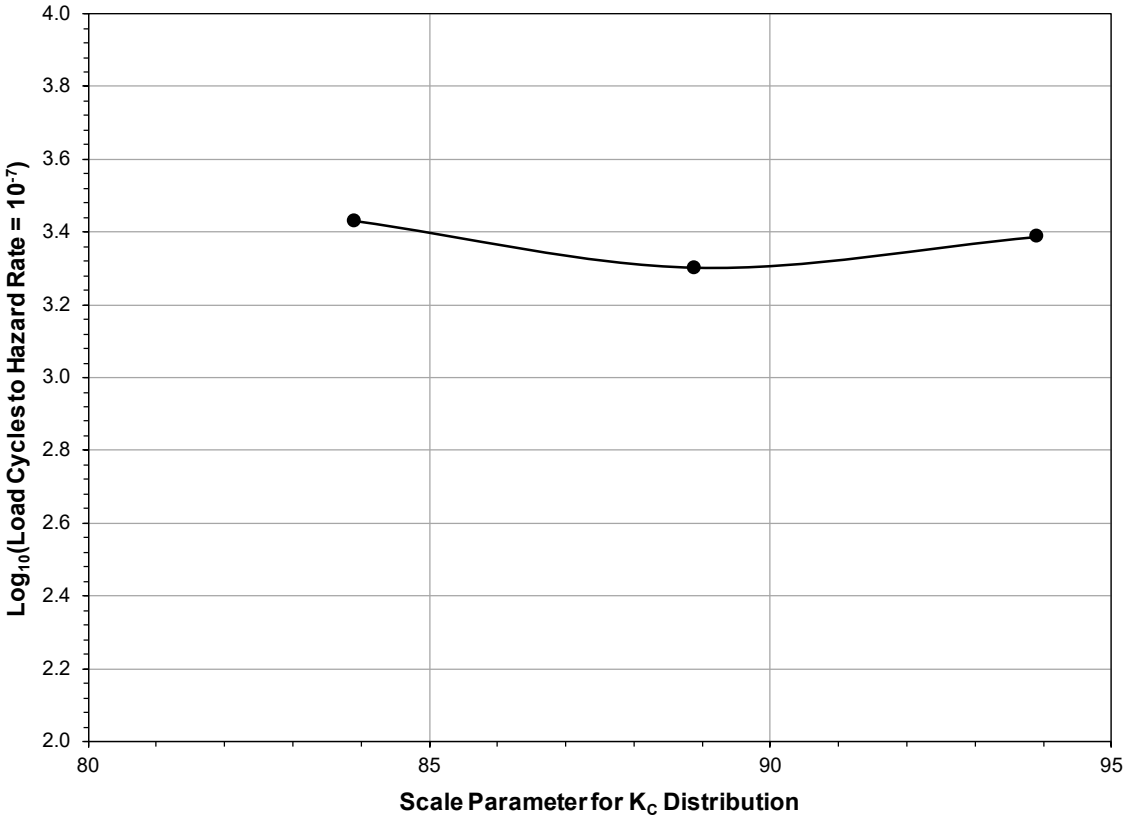

Figure 32. Sensitivity to the Scale Parameter of the K_C Distribution

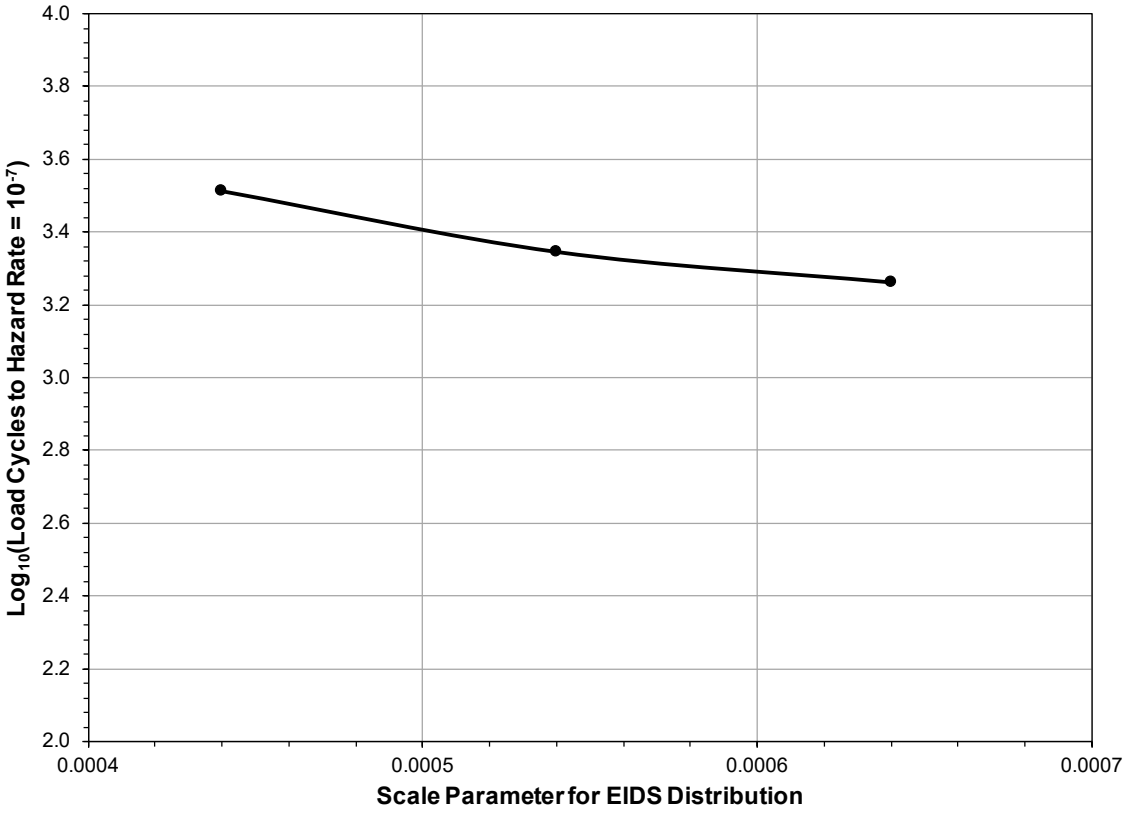

Figure 33. Sensitivity to the Scale Parameter of the EIDS Distribution

3.3 Hole Specimen under Spectrum Loading

This example is a panel with a central hole under spectrum loading. The spectrum used for this example is the standard fighter wing bending moment spectrum, FALSTAFF [17, 18].

This example contains three random variables: fracture toughness, K_c, the EIDS, a_o, and the maximum stress during a flight, σ_{max}. Fracture toughness determines when fracture occurs. The EIDS determines how quickly fracture will occur. The maximum stress during a flight determines whether a crack of a given size will fail during that flight. First, the reliability of the specimen as a function of crack size and as a function of load cycles is determined. Then the POF function is found. Finally, the hazard rate function is calculated. A flowchart for the MCS procedure is provided in Figure 34.

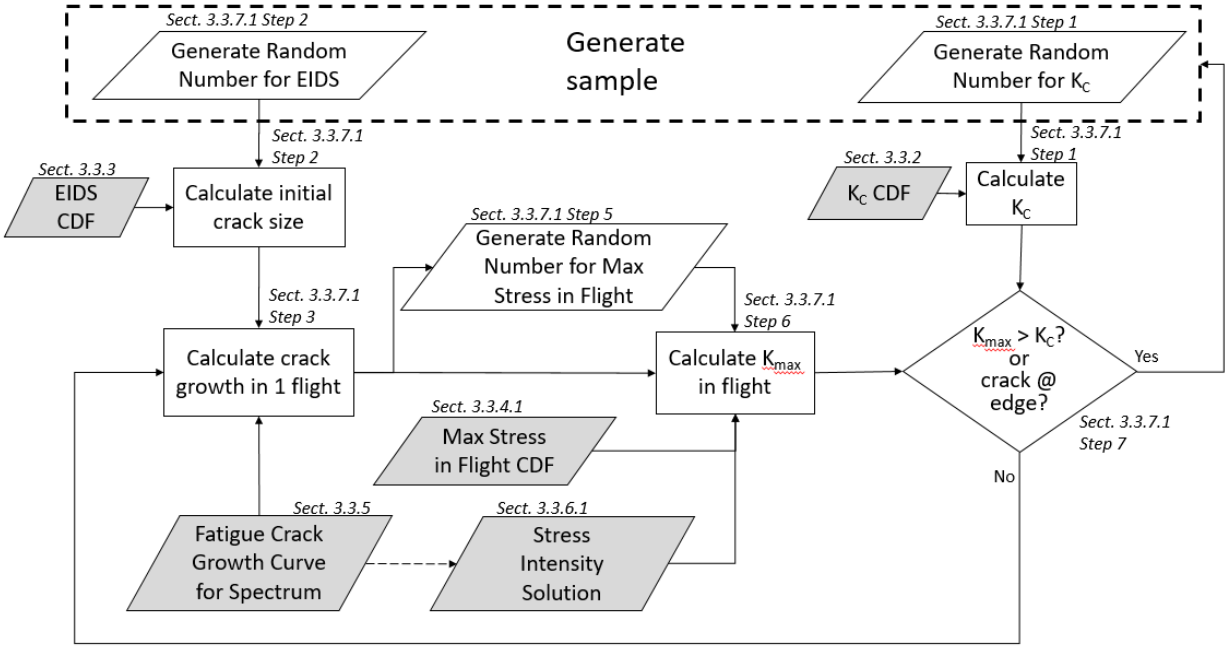

Figure 34. Flowchart of MCS for Hole Specimen under Spectrum Loading

3.3.1 Test Conditions

The specimen geometry (Figure 35), the material, and loading orientation are the same as for the previous example discussed in Section 3.2. The test is conducted at room temperature in laboratory air.

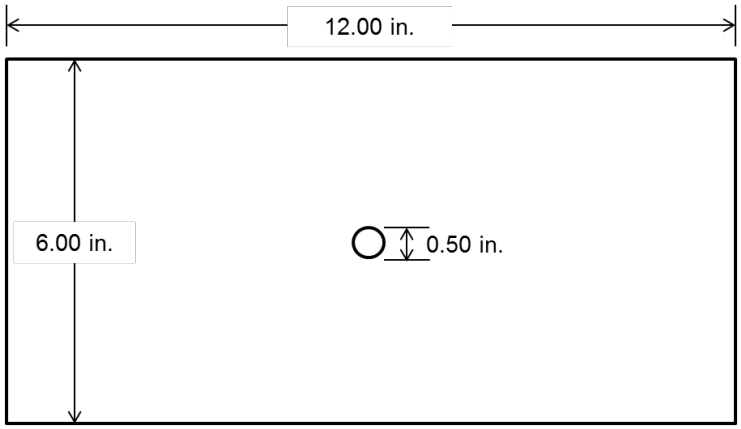

Figure 35. Hole Specimen Geometry

3.3.2 Material Properties

The fracture toughness distribution is the same as that discussed in Section 3.2.2. The distributions used to model the variability in the fracture toughness and yield strength are summarized here. The full development of the distributions can be found in Section 3.2.2. The fracture toughness variability for 0.063-inch-thick 7475-T61 aluminum sheet in the L-T orientation is modeled with a two-parameter Weibull distribution with a shape parameter of 12.49 and a scale parameter of 88.89 ksi√in as in the previous two examples (Sections 3.1.2 and 3.2.2).

Fatigue crack growth analysis was performed using AFGROW. The NASGRO model for the fatigue crack growth curve for aluminum 7475-T61 clad plate in the L-T orientation contained in AFGROW was used.

3.3.3 Equivalent Initial Damage Size

The equivalent initial damage size (EIDS) developed in Section 3.2.3 is used in this example. The EIDS distribution is a Weibull distribution with a shape parameter of 0.374 and a scale parameter of 0.00054 inch as in the previous example (Section 3.2.3).

3.3.4 Loading

This example considers a crack growing under variable amplitude loading, aka spectrum loading. The spectrum used is the Fighter Aircraft Loading STAndard For Fatigue (FALSTAFF) which is representative of fighter aircraft wing bending due primarily to maneuver loadings [17, 18]. A FALSTAFF spectrum file is widely available, including in the basic AFGROW installation. Figure 36 shows the plot of normalized load exceedances for FALSTAFF.

The FALSTAFF spectrum available with AFGROW contains 17,983 normalized peak-valley pairs representing 200 flights. The average duration of a flight is one hour. The normalized peaks and valleys were multiplied by a reference stress of 16 ksi in this example. This spectrum is used in conjunction with the material fatigue crack growth rate data and the stress intensity solution for the prescribed geometry in a crack growth code to calculate the fatigue crack growth curve for the specimen. The spectrum is also used to determine the probability of the maximum stress at the hole exceeding any specified value during a single flight.

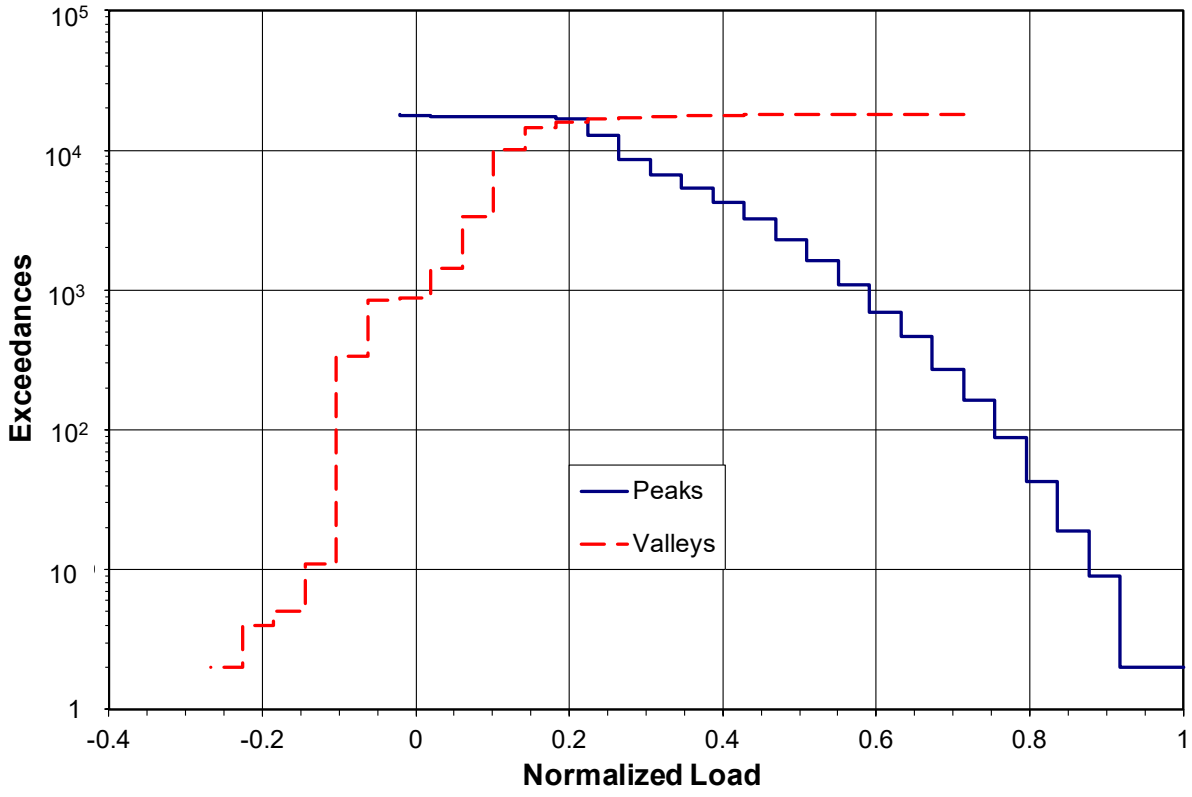

Figure 36. Exceedance Plot for FALSTAFF Spectrum

3.3.4.1 Maximum Stress in a Flight

Fracture during a flight is assumed to be caused by the largest stress that occurs during that flight. The probability that the maximum stress during a flight reaches any specified value must be determined in order to calculate the probability of failure. This is most easily done with a MCS of the peak stresses during a flight assuming that the peak loads occur randomly throughout the life of the aircraft. The average number of load peaks during a single flight is 17,983/200 = 89.92 or 90 peaks. For each flight, 90 values are randomly drawn from the probability distribution of normalized load peaks. After this has been done for a sufficient number of individual flights, the maximum stress in each flight is determined. The probability distribution of these maximum stresses is then determined. Because the mean and standard deviation, or their equivalent depending upon the type of distribution, are all that is needed, and not the low probability tails of the distribution, less than a couple thousand flights need to be sampled. This is easily done in Microsoft Excel®.

The probability distribution for the normalized load peaks is 1 minus the exceedance distribution. The probability distribution for the normalized load peaks in the FALSTAFF spectrum is presented in Table 16 and Figure 37.

Table 16. Normalized Load Peaks Statistics for FALSTAFF spectrum

Normalized Peak	Occurrences	Exceedances	Exceedance Distribution	Probability Distribution
-0.0214	0	17983	1	0
-0.0215	155	17828	0.99138	0.00862
0.0193	445	17383	0.96664	0.03336
0.1419	43	17340	0.96424	0.03576
0.1828	493	16847	0.93683	0.06317
0.2236	4058	12789	0.71117	0.28883
0.2645	4145	8644	0.48068	0.51932
0.3054	1999	6645	0.36952	0.63048
0.3462	1282	5363	0.29823	0.70177
0.3871	1151	4212	0.23422	0.76578
0.4279	987	3225	0.17934	0.82066
0.4688	954	2271	0.12629	0.87371
0.5097	640	1631	0.09070	0.90930
0.5505	533	1098	0.06106	0.93894
0.5914	404	694	0.03859	0.96141
0.6322	233	461	0.02564	0.97436
0.6731	193	268	0.01490	0.98510
0.714	104	164	0.00912	0.99088
0.7548	76	88	0.00489	0.99511
0.7957	45	43	0.00239	0.99761
0.8366	24	19	0.00106	0.99894
0.8774	10	9	0.00050	0.99950
0.9183	7	2	0.00011	0.99989
1	2	0	0	1

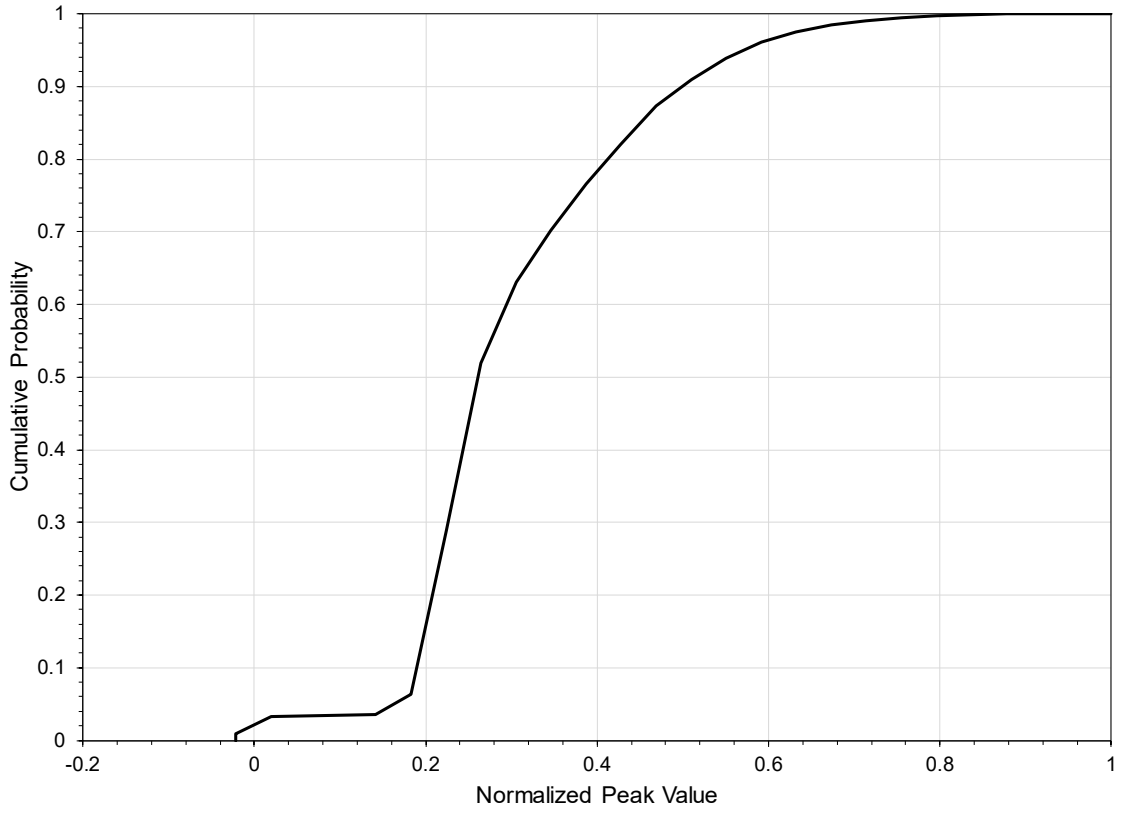

Figure 37. Normalized Load Peaks in FALSTAFF Spectrum Cumulative Probability

The probability distribution for the maximum stress that occurs during a flight is found for 1,000 flights with the following steps.

Step 1. Establish the relationship between the cumulative probability value and the value of the normalized peak in preparation for performing a MCS. The midpoint between the probabilities of occurrence for adjacent normalized peaks in Table 16 was set as the dividing point as shown in Table 17. Thus, if a random number of 0.5 is drawn in the MCS, the value assigned to that normalized peak in the flight would be 0.2645.

Table 17. Mapping of Cumulative Probability to Normalized Peak

Maximum Probability	Normalized Peak
0.00431	-0.0214
0.02099	-0.0215
0.03456	0.0193
0.04946	0.1419
0.17600	0.1828
0.40408	0.2236
0.57490	0.2645
0.66613	0.3054
0.73378	0.3462
0.79322	0.3871
0.84719	0.4279
0.89151	0.4688
0.92412	0.5097
0.95018	0.5505
0.96789	0.5914
0.97973	0.6322
0.98799	0.6731
0.99299	0.714
0.99636	0.7548
0.99828	0.7957
0.99922	0.8366
0.99969	0.8774
0.99994	0.9183
	1

Step 2. Perform the MCS for a single flight by using a random number generator to generate 90 random numbers between 0 and 1. Convert these random numbers to normalized peak using the mapping in Table 17.

A simple routine for performing this MCS is presented in Appendix B.6. The routine is written as a VBA macro inside a Microsoft Excel® workbook.

Step 3. Determine the maximum normalized peak during the flight and record that value.

Step 4. Repeat Steps 2 and 3 another 999 times.

Step 5. Rank order the 1,000 maximum normalized peaks in each flight. Calculate the mean rank of each point. This table can be used as the probability distribution for the maximum stress that occurs during a flight, or a parametric distribution such as a normal distribution, etc., can be determined.

The distribution in Step 5 is a distribution of the maximum stress that occurs in each flight which is a collection of random samples from the distribution of peaks in the FALSTAFF spectrum. The Gumbel distribution [19] is known to fit the distribution of maximum values of a number of

samples from another distribution. The CDF for the Gumbel distribution is described by equation (20), which can be rearranged as

$$MaxStress = \alpha + \beta\{-ln[-ln(rank)]\}. \quad (65)$$

Thus, the maximum stress plotted versus {-*ln*[-*ln*(*rank*)]} will produce a straight line if the maximum stress fits a Gumbel distribution. The rank ordered maximum stresses from the MCS are plotted on a Gumbel probability graph in Figure 38. A least squares line fit to the data is also shown. The correlation coefficient, R^2, of the data to this line is 0.939. The slope of line, β, is 0.060 and the value of the location parameter, α, is 0.699.

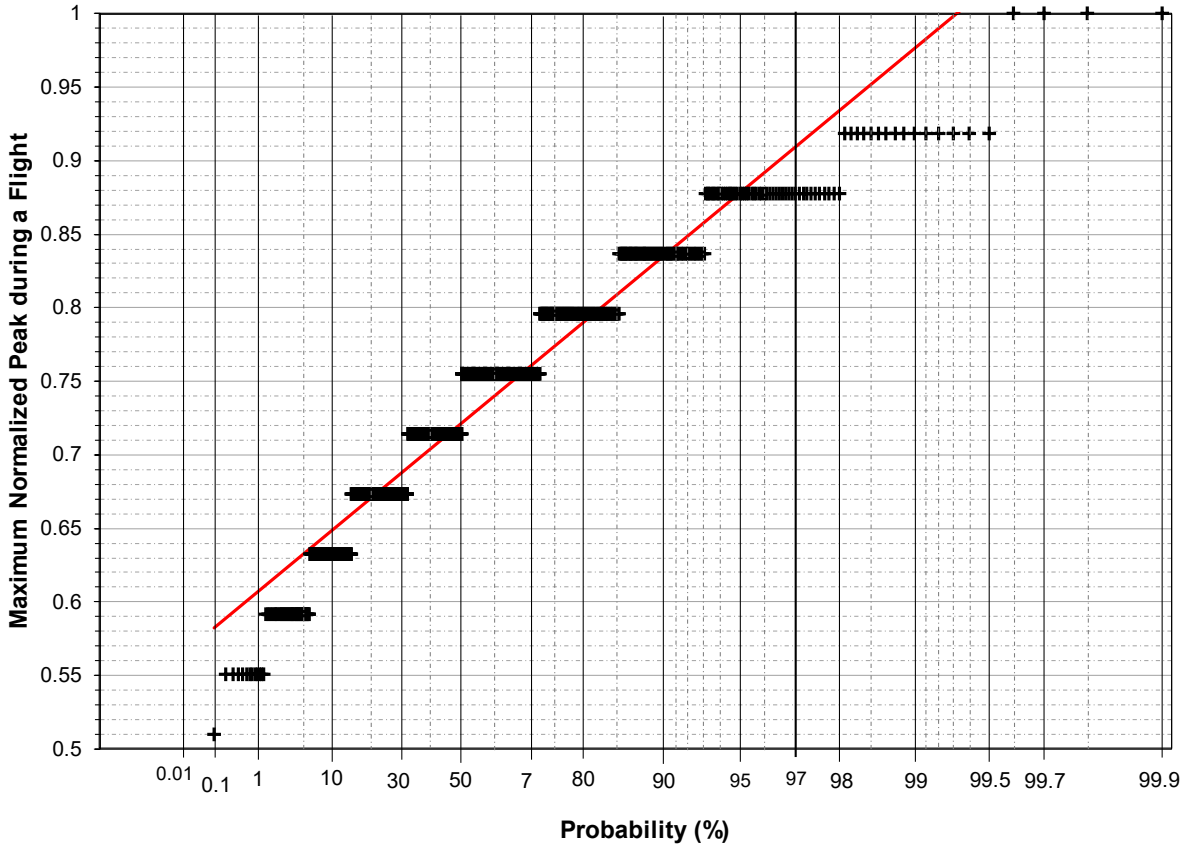

Figure 38. Gumbel Probability Plot of Maximum Stress in 1,000 Random Flights from FALSTAFF

While this Gumbel distribution does not model the high and low ends of the data accurately, it is sufficient for this problem considering all the assumptions and uncertainties involved in the problem. This Gumbel distribution predicts that flights with the highest maximum stresses (0.9 to 1.0) will occur more frequently than they did in this 1,000 flight sample, and the flights with the lowest maximum stresses will occur less often. This is conservative since higher maximum stresses will cause fracture at smaller crack sizes.

3.3.5 Crack Growth

A full range master crack growth curve is developed prior to performing the reliability calculation. This is more efficient than calculating crack growth for each sample in the MCS when dealing with spectrum loading. The master crack growth curve is used as a lookup table to calculate the life for each MC sample. It is important that the master crack growth curve start at

the smallest crack size possible and extend all the way to failure in order to cover all possible samples in the MCS.

If the fatigue crack growth analysis cannot be made to grow from sufficiently small cracks, the crack growth curve must be extended down to smaller crack sizes. Typically, the extrapolation is made with an exponential curve. The exponential extrapolation should be made to match the slope of the crack growth curve at the lowest value of the crack growth analysis in order to avoid discontinuities that could disrupt subsequent calculations.

The assumed cracking scenario is a corner crack from a centered hole in a plate. The classical model for this scenario in AFGROW was used to calculate the stress intensities. Since this problem does not involve a fastened joint, the through stress fraction was 1.0 and the bearing and bending fractions were 0. The analysis here started with a semi-circular crack of radius 0.0015 inch. The aspect ratio of the crack was constrained to be 1. Only the surface crack dimension, *c*, is used in the reliability calculation since that is what will fail the part.

The crack growth rate data for aluminum 7475-T761 plate in the L-T orientation from the NASGRO database contained in AFGROW was used. The loading was the FALSTAFF spectrum with a stress multiplication factor of 16 ksi. The resulting master crack growth curve is shown in Figure 39. A sample of the AFGROW output is given in Table 18.

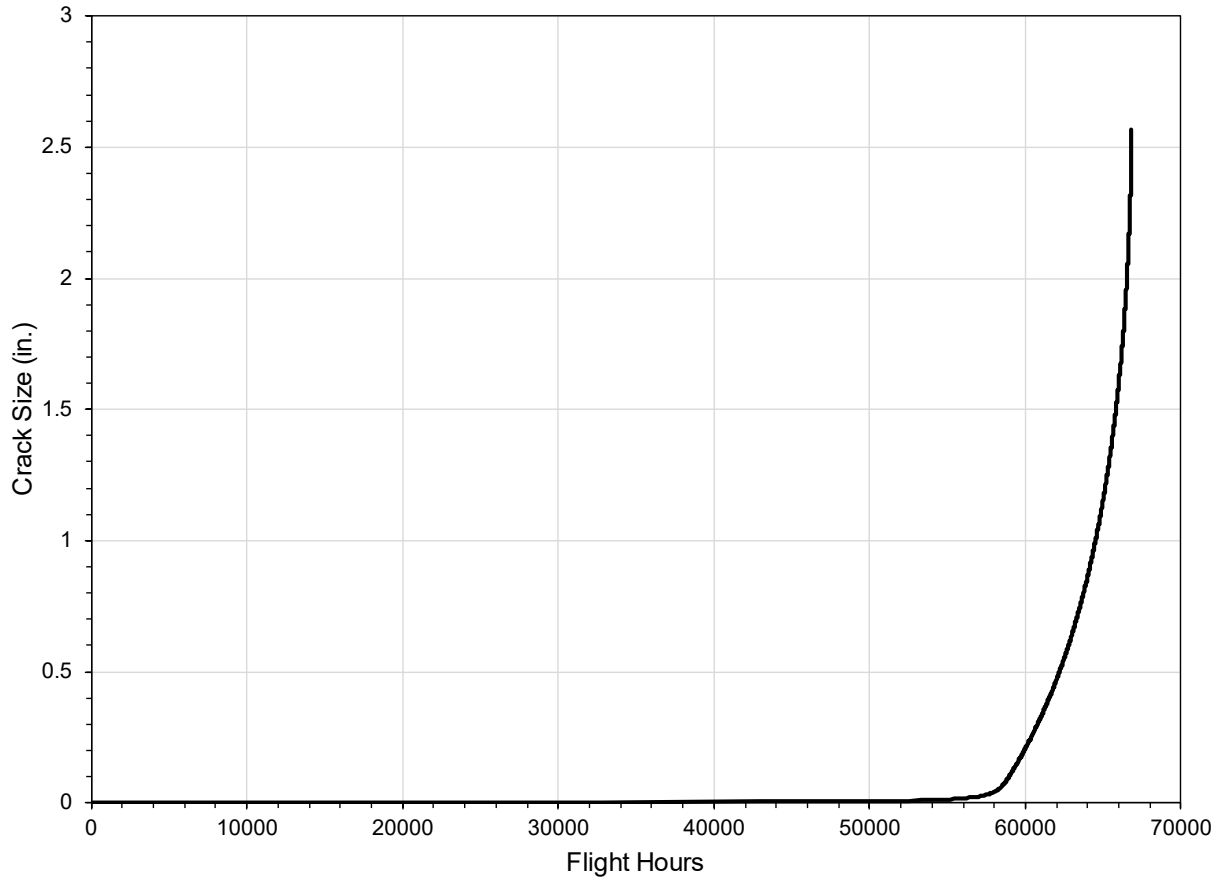

Figure 39. Fatigue Crack Growth Curve

Table 18. Sample of Fatigue Crack Growth Output from AFGROW

Surface Length, *c*	Bore Length, *a*	Beta Surface	Beta Bore	R(k) Surface	R(k) Bore	R(final) Surface	R(final) Bore	DeltaK Surface	DeltaK Bore	d*c* /dN	d*a* /dN	Cycles	Max Stress	R	Sub Spectrum	Pass	Life (FH)
0.003	0.003	2.008862596	2.007243419	-5.352331606	-5.352331606	-0.3	-0.3	6.02E-02	6.02E-02	0.00E+00	0.00E+00	0	0.3088	-5.35	0	1	0
0.0040001	0.0040001	2.007691531	2.012742819	0.261172824	0.261172824	0.261172824	0.261172824	1.03E+00	1.03E+00	0.00E+00	0.00E+00	2945328	6.1936	0.26	160	164	32756.804
0.005	0.005	2.004664332	2.017840438	-3.233160622	-3.233160622	-0.3	-0.3	7.76E-02	7.81E-02	0.00E+00	0.00E+00	3858359	0.3088	-3.23	111	215	42911.183
0.0050003	0.0050003	2.004664332	2.017840438	0.618135078	0.618135078	0.618135078	0.618135078	6.57E-01	6.61E-01	0.00E+00	0.00E+00	3858368	6.8464	0.62	111	215	42911.283
0.0060001	0.0060001	2.000715817	2.021533251	0.464636542	0.464636542	0.464636542	0.464636542	7.19E-01	7.26E-01	0.00E+00	0.00E+00	4256108	4.8864	0.46	130	237	47334.794
0.0060004	0.0060004	2.000715817	2.021533251	-0.036354413	-0.036354413	-0.036354413	-0.036354413	2.60E+00	2.63E+00	0.00E+00	0.00E+00	4256120	9.4624	-0.04	130	237	47334.927
0.0070002	0.0070002	1.996799791	2.024033775	0.472229398	0.472229398	0.472229398	0.472229398	9.68E-01	9.81E-01	0.00E+00	0.00E+00	4480736	6.1936	0.47	36	250	49833.02
0.0070005	0.0070005	1.996799791	2.024033775	0.366571945	0.366571945	0.366571945	0.366571945	1.16E+00	1.18E+00	0.00E+00	0.00E+00	4480753	6.1936	0.37	37	250	49833.209
0.0080002	0.0080002	1.992054649	2.026279019	0.382230624	0.382230624	0.382230624	0.382230624	8.26E-01	8.40E-01	0.00E+00	0.00E+00	4622433	4.232	0.38	10	258	51408.92
0.0080006	0.0080006	1.992054649	2.026279019	0.197118533	0.197118533	0.197118533	0.197118533	1.24E+00	1.26E+00	0.00E+00	0.00E+00	4622436	4.8864	0.2	10	258	51408.953
0.0090003	0.0090003	1.988454232	2.027623973	0.382230624	0.382230624	0.382230624	0.382230624	8.74E-01	8.91E-01	0.00E+00	0.00E+00	4720686	4.232	0.38	104	263	52501.652
0.0090008	0.0090008	1.988454232	2.027623973	0.141596639	0.141596639	0.141596639	0.141596639	3.28E+00	3.34E+00	3.58E-07	3.85E-07	4720794	11.424	0.14	105	263	52502.853
0.0100004	0.0100004	1.984532985	2.028846539	0.409878683	0.409878683	0.409878683	0.409878683	1.15E+00	1.18E+00	0.00E+00	0.00E+00	4791132	5.5392	0.41	92	267	53285.125
0.0100008	0.0100008	1.984532985	2.028846539	0.713718158	0.713718158	0.7	0.7	6.90E-01	7.05E-01	0.00E+00	0.00E+00	4791141	6.8464	0.71	92	267	53285.225
0.0110006	0.0110006	1.980332412	2.029949119	0.382230624	0.382230624	0.382230624	0.382230624	9.63E-01	9.87E-01	0.00E+00	0.00E+00	4845942	4.232	0.38	99	270	53894.701
0.011001	0.011001	1.980332412	2.029949119	0.29202773	0.29202773	0.29202773	0.29202773	1.44E+00	1.48E+00	0.00E+00	0.00E+00	4845957	5.5392	0.29	99	270	53894.867
0.0120006	0.0120006	1.975922078	2.030935838	0.64586944	0.64586944	0.64586944	0.64586944	7.53E-01	7.74E-01	0.00E+00	0.00E+00	4889105	5.5392	0.65	181	272	54374.743
0.0120011	0.0120011	1.975922078	2.030935838	0.227599244	0.227599244	0.227599244	0.227599244	1.25E+00	1.29E+00	0.00E+00	0.00E+00	4889121	4.232	0.23	181	272	54374.921
0.0130007	0.0130007	1.971388242	2.03181726	0.409878683	0.409878683	0.409878683	0.409878683	1.30E+00	1.34E+00	0.00E+00	0.00E+00	4925041	5.5392	0.41	181	274	54774.409
0.0130011	0.0130011	1.971388242	2.03181726	0.331041257	0.331041257	0.331041257	0.331041257	1.30E+00	1.34E+00	0.00E+00	0.00E+00	4925046	4.8864	0.33	181	274	54774.465
0.0140009	0.0140009	1.969110622	2.032222864	0.072967864	0.072967864	0.072967864	0.072967864	1.62E+00	1.67E+00	0.00E+00	0.00E+00	4956650	4.232	0.07	124	276	55125.952
0.0140012	0.0140012	1.969110622	2.032222864	0.382230624	0.382230624	0.382230624	0.382230624	1.08E+00	1.11E+00	0.00E+00	0.00E+00	4956660	4.232	0.38	125	276	55126.064
0.0150009	0.0150009	1.966848496	2.032608096	0.382230624	0.382230624	0.382230624	0.382230624	1.12E+00	1.15E+00	0.00E+00	0.00E+00	4980351	4.232	0.38	193	277	55389.546
0.0150013	0.0150013	1.966848496	2.032608096	0.536483932	0.536483932	0.536483932	0.536483932	8.38E-01	8.66E-01	0.00E+00	0.00E+00	4980391	4.232	0.54	193	277	55389.991
0.0160011	0.0160011	1.96245532	2.033327846	0.29202773	0.29202773	0.29202773	0.29202773	1.73E+00	1.79E+00	0.00E+00	0.00E+00	5002344	5.5392	0.29	37	279	55634.143
0.0160014	0.0160014	1.96245532	2.033327846	0.438689425	0.438689425	0.438689425	0.438689425	2.01E+00	2.09E+00	1.29E-07	1.54E-07	5002348	8.1552	0.44	37	279	55634.188
0.0170012	0.0170012	1.960373306	2.033668179	0.452146691	0.452146691	0.452146691	0.452146691	8.88E-01	9.21E-01	0.00E+00	0.00E+00	5022325	3.5776	0.45	59	280	55856.364
0.0170015	0.0170015	1.960373306	2.033668179	0.452146691	0.452146691	0.452146691	0.452146691	8.88E-01	9.21E-01	0.00E+00	0.00E+00	5022345	3.5776	0.45	60	280	55856.587
0.0180016	0.0180016	1.958403914	2.033999864	0.329321663	0.329321663	0.329321663	0.329321663	9.14E-01	9.49E-01	0.00E+00	0.00E+00	5039058	2.9248	0.33	45	281	56042.462
0.0190012	0.0190012	1.956577679	2.034326401	0.536483932	0.536483932	0.536483932	0.536483932	9.38E-01	9.75E-01	0.00E+00	0.00E+00	5054905	4.232	0.54	25	282	56218.707
0.0190022	0.0190022	1.956577679	2.034326401	0.045103996	0.045103996	0.045103996	0.045103996	3.13E+00	3.25E+00	1.77E-07	2.21E-07	5054911	6.8464	0.05	25	282	56218.773
0.0200015	0.0200015	1.954931714	2.034650628	-3.233160622	-3.233160622	-0.3	-0.3	1.51E-01	1.58E-01	0.00E+00	0.00E+00	5068930	0.3088	-3.23	181	282	56374.687
0.0200023	0.0200023	1.954931714	2.034650628	0.64586944	0.64586944	0.64586944	0.64586944	9.61E-01	1.00E+00	0.00E+00	0.00E+00	5068935	5.5392	0.65	181	282	56374.743
0.0210018	0.0210018	1.953502558	2.034975876	0.452146691	0.452146691	0.452146691	0.452146691	9.84E-01	1.03E+00	0.00E+00	0.00E+00	5082832	3.5776	0.45	126	283	56529.3
0.0210024	0.0210024	1.953502558	2.034975876	0.64586944	0.64586944	0.64586944	0.64586944	9.84E-01	1.03E+00	0.00E+00	0.00E+00	5082843	5.5392	0.65	126	283	56529.422
0.0220026	0.0220026	1.952332224	2.035304674	0.409878683	0.409878683	0.409878683	0.409878683	1.68E+00	1.75E+00	0.00E+00	0.00E+00	5092515	5.5392	0.41	40	284	56636.99
0.0230023	0.0230023	1.951466087	2.035638839	-3.233160622	-3.233160622	-0.3	-0.3	1.62E-01	1.69E-01	0.00E+00	0.00E+00	5103677	0.3088	-3.23	167	284	56761.13
0.0230027	0.0230027	1.951466087	2.035638839	0.331041257	0.331041257	0.331041257	0.331041257	1.72E+00	1.79E+00	0.00E+00	0.00E+00	5103722	4.8864	0.33	168	284	56761.63
0.0240025	0.0240025	1.950952937	2.035979265	0.302687713	0.302687713	0.302687713	0.302687713	2.80E+00	2.92E+00	3.11E-07	3.63E-07	5113763	7.5008	0.3	80	285	56873.303
0.0240028	0.0240028	1.950952937	2.035979265	0.64586944	0.64586944	0.64586944	0.64586944	1.05E+00	1.10E+00	0.00E+00	0.00E+00	5113764	5.5392	0.65	80	285	56873.314
0.0250029	0.0250029	1.950846001	2.036324778	0.382230624	0.382230624	0.382230624	0.382230624	1.43E+00	1.49E+00	0.00E+00	0.00E+00	5122546	4.232	0.38	178	285	56970.984

3.3.5.1 Crack Growth per Flight

Crack size is given as a function of cycles or flight hours in Table 18, but the MCS is performed in terms of discrete flights. The crack extension per flight, *dc/d(flight)*, i.e., the slope of the crack growth curve, as a function of crack size is needed. *dc/d(flight)* can be found using any number of numerical differentiation methods. For this example, it was found to be just as easy to break the master crack growth curve into sections and fit a curve to each section forcing continuity across each boundary. The details of this process are explained in Appendix C. The steps are summarized below.

First, cycles were converted to flights by multiplying the cycle count by (200 flights/17,983 cycles). Examples of this conversion are shown in Table 19. Then, polynomials were fit piecewise to segments of the crack growth curve. These polynomials gave the crack size as a function of flights. The polynomials were differentiated to obtain *dc/d(flight)* at each crack size in the AFGROW output. *dc/d(flight)* was plotted versus crack size and equations were fit piecewise to segments of this curve. An exponential function was used to extrapolated back to a crack size of zero. Example values are given in Table 19 and the equations are given below.

For $c < 0.00327$ inch,

$$\frac{dc}{d(flight)} = 1.86251E-11\ exp(2192.92\ c) \qquad (66a)$$

For $0.00372 \le c \le 0.01292$ inches,

$$\frac{dc}{d(flight)} = -34.027c^4 + 0.748c^3 + 0.0208c^2 - (1.219 \times 10^{-4})c + 1.785 \times 10^{-7} \qquad (66b)$$

For $0.01292 \le c \le 0.0682$ inch,

$$\frac{dc}{d(flight)} = 0.0336c^3 + 0.0152c^2 - (9.936 \times 10^{-5})c + 1.416 \times 10^{-6} \qquad (66c)$$

For $0.0682 \le c \le 1.4973$ inch,

$$\frac{dc}{d(flight)} = -(2.64 \times 10^{-4})c^6 + 0.001485c^5 - 0.003362c^4 + 0.00379c^3 - 0.002034c^2 + (6.42 \times 10^{-4})c + 4.03 \times 10^{-5} \qquad (66d)$$

For $1.4973 \le c \le 2.2384$ inch,

$$\frac{dc}{d(flight)} = -0.0101c^6 + 0.1266c^5 - 0.6564c^4 + 1.8044c^3 - 2.7707c^2 + 2.253c - 0.7572 \qquad (66e)$$

For $c \ge 2.2384$ inch,

$$\frac{dc}{d(flight)} = 0.3278c^3 - 2.2877c^2 + 5.3332c - 4.1504 \qquad (66f)$$

3.3.6 Fracture Criterion

The primary failure mechanism of concern is fracture of the specimen. It is assumed that fracture, if it occurs, will happen when the maximum stress intensity during a flight equals or exceeds the fracture toughness for a particular MC sample. Hence, the maximum stress intensity must be calculated for each flight in the MCS.

3.3.6.1 Calculation of the Maximum Stress Intensity during a Flight

The stress intensity, K, is commonly calculated with the equation

$$K = \beta\sigma\sqrt{\pi c} \tag{67}$$

where σ is the applied stress, c is the crack size, and β is a factor dependent upon the geometry and the crack size. The maximum stress intensity during a flight, K_{max}, uses the maximum stress during a flight, σ_{max}, discussed in Section 3.3.4.1. The crack size, c, at the beginning of a flight will be used since generally the crack only grows a little during a single flight and fracture can be checked for before calculating the crack extension during the flight. The crack size at the end of the flight could be used and the flight at which fracture occurs might change by a few flights.

There are numerous handbooks and papers providing equations for the geometry factor β [16, 7]. Most fatigue crack growth software also provide values of β associated with each crack size. The output from AFGROW in Table 18 lists the β values for the surface crack tip in the third column. Polynomials were fit piecewise to the β versus crack size data from Table 18 in Figure 40 to Figure 43. The equations for each fit are given in each figure. The values were extrapolated back to a crack size of zero and forward to a crack size of 2.75 inches, the distance from the edge of the hole to the edge of the specimen. Remember that it is assumed that the crack becomes a through crack at a crack size of 0.060 inch.

Table 19. Crack Length vs. Flight and Crack Extension per Flight Example

c Length	Cycles	Flights	dc /d(*flight*)
0.003	0	0	3.05311E-08
0.0040001	2945328	32756.80365	9.84698E-08
0.005	3858359	42911.18278	2.99717E-06
0.0050003	3858368	42911.28288	2.2602E-07
0.0060001	4256108	47334.79397	2.24788E-06
0.0060004	4256120	47334.92743	4.00225E-07
0.0070002	4480736	49833.02007	1.58674E-06
0.0070005	4480753	49833.20914	6.34444E-07
0.0080002	4622433	51408.91954	1.19887E-05
0.0080006	4622436	51408.9529	9.14891E-07
0.0090003	4720686	52501.65156	4.16273E-07
0.0090008	4720794	52502.85269	1.27782E-06
0.0100004	4791132	53285.12484	3.99622E-06
0.0100008	4791141	53285.22493	1.64043E-06
0.0110006	4845942	53894.70055	2.39773E-06
0.011001	4845957	53894.86737	2.08304E-06
0.0120006	4889105	54374.74281	2.80984E-06
0.0120011	4889121	54374.92076	2.5022E-06
0.0130007	4925041	54774.40916	7.1932E-06
0.0130011	4925046	54774.46477	2.84448E-06
0.0140009	4956650	55125.95229	2.69745E-06
0.0140012	4956660	55126.0635	3.79418E-06
0.0150009	4980351	55389.54568	8.9915E-07
0.0150013	4980391	55389.99055	4.09498E-06
0.0160011	5002344	55634.14336	6.74363E-06
0.0160014	5002348	55634.18784	4.50003E-06
0.0170012	5022325	55856.36434	1.34873E-06
0.0170015	5022345	55856.58678	5.38048E-06
0.0180016	5039058	56042.46233	5.67168E-06
0.0190012	5054905	56218.70656	1.49858E-05
0.0190022	5054911	56218.77329	6.40931E-06
0.0200015	5068930	56374.6872	1.43864E-05
0.0200023	5068935	56374.74281	6.46687E-06
0.0210018	5082832	56529.29989	4.90445E-06
0.0210024	5082843	56529.42223	9.29828E-06
0.0220026	5092515	56636.99049	8.05304E-06
0.0230023	5103677	56761.12996	7.99244E-07
0.0230027	5103722	56761.63043	8.95299E-06
0.0240025	5113763	56873.30256	2.69745E-05
0.0240028	5113764	56873.31369	1.02396E-05
0.0250029	5122546	56970.98371	1.02572E-05

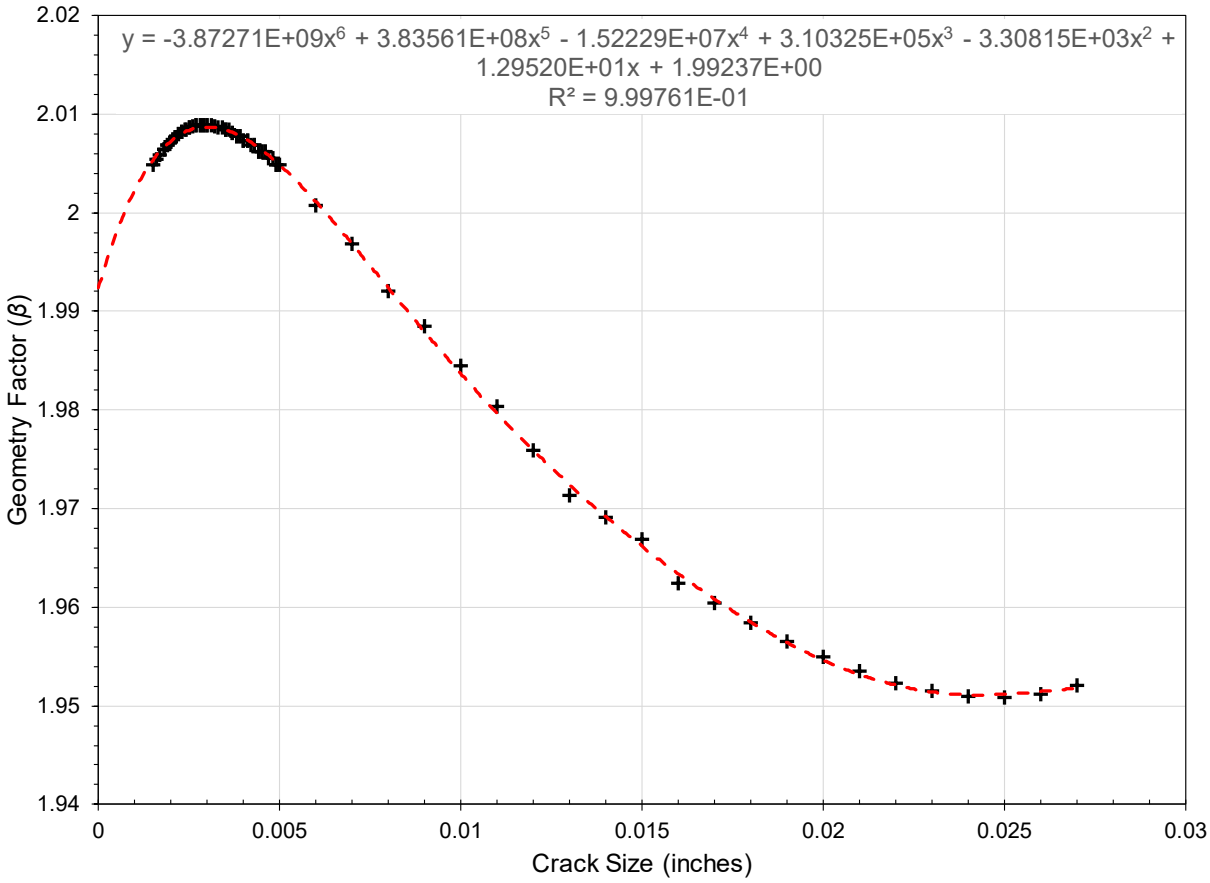

Figure 40. Stress Intensity Geometry Factors for $c \leq 0.02746$ Inch

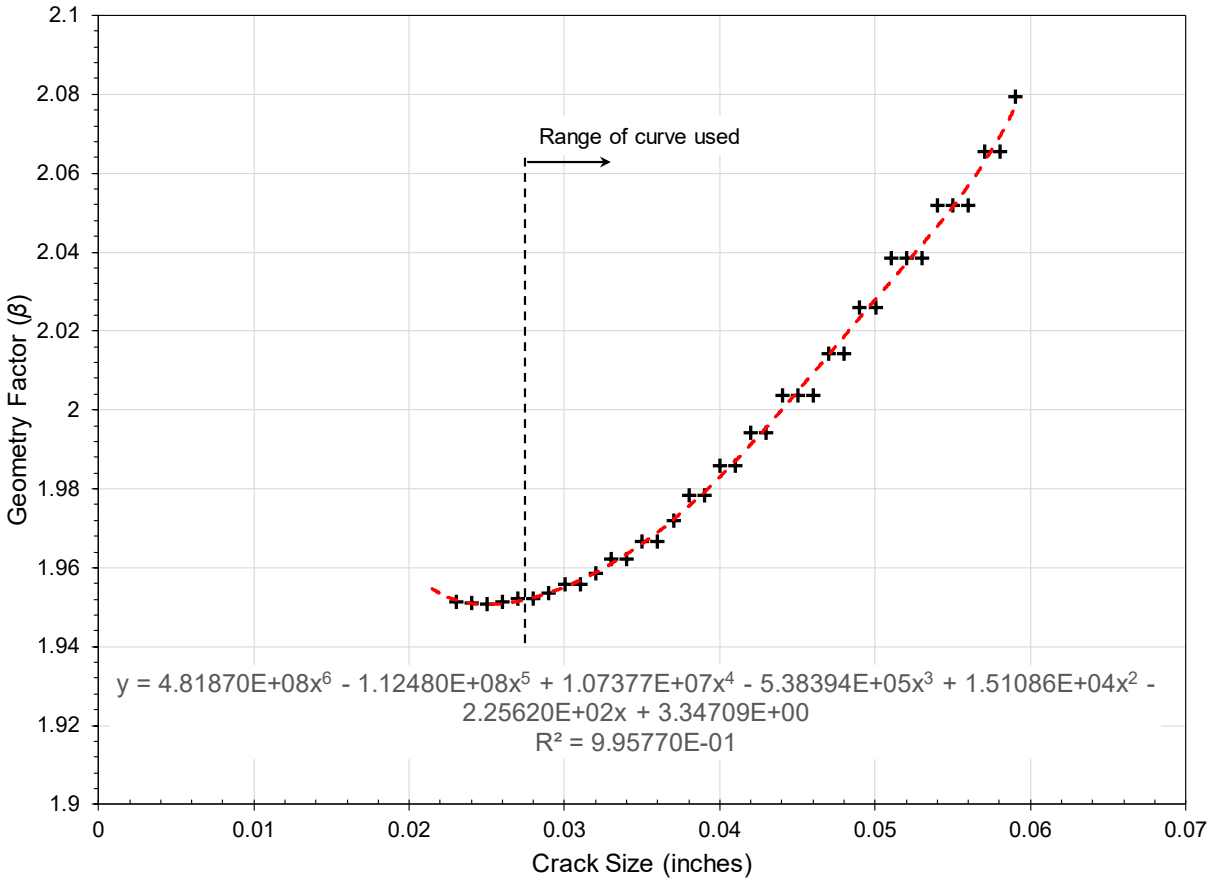

Figure 41. Stress Intensity Geometry Factors for 0.02746 < *c* < 0.0598 Inch

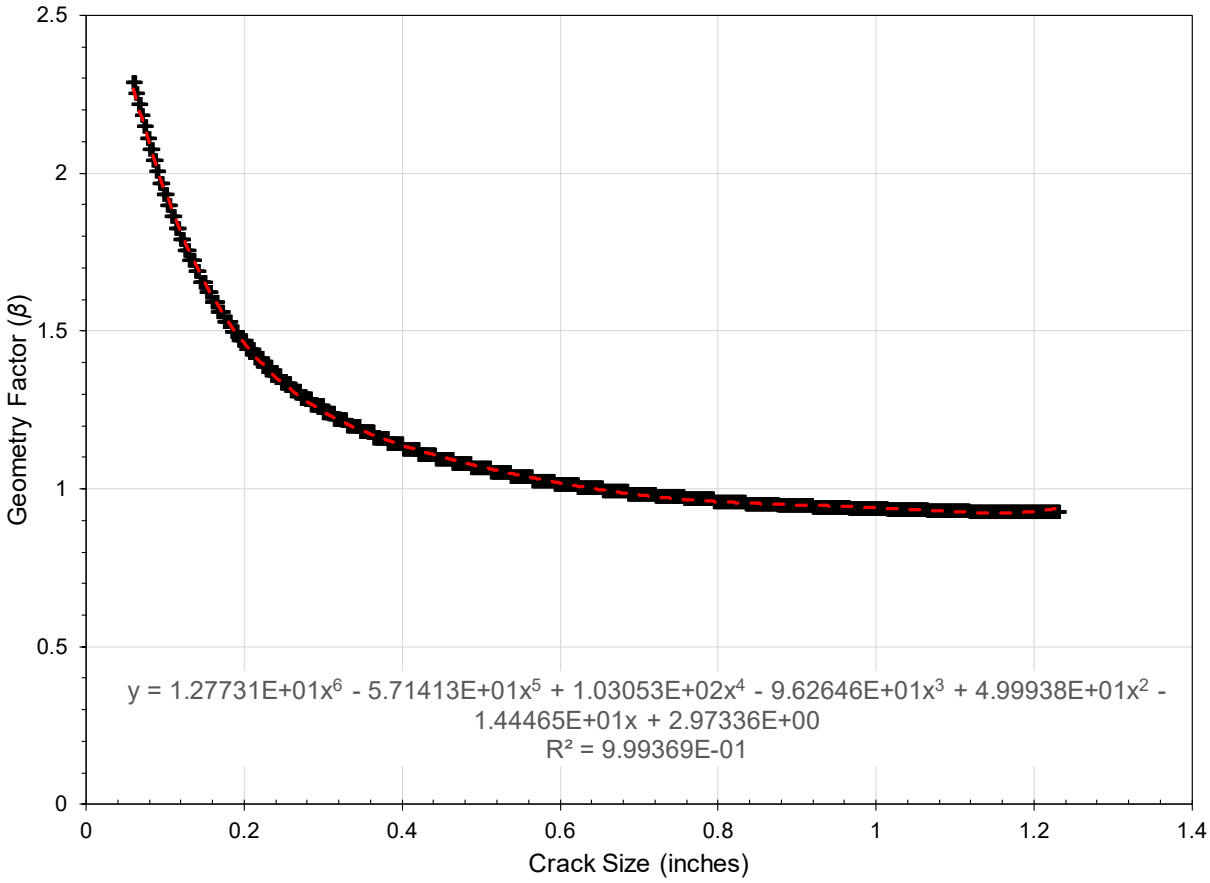

Figure 42. Stress Intensity Geometry Factors for $0.0598 \leq c \leq 1.201$ Inches

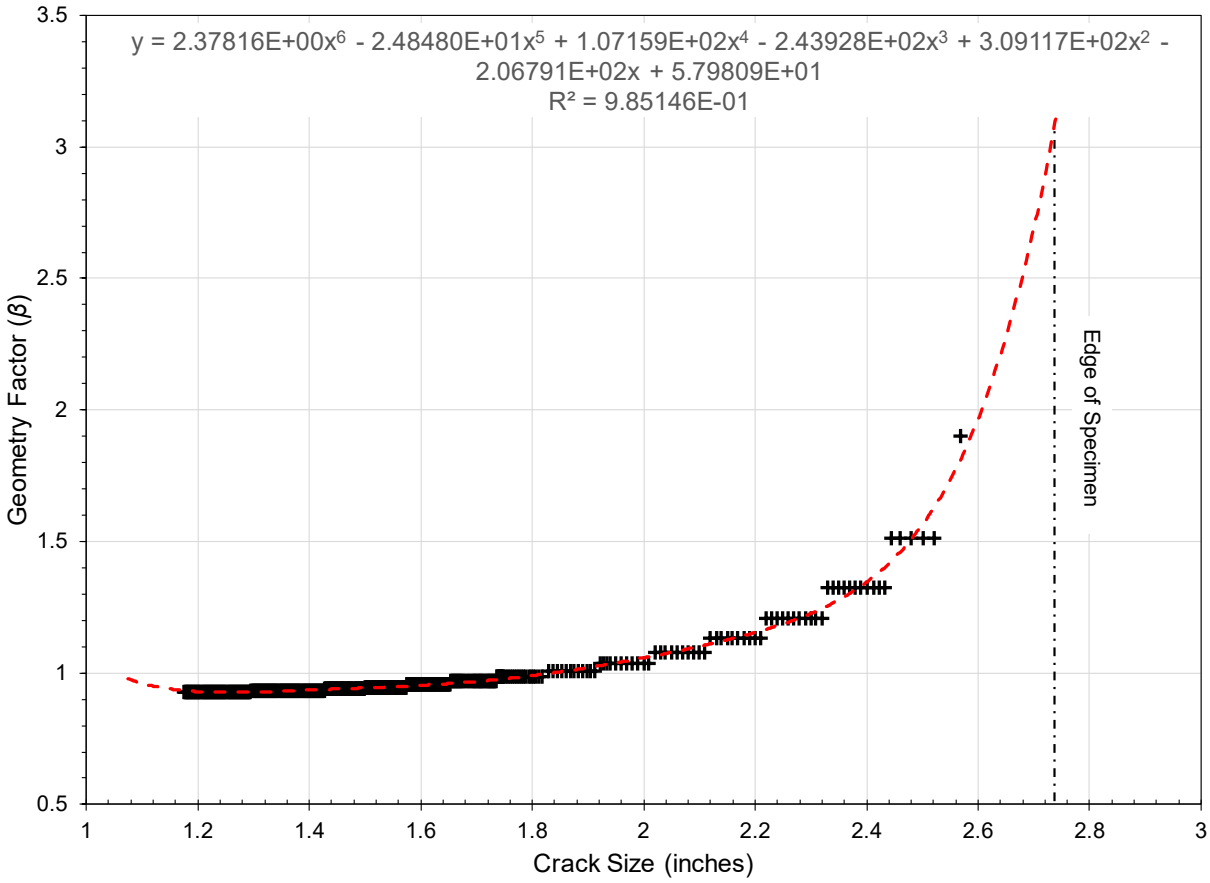

Figure 43. Stress Intensity Geometry Factors for $c > 1.201$ Inches

3.3.7 POF Calculation

MCS will be used to calculate the determine the failure CDF as a function cycles, $F_T(n)$. The failure PDF as a function of cycles, $f_T(n)$, is determined from $F_T(n)$. Finally, the HRF as a function of cycles, $h_T(n)$, is found.

3.3.7.1 Monte Carlo Simulation

The general steps in the MCS process are:

1. Randomly choose the starting conditions (i.e., K_C and EIDS) for a sample that is representative of a physical specimen.
2. Perform a fatigue crack growth analysis for this sample from the EIDS to failure, i.e., the applied stress intensity equals or exceeds K_C.
3. Record the flight hours when this sample fails.
4. Repeat this process of creating samples and modeling the fatigue crack growth until a sufficiently large number of samples have been generated that reliability, or its inverse, POF, can be estimated with acceptable confidence.

The MCS is performed using a Microsoft Excel® macro which is listed in Appendix B.3. The detailed MCS steps for this example problem are outlined below. Results for the first 50 samples are presented in Table 20.

First, 12,000 random samples of fracture toughness and EIDS pairs were generated as follows:

1. Randomly select K_C for MCS sample. As in Step 1 of Section 3.2.5.1, randomly generate a number between 0 and 1 using a (pseudo-) random number generator. Recall that the CDF has a range of 0 to 1. The random number is the CDF value, P, of K_C. Plug the random number into the inverse CDF for K_C. The inverse CDF for the Weibull distribution used for K_C is

$$K_C = \beta \left[LN\left(\frac{1}{1-P}\right)\right]^{1/\alpha} \tag{68}$$

   where here α is the shape parameter, 12.49, and β is scale parameter, 88.89 ksi√in. The samples for K_C from the example in Section 3.2 are used here since the fracture toughness distribution is the same. Values of K_C are given in column 2 of Table 20.

2. Randomly select an EIDS value for the MCS sample. As in Step 2 of Section 3.2.5.1, randomly generate a number, P, between 0 and 1 using a (pseudo-) random number generator. Plug the random number into the inverse CDF for the EIDS. The CDF for EIDS is also a Weibull distribution, so

$$EIDS = \beta \left[LN\left(\frac{1}{1-P}\right)\right]^{1/\alpha} \tag{69}$$

   with α equal to 0.374 and β equal to 0.00054 inches. The initial crack size samples from the example in Section 3.2 are used here also since the EIDS distributions are the same in both examples. Values for EIDS are given in column 3 of Table 20.

Then the crack growth simulation was run using the following steps.

Step 1. Start the crack growth simulation. If this is the first flight, then set $c_{start(f)}$, column 5 of Table 20, equal to the EIDS for this sample. Otherwise, set column 5 equal to $c_{end(f)}$, the last column, from the previous flight. Determine the crack extension during the current flight, $\Delta c(f)$ (column 9), based upon the crack size at the start of the flight and the equations for $dc/d(flight)$ in Section 3.3.5.1. Add column 2 and column 9 to get $c_{end(f)}$, column 10.

If $\Delta c(f)$ during the first flight was less than 10^{-13} inches/flight, the simulation stopped and execution jumped to Step 6. This sample has a long life that will not contribute to the early failure, low probability end of the POF distribution. The sample was still counted in the total number of samples when rank ordering the samples, but the sample was ranked above all the samples that failed. This reduced the MCS execution time.

Table 20. Sample of Monte Carlo Simuluation Results

Trial #	K_c (ksi√inch)	EIDS (inch)	Flight Count, f	$c_{start}(f)$ (inch)	$\sigma_{max}(f)$ (ksi)	β	$K_{max}(f)$ (ksi√inch)	$\Delta c(f)$ (inch)	$c_{end}(f)$ (inch)
1	96.01	0.005427765	22088	2.65171	17.20	2.274840	112.92	1.78E-02	2.66948
2	94.46	2.66785E-05	23127371	2.71529	13.62	2.823115	112.28	2.65E-02	2.74177
3	89.40	0.000174529	16732768	2.71428	11.92	2.812821	97.87	2.63E-02	2.74060
4	82.78	0.000266015	13697476	2.67064	12.22	2.418564	85.61	2.01E-02	2.69071
5	79.44	1.1517E-05	23908050	2.67810	15.98	2.479447	114.91	2.10E-02	2.69914
6	85.71	1.08303E-05	23944030	2.66742	13.14	2.393031	90.99	1.97E-02	2.68709
7	79.80	0.000654849	5858831	2.62659	13.47	2.106330	81.47	1.51E-02	2.64165
8	97.65	1.60943E-05	23669622	2.70936	14.00	2.763632	112.89	2.56E-02	2.73491
9	78.71	0.000258134	13935646	2.61758	15.93	2.051575	93.69	1.42E-02	2.63176
10	87.49	0.000565666	7116843	2.72146	11.51	2.887052	97.11	2.75E-02	2.74894
11	87.63	5.08976E-05	21932913	2.69243	12.91	2.603748	97.74	2.30E-02	2.71545
12	92.07	0.000713033	5161200	2.70165	12.95	2.688970	101.43	2.44E-02	2.72602
13	91.30	0.000854862	3790927	2.71413	11.29	2.811325	92.69	2.63E-02	2.74043
14	72.12	0.00018973	16185348	2.61835	12.50	2.056134	73.67	1.43E-02	2.63260
15	93.21	0.001427376	1105129	2.72079	12.52	2.880002	105.39	2.74E-02	2.74816
16	100.44	1.20366E-05	23880867	2.74437	10.98	3.143624	101.32	3.15E-02	2.77584
17	91.77	2.97344E-07	24502709	2.69451	13.25	2.622616	101.09	2.33E-02	2.71783
18	77.27	8.08029E-06	24088649	2.66314	12.25	2.359736	83.59	1.91E-02	2.68226
19	92.60	3.66128E-07	24499017	2.66297	13.89	2.358445	94.74	1.91E-02	2.68208
20	86.79	9.78383E-07	24466196	2.73301	11.70	3.012644	103.29	2.94E-02	2.76246
21	67.64	8.42643E-05	20387828	2.53708	14.35	1.672365	67.74	8.24E-03	2.54532
22	81.27	0.000608028	6488579	2.62953	13.56	2.124828	82.80	1.54E-02	2.64489
23	69.51	0.002785956	89277	2.64892	11.43	2.254860	74.34	1.74E-02	2.66636
24	92.09	0.012997186	12454	2.71798	13.28	2.850750	110.61	2.69E-02	2.74490
25	84.88	8.80299E-05	20220464	2.68506	11.95	2.538613	88.08	2.20E-02	2.70705
26	75.40	0.002533021	129608	2.64500	12.22	2.227428	78.46	1.70E-02	2.66201
27	66.47	0.01942764	10771	2.58459	13.59	1.873952	72.55	1.14E-02	2.59595
28	94.64	3.25505E-06	24344524	2.70118	12.90	2.684503	100.86	2.43E-02	2.72548
29	91.22	2.96511E-07	24502755	2.72629	10.33	2.938627	88.81	2.83E-02	2.75458
30	90.02	0.001230616	1682558	2.64993	14.06	2.262065	91.75	1.76E-02	2.66749
31	83.21	0.002619548	113236	2.66017	13.04	2.337156	88.10	1.88E-02	2.67893
32	86.79	7.5561E-05	20780021	2.70326	11.47	2.704300	90.40	2.46E-02	2.72787
33	90.24	5.82979E-05	21580415	2.73081	11.18	2.988131	97.78	2.91E-02	2.75988
34	81.65	0.000810895	4171104	2.63237	16.22	2.142986	99.92	1.56E-02	2.64802
35	78.33	2.57983E-05	23171984	2.67605	11.48	2.462461	81.96	2.08E-02	2.69682
36	93.22	7.54546E-08	24514612	2.60376	18.60	1.972972	104.95	1.29E-02	2.61669
37	82.62	0.00039572	10315178	2.64546	13.58	2.230602	87.33	1.71E-02	2.66251
38	69.59	0.001676536	654590	2.65359	10.72	2.288410	70.82	1.80E-02	2.67157
39	69.42	0.000165947	17049993	2.60406	15.74	1.974607	88.88	1.30E-02	2.61702
40	84.91	0.016196373	11478	2.69920	14.56	2.665870	113.01	2.40E-02	2.72320
41	86.19	0.002464727	144915	2.68206	12.05	2.512868	87.88	2.16E-02	2.70364
42	83.01	0.000111248	19218440	2.69806	11.07	2.655241	85.57	2.38E-02	2.72189
43	87.38	3.1519E-07	24501750	2.66551	14.62	2.378042	100.56	1.94E-02	2.68493
44	95.00	0.001660598	676634	2.67590	16.76	2.461234	119.61	2.08E-02	2.69665
45	88.55	0.000311567	12398631	2.69946	14.75	2.668396	114.60	2.40E-02	2.72351
46	90.85	4.32487E-06	24287562	2.74942	10.36	3.204457	97.51	3.24E-02	2.78183
47	80.37	1.14633E-06	24457195	2.63481	14.66	2.158857	91.03	1.59E-02	2.65072
48	87.97	0.002070422	296134	2.70250	11.96	2.697035	93.95	2.45E-02	2.72700
49	77.37	0.000132447	18347057	2.58720	14.40	1.886792	77.44	1.16E-02	2.59876
50	87.46	2.13267E-05	23399974	2.61774	15.48	2.052549	91.11	1.42E-02	2.63194

Step 2. Determine the geometry factor, β, for the stress intensity for $c_{start}(f)$ using the equations for β in Section 3.3.6.1.

Step 3. Randomly select the maximum stress for this flight, $\sigma_{max}(f)$ (column 6 in Table 20). Randomly generate a number, p, between 0 and 1 using a (pseudo-) random number generator. Plug the random number into the inverse Gumbel CDF for the maximum stress in a flight,

$$\sigma_{max}(f) = \sigma_{ref}\left(\alpha - \beta \cdot ln\left[ln\left(\frac{1}{p}\right)\right]\right) \qquad (70)$$

where α is equal to 0.699, β is equal to 0.060, and σ_{ref} is 16 ksi. The maximum stress value changes with every flight. The values shown in Table 20 are for the last flight for each sample.

Step 4. Compute the maximum applied stress intensity in the flight, $K_{max}(f)$ (column 8 in Table 20). Calculate the maximum applied stress intensity during the flight from

$$K_{max}(f) = \beta \cdot \sigma_{max}(f) \cdot \sqrt{\pi \cdot c_{start}(f)} \qquad (71)$$

$K_{max}(f)$ values for the last flight of each sample are in column 8, *Kmax(f)*, of Table 20.

Step 5. If any of the following criteria are met go to Step 6. Otherwise, loop back to Step 1

1) $c_{end}(f)$ (column 10) is greater than or equal to distance from the edge of the hole to the edge of the specimen, 2.75 inches, or
2) $K_{max}(f)$ (column 8) is greater than or equal to K_C (column 2), or
3) *Flight Count* (column 4) times the average flight time equals the flight hours specified for an inspection.

Step 6. Move the ActiveCell down one row to the next sample. Increment the sample number, *i*, and loop back to Step 1 until *i* is greater than 12,000.

Theoretically, millions of samples are required to accurately obtain POF values in the 10^{-7} range. However, this assumes that the tails of the input distributions are accurately defined. Sufficient data to define the tails of the input distributions are rarely available. So, the tails of the input distributions are usually extrapolations. Generating millions of samples from extrapolations does not increase the accuracy of the extrapolation. The approach taken here is to generate enough samples to define the centroid of the POF distribution well. Then extrapolate to lower values using functions fit to the low probability tail of the POF distribution.

3.3.7.2 SFPOF Calculation

SFPOF as a function of flights was calculated using the number of flights to failure from the MCS samples. First, find the CDF of the failure time distribution, $F_T(n)$. This establishes the failure time PDF, $f_T(n)$. Finally, calculate the hazard rate, $h_T(n)$, which when multiplied by a time period of one flight is the SFPOF.

The first step in determining $F_T(n)$ is to rank order the number of flights to failure from shortest to longest. The number for flights to failure should also be converted to flight hours (FH) to failure to provide a continuous failure distribution, $F_T(t)$. This is easily done in this example since the average FH per flight is one hour. Sort the samples from shortest life to longest life. Assign the median rank to each sample using Benard's approximation (Section 2.3.1). Then, fit a function to the low life tail of the cumulative failure distribution. It is unlikely that the reliability function can be completely described by a single standard distribution. However, because fatigue failures are usually well described by the Weibull distribution, the rank ordered failure data were plotted on a Weibull probability plot as shown in Figure 44. The failure data does not plot as a straight line. There are three nearly straight line sections in the plot. $F_T(t)$ can be represented piecewise by three Weibull functions. When dealing with experimental data, a change in slope is usually associated with a change in mechanism. Since these are simulations, it is difficult to determine what the cause of the slope changes is.

The early failures, lives less than 10,000 FH, are of most interest. A Weibull function was fit to all failures times less than 10,000 FH using their rank order in the complete set of failure data. The resulting Weibull function fit is the dashed red line in Figure 44 and described by the equation

$$F_T(t) = 1 - exp\left[-\left(\frac{t}{13823.8}\right)^{12.42}\right] \text{ for } t \leq 10{,}000\ FH \quad (72)$$

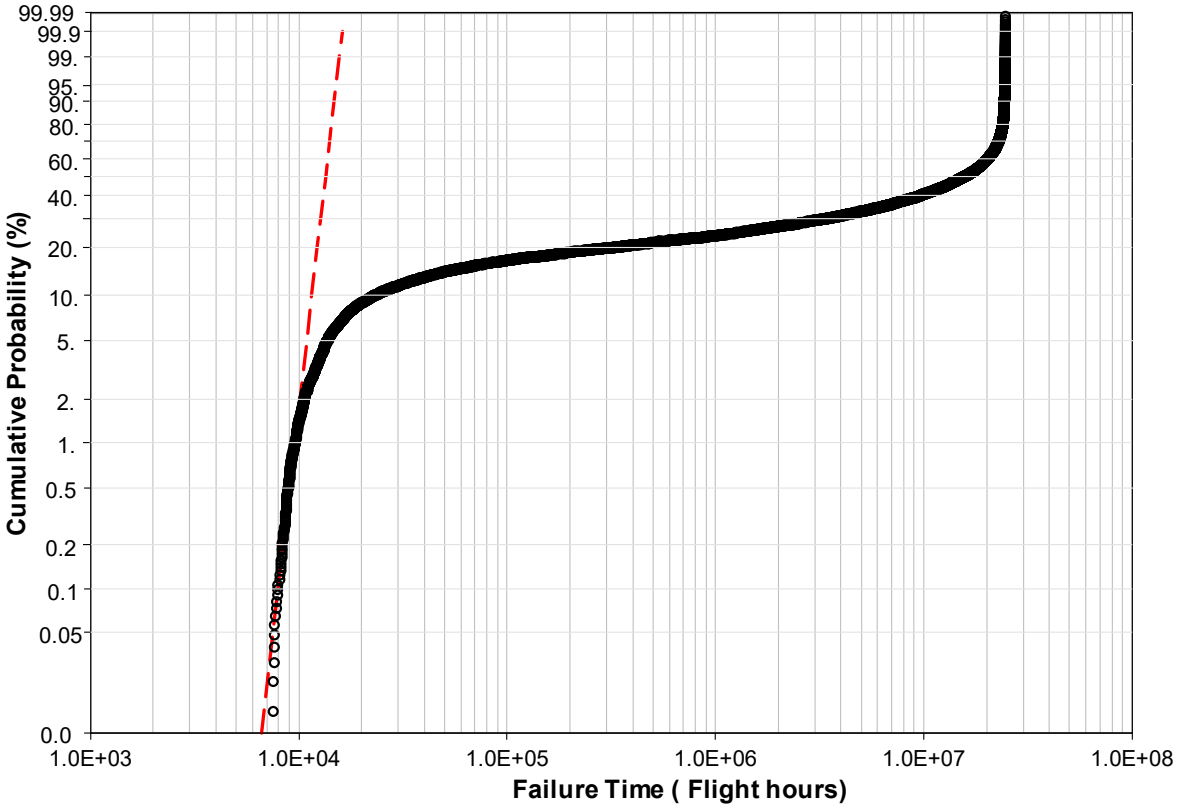

Figure 44. Weibull Probability Plot of Rank Ordered Failures

While performing the sensitivity analysis described in the next section, it was observed that the samples below a POF of 0.1% (8,000 FH) described a line with a different slope than the line through the samples with POF greater than 0.1% and less than 1.0% (10,000 FH). So, an additional Weibull function was fit to the samples that failed in less than 8,000 FH as in Figure 45. The resulting Weibull function fit shown by the dashed blue line in Figure 45 is described by the equation

$$\mathrm{F_T(t)} = 1 - \exp\left[-\left(\frac{\mathrm{n}}{13651.9}\right)^{13.17}\right] \text{ for } \mathrm{t} < 8{,}000\ \mathrm{FH} \quad (73)$$

The red dashed line is still described by equation (72). The larger exponent (shape parameter) in equation (73) means that there is less variability (smaller standard deviation if you will) in the tail of the distribution with this revised fit. There is not much change in the value of the scale parameter (the denominator).

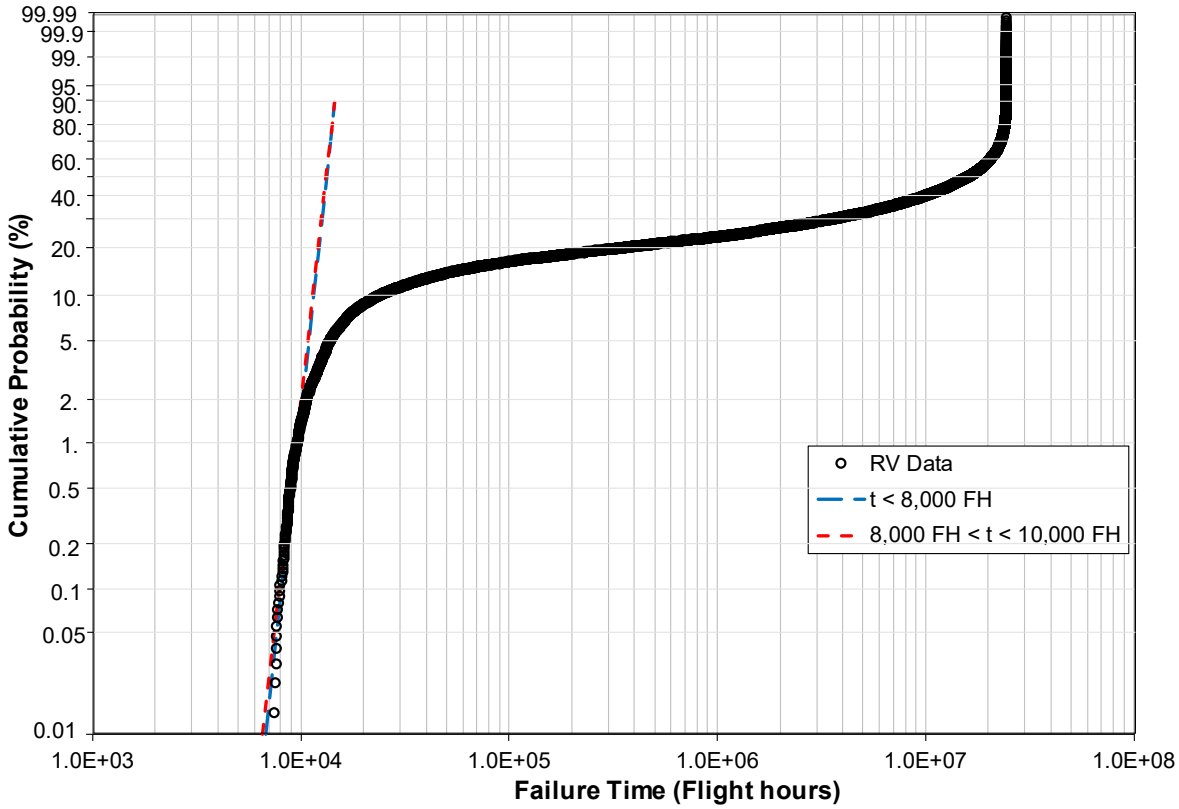

Figure 45. Revised Fit to Low Probability Tail of Failure Distribution

Remember, the hazard rate, $h_T(N)$, is defined as

$$h_T(t_f) = \frac{f_T(t_f)}{(1 - F_T(t_f))} \tag{74}$$

This calculation is straightforward since a Weibull distribution fit the tail of $F_T(t)$ well. The hazard rate in the short life tail (t_f < 8,000 FH) is

$$h_T(t_f) = \frac{13.17}{13651.9}\left(\frac{t_f}{13651.9}\right)^{12.17} \tag{75}$$

The resulting SFPOF values for FH values up to 8,000 FH are given in Table 21. The SFPOF is equal to 10^{-7} at about 6,424 FH which corresponds to a cumulative probability of failure of 4.88×10^{-5}.

Table 21. SFPOF Values for Select Flight Hours to Failure

N_f	SFPOF
1000	1.47E-17
1250	2.22E-16
1500	2.05E-15
1750	1.34E-14
2000	6.79E-14
2250	2.85E-13
2500	1.03E-12
2750	3.27E-12
3000	9.44E-12
3250	2.50E-11
3500	6.16E-11
3750	1.43E-10
4000	3.13E-10
4250	6.55E-10
4500	1.31E-09
4750	2.53E-09
5000	4.73E-09
5250	8.57E-09
5500	1.51E-08
5750	2.59E-08
6000	4.35E-08
6250	7.15E-08
6500	1.15E-07
6750	1.83E-07
7000	2.84E-07
7250	4.36E-07
7500	6.58E-07
7750	9.81E-07
8000	1.44E-06

3.3.8 Sensitivity Study

As was done in the previous examples, the methods of Robust Design and ANOVA [10] were employed to perform a sensitivity study to determine how sensitive the FHs when SFPOF equals 10^{-7} are to the parameters of the three distributions. The three random variables in this example should be considered in the sensitivity analysis: fracture toughness, EIDS, and the maximum stress in a flight. Since the distribution for each random variable is defined by two parameters, there are six parameters to be varied in the sensitivity study. A sensitivity study that includes every combination of parameters would involve 3^6, or 729, different MCS runs. The $L_{18}(2^1x3^7)$ orthogonal array shown in Table 22 can be used to perform a three-level sensitivity study for six parameters. Note the first two columns of the array are not assigned a variable. The values for the shape factor of the fracture toughness distribution were 14.5, 12.49, and 10.5, and the scale factor values were 93.9, 88.89, and 83.9. The values for the shape factor of the EIDS distribution

were 0.424, 0.374, and 0.324, and the scale factor values were 0.00064, 0.00054, and 0.00044. These are the same values used in sensitivity study in Section 3.2.6. The values for the dispersion parameter, β, of the Gumbel distribution for the maximum stress during a flight were 0.1, 0.06, and 0.02. The values for the characteristic value, α, of the Gumbel distribution for the maximum stress during a flight were 0.75, 0.699, and 0.65.

Table 22. $L_{18}(2^1x3^7)$ Orthogonal Array for Sensitivity Analysis

	Variable							
Trial No.	**1 (unused)**	**2 (unused)**	**Shape (K_C)**	**Scale (K_C)**	**Shape (EIDS)**	**Scale (EIDS)**	**β (Max Stress)**	**α (Max Stress)**
1	1	1	12.49	88.89	0.374	0.00054	0.06	0.699
2	1	1	14.5	93.9	0.424	0.00064	0.1	0.75
3	1	1	10.5	83.9	0.324	0.00044	0.02	0.65
4	1	2	12.49	88.89	0.424	0.00064	0.02	0.65
5	1	2	14.5	93.9	0.324	0.00044	0.06	0.699
6	1	2	10.5	83.9	0.374	0.00054	0.1	0.75
7	1	3	12.49	93.9	0.374	0.00044	0.1	0.65
8	1	3	14.5	83.9	0.424	0.00054	0.02	0.699
9	2	3	10.5	88.89	0.324	0.00064	0.06	0.75
10	2	1	12.49	83.9	0.324	0.00064	0.1	0.699
11	2	1	14.5	88.89	0.374	0.00044	0.02	0.75
12	2	1	10.5	93.9	0.424	0.00054	0.06	0.65
13	2	2	12.49	93.9	0.324	0.00054	0.02	0.75
14	2	2	14.5	83.9	0.374	0.00064	0.06	0.65
15	2	2	10.5	88.89	0.424	0.00044	0.1	0.699
16	2	3	12.49	83.9	0.424	0.00044	0.06	0.75
17	2	3	14.5	88.89	0.324	0.00054	0.1	0.65
18	2	3	10.5	93.9	0.374	0.00064	0.02	0.699

A MCS was performed with the set of parameters in each row for a total of eighteen trials. Note that Trial 1 is the same as the baseline analysis. The 12,000 samples in each trial were rank ordered using Benard's median rank approximation and then plotted on a Weibull probability plot. The samples with a POF less than 0.1% were fit with a line as shown in Figure 46 to Figure 63. The values of the Weibull shape and scale parameters, as well as the FHs at which SFPOF equals 10^{-7}, for each of these fits are given in Table 23. An SFPOF of 10^{-7} was reached before the POF reached 0.1% in every trial, so the FH to an SFPOF of 10^{-7} lies within the range of the curve fits to low POF tail of the failure distribution for each run.

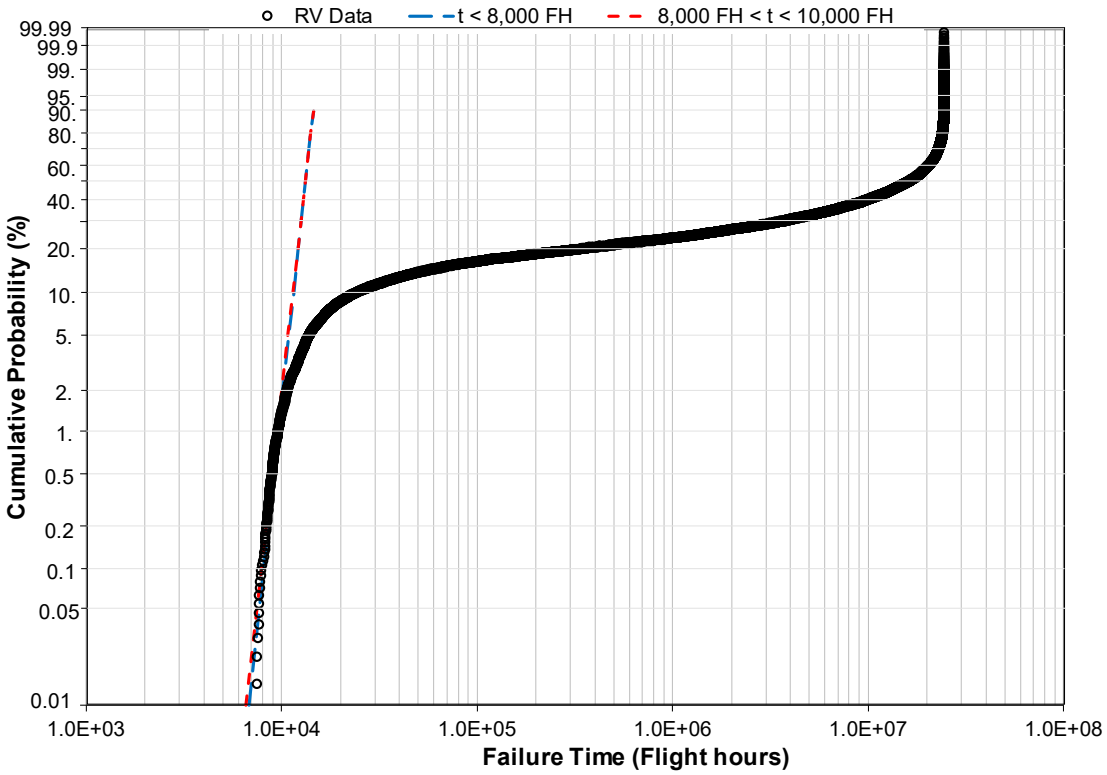

Figure 46. Weibull Plot and Fit to Tail for Trial 1

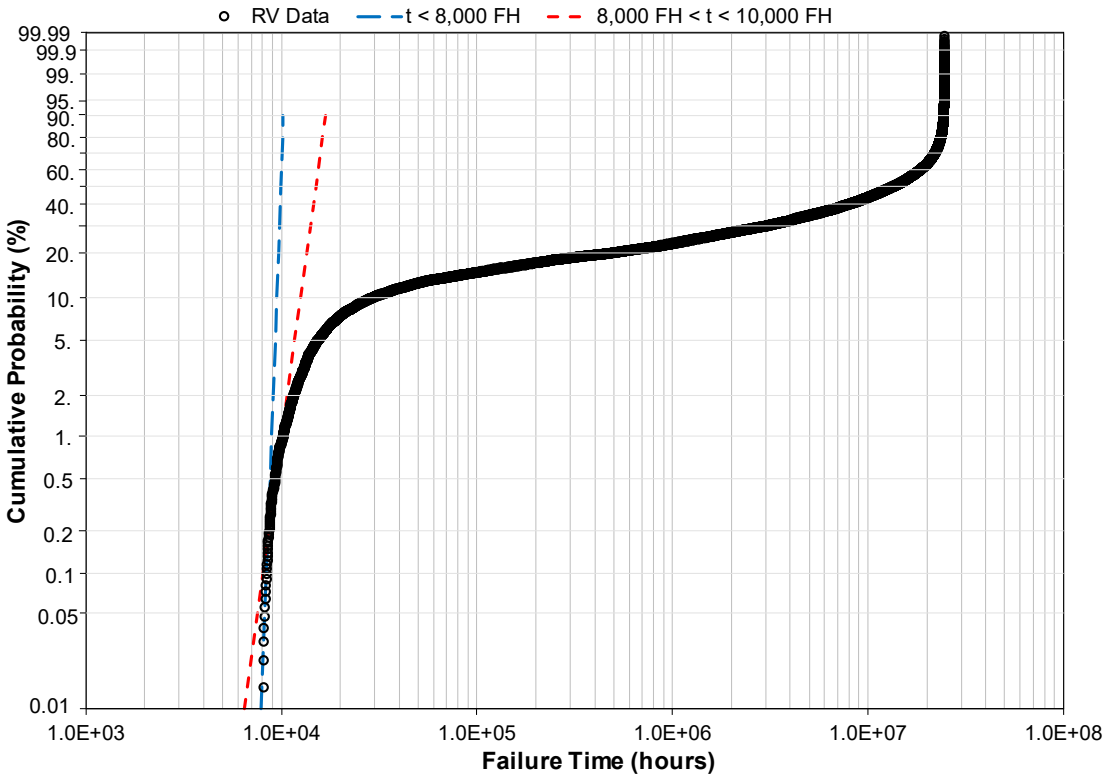

Figure 47. Weibull Plot and Fit to Tail for Trial 2

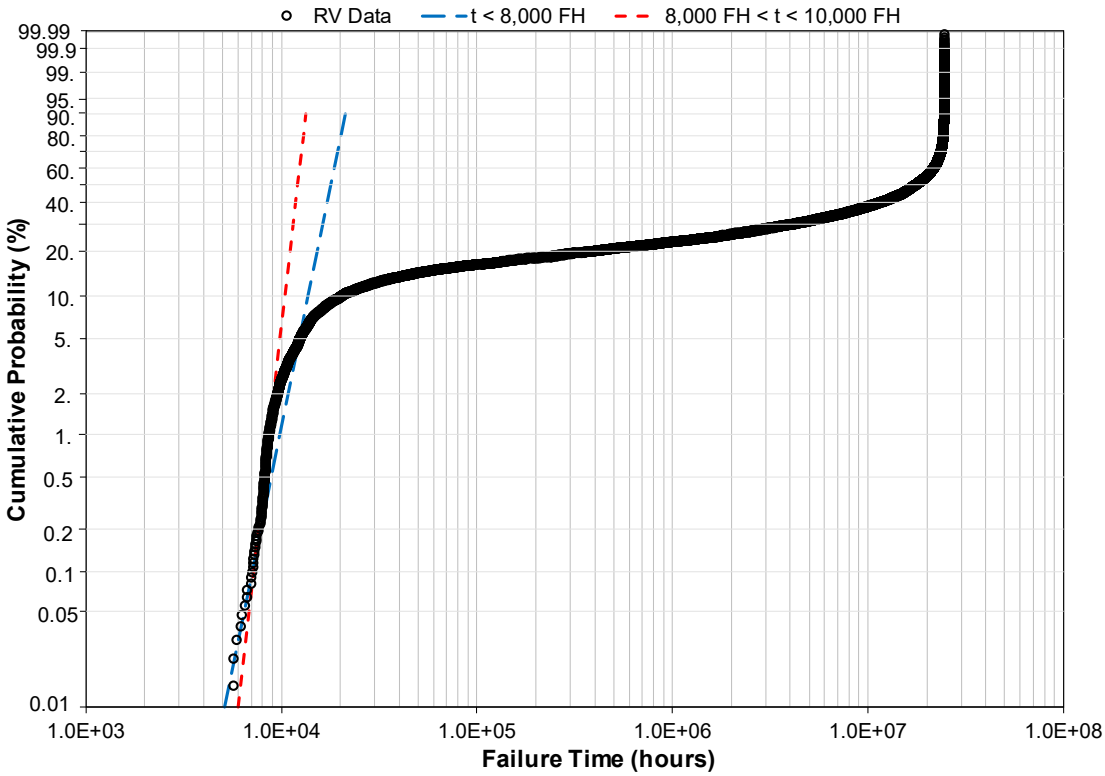

Figure 48. Weibull Plot and Fit to Tail for Trial 3

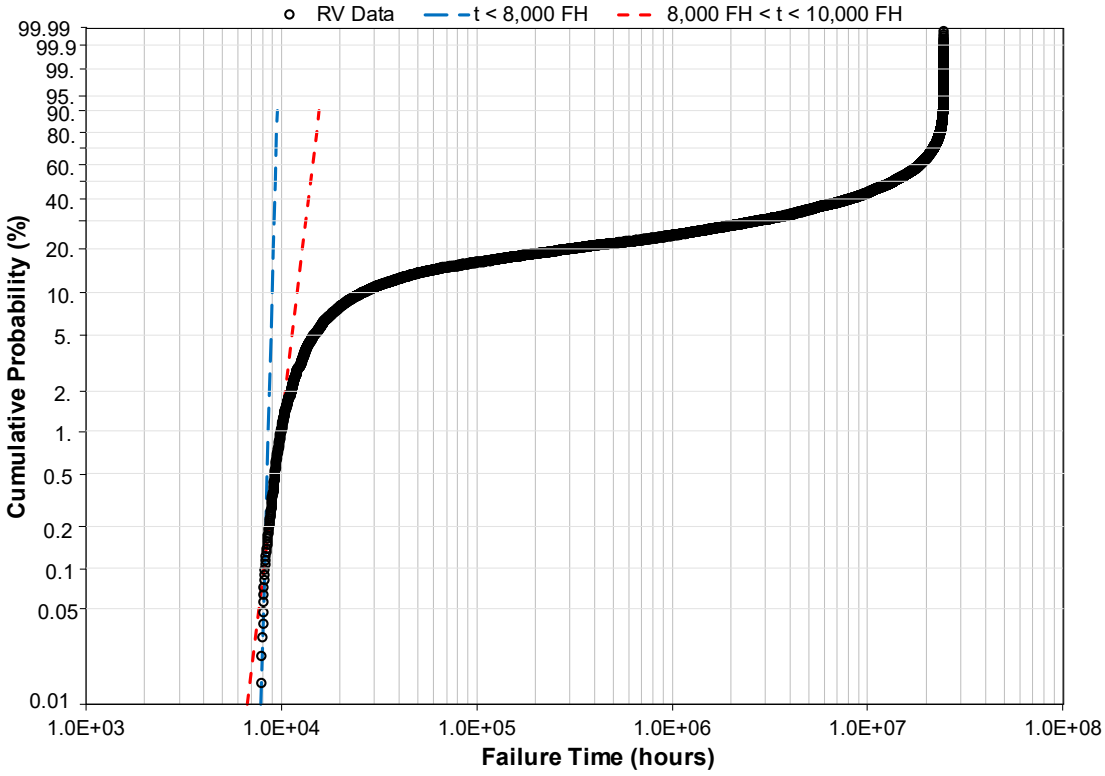

Figure 49. Weibull Plot and Fit to Tail for Trial 4

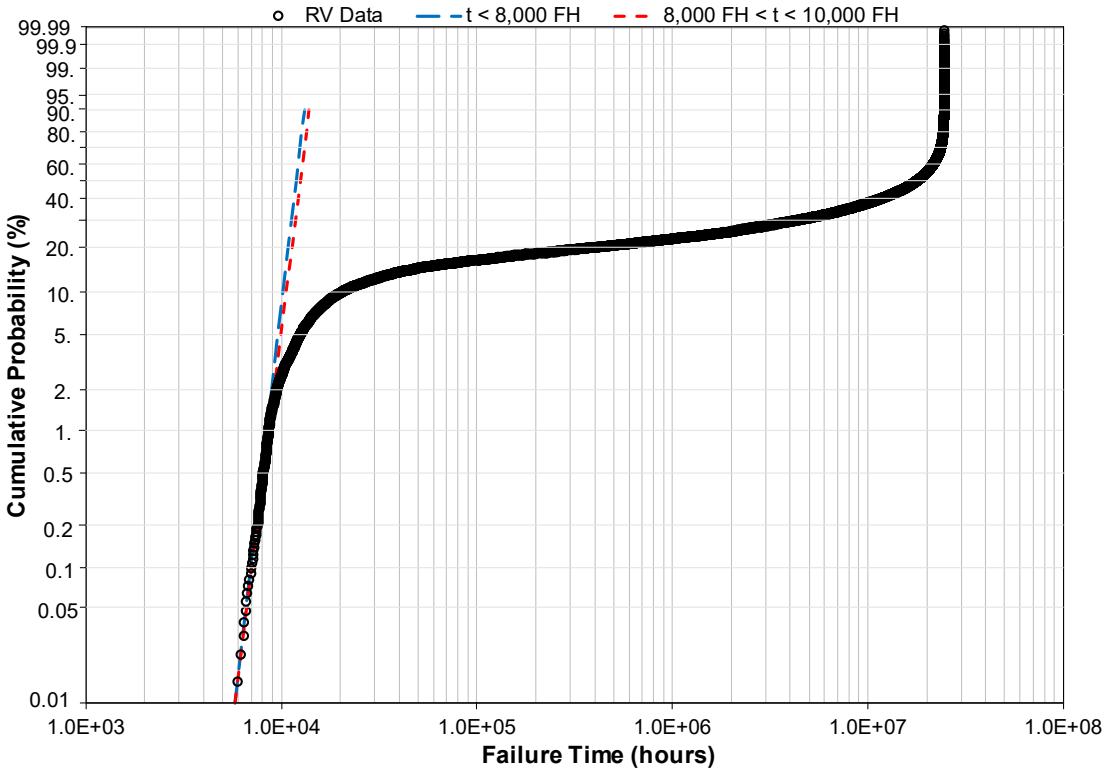

Figure 50. Weibull Plot and Fit to Tail for Trial 5

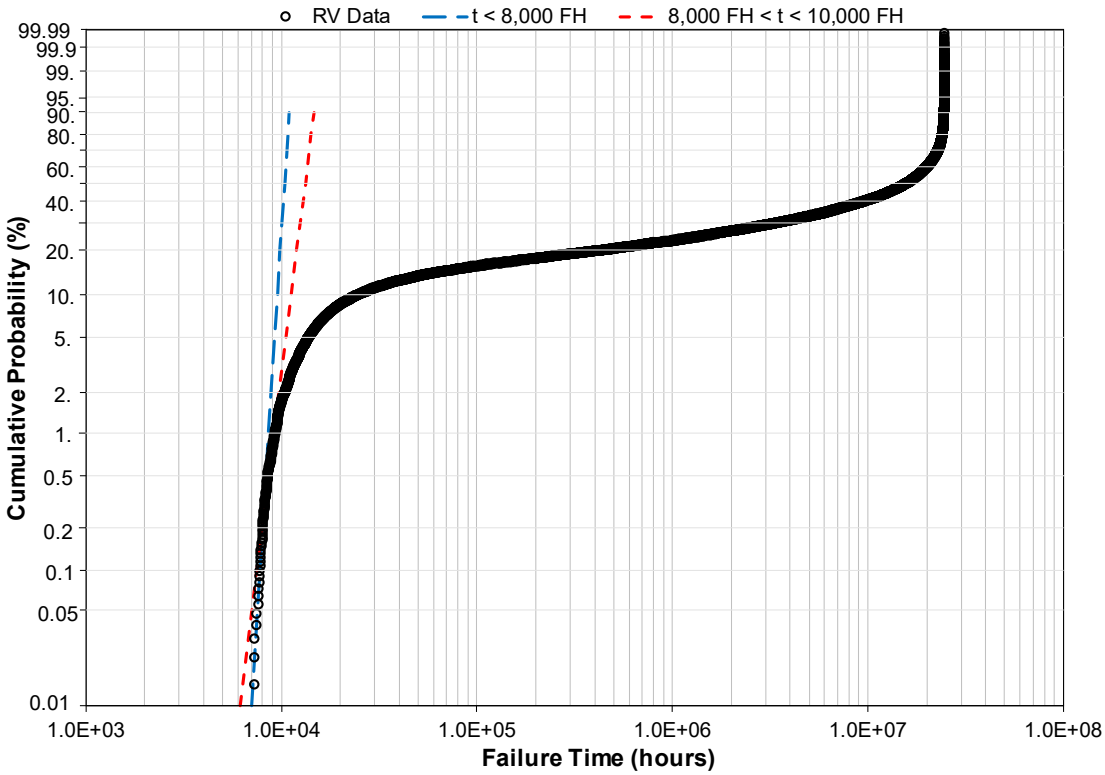

Figure 51. Weibull Plot and Fit to Tail for Trial 6

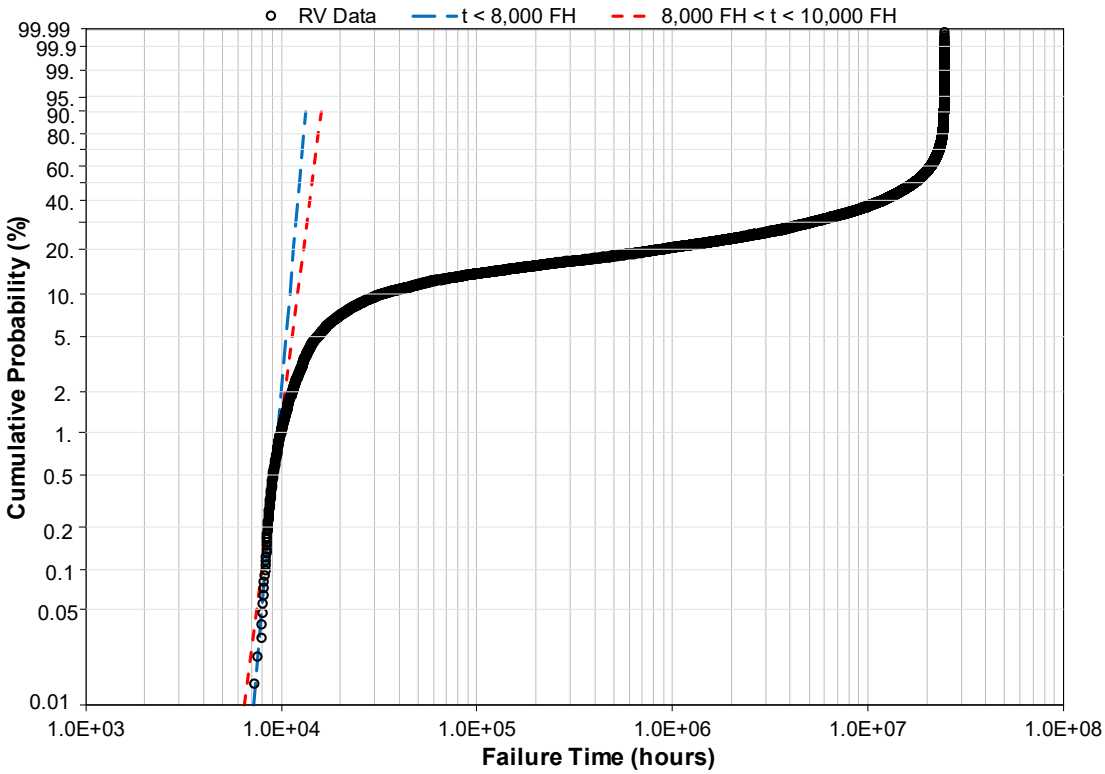

Figure 52. Weibull Plot and Fit to Tail for Trial 7

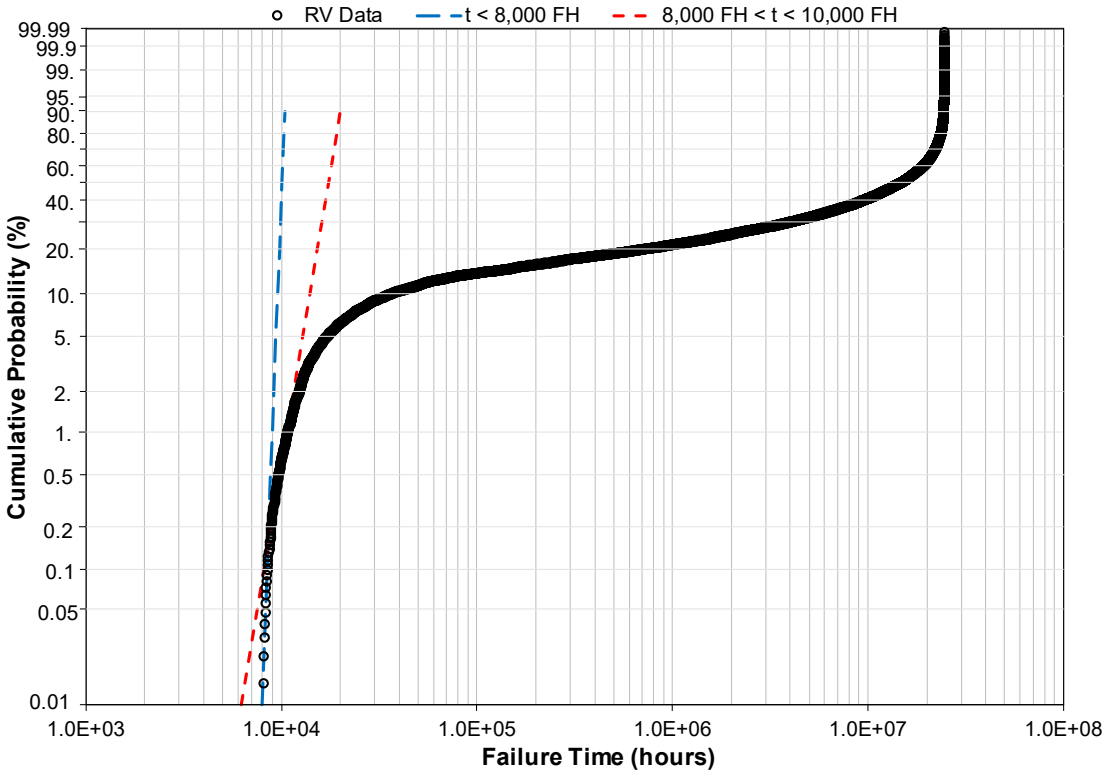

Figure 53. Weibull Plot and Fit to Tail for Trial 8

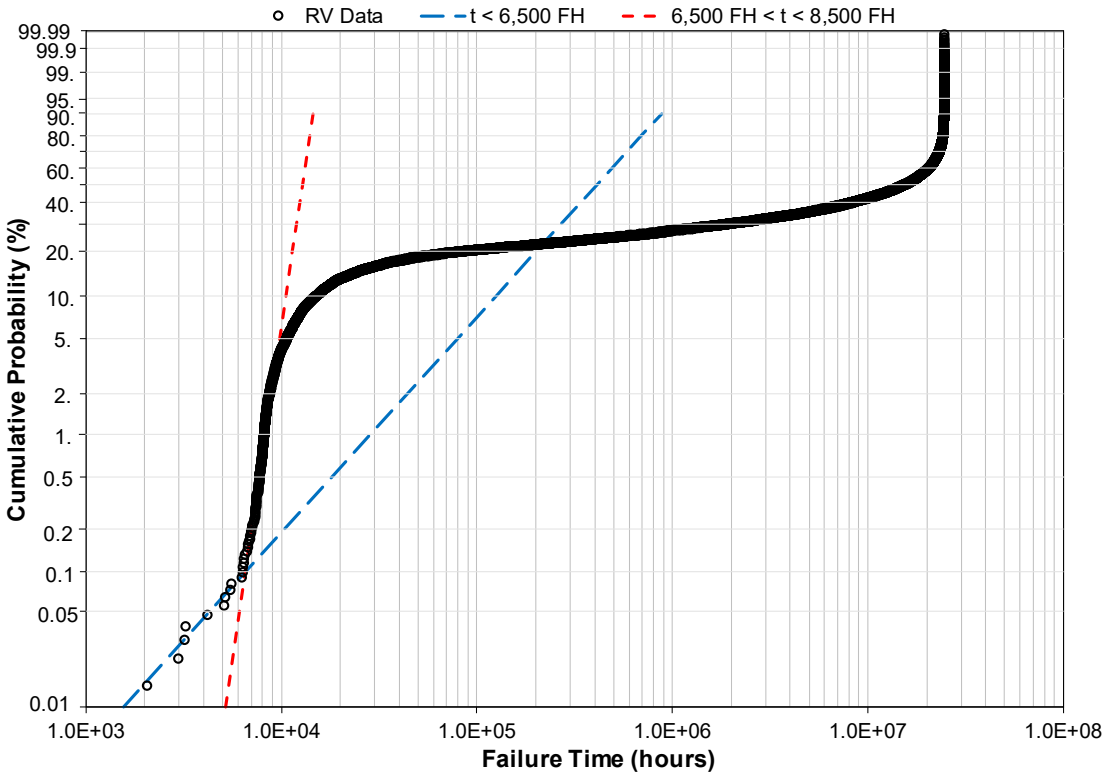

Figure 54. Weibull Plot and Fit to Tail for Trial 9

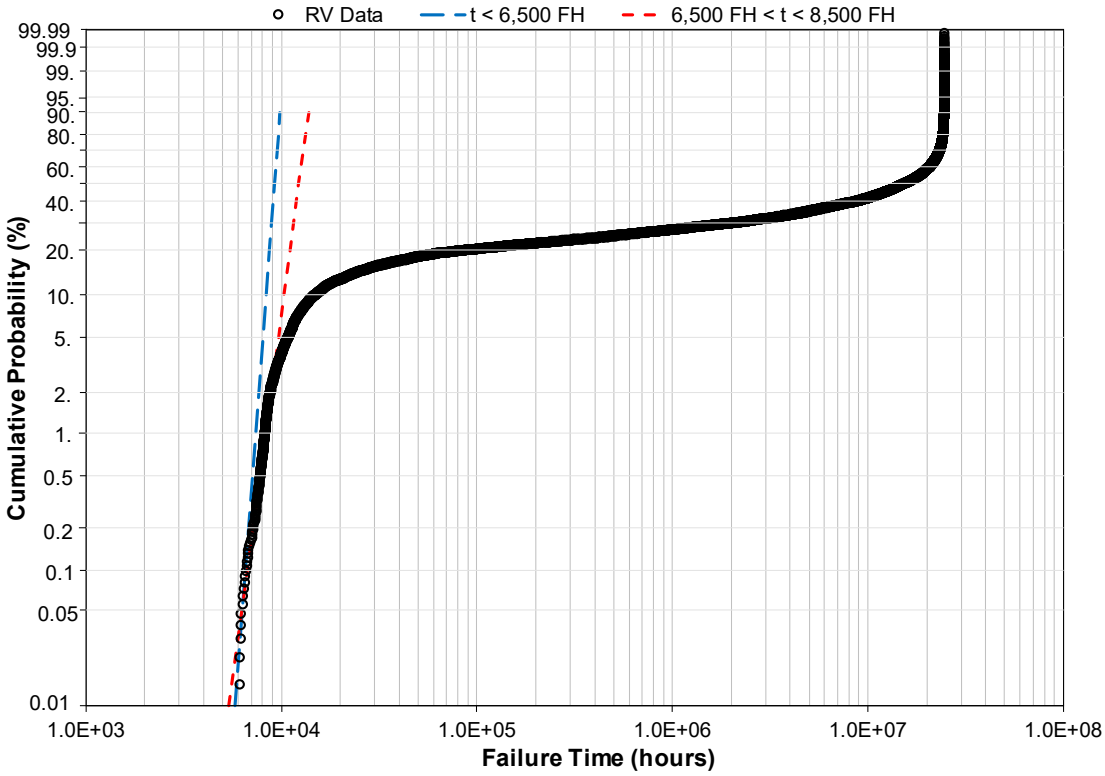

Figure 55. Weibull Plot and Fit to Tail for Trial 10

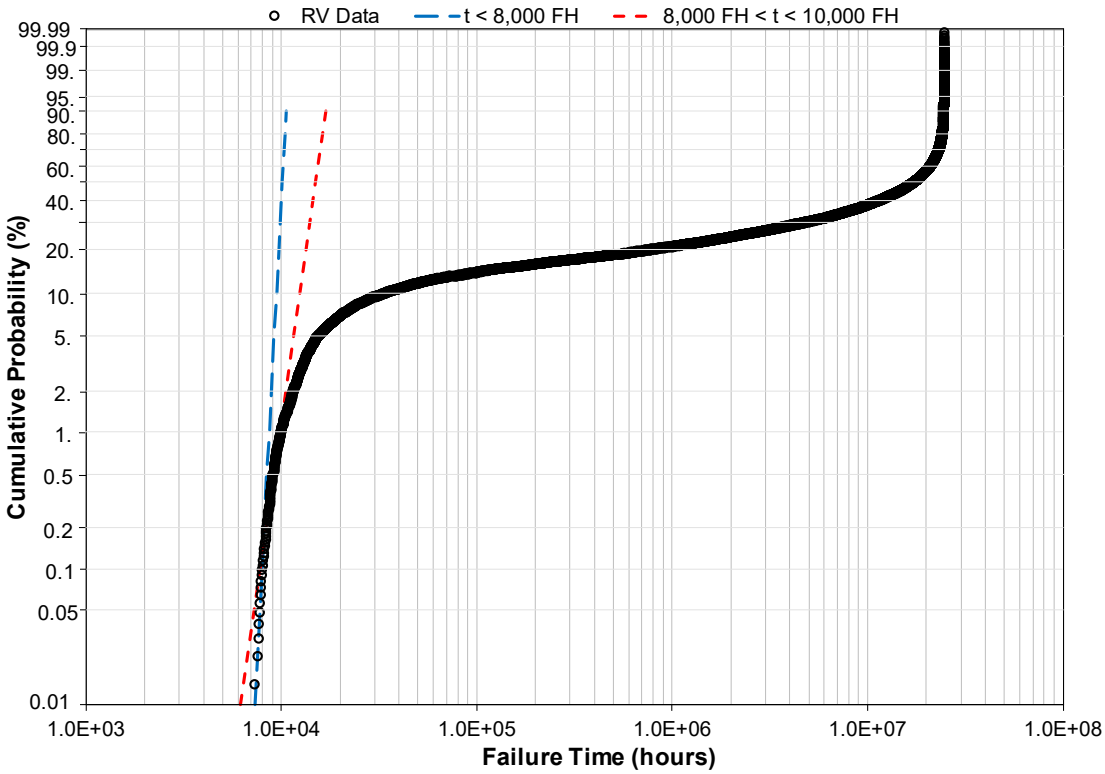

Figure 56. Weibull Plot and Fit to Tail for Trial 11

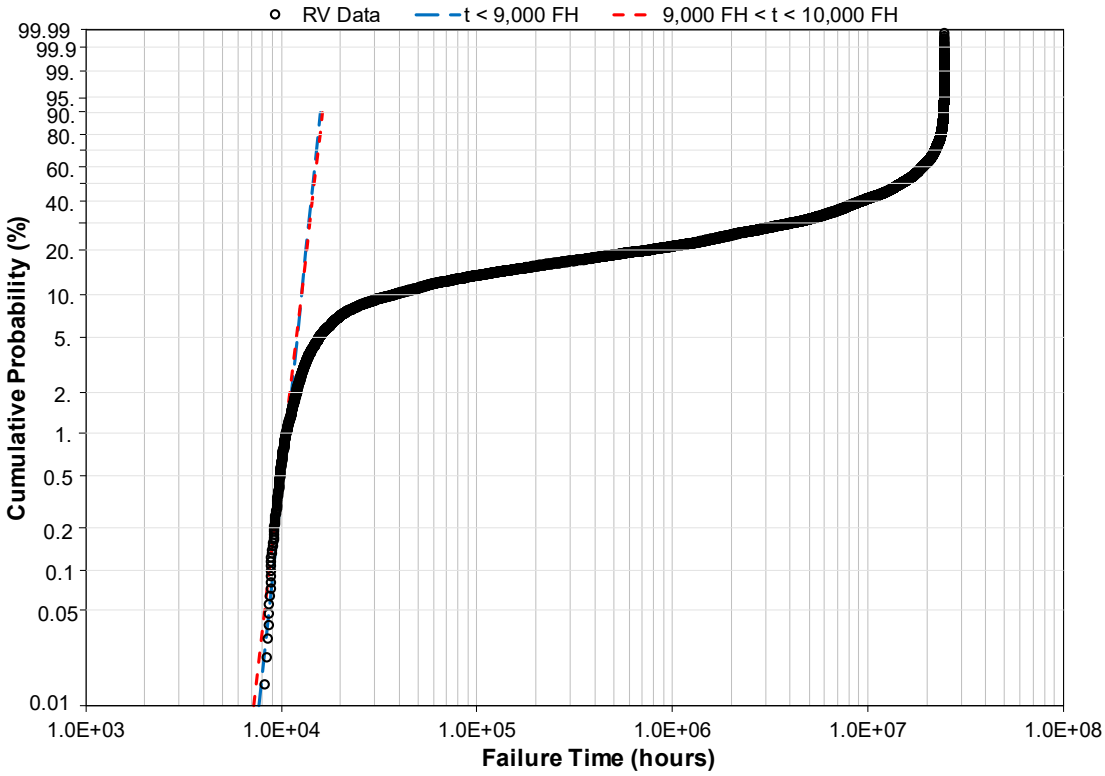

Figure 57. Weibull Plot and Fit to Tail for Trial 12

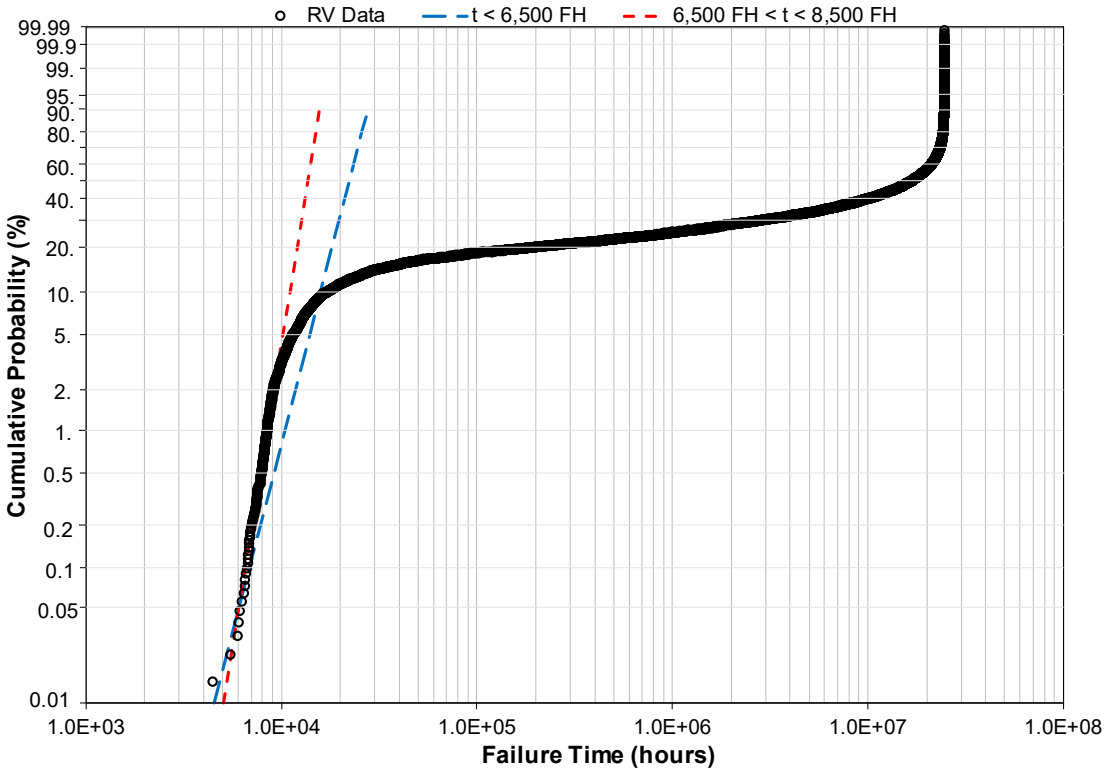

Figure 58. Weibull Plot and Fit to Tail for Trial 13

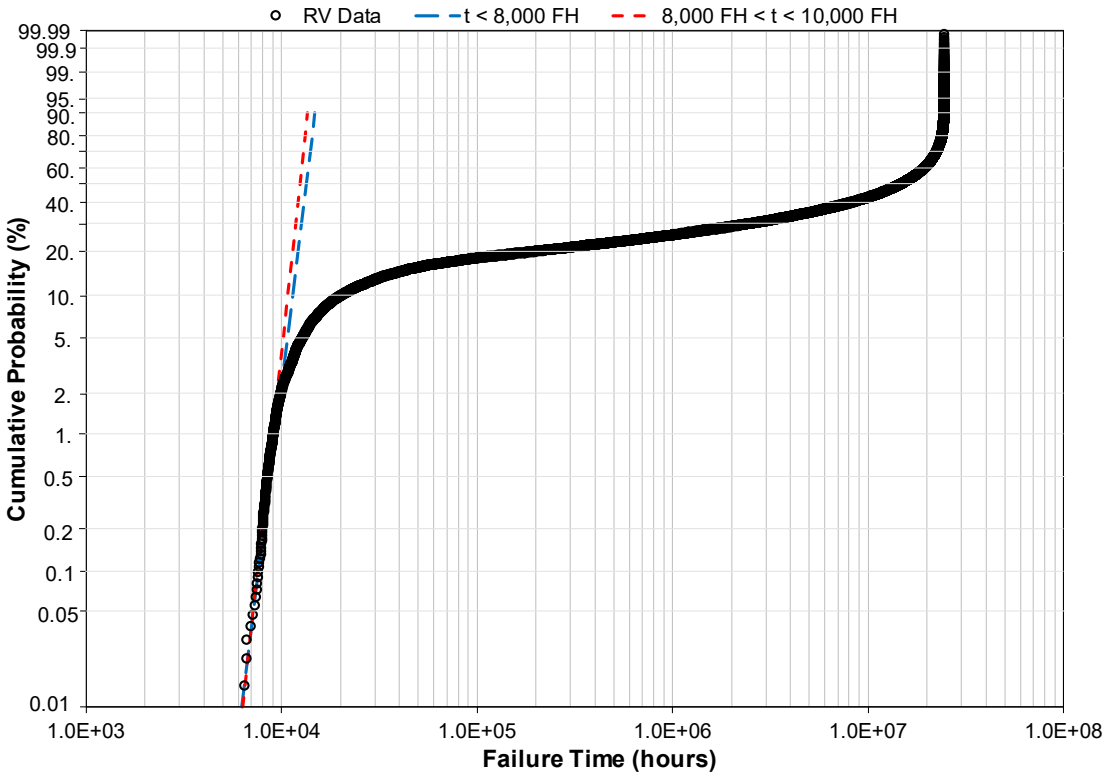

Figure 59. Weibull Plot and Fit to Tail for Trial 14

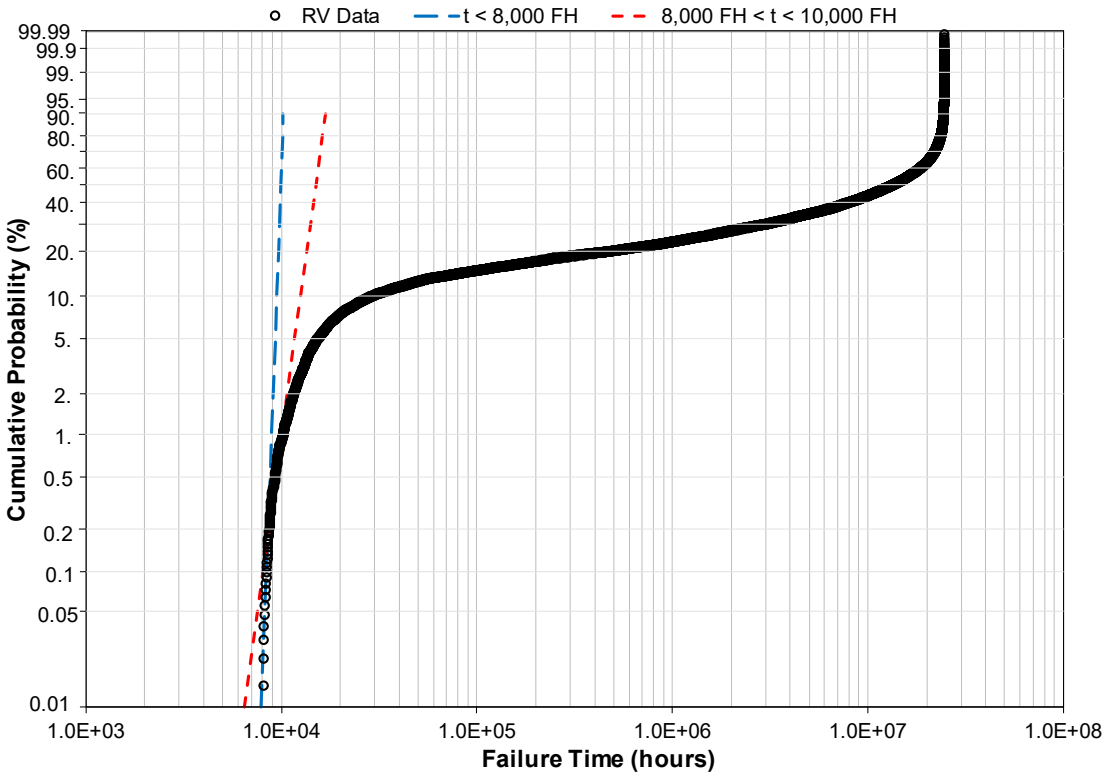

Figure 60. Weibull Plot and Fit to Tail for Trial 15

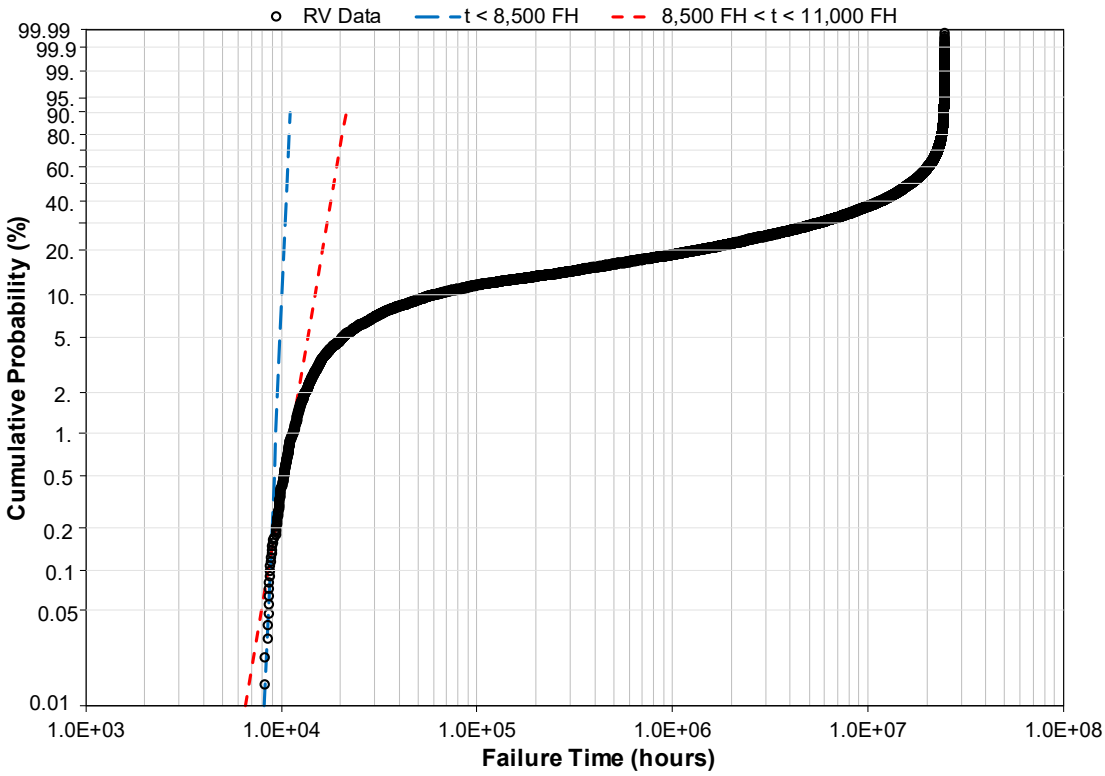

Figure 61. Weibull Plot and Fit to Tail for Trial 16

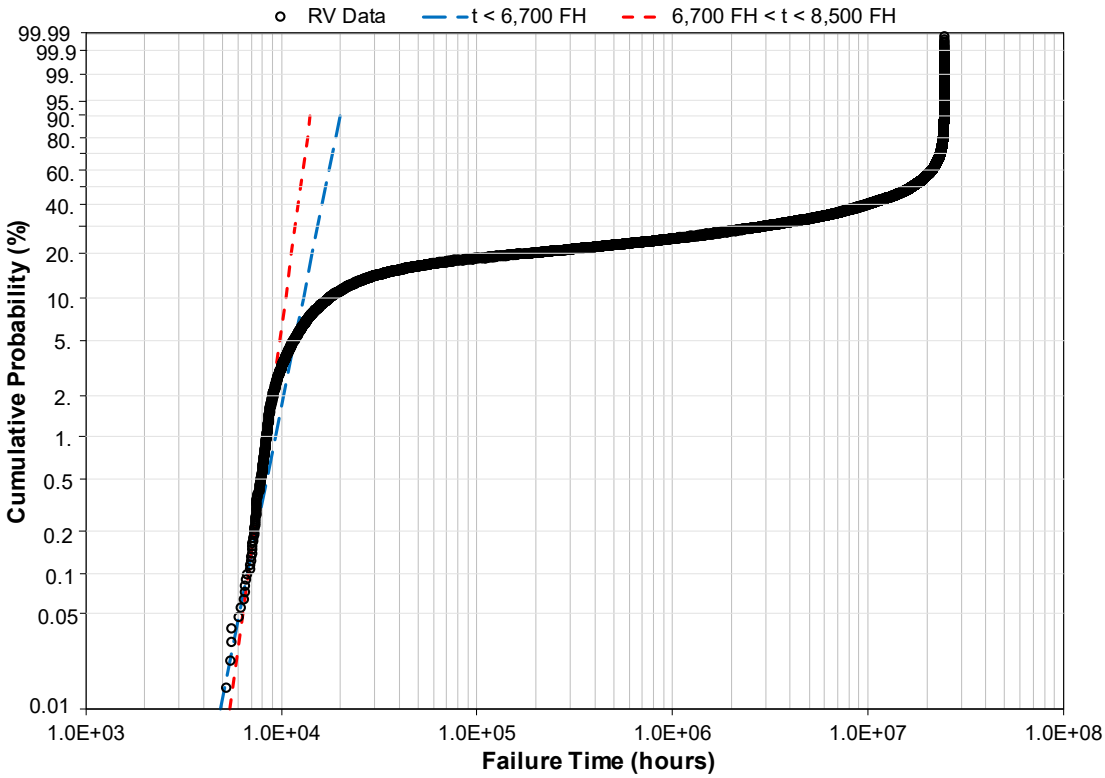

Figure 62. Weibull Plot and Fit to Tail for Trial 17

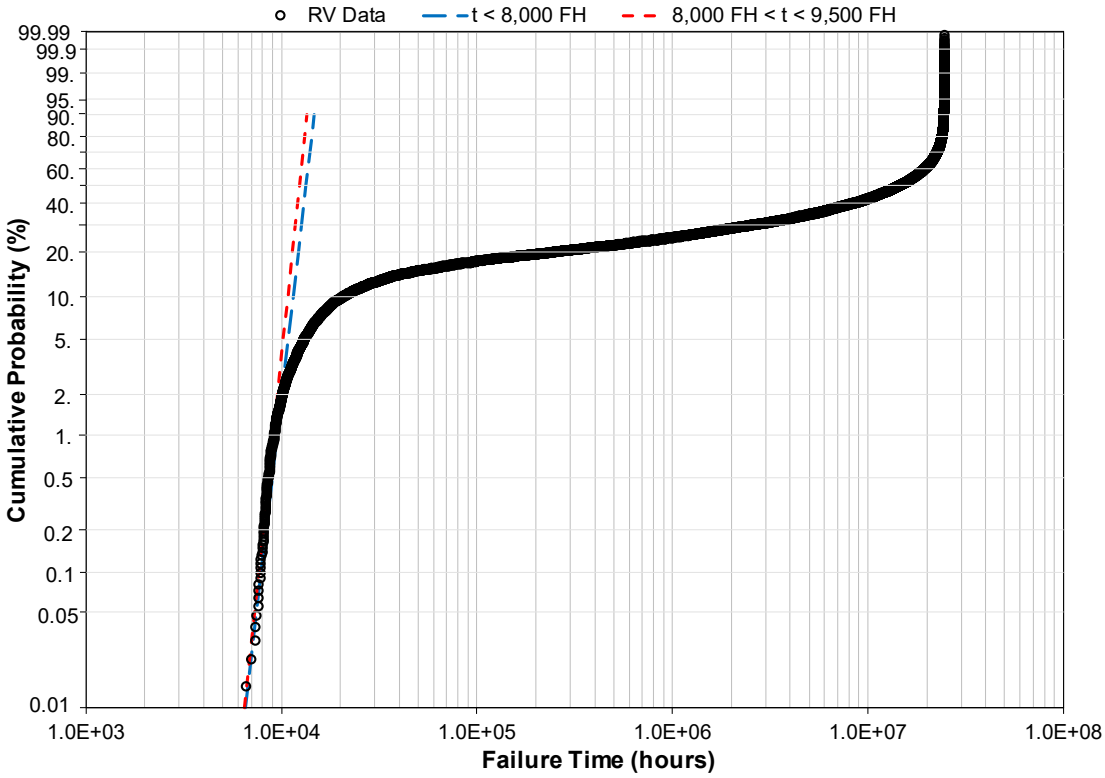

Figure 63. Weibull Plot and Fit to Tail for Trial 18

Table 23. Summary of Sensitivity Trials

	Variable						Results		
Trial No.	Shape (K_C)	Scale (K_C)	Shape (EIDS)	Scale (EIDS)	β (Max Stress)	α (Max Stress)	Shape Param POF < 0.001	Scale Param POF < 0.001	FH for SFPOF = 10^{-7}
1	12.49	88.89	0.374	0.00054	0.06	0.699	13.1712	13651.93	6424.34
2	14.5	93.9	0.424	0.00064	0.1	0.75	39.0665	10003.89	7577.88
3	10.5	83.9	0.324	0.00044	0.02	0.65	7.0454	18882.39	4844.17
4	12.49	88.89	0.424	0.00064	0.02	0.65	51.5036	9387.34	7563.13
5	14.5	93.9	0.324	0.00044	0.06	0.699	12.3235	12222.1	5414.79
6	10.5	83.9	0.374	0.00054	0.1	0.75	22.5702	10531.04	6632.57
7	12.49	93.9	0.374	0.00044	0.1	0.65	16.3088	12672.89	6830.18
8	14.5	83.9	0.424	0.00054	0.02	0.699	37.7633	10146.03	7620.20
9	10.5	88.89	0.324	0.00064	0.06	0.75	1.586	518090.9	1509.19
10	12.49	83.9	0.324	0.00064	0.1	0.699	19.1608	9390.91	5437.50
11	14.5	88.89	0.374	0.00044	0.02	0.75	27.3881	10231.76	6952.84
12	10.5	93.9	0.424	0.00054	0.06	0.65	13.8218	14920.57	7318.26
13	12.49	93.9	0.324	0.00054	0.02	0.75	5.5696	23791.11	4355.74
14	14.5	83.9	0.374	0.00064	0.06	0.65	11.615	13807.96	5893.59
15	10.5	88.89	0.424	0.00044	0.1	0.699	39.0665	10003.89	7577.88
16	12.49	83.9	0.424	0.00044	0.06	0.75	32.7244	10787.28	7791.73
17	14.5	88.89	0.324	0.00054	0.1	0.65	7.1392	17695.3	4576.35
18	10.5	93.9	0.374	0.00064	0.02	0.699	12.443	13711.53	6183.18

The effect of the distribution parameters on the FHs to an SFPOF of 10^{-7} are of interest. The average of the FHs for each parameter value are determined. For example, the average FHs for a value of the fracture toughness shape parameter equal to 12.49 is the average of the FHs from trials 1, 4, 7, 10, 13, and 16. When working with large numbers like these, it is easier to identify differences using common logarithms.

The average log FHs for each value of the parameters for the three distributions are compiled in Table 24. The average log FHs are considered in order to determine which parameters account for the most variation in FHs to SFPOF equal 10^{-7}. The results are most sensitive to these parameters. Plots of the average log FH versus the values of each parameter along with the actual data points are presented in Figure 64 to Figure 69.

Table 24. Average Log FHs to SFPOF=10^{-7} for Parameter Values of the Distributions

Fracture Toughness	
Shape	Avg Log FHs
10.5	3.703468925
12.49	3.797842926
14.5	3.794692719
Scale	
83.9	3.797713582
88.89	3.707917346
93.9	3.790373643

EIDS	
Shape	Avg Log FHs
0.324	3.605420984
0.374	3.811282793
0.424	3.879300794
Scale	
0.00044	3.811096108
0.00054	3.779244165
0.00064	3.705664298

Max. Stress	
Beta	Avg Log FHs
0.02	3.78638716
0.06	3.707762796
0.1	3.801854615
Alpha	
0.65	3.782276726
0.699	3.804922467
0.75	3.708805378

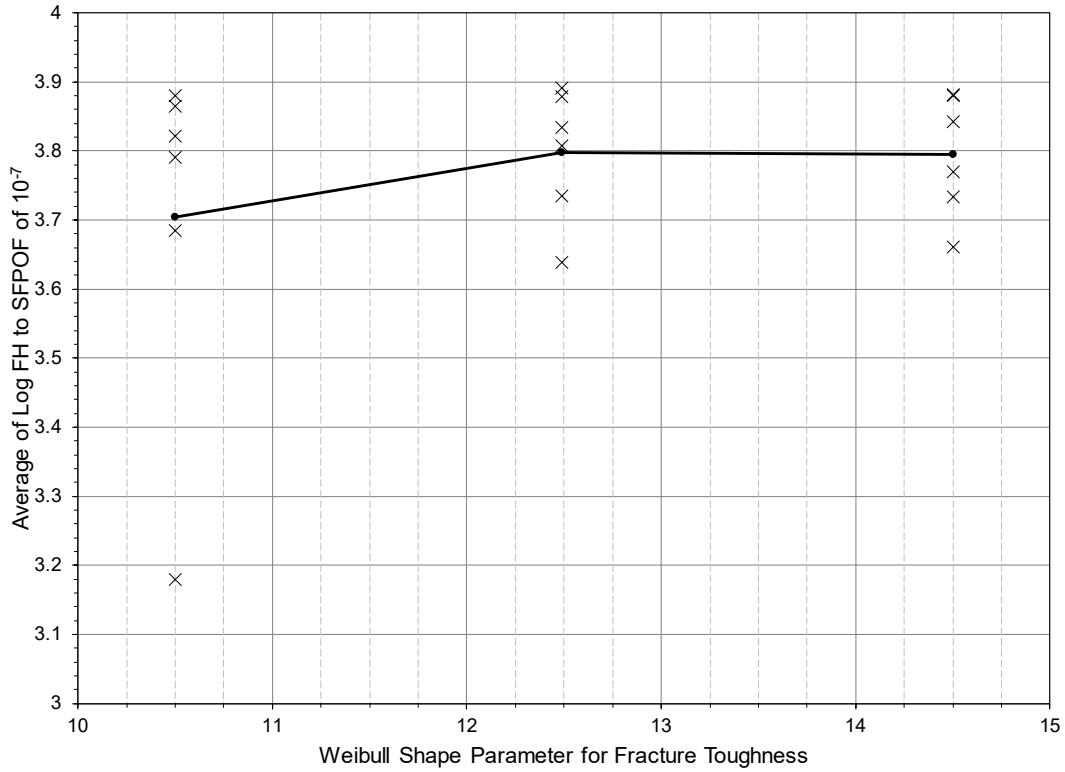

Figure 64. Average Log FHs vs. Shape Parameter for Fracture Toughness Distribution

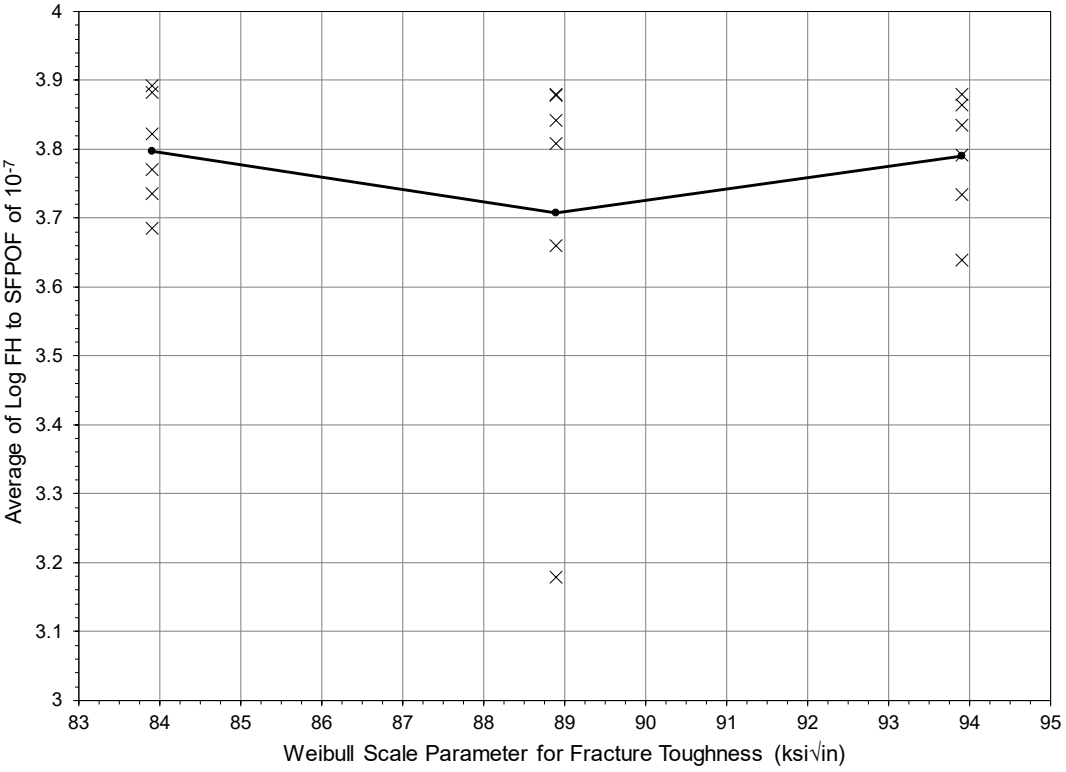

Figure 65. Average Log FHs vs. Scale Parameter for Fracture Toughness Distribution

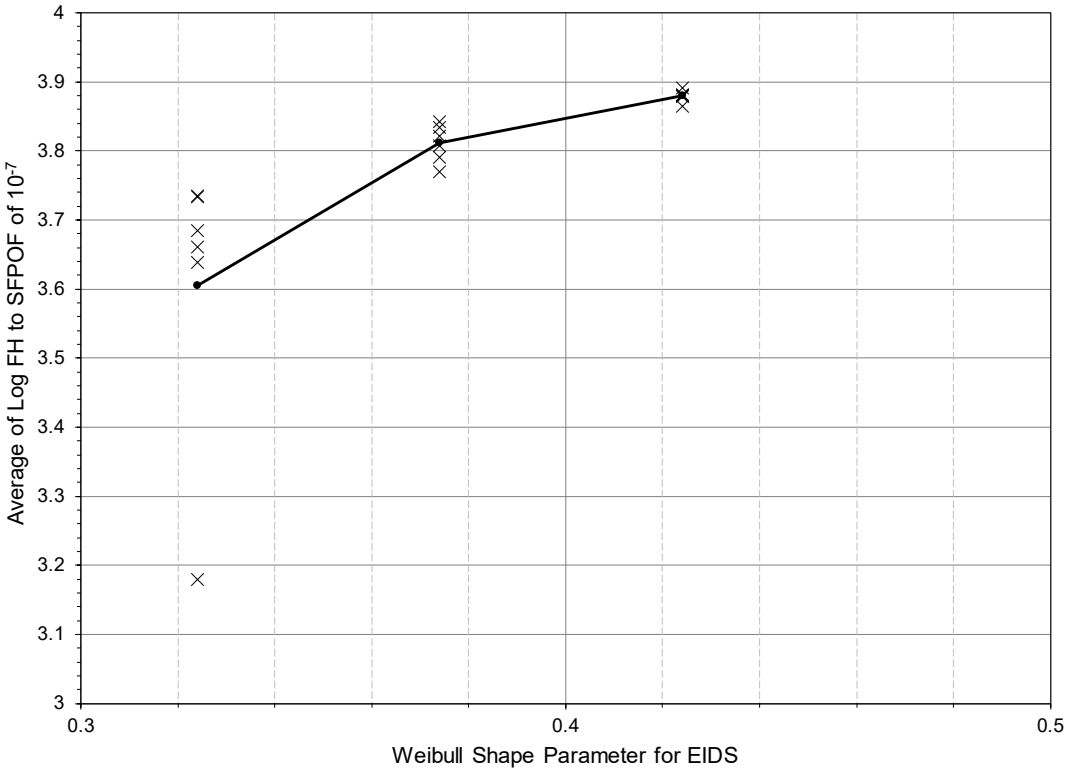

Figure 66. Average Log FHs vs. Shape Parameter for EIDS Distribution

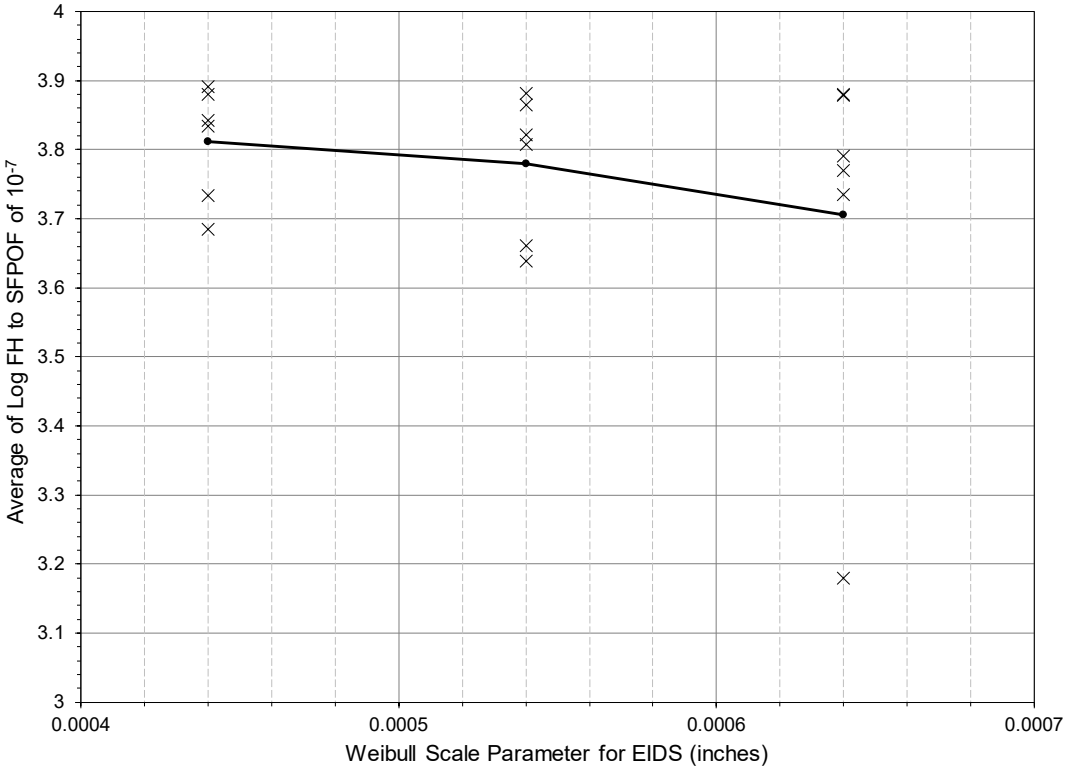

Figure 67. Average Log FHs vs. Scale Parameter for EIDS Distribution

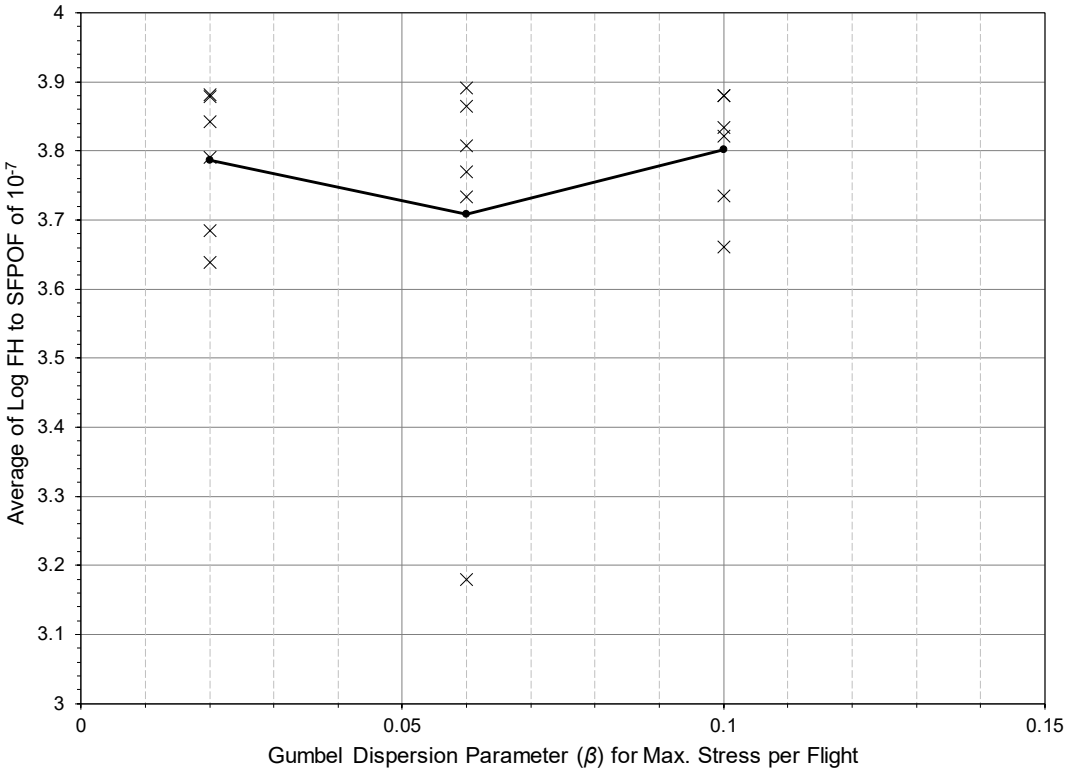

Figure 68. Average Log FHs vs. Dispersion Parameter for Max. Stress Distribution

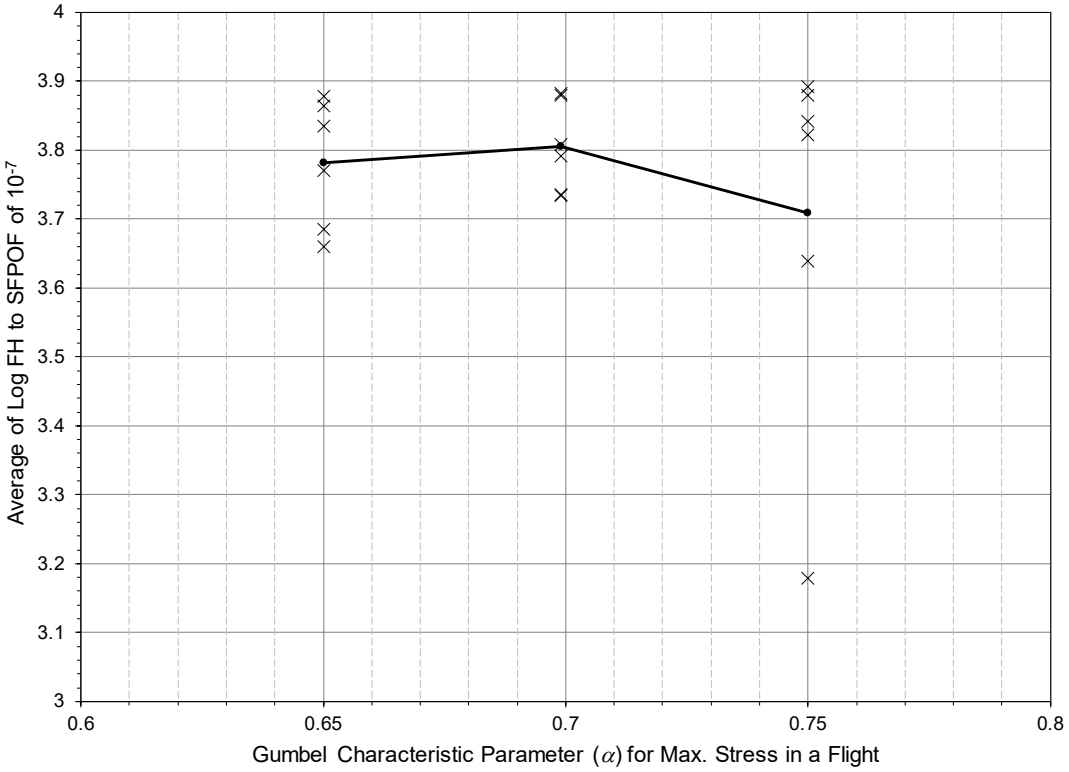

Figure 69. Average Log FHs vs. Characteristic Value for Max. Stress Distribution

The log FHs for all but Trial 9 are between 3.6 and 3.9 (3981 to 7943 FHs) for the range of values chosen. Trial 9 had a log FHs of just under 3.18 or 1509 FHs. For most of the distribution parameters, the log FHs are scattered across the range of 3.6 to 3.9 for every value of the parameter. However, the log FHs for the shape parameter of the EIDS distribution form tight clusters at each of the three values chosen for the sensitivity study – with the exception of Trial 9. This indicates that the shape parameter for the EIDS distribution has a dominant effect on the FHs to SFPOF equals 10^{-7}. In addition, the average log FHs for the shape parameter of the EIDS distribution span the entire range of log FHs, 3.6 to 3.9. The range of average log FHs for all of the other parameters is from 3.7 to 3.8 (5012 to 6310 FHs) which indicates that the FHs to SFPOF equals 10^{-7} is less sensitive to these other parameters.

It is also interesting to note that the average log FHs plots for the fracture toughness and maximum stress distributions show either a peak or a valley at the intermediate value for each parameter. The average log FHs for the EIDS distribution parameters show a monotonic trend: increasing life with increasing shape parameter, and decreasing life with increasing scale parameter. An increasing shape parameter indicates less scatter in the EIDS distribution and lower probability of a large EIDS that results in shorter life. An increasing scale parameter shifts the entire EIDS distribution to larger damage sizes.

3.4 Summary

In this section, the MCS process for determining the POF for a structural detail with deterioriating resistance to fracture was demonstrated. The MCS process can be idealized as selecting many different samples of a structural detail from the population of all possible details of this type that could be produced. Each sample will have a different EIDS. The growth of the EIDS in each sample is then simulated using a master crack growth curve. A maximum stress for a flight is selected at the start of each flight for each sample. The maximum stress for a flight and the crack size at the start of the flight are used to calculate the maximum stress intensity experienced during that flight. If the maximum stress intensity for a flight equals or exceeds the fracture toughness for that sample, fracture occurs during that flight. After any given flight, the fraction of the samples that have failed gives an estimate of the POF at that flight.

While a maximum of three random variables was used in these examples, additional random variables can be included if it is deemed that they are significant. Including more than three random variables eliminates some solution methods such as integration. However, MCS is able to handle however many random variables the analyst chooses to use.

Because of the uncertainty in the random variables used in the reliability assessment, sensitivity studies should be performed to see how sensitive the POF and SFPOF are to any assumptions, or lack of knowledge, about any of the random variables. A structured process using orthogonal arrays to reduce the number of additional reliability assessments required for a sensitivity study was demonstrated.

While it did not cause any issues in this example, the Weibull distribution for the EIDS has non-zero probability of having a crack greater than 2.75 inches, the physical limit of the part. It can be argued that an EIDS bigger than 1.0 inch is unlikely since it would be seen visually and repaired. Yet, the Weibull distribution has a small, but non-zero, probability for such an EIDS. This is not much of an issue in a MCS because drawing a sample with such a large EIDS is very unlikely. However, if a sample with 2.75 inches or larger EIDS was generated, it would result in

a very early failure increasing the POF unrealistically early in the life. For this reason, some analysts recommend using the beta distribution for the EIDS.

The beta distribution has upper and lower bounds, which eliminates the possibility of obtaining non-physical EIDS values [20]. The equation for the PDF of the beta distribution is

$$f(x) = \frac{(x-a)^{p-1}(b-x)^{q-1}}{B(p,q)(b-a)^{p+q-1}} \quad a \le x \le b; p, q > 0 \quad (76)$$

where *B(p,q)* is the beta function

$$B(\alpha,\beta) = \int_0^1 t^{\alpha-1}(1-t)^{\beta-1}dt \quad (77)$$

The lower and upper bounds of the distribution are *a* and *b*, respectively. The shape parameters are *p* and *q*. The beta distribution can take any number of shapes depending upon the values of *p* and *q*.

If obtaining an accurate value of the POF is goal of the reliability assessment, then using the beta distribution for the EIDS is desirable. If obtaining the order of magnitude of the POF is the objective, because of the uncertainties in the distributions of all the random variables, then a Weibull distribution for the EIDS may be satisfactory.

A similar argument can be made against using a normal distribution for the fracture toughness as the normal distribution extends infinitely in both directions. Negative fracture toughness values are unphysical. A beta distribution can be used for the fracture toughness as well, if the analyst wants to eliminate any possibility of unphysical results.

4 INSPECTIONS DURING THE LIFE

NDI of the location can be performed at selected times during the life of the specimen. The MCS described in Section 3.3 can be interrupted at prescribed inspection times, instead of running every sample to failure. The expected crack size distribution at the inspection time can be determined from the crack sizes recorded in the MCS. The effectiveness of the NDI can be modeled using a separate MCS. Any sample for which a crack is found with NDI can be repaired by drawing a new equivalent damage size for the sample from an equivalent repair damage size (ERDS) distribution. Then the overall MCS for flying the part can be resumed. An important part of modeling the impact of an inspection is determining the SFPOF prior to the inspection and after repairing any crack found. The algorithms for modeling all these actions are described in the following sections.

4.1 Example Definition

The example from Section 3.3 will be used here. The MCS is stopped at 5,000 FH to allow for an inspection. The shortest life for the example of Section 3.3 was 6,334 FH, so there are not any failures prior to this inspection. However, there will be some large cracks to be repaired.

Additional information needed for this example are the POD curve for the nondestructive inspection (NDI) used, and the equivalent repair damage size distribution (ERDS).

4.1.1 POD Curve for a NDI Procedure

The POD curve for a NDI procedure gives the probability of detecting a crack of a given size with that procedure. Many parameters affect the POD [21], so do not assume that the POD for a given sensor type on a particular structural component is transferable to a different component. Consult your local NDI expert before deciding on a POD curve to use in a risk analysis. The POD curve used in this example was created to illustrate features of the risk analysis for the crack sizes in the MCS. Any similarity to actual POD curves is coincidental. Do not use the example POD curve for a real aircraft risk analysis.

A number of different equations have been used to describe the POD [21, 22]. Table 25 lists several of these.

Table 25. Common Equations for Modeling POD

Name	Functional Form
Lockheed	$P(c) = exp\left[-\alpha \cdot c^{1-\beta}\right]$
Weibull	$P(c) = 1 - exp\left[-\alpha \cdot c^{\beta}\right]$
Probit	$P(c) = \Phi(\alpha + \beta c)^{*}$
Log Probit	$P(c) = \Phi(\alpha + \beta \cdot \ln(c))^{*}$
Log Odds – linear scale	$P(c) = \frac{exp[\alpha + \beta c]}{1 + exp[\alpha + \beta c]}$
Log Odds – log scale	$P(c) = \frac{\alpha \cdot c^{\beta}}{1 + \alpha \cdot c^{\beta}}$
Arcsine	$P(c) = sin^2(\alpha + \beta c)$

* Φ(x) is the CDF for the standard normal distribution

This example used the Log Odds – log scale equation for POD, equation (78). The graph of the POD is shown in Figure 70. Note that the numbers in equation (78) were chosen to give a POD curve that would give interesting results in the MCS. There is no rational method for developing this curve. You must work with your NDI experts to develop a realistic POD model for your particular situation.

$$P(c) = \frac{13{,}000 \cdot c^5}{1 + 13{,}000 \cdot c^5} \tag{78}$$

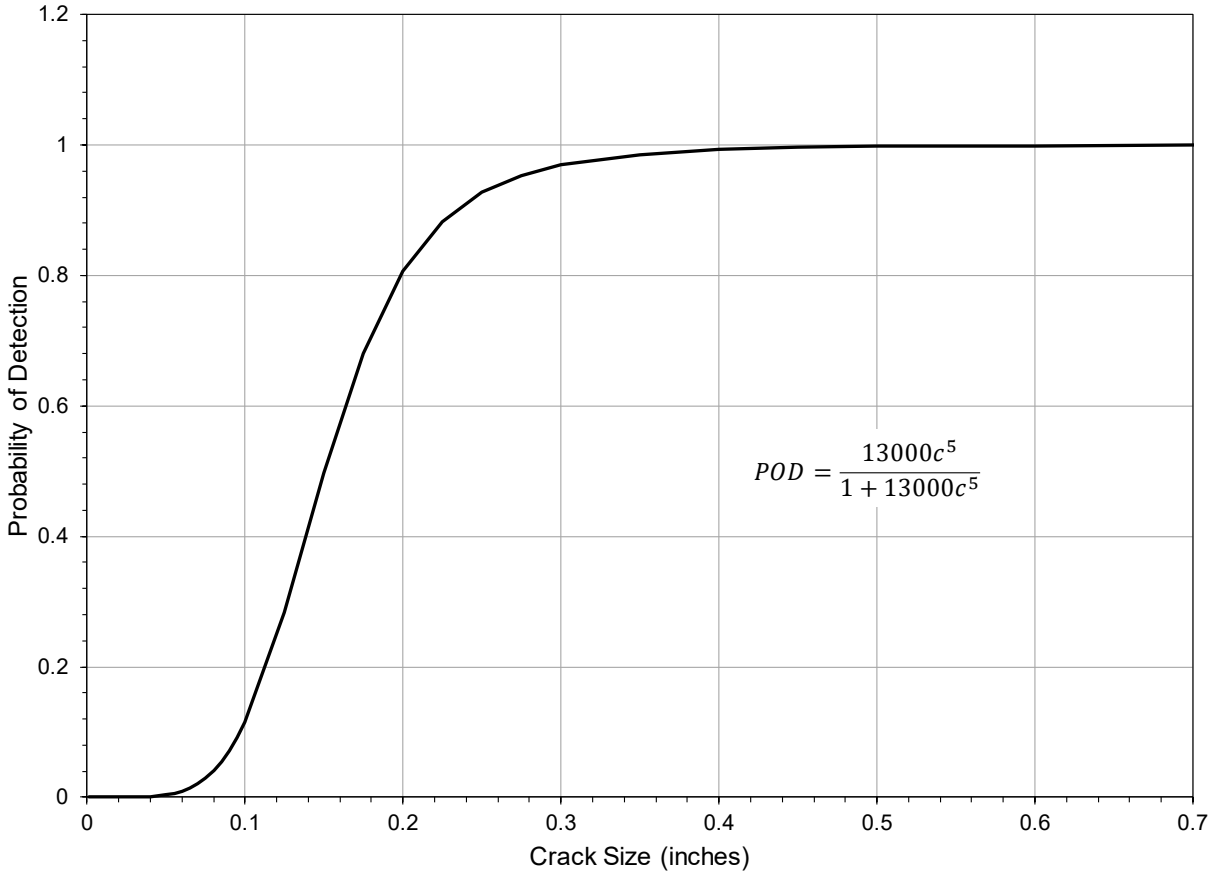

Figure 70. POD Plot

4.1.2 Equivalent Repair Damage Size Distribution

Whenever a crack is found by the inspection, it is assumed that it is repaired. The repair does not take the equivalent damage size to zero, but to a smaller size than before. Determining the distribution of equivalent damage sizes after a repair is just as difficult, if not harder, as determining the EIDS. No organization want to pay to conduct a large-scale test program on repaired structure to determine the size of the damage from which cracks form. As a result, the EIDS distribution is often used as the post-repair damage size distribution, ERDS. In the absence of data, a sensitivity study with different ERDS distributions can be performed to see how much the ERDS distribution effects how the aircraft will be managed and maintained.

For this example, the ERDS distribution is a modification to the EIDS distribution in Section 3.2.3. Recognizing that repairs may not be made under conditions as well controlled as initial

manufacture, the shape parameter for the EIDS distribution was decreased from 0.374 to 0.35 to reflect the potential for more variation in the equivalent damage size. The scale parameter for the EIDS distribution was increased from 0.00054 to 0.00075 inch to reflect the potential for the mean damage size being slightly larger. The ERDS distribution is compared to the EIDS distribution in Figure 71.

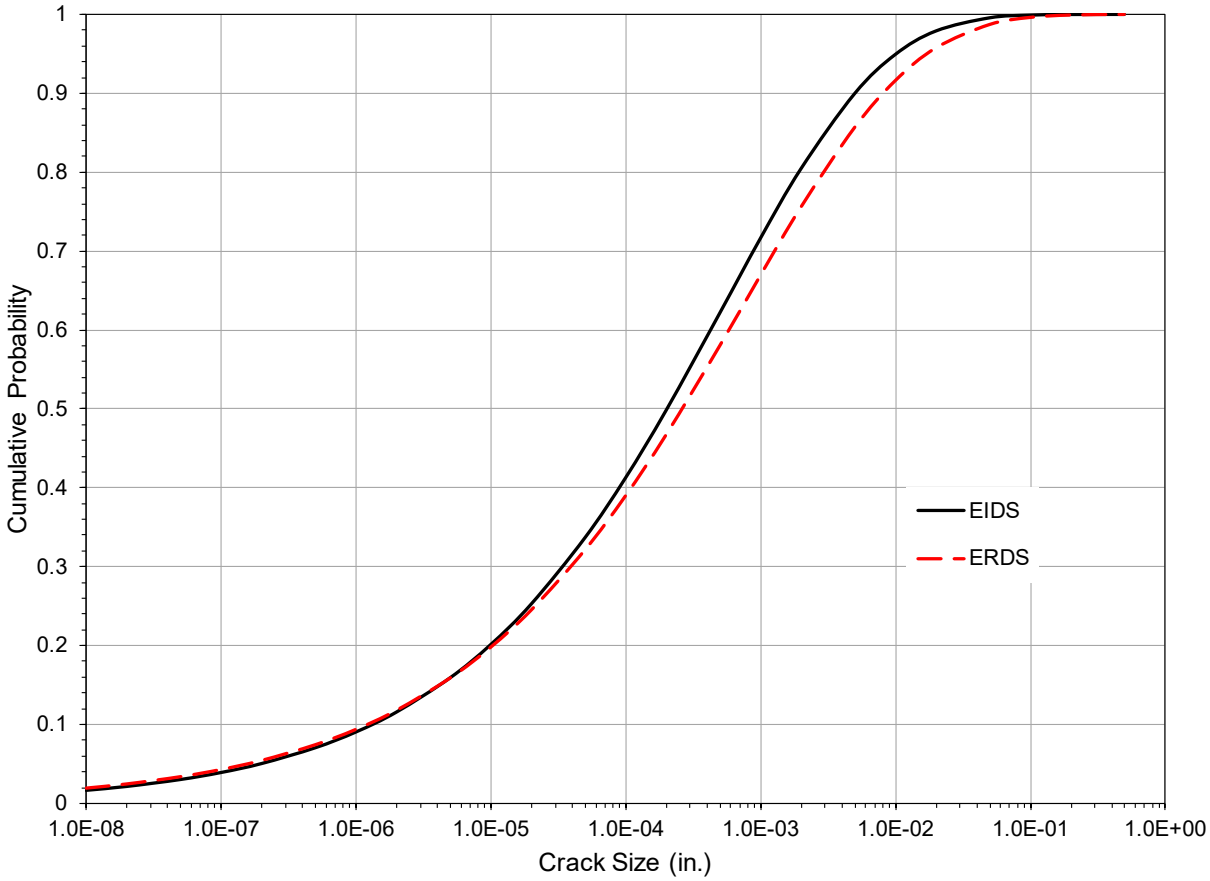

Figure 71. Comparison of EIDS and ERDS Distributions

4.2 Inspection and Repair

The inspection at 5,000 FH is simulated using the POD curve previous specified in Section 4.1.1. It is assumed that whenever a crack is detected in the simulation that it is repaired with the resulting equivalent damage size after the repair drawn from the ERDS distribution. The simulation marches through each of the 12,000 samples of cracks after 5,000 flights one at a time. The process is as follows and the subroutine is given in Appendix B.4.

Step 1. Determine the POD for the crack size of sample *i*. For the *i*th sample, put the crack size at the end of 5,000 flights into the POD equation to obtain the probability of detecting the crack, POD_i.

Step 2. Was the crack detected? Using a (pseudo-) random number generator, generate a number, *P*, between 0 and 1 that represents the probability that the crack will be detected. If $P \leq POD_i$, the crack was detected. Go to Step 3 to repair the crack.

If $P > POD_i$, the crack was not detected. Move to the next sample, $i+1$, and go to Step 1.

Step 3. Determine the crack size after repair. Using a (pseudo-) random number generator, generate a number, P, between 0 and 1 that represents the CDF of the equivalent repaired damage size, $ERDS_i$. Use P in the inverse CDF equation for the Weibull distribution to find the equivalent damage size after repair for this sample. The inverse CDF for the Weibull distribution is

$$ERDS_i = \alpha \left[LN\left(\frac{1}{1-P}\right)\right]^{1/\beta} \quad (79)$$

where β is the shape parameter and α is the scale parameter, 0.35 and 0.00075 respectively in this example. Replace the crack size after 5,000 flights with $ERDS_i$.

Move to the next sample, $i+1$, and go to Step 1.

Repeat these three steps until all MCS crack growth samples have been inspected. The effect of the inspection can be seen by comparing the crack size distributions at the end of flight 5,000 and after the inspection.

4.2.1 Crack Size Distribution Prior to an Inspection

The first 50 samples obtained by for this example are presented in Table 26. The crack sizes in the last column, $c_{end(f)}$, are the crack sizes prior to the inspection. The CDF of the crack size distribution prior to inspection is found by rank ordering the crack sizes in the last column, $c_{end(f)}$, using median rank (Section 2.3.1). If any of the samples failed before flight 5,000, the crack size should be treated as the largest crack physically possible in the ranking. If there were any failures prior to inspection, the time to the inspection needs to be shorter since the goal is to find cracks before they cause failure.

The resulting crack size CDF prior to inspection for this example is plotted on a Weibull graph in Figure 72. The plot shows four distinct regions that are nearly straight lines. This indicates that a Weibull distribution can be used to model each of the distinct regions of the curve. The CDF is represented as the following piecewise function.

$$Pr(C \le c) = 1 - exp\left[-\left(\frac{c}{1.01 \times 10^{-7}}\right)^{70.1}\right] \text{for } c \le 9.64E-08 \quad (80a)$$

$$Pr(C \le c) = 1 - exp\left[-\left(\frac{c}{0.00054}\right)^{0.377}\right] \text{ for } 9.64E\text{-}08 \le c \le 0.00482 \quad (80b)$$

$$Pr(C \le c) = 1 - exp\left[-\left(\frac{c}{3.4098 \times 10^{-6}}\right)^{0.11378}\right] \text{ for } 0.00482 \le c \le 0.449 \quad (80c)$$

$$Pr(C \le c) = 1 - exp\left[-\left(\frac{c}{0.11205}\right)^{0.96586}\right] \quad for\ 0.449 < c \quad (80d)$$

Figure 73 shows a close-up of the upper tail of the distribution, which is the region of most interest for failure.

Table 26. Example Results of MCS to 5,000 Flights

Trial #	K_c (ksi√inch)	Flight Count, f	$c_{start}(f)$ (inch)	$\sigma_{max}(f)$ (ksi)	$K_{max}(f)$ (ksi√inch)	$c_{end}(f)$ (inch)
1	96.01	5000	0.00717	12.85	3.85	0.00717
2	94.46	5000	0.00003	12.32	0.23	0.00003
3	89.40	5000	0.00017	12.42	0.58	0.00017
4	82.78	5000	0.00027	11.22	0.65	0.00027
5	79.44	5000	0.00001	10.60	0.13	0.00001
6	85.71	5000	0.00001	11.62	0.14	0.00001
7	79.80	5000	0.00066	11.74	1.07	0.00066
8	97.65	5000	0.00002	12.25	0.17	0.00002
9	78.71	5000	0.00026	9.51	0.54	0.00026
10	87.49	5000	0.00057	14.25	1.20	0.00057
11	87.63	5000	0.00005	12.57	0.32	0.00005
12	92.07	5000	0.00071	12.07	1.14	0.00071
13	91.30	5000	0.00086	12.83	1.33	0.00086
14	72.12	5000	0.00019	11.56	0.56	0.00019
15	93.21	5000	0.00143	10.48	1.41	0.00143
16	100.44	5000	0.00001	11.79	0.15	0.00001
17	91.77	5000	3.91E-07	11.43	0.03	3.91E-07
18	77.27	5000	0.00001	11.00	0.11	0.00001
19	92.60	5000	4.59E-07	11.39	0.03	4.59E-07
20	86.79	5000	1.07E-06	11.06	0.04	1.07E-06
21	67.64	5000	0.00008	10.36	0.34	0.00008
22	81.27	5000	0.00061	14.79	1.29	0.00061
23	69.51	5000	0.00283	12.05	2.28	0.00283
24	92.09	5000	0.14055	11.53	13.03	0.14065
25	84.88	5000	0.00009	11.76	0.39	0.00009
26	75.40	5000	0.00256	11.26	2.03	0.00256
27	66.47	5000	0.33798	11.00	13.56	0.33812
28	94.64	5000	3.35E-06	10.42	0.07	3.35E-06
29	91.22	5000	3.90E-07	10.62	0.02	3.90E-07
30	90.02	5000	0.00123	11.65	1.45	0.00123
31	83.21	5000	0.00265	11.33	2.08	0.00265
32	86.79	5000	0.00008	10.71	0.33	0.00008
33	90.24	5000	0.00006	10.25	0.28	0.00006
34	81.65	5000	0.00081	14.52	1.47	0.00081
35	78.33	5000	0.00003	10.52	0.19	0.00003
36	93.22	5000	1.69E-07	13.92	0.02	1.69E-07
37	82.62	5000	0.00040	11.45	0.81	0.00040
38	69.59	5000	0.00168	11.14	1.62	0.00168
39	69.42	5000	0.00017	11.52	0.52	0.00017
40	84.91	5000	0.24883	11.24	13.26	0.24895
41	86.19	5000	0.00249	11.10	1.97	0.00249
42	83.01	5000	0.00011	13.97	0.52	0.00011
43	87.38	5000	0.00000	10.09	0.02	0.00000
44	95.00	5000	0.00166	13.69	1.99	0.00166
45	88.55	5000	0.00031	11.69	0.73	0.00031
46	90.85	5000	4.42E-06	12.98	0.10	4.42E-06
47	80.37	5000	1.24E-06	18.67	0.07	1.24E-06
48	87.97	5000	0.00208	11.88	1.93	0.00208
49	77.37	5000	0.00013	11.41	0.46	0.00013
50	87.46	5000	0.00002	11.07	0.18	0.00002

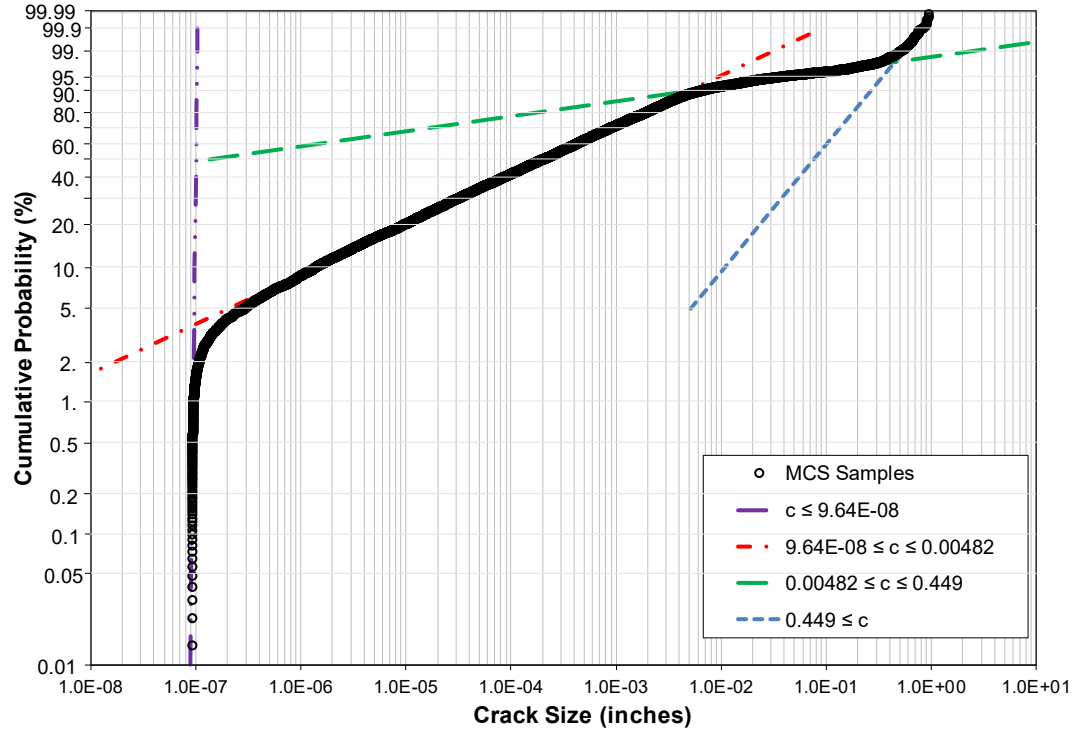

Figure 72. Weibull Plot of Crack Size Distribution after 5,000 Flights

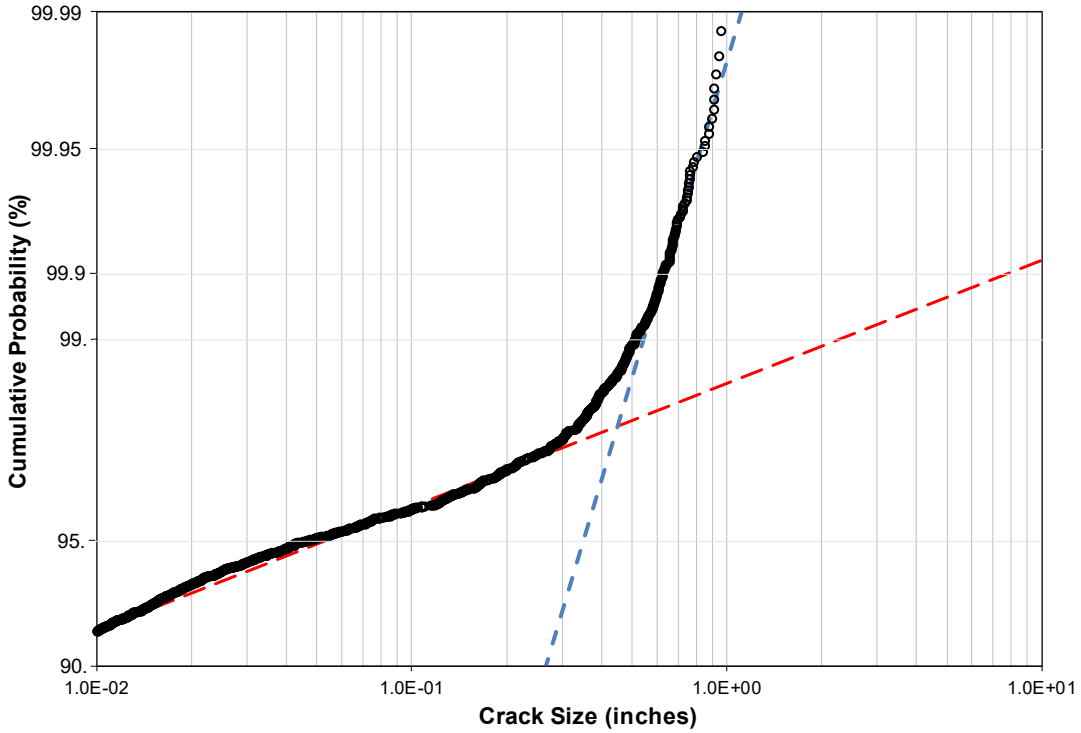

Figure 73. Distribution fit to Upper Tail of Crack Size Distribution at 5,000 Flights
Red dashed line is equation (87). Blue dashed line is equation (88).

4.2.2 Crack Size Distribution after Inspection and Repair

The first 50 samples of the crack size distribution after running the subroutine in Appendix B.4 using the POD function of Section 4.1.1 and the ERDS distribution of Section 4.1.2 are given in the last column, $c_{I\&R(f)}$, of Table 27. Rank ordering the 12,000 crack sizes in the last column of the table gives the CDF for the crack sizes after inspection and repair. This CDF is plotted on a Weibull graph in Figure 74. There are now five segments to the CDF which are described by the function

$$Pr(C \le c) = 1 - exp\left[-\left(\frac{c}{0.00441}\right)^{0.625}\right] for\ c \le 9.17E\text{-}08 \quad (81a)$$

$$Pr(C \le c) = 1 - exp\left[-\left(\frac{c}{1.01 \times 10^{-7}}\right)^{69.5}\right] \text{for } 9.17\text{E-}08 \le c \le 9.64\text{E-}08 \quad (81b)$$

$$Pr(C \le c) = 1 - exp\left[-\left(\frac{c}{0.000463}\right)^{0.383}\right] \text{ for } 9.64\text{E-}08 \le c \le 0.0052 \quad (81c)$$

$$Pr(C \le c) = 1 - exp\left[-\left(\frac{c}{8.56 \times 10^{-5}}\right)^{0.2256}\right] \text{ for } 0.0052 \le c \le 0.10881 \quad (81d)$$

$$Pr(C \le c) = 1 - exp\left[-\left(\frac{c}{0.005618}\right)^{0.5441}\right] \ for\ 0.10881 < c \quad (81e)$$

Note that the large cracks in the distribution of Figure 73 are not in Figure 74. There is an additional segment for very small cracks in Figure 74 because of the large cracks that were detected and repaired. The middle part of the distribution is unaffected.

Table 27. Example of Crack Sizes after Inspection and Repair

Trial #	Flight Count, *f*	$c_{start}(f)$ (inch)	$K_{max}(f)$ (ksi√inch)	$c_{end}(f)$ (inch)	Inspection (Detect or Not)	$c_{I\&R}(f)$ (inch)
1	5000	0.00717	3.85	0.00717	N	0.00717
2	5000	0.00003	0.23	0.00003	N	0.00003
3	5000	0.00017	0.58	0.00017	N	0.00017
4	5000	0.00027	0.65	0.00027	N	0.00027
5	5000	0.00001	0.13	0.00001	N	0.00001
6	5000	0.00001	0.14	0.00001	N	0.00001
7	5000	0.00066	1.07	0.00066	N	0.00066
8	5000	0.00002	0.17	0.00002	N	0.00002
9	5000	0.00026	0.54	0.00026	N	0.00026
10	5000	0.00057	1.20	0.00057	N	0.00057
11	5000	0.00005	0.32	0.00005	N	0.00005
12	5000	0.00071	1.14	0.00071	N	0.00071
13	5000	0.00086	1.33	0.00086	N	0.00086
14	5000	0.00019	0.56	0.00019	N	0.00019
15	5000	0.00143	1.41	0.00143	N	0.00143
16	5000	0.00001	0.15	0.00001	N	0.00001
17	5000	3.91E-07	0.03	3.91E-07	N	3.91E-07
18	5000	0.00001	0.11	0.00001	N	0.00001
19	5000	4.59E-07	0.03	4.59E-07	N	4.59E-07
20	5000	1.07E-06	0.04	1.07E-06	N	1.07E-06
21	5000	0.00008	0.34	0.00008	N	0.00008
22	5000	0.00061	1.29	0.00061	N	0.00061
23	5000	0.00283	2.28	0.00283	N	0.00283
24	5000	0.14055	13.03	0.14065	N	0.14065
25	5000	0.00009	0.39	0.00009	N	0.00009
26	5000	0.00256	2.03	0.00256	N	0.00256
27	5000	0.33798	13.56	0.33812	D	0.00125
28	5000	3.35E-06	0.07	3.35E-06	N	3.35E-06
29	5000	3.90E-07	0.02	3.90E-07	N	3.90E-07
30	5000	0.00123	1.45	0.00123	N	0.00123
31	5000	0.00265	2.08	0.00265	N	0.00265
32	5000	0.00008	0.33	0.00008	N	0.00008
33	5000	0.00006	0.28	0.00006	N	0.00006
34	5000	0.00081	1.47	0.00081	N	0.00081
35	5000	0.00003	0.19	0.00003	N	0.00003
36	5000	1.69E-07	0.02	1.69E-07	N	1.69E-07
37	5000	0.00040	0.81	0.00040	N	0.00040
38	5000	0.00168	1.62	0.00168	N	0.00168
39	5000	0.00017	0.52	0.00017	N	0.00017
40	5000	0.24883	13.26	0.24895	D	0.00006
41	5000	0.00249	1.97	0.00249	N	0.00249
42	5000	0.00011	0.52	0.00011	N	0.00011
43	5000	0.00000	0.02	0.00000	N	0.00000
44	5000	0.00166	1.99	0.00166	N	0.00166
45	5000	0.00031	0.73	0.00031	N	0.00031
46	5000	4.42E-06	0.10	4.42E-06	N	4.42E-06
47	5000	1.24E-06	0.07	1.24E-06	N	1.24E-06
48	5000	0.00208	1.93	0.00208	N	0.00208
49	5000	0.00013	0.46	0.00013	N	0.00013
50	5000	0.00002	0.18	0.00002	N	0.00002

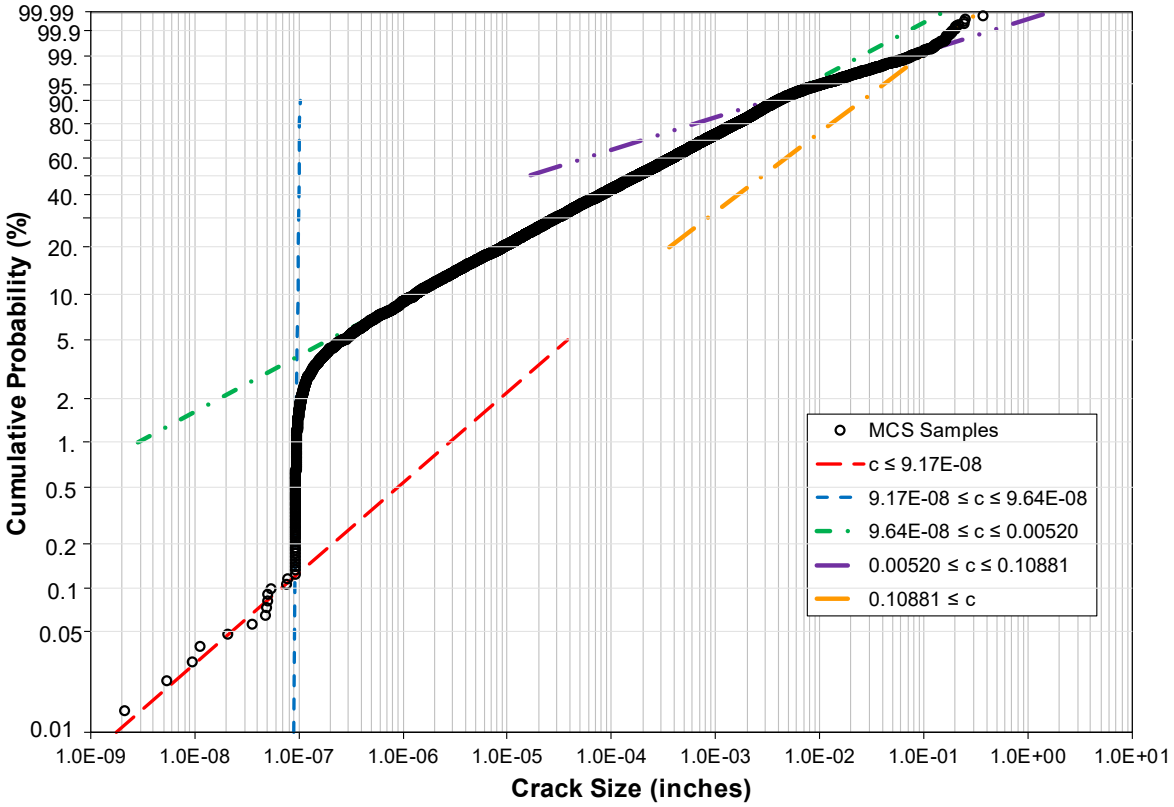

Figure 74. Plot of Post-Inspection and Repair Crack Size Distribution

4.2.3 Effect of Inspection on SFPOF

Another measure of the effectiveness of an inspection is the change in the SFPOF from before the inspection to after the inspection. Calculation of the SFPOF requires the values from the failure PDF and CDF. The PDF and CDF values from before and after the inspection are needed to make this comparison. The determination of the values, and the resulting SFPOFs, are presented in the following sections.

4.2.3.1 SFPOF Prior to Inspection

The SFPOF at the end of flight 5,000 and prior to any inspection and repair is calculated by determining the failure PDF and CDF at the end of flight 5,000. The value of the failure CDF, or the POF, at the end of flight 5,000 was found via MCS using the fracture toughness distribution (Section 3.3.2), the distribution of the maximum stress in a flight (Section 3.3.4.1), and the crack size distribution at the end of flight 5,000 (Section 4.2.1).

The failure PDF is the derivative of the failure CDF function. This was estimated as the difference in the value of failure CDF over one flight, i.e., from the start of flight 5,000 to the end of flight 5,000. The value of the failure CDF, or POF, at the start of flight 5,000 was found using the distribution $c_{start(f)}$ for flight 5,000, the fourth column of Table 26. The calculation of the POFs at the start and end of flight 5,000 are presented below along with the determination of the PDF and the SFPOF.

The crack size distribution is the only variable that changes in the POF calculations at the start and end of flight 5,000. The change in the crack size distribution is small since the cracks in the

MCS samples grow very little in one flight. Care must be taken to ensure that the difference between the two crack size distributions is captured.

4.2.3.1.1 POF at the End of Flight 5,000

The POF was calculated using the integral in equation (22). The integral was estimated using Importance Sampling (Section 2.3.3), drawing random values for each variable and seeing if the combination results in failure or not.

Since the crack size, c, fracture toughness, K_c, and peak stress during a flight, σ, are independent random variables, the joint pdf is the product of their individual pdfs,

$$f(x) = f_c(c) \cdot f_K(k) \cdot f_\sigma(s) \tag{82}$$

The POF integral becomes then

$$POF = \iiint_{-\infty}^{\infty} h(c,k,s) f_c(c) f_K(k) f_\sigma(s)\, dc\, dk\, ds \tag{83}$$

and the IS formulation becomes

$$\begin{aligned} POF &= \iiint_{-\infty}^{\infty} \frac{h(c,k,s) f_c(c) f_K(k) f_\sigma(s)}{g_c(c) g_K(k) g_\sigma(s)} g_c(c) g_K(k) g_\sigma(s)\, dc\, dk\, ds \\ &= E\left[\frac{h(c,k,s) f_c(c) f_K(k) f_\sigma(s)}{g_c(c) g_K(k) g_\sigma(s)}\right] \end{aligned} \tag{84}$$

The alternate sampling pdfs were selected to cover the regions most likely to cause failure so that fewer samples were required to obtain a good estimate of the POF. Uniform distributions were chosen for all three sampling distributions. The value of $g(x_i)$ is then constant for all x_i and equal to

$$g(x) = \frac{1}{UB - LB} \tag{85}$$

where *UB* and *LB* are the upper and lower bounds, respectively, of the uniform distribution.

Selecting the Sampling Distributions

Large crack sizes are more likely to fracture than small crack sizes. The largest crack size possible in the example is 2.75 inches, *UB* for $g_c(c)$. It was decided to have the crack size sampling distribution extend down to crack sizes unlikely to cause failure. A crack size of 0.07 inch was chosen as the *LB* for $g_c(c)$. Thus, g_c equals 0.3731.

Material with low K_c is more likely to fracture so sampling was done in the low tail of the K_c distribution. The *LB* was chosen to be 25 ksi√inches. The *UB* was chosen as the 50% value of the K_c distribution, 85 ksi√inches. Thus, g_K equals 0.0167.

A high σ_{max} during a flight is more likely to cause fracture, so sampling of the peak stress distribution focused on the high value tail. The *UB* was chosen as 1.4 times the reference stress of 16 ksi. A *LB* of 0.7 times the reference stress was selected. The values of g_σ is equal to 1/(0.7*16) or 0.893.

PDFs of the Original Distributions

The crack size CDF at the end of flight 5,000 is defined by equation (80). Because the sampling distribution is limited to cracks from 0.07 to 2.75 inches, only equations (80c) and (80d) are needed for the IS. Thus,

$$f_c(c) = \left[\left(\frac{0.11378}{3.4098E\text{-}06}\right)\left(\frac{c}{3.4098E\text{-}06}\right)^{(0.11378-1)}\right] exp\left\{-\left[\left(\frac{c}{3.4098E\text{-}06}\right)^{0.11378}\right]\right\} \quad \text{for } 0.07 \leq c \leq 0.449 \quad (86a)$$

$$f_c(c) = \left[\left(\frac{0.96586}{0.11205}\right)\left(\frac{c}{0.11205}\right)^{(0.96586-1)}\right] exp\left\{-\left[\left(\frac{c}{0.11205}\right)^{0.96586}\right]\right\} \quad \text{for } c \geq 0.449 \quad (86b)$$

The fracture toughness PDF is

$$f_k(k) = \left(\frac{12.49}{93.9}\right)\left(\frac{k}{93.9}\right)^{(12.49-1)} exp\left\{-\left[\left(\frac{k}{93.9}\right)^{12.49}\right]\right\} \quad (87)$$

The PDF for the maximum stress in a flight is

$$f_\sigma(s) = 0.06\, exp\left\{-0.06\left(\frac{s}{16} - 0.699\right) + exp\left[-0.06\left(\frac{s}{16} - 0.699\right)\right]\right\} \quad (88)$$

Performing MCS with IS

Determination of the POF using MCS with IS was accomplished with the following steps which are coded in the subroutine in Appendix B.5.

Step 1. Randomly obtain K_c sample. Use a (pseudo-) random number generator to randomly generate a number between 0 and 1. Recall that the CDF has a range of 0 to 1. The random number is the CDF value, P, of the sampling distribution g_K. Plug the random number into the inverse CDF to determine K_i for this sample:

$$K_i = LB + \frac{P}{g_K} = 25 + \frac{P}{0.0167} \quad (89)$$

Determine the original pdf value, $f_K(K_i)$, for K_i with equation (87).

Step 2. Randomly obtain σ_{max} sample. Use a (pseudo-) random number generator to randomly generate a number, P, between 0 and 1. Plug the random number into the inverse CDF for g_σ to determine s_i for this sample:

$$s_i = LB + \frac{P}{g_\sigma} = 11.2 + \frac{P}{0.0893} \quad (90)$$

Determine the original pdf value, f_σ, for s_i from equation (88).

Step 3. Randomly obtain a crack size, c, sample. Use a (pseudo-) random number generator to randomly generate a number, P, between 0 and 1. Plug the random number into the inverse CDF for g_c to determine c_i for this sample:

$$c_i = LB + \frac{P}{g_c} = 0.07 + \frac{P}{0.3731} \tag{91}$$

Determine the original pdf value, $f_c(c)$, for c_i from equation (86). For $0.07 \le c_i \le 0.4498$,

Step 4. Calculate the maximum stress intensity during the flight. First, calculate the geometry factor based on the crack size from the equations in Section 3.3. For $0.07 \le c_i \le 1.2$,

$$\beta(c_i) = 12.7731c_i^6 - 57.1413c_i^5 + 103.053c_i^4 - 96.2646c_i^3 + 49.9938c_i^2 - 14.4465c_i + 2.9734 \tag{92}$$

For $1.2 \le c_i \le 2.75$,

$$\beta(c_i) = 2.3781c_i^6 - 24.848c_i^5 + 107.159c_i^4 - 243.928c_i^3 + 309.1178c_i^2 - 206.791c_i + 57.9809 \tag{93}$$

Then calculate the maximum stress intensity during the flight.

$$k_i(f) = \beta(c_i) \cdot s_i \cdot \sqrt{\pi \cdot c_i} \tag{94}$$

Step 5. Determine if this sample would fail. Compare $k_i(f)$ to K_i. If $k_i(f) \ge K_i$, then failure occurred with this sample. Set $h(c_i, K_i, s_i)$ equal to 1. Otherwise, $h(c_i, K_i, s_i)$ is equal to 0.

Step 6. Compute $\frac{h(c,k,s)f_c(c)f_K(k)f_\sigma(s)}{g_c(c)g_K(k)g_\sigma(s)}$ for this sample. Add this value to the running total for all samples and increment the number of samples, N, by 1. Calculate $E\left[\frac{h(c,k,s)f_c(c)f_K(k)f_\sigma(s)}{g_c(c)g_K(k)g_\sigma(s)}\right]$ as in equation (24).

Step 7. Compute $\left(\frac{h(c,k,s)f_c(c)f_K(k)f_\sigma(s)}{g_c(c)g_K(k)g_\sigma(s)}\right)^2$ for this sample. Add this value to the total sum of squares for all samples. Calculate $E\left[\left(\frac{h(c,k,s)f_c(c)f_K(k)f_\sigma(s)}{g_c(c)g_K(k)g_\sigma(s)}\right)^2\right]$. Then calculate the variance as in equation (25).

Step 8. If the variance is too large, go to Step 1 and select another sample. If the variance is acceptable, stop.

After 12,000 samples, the POF at the start of flight 5,000 was found to be 6.71×10^{-9} with a variance of 5.20×10^{-15} (the bottom row of Table 28).

Table 28. POF at the Start and End of 5,000 Flights Prior to Inspection

	# of Samples	Sum of POFs	Expected Value of POF	Sum of Squares for POFs	Expected Std. Error	Variance
start of flight 5,000	12000	8.02E-05	6.68E-09	6.3187E-11	5.27E-15	5.22E-15
end of flight 5,000	12000	8.06E-05	6.71E-09	6.2914E-11	5.24E-15	5.20E-15

4.2.3.1.2 POF at the Start of Flight 5,000

The POF at the start of flight 5,000 was found with the same procedure as for the POF at the end of flight 5,000 except that the distribution for $c_{start(f)}$ for flight 5,000 was used. So, the crack size distribution at the start of flight 5,000 needs to be determined. Following the procedure in Section 4.2.1, the crack sizes in the fifth column of the spreadsheet represented in Table 26 were rank ordered using median rank. The 12,000 samples were then plotted on a Weibull graph in Figure 75. Again, the CDF is described piecewise by four straight lines on the Weibull graph. The distribution of $c_{start(f)}$ at flight 5,000 is described by the function

$$Pr(C \le c) = 1 - exp\left[-\left(\frac{c}{1.01 \times 10^{-7}}\right)^{70}\right] \text{ for } c \le 9.64\text{E-}08 \quad (95a)$$

$$Pr(C \le c) = 1 - exp\left[-\left(\frac{c}{0.00054}\right)^{0.377}\right] \text{ for } 9.64\text{E-}08 \le c \le 0.00483 \quad (95b)$$

$$Pr(C \le c) = 1 - exp\left[-\left(\frac{c}{3.3945 \times 10^{-6}}\right)^{0.11374}\right] \text{ for } 0.00483 \le c \le 0.4492 \quad (95c)$$

$$Pr(C \le c) = 1 - exp\left[-\left(\frac{c}{0.11201}\right)^{0.96584}\right] \text{ for } 0.4492 < c \quad (95d)$$

The original PDF for $c_{start(f)}$ at flight 5,000 over the size range of interest is

$$f_c(c) = \left[\left(\frac{0.11374}{3.3945E\text{-}06}\right)\left(\frac{c}{3.3945E\text{-}06}\right)^{(0.11374-1)}\right] exp\left\{-\left[\left(\frac{c}{3.3945E\text{-}06}\right)^{0.11374}\right]\right\}$$

$$\text{for } 0.07 \le c \le 0.4492 \quad (96a)$$

$$f_c(c) = \left[\left(\frac{0.96584}{0.11201}\right)\left(\frac{c}{0.11201}\right)^{(0.96584-1)}\right] exp\left\{-\left[\left(\frac{c}{0.11201}\right)^{0.96584}\right]\right\}$$

$$\text{for } c \ge 0.4492 \quad (96b)$$

All of the other PDFs remain the same as they were for the end of flight 5,000. Performing the MCS with IS as above, after 12,000 samples the POF at the start of flight 5,000 was found to be 6.68×10^{-9} with a variance of 5.22×10^{-15} (Table 28).

4.2.3.1.3 SFPOF at Flight 5,000 Prior to Inspection

The estimated value of the PDF at the end of flight 5,000 was found by subtracting the POF at the start of flight 5,000 from the POF at the end of flight 5,000. This gives a value of 3.17×10^{-11}. The HRF at the end of flight 5,000 was found to be 3.17×10^{-11} using equation (5). The SFPOF is just the HRF multiplied by one flight. So, the SFPOF at the end of flight 5,000 prior to inspection is also 3.17×10^{-11}. This value is lower than the SFPOF of 4.73×10^{-9} estimated for flight 5,000 in Table 21 of Section 3.3.7.2.

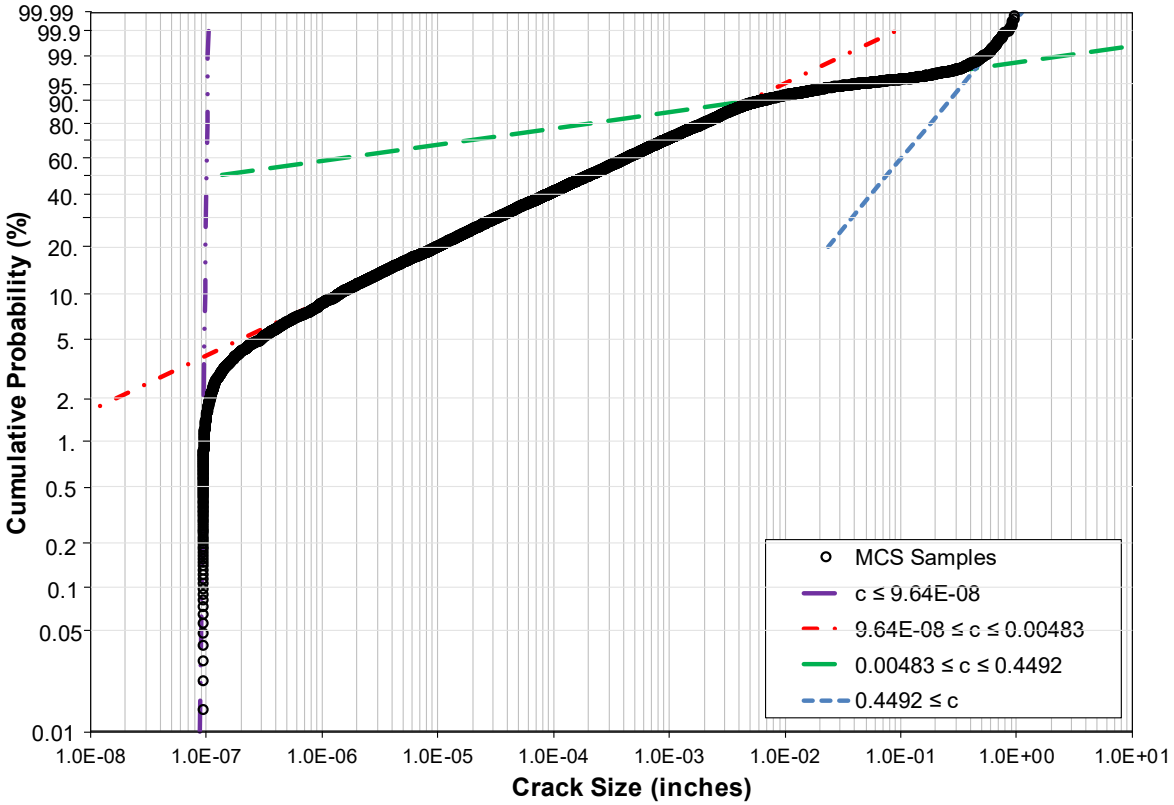

Figure 75. Weibull Graph of the Crack Size Distribution at the Start of Flight 5,000

4.2.4 Post-Inspection SFPOF

The post-inspection SFPOF was found using the same process used for the pre-inspection SFPOF. The crack size distributions after the inspection and repair (at the start of flight 5,001) and at the end of flight 5,001 are needed. Only the original PDFs for the crack size distributions change. Since the crack growth in a single flight is small, it is not necessary to change the sampling distribution for the crack size in the IS routine.

4.2.4.1 POF at the Start of Flight 5,001

The crack size CDF at the start of flight 5,001 (after inspection and repair) was given previously in equation (81). The original PDF for the two large crack segments of the crack size distribution is described by the equation

$$f_c(c) = \left[\left(\frac{0.2256}{8.56\text{E-}05}\right)\left(\frac{c}{8.56\text{E-}05}\right)^{(0.2256-1)}\right] exp\left\{-\left[\left(\frac{c}{8.56\text{E-}05}\right)^{0.2256}\right]\right\}$$

$$\text{for } 0.07 \leq c \leq 0.10881 \quad (97a)$$

$$f_c(c) = \left[\left(\frac{0.5441}{5.618\text{E-}03}\right)\left(\frac{c}{5.618\text{E-}03}\right)^{(0.5441-1)}\right] exp\left\{-\left[\left(\frac{c}{5.618\text{E-}03}\right)^{0.5441}\right]\right\}$$

$$\text{for } c \geq 0.10881 \quad (97b)$$

IS of 12,000 samples gives an expected value of the POF after inspection and repair at 5,000 flights (start of flight 5,001) of 1.02 x 10^{-11} (Table 29). This is two orders of magnitude lower than the POF at the end of flight 5,000 prior to the inspection (Section 4.2.3.1.1).

Table 29. POF at the Start and End of Flight 5,001

	# of Samples	Sum of POFs	Expected Value of POF	Sum of Squares for POFs	Expected Std. Error	Variance
start of flight 5001	12000	1.23E-07	1.02E-11	2.6502E-15	2.21E-19	2.21E-19
end of flight 5001	12000	3.65E-07	3.04E-11	1.8715E-14	1.56E-18	1.56E-18

4.2.4.2 POF at the End of Flight 5,001

The post-inspection and repair crack size samples, an example of which are shown in the last column of Table 27, need to be grown for a single flight to the end of flight 5,001. This is done with equation (66). A sample of these results are given in Table 30. The crack sizes at the end of flight 5,001 were rank ordered using median rank, equation (19), and plotted on a Weibull graph (Figure 76). The resulting CDF is described by the piecewise equations

$$Pr(C \le c) = 1 - exp\left[-\left(\frac{c}{0.00428}\right)^{0.626}\right] \text{ for } c \le 9.17\text{E-}08 \quad (98a)$$

$$Pr(C \le c) = 1 - exp\left[-\left(\frac{c}{1.01 \times 10^{-7}}\right)^{69.5}\right] \text{ for } 9.17\text{E-}08 \le c \le 9.64\text{E-}08 \quad (98b)$$

$$Pr(C \le c) = 1 - exp\left[-\left(\frac{c}{0.000463}\right)^{0.383}\right] \text{ for } 9.64\text{E-}08 \le c \le 0.00525 \quad (98c)$$

$$Pr(C \le c) = 1 - exp\left[-\left(\frac{c}{8.42 \times 10^{-5}}\right)^{0.225}\right] \text{ for } 0.00525 \le c \le 0.10878 \quad (98d)$$

$$Pr(C \le c) = 1 - exp\left[-\left(\frac{c}{0.005629}\right)^{0.5443}\right] \text{ for } 0.10878 < c \quad (98e)$$

The original PDF for crack size at the end of flight 5,001 is

$$f_c(c) = \left[\left(\frac{0.225}{8.42\text{E-}05}\right)\left(\frac{c}{8.42\text{E-}05}\right)^{(0.225-1)}\right] exp\left\{-\left[\left(\frac{c}{8.42\text{E-}05}\right)^{0.225}\right]\right\}$$

$$\text{for } 0.07 \le c \le 0.10878 \quad (99a)$$

$$f_c(c) = \left[\left(\frac{0.5443}{5.629\text{E-}03}\right)\left(\frac{c}{5.629\text{E-}03}\right)^{(0.5443-1)}\right] exp\left\{-\left[\left(\frac{c}{5.629\text{E-}03}\right)^{0.5443}\right]\right\}$$

$$\text{for } c \ge 0.10878 \quad (99b)$$

Table 30. Sample of Crack Sizes at the End of 5,001 Flights

Sample #	Inspection (D or N)	c(f) after inspection	c(f) @ end of 5001 flights
1	N	0.007172547	0.007173105
2	N	2.67772E-05	2.67772E-05
3	N	0.000174666	0.000174666
4	N	0.000266182	0.000266182
5	N	1.16126E-05	1.16126E-05
6	N	1.09256E-05	1.09257E-05
7	N	0.000655241	0.000655241
8	N	1.61908E-05	1.61908E-05
9	N	0.000258298	0.000258298
10	N	0.000565988	0.000565988
11	N	5.10017E-05	5.10018E-05
12	N	0.000713477	0.000713478
13	N	0.00085547	0.00085547
14	N	0.000189871	0.000189871
15	N	0.001429511	0.001429511
16	N	1.21322E-05	1.21323E-05
17	N	3.90539E-07	3.90558E-07
18	N	8.17509E-06	8.17511E-06
19	N	4.59338E-07	4.59356E-07
20	N	1.07172E-06	1.07174E-06
21	N	8.43763E-05	8.43763E-05
22	N	0.000608382	0.000608382
23	N	0.00282992	0.002829929
24	N	0.140651107	0.140750867
25	N	8.81429E-05	8.81429E-05
26	N	0.002557747	0.002557753
27	D	0.001250208	0.001250208
28	N	3.34886E-06	3.34887E-06
29	N	3.89707E-07	3.89725E-07
30	N	0.001232002	0.001232002
31	N	0.002649615	0.002649621
32	N	7.56709E-05	7.56709E-05
33	N	5.84038E-05	5.84038E-05
34	N	0.000811446	0.000811446
35	N	2.58969E-05	2.58969E-05
36	N	1.68605E-07	1.68624E-07
37	N	0.000395942	0.000395942
38	N	0.001680231	0.001680231
39	N	0.000166081	0.000166081
40	D	6.23313E-05	6.23313E-05

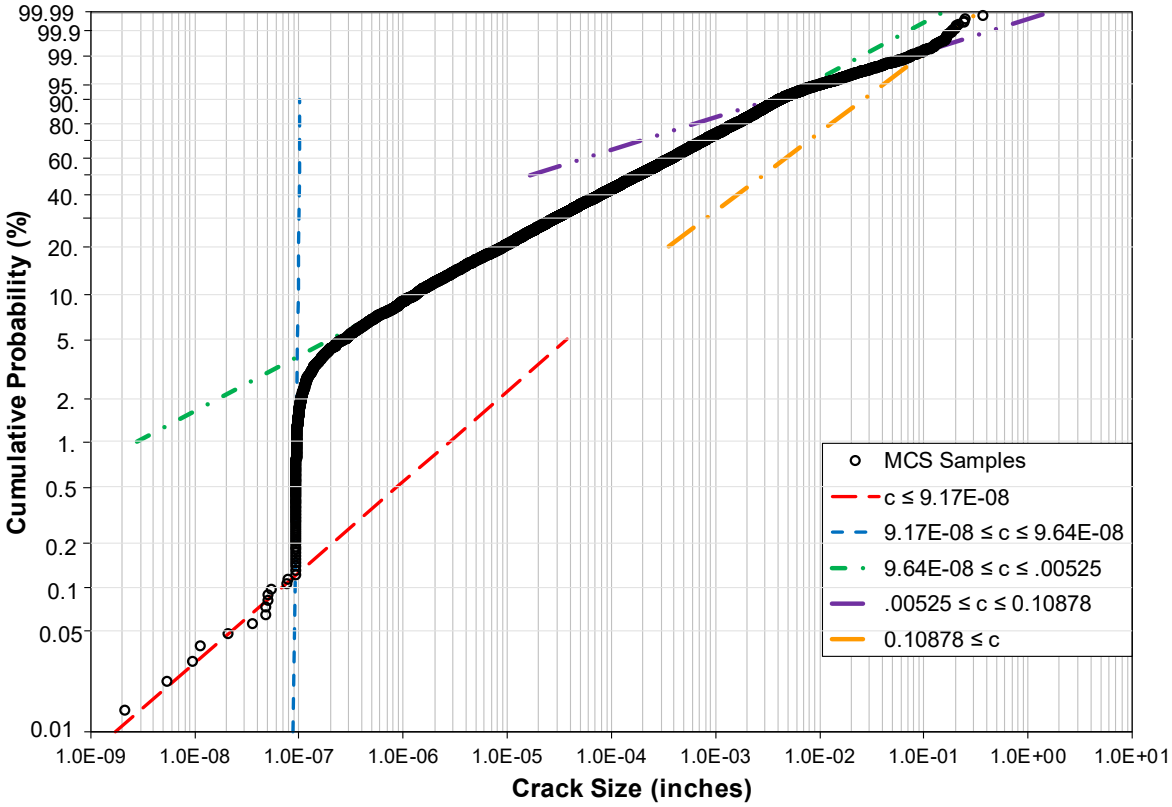

Figure 76. Weibull Graph of the Crack Size Distribution at the End of 5,001 Flights

Using 12,000 samples, the expected value of the POF at the end of flight 5,001 is 3.04 x 10^{-11} with a variance of 1.56 x 10^{-18} (Table 29). This value is slightly larger than the POF at the start of flight 5,001 as expected.

4.2.4.3 SFPOF after Inspection and Repair

The value of the failure PDF after the inspection and repair (at the start of flight 5,001) was estimated as the difference between the expected values of the failure CDFs at the end and the start of flight 5,001. This value is 2.02 x 10^{-11}. The HRF after the inspection and repair is also 2.02 x 10^{-11} using equation (5). Multiplying the HRF by one flight gives the SFPOF. So, the SFPOF at the start of flight 5,001 is also 2.02 x 10^{-11}. The SFPOF is only slightly smaller than it was prior to the inspection, 2.02 x 10^{-11} versus 3.17 x 10^{-11}. The inspection and repair at 5,000 flights was not especially effective at reducing the SFPOF since it was not high to begin with.

4.2.5 Sensitivity Study

A sensitivity study should be performed to assess the impact of each of the random variables on the reliability of the detail. Now there are ten random variables:

1) the shape and scale parameters of the fracture toughness distribution,
2) the shape and scale parameters of the EIDS distribution,
3) the dispersion parameter and characteristic value of the maximum stress distribution,
4) the coefficient and exponent of the POD distribution, and
5) the shape and scale parameters of the ERDS distribution.

If three values were selected for each parameter, performing a sensitivity study for every combination of values would require 3^{10}, or 59,049, MCS runs. Using an $L_{27}(3^{13})$ orthogonal array reduces the MCS runs to 27. The basic layout for this orthogonal array is shown in Table 31 where 1, 2, and 3 in the array represent the three different values for each variable. Only 10 columns of this array are needed for the variables. The time when the inspections are performed can be included as another variable to the sensitivity study. This would use another column of the orthogonal array.

The procedure for the sensitivity study is the same as that for the sensitivity studies in Section 3. Additional outputs, besides the number of flights to a SFPOF of 10^{-7}, can be considered in the sensitivity study. These outputs include the SFPOF reached before an inspection, the SFPOF after each inspection, or the number of cracks found by an inspection. Since the overall process for the sensitivity study is the same, the sensitivity study will not be performed for this example.

Table 31. $L_{27}(3^{13})$ Orthogonal Array

Trial No.	Variable 1	Variable 2	Variable 3	Variable 4	Variable 5	Variable 6	Variable 7	Variable 8	Variable 9	Variable 10	Variable 11	Variable 12	Variable 13
1	1	1	1	1	1	1	1	1	1	1	1	1	1
2	1	1	1	1	2	2	2	2	2	2	2	2	2
3	1	1	1	1	3	3	3	3	3	3	3	3	3
4	1	2	2	2	1	1	1	2	2	2	3	3	3
5	1	2	2	2	2	2	2	3	3	3	1	1	1
6	1	2	2	2	3	3	3	1	1	1	2	2	2
7	1	3	3	3	1	1	1	3	3	3	2	2	2
8	1	3	3	3	2	2	2	1	1	1	3	3	3
9	1	3	3	3	3	3	3	2	2	2	1	1	1
10	2	1	2	3	1	2	3	1	2	3	1	2	3
11	2	1	2	3	2	3	1	2	3	1	2	3	1
12	2	1	2	3	3	1	2	3	1	2	3	1	2
13	2	2	3	1	1	2	3	2	3	1	3	1	2
14	2	2	3	1	2	3	1	3	1	2	1	2	3
15	2	2	3	1	3	1	2	1	2	3	2	3	1
16	2	3	1	2	1	2	3	3	1	2	2	3	1
17	2	3	1	2	2	3	1	1	2	3	3	1	2
18	2	3	1	2	3	1	2	2	3	1	1	2	3
19	3	1	3	2	1	3	2	1	3	2	1	3	2
20	3	1	3	2	2	1	3	2	1	3	2	1	3
21	3	1	3	2	3	2	1	3	2	1	3	2	1
22	3	2	1	3	1	3	2	2	1	3	3	2	1
23	3	2	1	3	2	1	3	3	2	1	1	3	2
24	3	2	1	3	3	2	1	1	3	2	2	1	3
25	3	3	2	1	1	3	2	3	2	1	2	1	3
26	3	3	2	1	2	1	3	1	3	2	3	2	1
27	3	3	2	1	3	2	1	2	1	3	1	3	2

4.3 Recurring Inspections

In this example, POD is modeled with a deterministic equation. The inspection for each sample has exactly the same POD. This is not a realistic scenario, even if it is assumed that the same NDI sensor and other equipment are used for every inspection. Placement of the sensor on the part, the shape and depth of the crack, and local residual stresses, for example, can effect the sensitivity of the NDI method. Therefore, it is recommended that a random noise term be added to the POD equation, at the very least. This will introduce needed variability into the POD of a single inspection of a MCS. A commonly used random noise term is a normal distribution with a mean of zero and a standard deviation that captures the variability in the NDI readings.

Furthermore, when considering recurring inspections over the lifetime of an aircraft fleet, it is unlikely that the same NDI sensor and instruments will be used for every inspection of a widely dispersed fleet over a period of 20 or 30 years. There will be small, but potentially significant, variations in NDI POD with each inspection that should be modelled by including a random

noise term in the POD equation. Appendix G of Mil-Hdbk-1823 [23] provides a thorough discussion of how to quantify and model the variability in NDI. Subject matter experts in nondestructive evaluation systems should be consulted if there are any questions or concerns about properly modelling POD in a risk assessment.

The POD is often multiplied by the probability of inspection (POI), which is meant to reflect the probability that an inspection was performed correctly. POI is intended to cover the possibility that any of a multitude of things may have prevented the inspection from being performed as specified. The value of POI is typically chosen to be between 0.95 and 0.90, though lower values can be chosen if an inspection is particularly difficult to perform. A POI greater than 0.95 is rarely used and requires justification. POI is usually treated as a deterministic value for every inspection, but it also could be treated as a random variable for each inspection if the added complexity was warranted.

4.4 Summary

This example demonstrated a MCS for a single inspection and repair scenario. Two additional random variables were introduced, POD and ERDS. A procedure for determining the SFPOF before and after an inspection using IS was demonstrated. A third variable, POI, was briefly discussed. Recurring inspections would repeat the MCS for each subsequent inspection. The importance of adding variability to the POD for subsequent inspections was briefly discussed.

5 CONCLUSION

This handbook demonstrated how to calculate the risk of structural failure due to fracture using MCS. MCS is the standard against which all other calculation methods are compared. Thus, the reader is provided with an approach for verifying any other risk calculation method. And since MCS is somewhat intuitive in calculating reliability, it is hoped that the reader developed some understanding and comfort with risk and reliability calculations.

6 REFERENCES

[1] E. J. Tuegel, R. P. Bell, A. P. Berens, T. Brussat, J. W. Cardinal, J. P. Gallagher and J. Rudd, "Aircraft Structural Reliability and Risk Analysis Handbook - Volume 1: Basic Analysis Methods," Air Force Research Laboratory, Wright-Patterson AFB, OH, 2018.

[2] National Institute of Standards and Technology, "NIST/SEMATECH e-Handbook of Statistical Methods," 1 April 2012. [Online]. Available: http://www.itl.nist.gov/div898/handbook/. [Accessed 4 February 2013].

[3] USAF Center of Excellence for Airworthiness, *United States Air Force (USAF) Airworthiness Bulletin (AWB)-150A,* Wright-Patterson Air Force Base, OH: Air Force Life Cycle Management Center, 2017.

[4] K. C. Kapur and L. R. Lamberson, Reliability in Engineering Design, New York: John Wiley & Sons, 1977.

[5] R. Y. Rubinstein and D. P. Kroese, Simulation and the Monte Carlo Method, Second ed., Hoboken, NJ: John Wiley & Sons, Inc., 2008.

[6] ASTM International, *Annual Book of Standards,* vol. 03.01, West Conshohocken, PA: ASTM International, 2014.

[7] D. A. Skinn, J. P. Gallagher, A. P. Berens, P. D. Huber and J. Smith, Damage Tolerant Design Handbook, Vols. Vol. 4, Chapter 8, Table 8.7.2.1, Wright-Patterson AFB, OH 45433: Wright Laboratory, 1994.

[8] O. A. Yakimenko, Engineering Computations and Modeling in MATLAB(R)/Simulink(R), Reston, VA: American Institute of Aeronautics and Astronautics, Inc., 2011.

[9] A. Saltelli, M. Ratto, T. Andres, F. Campolongo, J. Cariboni, D. Gatelli, M. Saisana and S. Tarantola, Global Sensitivity Analysis. The Primer, Chicester, West Sussex, England: John Wiley & Sons Ltd., 2008.

[10] M. S. Phadke, Quality Engineering Using Robust Design, Englewood Cliffs, New Jersey: PTR Prentrice-Hall, Inc., 1989.

[11] S. D. Manning, W. R. Garver, S. P. Henslee, J. W. Norris, B. J. Pendley, S. M. Speaker, V. D. Smith, B. W. Yee, M. Shinozuka and J. N. Yang, "Durability Methods Development," U.S. Air Force Flight Dynamics Laboratory, Wright-Patterson AFB, OH, 1979.

[12] E. L. Anagnostou, S. J. Engel, D. Fridline, D. H. Hoitsma, J. S. Madsen, J. A. Nardiello and J. M. Papazian, "Science-based Multiscale Modeling of Fatigue Damage for Structural Prognosis," in *51st AIAA/ASME/ASCE/AHS/ASC Structures, Structural Dynamics, and Materials Conference*, Orlando, FL, 2010.

[13] E. A. DeBartolo and B. M. Hillberry, "A model of initial flaw sizes in aluminum alloys," *International Journal of Fatigue,* vol. 23, pp. S79-S86, 2001.

[14] Y. Liu and S. Mahadevan, "An efficient method for equivalent initial flaw size (EIFS) calculation," in *49th AIAA/ASME/ASCE/AHS/ASC Structures, Structural Dynamics and Materials Conference*, Schaumburg, IL, 2008.

[15] L. Molent, "A review of equivalent pre-crack sizes in aluminium alloy 7050-T7451," *Fatigue and Fracture of Engineering Materials and Structures,* vol. 37, pp. 1055-1074, 2014.

[16] P. C. Miedlar, A. P. Berens, A. Gunderson and J. P. Gallagher, "USAF Damage Tolerant Design Handbook: Guidelines for the Analysis and Design of Damage Tolerant Aircraft Structures," U.S. Air Force Research Laboratory, Wright-Patterson Air Force Base, OH, 2002.

[17] Flugzeugwerke Emmen, (F+W) Switzerland, "FALSTAFF - Description of a Fighter Aircraft Loading Standard for Fatigue Evaluation," 1976.

[18] G. M. van Dijk and J. B. de Jonge, "Introduction to a Fighter Aircraft Loading Standard for Fatigue Evaluation - "FALSTAFF"," NLR (National Aerospace Laboratory) The Netherlands, 1975.

[19] K. Worden, D. W. Allen, H. Sohn, D. W. Stinemates and C. R. Farrar, "Extreme Value Statistics for Damage Detection in Mechanical Structures," Los Alamos National Laboratory, 2002.

[20] National Institute of Standards and Technology, "Engineering Statistics Handbook," [Online]. Available: https://www.itl.nist.gov/div898/handbook/eda/section3/eda366h.htm. [Accessed 23 December 2019].

[21] U.S. Dept. of Defense, "Nondestructive Evaluation System Reliability Assessment," U.S. Air Force, Wright-Patterson AFB, OH, 2009.

[22] A. P. Berens and P. W. Hovey, "Evaluation of NDE Reliability Characterization," Air Force Wright Aeronautical Laboratories, Wright-Patterson AFB, OH, 1981.

[23] Department of Defense, Nondestructive Evaluation System Reliability Assessment, Wright-Patterson AFB, OH: Air Force Life Cycle Management Center, 2009.

[24] J. Bakuckas, J. L. Jackson, R. C. Rice and S. Thompson, Eds., Metallic Materials Property Development and Standardization, Federal Aviation Administration, 2003.

[25] D. O. Cornog and J. W. Lincoln, "Risk Assessment of the F-16 Wing," in *Proceedings of the 1988 Structural Integrity Conference*, San Antonio, TX, 1989.

[26] A. M. Freudenthal, "Reliability Assessment of Aircraft Structures Based on Probabilistic Interpretation of the Scatter Factor," Air Force Materials Laboratory, Wright-Patterson AFB, OH, 1975.

[27] "Dept. of Defense Standard Practice - Aircraft Structural Integrity Program (ASIP)," Dept. of Defense, Wright-Patterson AFB, OH 45433, 2005.

[28] W. Nelson, Applied Life Data Analysis, New York: John Wiley & Sons, 1982.

[29] A. M. Freudenthal, J. M. Garrelts and M. Shinozuka, "The Analysis of Structural Safety," *Proc. of the American Society of Civil Engineers, Structural Division,* vol. 92, no. ST1, pp. 267-325, February 1966.

[30] J. W. Lincoln, "Method for Computation of Structural Failure Probability for an Aircraft," Aeronautical Systems Division, Wright-Patterson Air Force Base, 1980.

[31] J. W. Lincoln, "Risk Assessment of an Aging Military Aircraft," *J. of Aircraft,* vol. 22, no. 8, pp. 687-691, 1985.

[32] A. P. Berens, P. W. Hovey and D. A. Skinn, "Risk Analysis for Aging Aircraft Fleets," Wright Laboratory, Wright-Patterson Air Force Base, 1991.

[33] B. Lundberg, "Fatigue Life of Airplane Structures: the 18th Wright Brothers Lecture," *J. of Aeronautical Sciences,* vol. 22, no. 6, pp. 349-402, 1955.

[34] Structures Branch, Engineering Directorate, Aeronautical Systems Center, "Methodology for Determination of Equivalent Flight Hours and Approaches to Communicate Usage Severity," ASC/EN, Wright-Patterson Air Force Base, OH, 2009.

[35] "Dept. of Defense Standard Practice for System Safety," Dept. of Defense, 2012.

[36] A. M. Freudenthal and P. Y. Wang, "Ultimate Strength Analysis," Air Force Materials Laboratory, Wright-Patterson Air Force Base, 1969.

[37] M. C. Campion, L. C. Hanson and D. S. Morcock, "Implementation Studies for a Reliability-Based Static Strength Criteria System," Air Force Flight Dynamics Laboratory, Wright-Patterson Air Force Base, 1972.

[38] R. J. Veldman and C. Peckham, "Handbook of Military Aircraft Design Normal Load Factor Exceedance Data," Aeronautical Systems Division; Air Force Systems Command, Wright-Patterson Air Force Base, 1982.

[39] C. A. Babish IV, *Aircraft Structure Risk and Reliability Analysis Course,* Dayton, OH, 2004.

[40] S. D. Manning and J. N. Yang, "USAF Durability Design Handbook: Guidelines for the Analysis and Design of Durable Aircraft Structures," Air Force Wright Aeronautical Laboratories, Wright-Patterson AFB, OH, 1989.

[41] National Institute of Standards and Technology, "NIST/SEMATECH e-Handbook of Statistical Methods," 30 October 2013. [Online]. Available: https://www.itl.nist.gov/div898/handbook/eda/section3/eda366g.htm. [Accessed 26 December 2019].

SYMBOLS AND ABBREVIATIONS

a	length of part-through crack in the thickness direction
c	length of crack on the surface
CDF	cumulative distribution function
EIDS	equivalent initial damage size
ERDS	equivalent damage size after a repair
f	number of flights
FH	flight hours
HRF	hazard rate function (also known as the failure rate)
IS	importance sampling
K_c	fracture toughness
K, k	stress intensity
LSE	least squares estimation
MCS	Monte Carlo simulation
N	number of samples in MCS
N_f	flights to failure
PDF	probability density function
POF	probability of failure
SFPOF	single flight probability of failure
α	parameter in a probability distribution
β	parameter in a probability distribution
σ	stress

APPENDIX A. FRACTOGRAPHIC ESTIMATION OF EIDS

A.1 Introduction

The crack size data used to establish the EIDS distribution in Section 3.2 are presented here along with the analysis to estimate the EIDS for each specimen. These data are from the no load transfer specimens tested under the F-16 400 hr. block spectrum reported in volume VIII of [11].

The specimens were made from 7475-T7351 aluminum. This is a different temper than used in the example in Section 3.2, -T7651 vs. –T7351. Studies have shown that fatigue cracks nucleate at the iron-bearing particles in the alloy or at scratches from drilling the hole. The iron-bearing particles are impurities in the alloy. Their size and shape are affected by the alloy composition, not the heat treatment/temper. Crack formation for 7475-T7351 should be similar to that for 7475-T7651.

Two specimen geometries were used in these tests. The basic configuration is shown in Figure A-1. The gage section thickness, t, for type A specimens was 0.375 inch and 0.275 inch for type B specimens. The two fastener holes were spaced 1.0 inch or 3.0 inches apart. (There was no indication in the report which specimens had which fastener spacing.) The fasteners used were $^{3}/_{16}$ and ¼ inch diameter MS-90353 rivets and ¼-inch-diameter NAS 1580 countersunk bolts.

Three different reference stress levels were used: 32 ksi, 34 ksi, and 38 ksi. The F-16 400-hour block spectrum shown in Figure A-2 created marker bands on the crack faces which were used to determine crack length at specific times during each test via fractography.

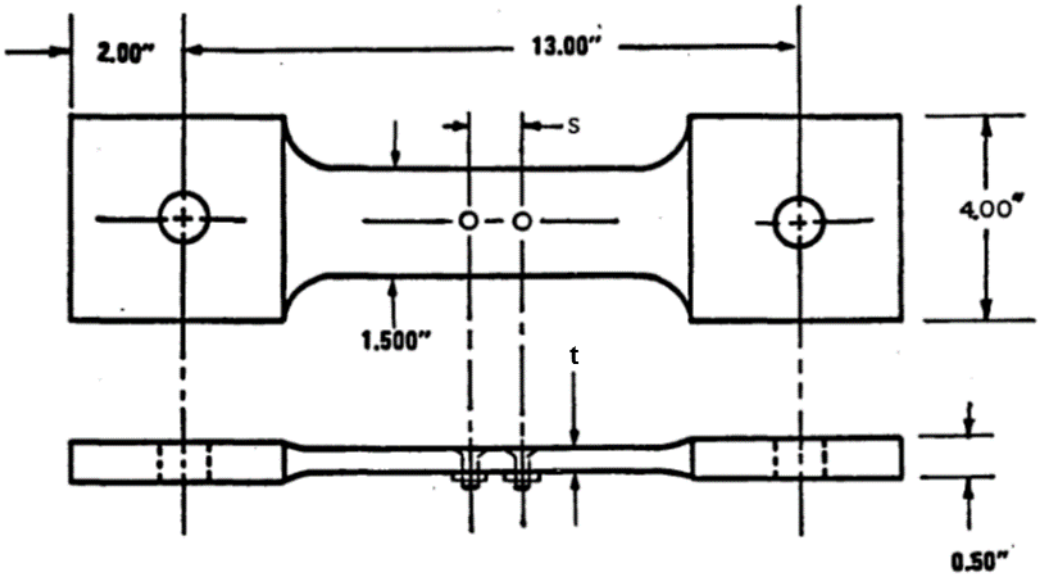

Figure A-1. No Load Transfer Specimen Geometry [11]

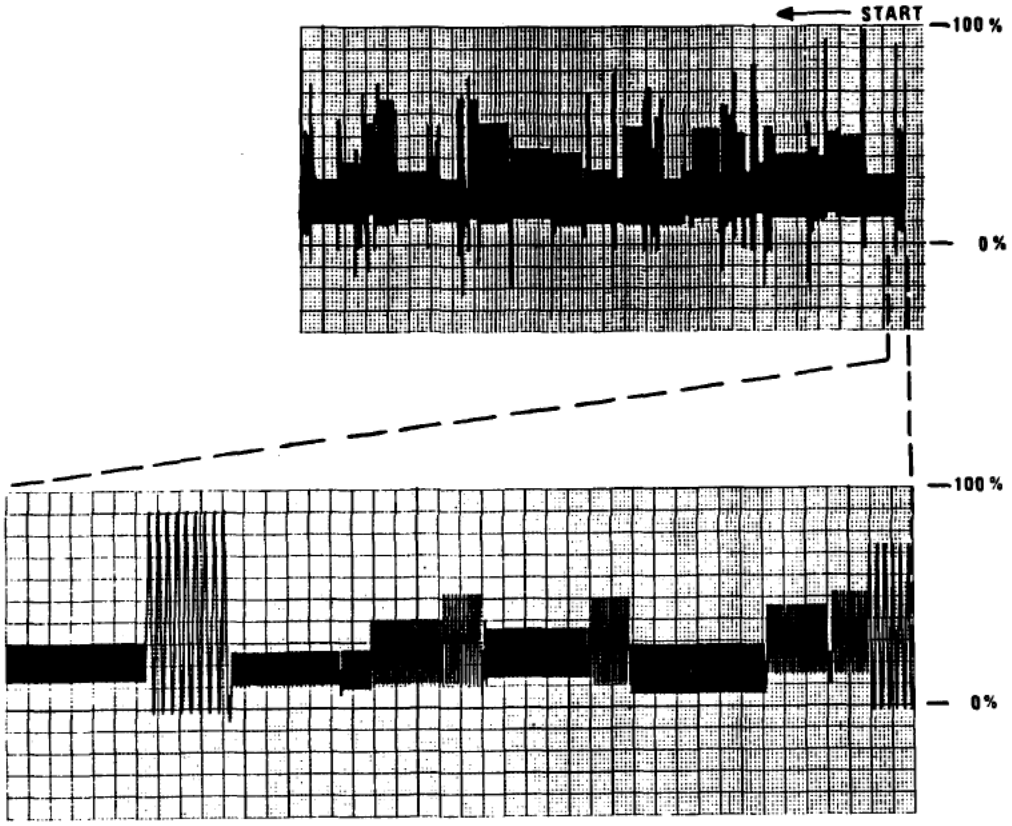

Figure A-2. F-16 400-hour Block Spectrum [11]

A.2 Fractographic Data

The letter after the specimen number designates the hole in which the crack formed. The hole specified as A was nearest the specimen end marked with the specimen identification. Hole B was furthest from that end. Only those crack sizes less than 0.0393 inch (1 mm) were used in determining EIDS following the approach in reference [15]. The fractographic measurements for each specimen are given in Table A-1 to Table A-32.

Table A-1. Fractographic Results for Specimen 99

Specimen	99A
Fastener	MS-90353 (3/16 in.)
Stress	32 ksi
Test Date	5/12/1980
Fatigue Life	29948 hrs
Location:	Bore
Flight Hrs	**Crack Size**
19600	0.0244
20000	0.0265
20400	0.0281
20800	0.0309
21200	0.0349
21600	0.039
22000	0.0439
22400	0.049
22800	0.0545
23200	0.0609
23600	0.0675
24000	0.0758
24400	0.0834
24800	0.0938
25200	0.1022
25600	0.1135
26000	0.1258
26400	0.1391
26800	0.1537
27200	0.1705
27600	0.188
28000	0.2067
28400	0.2273
28800	0.2514
29200	0.2806

Specimen	99B
Fastener	MS-90353 (3/16 in.)
Stress	32 ksi
Test Date	5/12/1980
Fatigue Life	29948 hrs
Location:	Unkown
Flight Hrs	**Crack Size**
14800	0.0117
15200	0.0128
15600	0.014
16000	0.0153
16400	0.0173
16800	0.0189
17200	0.0205
17600	0.0227
18000	0.0255
18400	0.0276
18800	0.0295
19200	0.0324
19600	0.0362
20000	0.039
20400	0.0434
20800	0.0482
21200	0.0542
21600	0.0593
22000	0.0656
22400	0.0728
22800	0.0805
23200	0.0885
23600	0.0974
24000	0.1074
24400	0.118
24800	0.1293
25200	0.1417
25600	0.1541
26000	0.1687
26400	0.1856
26800	0.2026
27200	0.2223
27600	0.2437
28000	0.269
28400	0.3008
28800	0.3408
29200	0.3922
29948	0.4801

Table A-2. Fractographic Results for Specimens 100 and 101

Specimen	100A
Fastener	MS-90353 (3/16 in.)
Stress	32 ksi
Test Date	5/12/1980
Fatigue Life	23600 hrs
Location	Bore

Flight Hrs	Crack Size
6400	0.0107
6800	0.0122
7200	0.0132
7600	0.0157
8000	0.0178
8400	0.0196
8800	0.0224
9200	0.0252
9600	0.0283
10000	0.0304
10400	0.0327
10800	0.035
11200	0.0377
11600	0.0413
12000	0.0443
12400	0.0479
12800	0.0513
13200	0.057
13600	0.0635
14000	0.0687
14400	0.0743
14800	0.0793
15200	0.0875
15600	0.0942
16000	0.1031
16400	0.113
16800	0.1213
17200	0.1319
17600	0.1421
18000	0.154
18400	0.1672
18800	0.1813
19200	0.1947
19600	0.209
20000	0.2277
20400	0.2461
20800	0.2694
21200	0.2968
21600	0.3259
22000	0.3575
22400	0.3943
22800	0.4437
23200	0.501
23600	0.5653

Specimen	101A
Fastener	MS-90353 (3/16 in.)
Stress	32 ksi
Test Date	5/15/1980
Fatigue Life	23600 hrs
Location	Bore

Flight Hrs	Crack Size
8800	0.0121
9200	0.0132
9600	0.0147
10000	0.0162
10400	0.0178
10800	0.0195
11200	0.0209
11600	0.0233
12000	0.0258
12400	0.0278
12800	0.0313
13200	0.0348
13600	0.0388
14000	0.0429
14400	0.0479
14800	0.053
15200	0.0582
15600	0.0634
16000	0.07
16400	0.0777
16800	0.0863
17200	0.0943
17600	0.1032
18000	0.1131
18400	0.1234
18800	0.1344
19200	0.1482
19600	0.1615
20000	0.1775
20400	0.1941
20800	0.2145
21200	0.2372
21600	0.2607
22000	0.29
22400	0.3285
22800	0.3785
23200	0.439
23600	0.4871

Table A-3. Fractographic Results for Specimens 621 and 623

Specimen	621A
Fastener	MS-90353 (3/16 in.)
Stress	32 ksi
Test Date	
Fatigue Life	16000 hrs
Location	Bore
Flight Hrs	**Crack Size**
8800	0.0069
9200	0.0078
9600	0.0092
10000	0.0107
10400	0.0127
10800	0.0145
11200	0.0167
11600	0.0192
12000	0.0219
12400	0.0246
12800	0.0274
13200	0.03
13600	0.0335
14000	0.0391
14400	0.0451
14800	0.0555
15200	0.0678
15600	0.0824
16000	0.098

Specimen	623B
Fastener	MS-90353 (3/16 in.)
Stress	32 ksi
Test Date	
Fatigue Life	16000 hrs
Location	Countersink
Flight Hrs	**Crack Size**
12800	0.0161
13200	0.017
13600	0.0179
14000	0.0194
14400	0.0208
14800	0.0221
15200	0.0239
15600	0.0255
16000	0.0275

Specimens 622 and 624 with 3/16-inch, MS-90353 rivets did not crack after 16,000 hours (4,000 passes through the spectrum).

Table A-4. Fractographic Results for Specimens 102 and 103

Specimen	102A
Fastener	MS-90353 (1/4 in.)
Stress	32 ksi
Test Date	5/16/1980
Fatigue Life	23606 hrs
Location	Bore
Flight Hrs	**Crack Size**
13600	0.0222
14000	0.0238
14400	0.0257
14800	0.0277
15200	0.0302
15600	0.0324
16000	0.0347
16400	0.0376
16800	0.0419
17200	0.0462
17600	0.0523
18000	0.0588
18400	0.0657
18800	0.0732
19200	0.0822
19600	0.092
20000	0.1031
20400	0.1146
20800	0.1275
21200	0.1436
21600	0.1616
22000	0.1842
22400	0.2108
22800	0.2473
23200	0.2953
23606	0.3702

Specimen	103B
Fastener	MS-90353 (1/4 in.)
Stress	32 ksi
Test Date	5/16/1980
Fatigue Life	24750 hrs
Location	Bore
Flight Hrs	**Crack Size**
12000	0.0208
12400	0.0221
12800	0.0241
13200	0.026
13600	0.0284
14000	0.0323
14400	0.0356
14800	0.041
15200	0.0472
15600	0.0536
16000	0.0596
16400	0.0654
16800	0.0723
17200	0.0776
17600	0.0858
18000	0.0938
18400	0.102
18800	0.1135
19200	0.125
19600	0.1373
20000	0.1504
20400	0.1644
20800	0.1797
21200	0.1978
21600	0.2161
22000	0.238
22400	0.2611
22800	0.2894
23200	0.323
23600	0.3622
24000	0.4147
24400	0.481
24750	0.524

Table A-5. Fractographic Results for Specimens 104 and 108

Specimen	104B
Fastener	MS-90353 (1/4 in.)
Stress	32 ksi
Test Date	5/19/1980
Fatigue Life	16000 hrs
Location	Unknown
Flight Hrs	**Crack Size**
10800	0.0113
11200	0.0121
11600	0.0131
12000	0.014
12400	0.0149
12800	0.016
13200	0.0171
13600	0.0183
14000	0.0198
14400	0.0212
14800	0.0228
15200	0.0257
15600	0.0291
16000	0.03

Specimen	108B
Fastener	MS-90353 (1/4 in.)
Stress	32 ksi
Test Date	5/30/1980
Fatigue Life	16000 hrs
Location	Unknown
Flight Hrs	**Crack Size**
12800	0.0201
13200	0.0222
13600	0.0251
14000	0.0284
14400	0.0324
14800	0.0367
15200	0.042
15600	0.0484
16000	0.0532

Table A-6. Fractographic Results for Specimen 105

Specimen	105A
Fastener	MS-90353 (1/4 in.)
Stress	32 ksi
Test Date	5/19/1980
Fatigue Life	25235 hrs
Location	Unknown
Flight Hrs	**Crack Size**
12800	0.0195
13200	0.0223
13600	0.0247
14000	0.0266
14400	0.029
14800	0.0326
15200	0.0368
15600	0.0396
16000	0.0437
16400	0.0485
16800	0.0548
17200	0.0602
17600	0.0666
18000	0.0733
18400	0.0817
18800	0.089
19200	0.0978
19600	0.107
20000	0.1166
20400	0.1295
20800	0.1399
21200	0.1531
21600	0.1681
22000	0.1798
22400	0.1944
22800	0.2123
23200	0.2311
23600	0.254
24000	0.2798
24400	0.3113
24800	0.3541
25235	0.4162

Specimen	105B
Fastener	MS-90353 (1/4 in.)
Stress	32 ksi
Test Date	5/19/1980
Fatigue Life	25235
Location	Unknown
Flight Hrs	**Crack Size**
15200	0.0197
15600	0.0209
16000	0.0223
16400	0.0244
16800	0.0259
17200	0.0277
17600	0.0299
18000	0.032
18400	0.0346
18800	0.0369
19200	0.0395
19600	0.0429
20000	0.0464
20400	0.0497
20800	0.0543
21200	0.0596
21600	0.0649
22000	0.07
22400	0.0763
22800	0.0834
23200	0.0921
23600	0.1006
24000	0.108
24400	0.1173
24800	0.1292
25200	0.1407
25235	0.1508

Table A-7. Fractographic Results for Specimen 106

Specimen	106A
Fastener	MS-90353 (1/4 in.)
Stress	32 ksi
Test Date	5/21/1980
Fatigue Life	28006 hrs
Location	Unknown
Flight Hrs	**Crack Size**
18000	0.0257
18400	0.0277
18800	0.0291
19200	0.0312
19600	0.0329
20000	0.0351
20400	0.038
20800	0.0418
21200	0.0464
21600	0.0491
22000	0.0549
22400	0.0594
22800	0.0653
23200	0.0718
23600	0.0794
24000	0.0881
24400	0.0967
24800	0.1075
25200	0.1197
25600	0.1341
26000	0.1525
26400	0.1728
26800	0.1999
27200	0.2357
27600	0.2845
28006	0.3708

Specimen	106B
Fastener	MS-90353 (1/4 in.)
Stress	32 ksi
Test Date	5/21/1980
Fatigue Life	28006 hrs
Location	Unknown
Flight Hrs	**Crack Size**
24000	0.0244
24400	0.0268
24800	0.0296
25200	0.0318
25600	0.0343
26000	0.0373
26400	0.0396
26800	0.0455
27200	0.0483
27600	0.053
28000	0.0581

Table A-8. Fractographic Results for Specimen 107

Specimen	107A
Fastener	MS-90353 (1/4 in.)
Stress	32 ksi
Test Date	5/21/1980
Fatigue Life	28806 hrs
Location	Unknown
Flight Hrs	**Crack Size**
21600	0.0193
22000	0.021
22400	0.0228
22800	0.0258
23200	0.029
23600	0.0321
24000	0.0348
24400	0.0363
24800	0.0389
25200	0.0418
25600	0.045
26000	0.0491
26400	0.0532
26800	0.0599
27200	0.0651
27600	0.0721
28000	0.0797
28400	0.0888
28800	0.097

Specimen	107B
Fastener	MS-90353 (1/4 in.)
Stress	32 ksi
Test Date	5/21/1980
Fatigue Life	28806 hrs
Location	Unknown
Flight Hrs	**Crack Size**
16800	0.0252
17200	0.0264
17600	0.0278
18000	0.0291
18400	0.0311
18800	0.0337
19200	0.0366
19600	0.0397
20000	0.0427
20400	0.0468
20800	0.0521
21200	0.0577
21600	0.0632
22000	0.0662
22400	0.0717
22800	0.0775
23200	0.0843
23600	0.0908
24000	0.0988
24400	0.1081
24800	0.1175
25200	0.1304
25600	0.1434
26000	0.1591
26400	0.1753
26800	0.1968
27200	0.2264
27600	0.2617
28000	0.319
28400	0.3765
28806	0.4147

Specimens 379, 380 and 381 with ¼-inch MS-90353 rivets did not crack after 16,000 hours (4,000 passes through the spectrum).

Table A-9. Fractographic Results for Specimen 109

Specimen	109A
Fastener	MS-90353 (1/4 in.)
Stress	34 ksi
Test Date	5/30/1980
Fatigue Life	16000 hrs
Location	Unknown

Flight Hrs	Crack Size
12000	0.0207
12400	0.0219
12800	0.024
13200	0.0256
13600	0.0276
14000	0.0306
14400	0.0335
14800	0.0359
15200	0.0394
15600	0.043
16000	0.0471

Specimen	109B
Fastener	MS-90353 (1/4 in.)
Stress	34 ksi
Test Date	5/30/1980
Fatigue Life	16000 hrs
Location	Unknown

Flight Hrs	Crack Size
9200	0.0148
9600	0.0161
10000	0.0172
10400	0.0188
10800	0.0202
11200	0.0214
11600	0.0232
12000	0.0245
12400	0.0264
12800	0.0287
13200	0.0307
13600	0.0331
14000	0.0361
14400	0.038
14800	0.0425
15200	0.0471
15600	0.0522
16000	0.0584

No cracking was found in Specimen 110 after 16,000 FH.

Table A-10. Fractographic Results for Specimen 111

Specimen	111A
Fastener	MS-90353 (1/4 in.)
Stress	34 ksi
Test Date	5/30/1980
Fatigue Life	21606 hrs
Location	Unknown

Flight Hrs	Crack Size
15200	0.0151
15600	0.0164
16000	0.0176
16400	0.0203
16800	0.0234
17200	0.026
17600	0.029
18000	0.0311
18400	0.0357
18800	0.0407
19200	0.0463
19600	0.053
20000	0.0603
20400	0.0688
20800	0.0788
21200	0.0904
21606	0.1041

Specimen	111B
Fastener	MS-90353 (1/4 in.)
Stress	34 ksi
Test Date	5/30/1980
Fatigue Life	21606 hrs
Location	Unknown

Flight Hrs	Crack Size
12000	0.0162
12400	0.0185
12800	0.0213
13200	0.0268
13600	0.0308
14000	0.0341
14400	0.0377
14800	0.0414
15200	0.0447
15600	0.0506
16000	0.0558
16400	0.0625
16800	0.0707
17200	0.079
17600	0.0897
18000	0.1011
18400	0.112
18800	0.1269
19200	0.1424
19600	0.1615
20000	0.1862
20400	0.2141
20800	0.2541
21200	0.3134
21600	0.4
21606	0.4158

Table A-11. Fractographic Results for Specimen 112

Specimen	112A
Fastener	MS-90353 (1/4 in.)
Stress	34 ksi
Test Date	6/2/1980
Fatigue Life	21635 hrs
Location	Unknown

Flight Hrs	Crack Size
13200	0.0185
13600	0.0226
14000	0.0258
14400	0.0302
14800	0.0346
15200	0.0397
15600	0.0455
16000	0.0511
16400	0.0584
16800	0.0666
17200	0.075
17600	0.0835
18000	0.0977
18400	0.1107
18800	0.123
19200	0.1375
19600	0.1563
20000	0.1757
20400	0.1998
20800	0.2294
21200	0.2718
21600	0.3156
21635	0.3372

Specimen	112B
Fastener	MS-90353 (1/4 in.)
Stress	34 ksi
Test Date	6/2/1980
Fatigue Life	21635 hrs
Location	Unknown

Flight Hrs	Crack Size
14400	0.0207
14800	0.0226
15200	0.025
15600	0.0267
16000	0.0286
16400	0.0307
16800	0.0341
17200	0.036
17600	0.0387
18000	0.04
18400	0.0437
18800	0.0482
19200	0.0542
19600	0.061
20000	0.0688
20400	0.0775
20800	0.0862
21200	0.0959
21600	0.1066
21635	0.119

Table A-12. Fractographic Results for Specimens 113 and 699

Specimen	113A
Fastener	MS-90353 (1/4 in.)
Stress	34 ksi
Test Date	6/3/1980
Fatigue Life	13055 hrs
Location	Unknown

Flight Hrs	Crack Size
4800	0.014
5200	0.0173
5600	0.0206
6000	0.0271
6400	0.0337
6800	0.0382
7200	0.0449
7600	0.0527
8000	0.0606
8400	0.0699
8800	0.0789
9200	0.0909
9600	0.1042
10000	0.1211
10400	0.1396
10800	0.1621
11200	0.1893
11600	0.2308
12000	0.2749
12400	0.3433
12800	0.3935
13055	0.4431

Specimen	699B
Fastener	MS-90353 (1/4 in.)
Stress	34 ksi
Test Date	Unknown
Fatigue Life	16000 hrs
Location	Countersink-Bore

Flight Hrs	Crack Size
3200	0.0032
3600	0.0042
4000	0.0051
4400	0.0063
4800	0.0079
5200	0.0098
5600	0.0117
6000	0.0134
6400	0.0152
6800	0.0165
7200	0.019
7600	0.0206
8000	0.0229
8400	0.0254
8800	0.0278
9200	0.0298
9600	0.033
10000	0.0366
10400	0.0398
10800	0.0436
11200	0.0464
11600	0.0511
12000	0.0558
12400	0.0602
12800	0.0644
13200	0.0688
13600	0.0742
14000	0.0798
14400	0.0854
14800	0.0919
15200	0.0992
15600	0.1064
16000	0.114

Table A-13. Fractographic Results for Specimen 114

Specimen	114A
Fastener	MS-90353 (1/4 in.)
Stress	34 ksi
Test Date	6/5/1980
Fatigue Life	23606 hrs
Location	Unknown

Flight Hrs	Crack Size
14000	0.0142
14400	0.0167
14800	0.0191
15200	0.0211
15600	0.0239
16000	0.0289
16400	0.0345
16800	0.0388
17200	0.0432
17600	0.0482
18000	0.0533
18400	0.0597
18800	0.0668
19200	0.0736
19600	0.0833
20000	0.0925
20400	0.1017
20800	0.1132
21200	0.1256
21600	0.1423
22000	0.1627
22400	0.1872
22800	0.2171
23200	0.2601
23606	0.3274

Specimen	114B
Fastener	MS-90353 (1/4 in.)
Stress	34 ksi
Test Date	6/5/1980
Fatigue Life	23606 hrs
Location	Unknown

Flight Hrs	Crack Size
15200	0.0198
15600	0.0219
16000	0.0247
16400	0.0286
16800	0.0337
17200	0.0383
17600	0.0418
18000	0.047
18400	0.054
18800	0.0619
19200	0.0698
19600	0.081
20000	0.0921
20400	0.1054
20800	0.1188
21200	0.1357
21600	0.1544
22000	0.1753
22400	0.2031
22800	0.2364
23200	0.2863
23606	0.3738

Table A-14. Fractographic Results for Specimen 115

Specimen	115A
Fastener	MS-90353 (1/4 in.)
Stress	34 ksi
Test Date	6/4/1980
Fatigue Life	25206 hrs
Location	Unknown

Flight Hrs	Crack Size
13600	0.0177
14000	0.0205
14400	0.0228
14800	0.0253
15200	0.0282
15600	0.0321
16000	0.0343
16400	0.0374
16800	0.0414
17200	0.0458
17600	0.051
18000	0.0563
18400	0.0634
18800	0.0717
19200	0.0791
19600	0.0869
20000	0.0945
20400	0.1074
20800	0.1147
21200	0.1247
21600	0.1385
22000	0.1525
22400	0.1697
22800	0.187
23200	0.2079
23600	0.2315
24000	0.2579
24400	0.2874
24800	0.3294
25206	0.3853

Specimen	115B1
Fastener	MS-90353 (1/4 in.)
Stress	34 ksi
Test Date	6/4/1980
Fatigue Life	25206 hrs
Location	Unknown

Flight Hrs	Crack Size
16400	0.0214
16800	0.0235
17200	0.0266
17600	0.031
18000	0.0338
18400	0.0382
18800	0.0429
19200	0.048
19600	0.0533
20000	0.0592
20400	0.067
20800	0.0749
21200	0.0858
21600	0.0966
22000	0.109
22400	0.1225
22800	0.1382
23200	0.1571
23600	0.1798
24000	0.2075
24400	0.2405
24800	0.2904
25206	0.3679

Table A-15. Fractographic Results for Specimen 116

Specimen	116A
Fastener	MS-90353 (1/4 in.)
Stress	34 ksi
Test Date	6/9/1980
Fatigue Life	19206 hrs
Location	Bore

Flight Hrs	Crack Size
8800	0.0109
9200	0.0122
9600	0.0136
10000	0.017
10400	0.0192
10800	0.0222
11200	0.0254
11600	0.028
12000	0.0307
12400	0.0348
12800	0.0405
13200	0.0447
13600	0.0501
14000	0.0574
14400	0.0658
14800	0.0754
15200	0.0856
15600	0.0972
16000	0.1091
16400	0.1225
16800	0.139
17200	0.1562
17600	0.1826
18000	0.2124
18400	0.2494
18800	0.3076
19206	0.4021

Specimen	116B1
Fastener	MS-90353 (1/4 in.)
Stress	34 ksi
Test Date	6/9/1980
Fatigue Life	19206 hrs
Location	Bore

Flight Hrs	Crack Size
16400	0.1005
16800	0.1123
17200	0.1248
17600	0.1366
18000	0.1499
18400	0.1656
18800	0.1849
19206	0.2039

Table A-16. Fractographic Results for Specimen 117

Specimen	117A
Fastener	MS-90353 (1/4 in.)
Stress	34 ksi
Test Date	6/9/1980
Fatigue Life	27206 hrs
Location	Bore - Sharp Groove in hole

Flight Hrs	Crack Size
14400	0.0155
14800	0.0167
15200	0.0182
15600	0.0198
16000	0.0211
16400	0.0235
16800	0.0259
17200	0.0276
17600	0.0298
18000	0.033
18400	0.036
18800	0.0395
19200	0.0432
19600	0.0468
20000	0.0517
20400	0.0564
20800	0.0616
21200	0.0685
21600	0.0754
22000	0.0834
22400	0.0915
22800	0.1002
23200	0.1096
23600	0.1203
24000	0.1323
24400	0.1453
24800	0.1607
25200	0.1776
25600	0.1982
26000	0.2262
26400	0.262
26800	0.3114
27206	0.396

Specimen	117B2
Fastener	MS-90353 (1/4 in.)
Stress	34 ksi
Test Date	6/9/1980
Fatigue Life	27206 hrs
Location	Bore

Flight Hrs	Crack Size
13600	0.0118
14000	0.0129
14400	0.0147
14800	0.0165
15200	0.0177
15600	0.0189
16000	0.0202
16400	0.0223
16800	0.024
17200	0.0257
17600	0.0277
18000	0.0303
18400	0.0331
18800	0.0356
19200	0.0387
19600	0.0416
20000	0.044
20400	0.0477
20800	0.0517
21200	0.0562
21600	0.0607
22000	0.0651
22400	0.0698
22800	0.0753
23200	0.0808
23600	0.0865
24000	0.0925
24400	0.1002
24800	0.1073
25200	0.1149
25600	0.1227
26000	0.1312
26400	0.1426
26800	0.1549
27206	0.1678

Specimen 118 was destroyed in the test fixture.

Table A-17. Fractographic Results for Specimens 696 and 697

Specimen	696A
Fastener	MS-90353 (1/4 in.)
Stress	34 ksi
Test Date	Unknown
Fatigue Life	16000 hrs
Location	Bore

Flight Hrs	Crack Size
7600	0.0013
8000	0.0016
8400	0.0018
8800	0.0019
9200	0.002
9600	0.0024
10000	0.0028
10400	0.0029
10800	0.0032
11200	0.0035
11600	0.0038
12000	0.0043
12400	0.0047
12800	0.0049
13200	0.0055
13600	0.0059
14000	0.0064
14400	0.0072
14800	0.0079
15200	0.0085
15600	0.0095
16000	0.0103

Specimen	697A
Fastener	MS-90353 (1/4 in.)
Stress	34 ksi
Test Date	Unknown
Fatigue Life	16000 hrs
Location	Countersink-Bore

Flight Hrs	Crack Size
8800	0.0063
9200	0.0067
9600	0.0076
10000	0.0086
10400	0.0094
10800	0.0105
11200	0.0116
11600	0.0126
12000	0.0136
12400	0.0158
12800	0.0171
13200	0.0188
13600	0.0209
14000	0.0239
14400	0.0274
14800	0.0313
15200	0.0352
15600	0.0416
16000	0.0482

Table A-18. Fractographic Results for Specimen 700

Specimen	700A
Fastener	MS-90353 (1/4 in.)
Stress	34 ksi
Test Date	Unknown
Fatigue Life	16000 hrs
Location	Bore

Flight Hrs	Crack Size
4800	0.0029
5200	0.0033
5600	0.0037
6000	0.0041
6400	0.0046
6800	0.005
7200	0.0056
7600	0.0063
8000	0.007
8400	0.0077
8800	0.0083
9200	0.009
9600	0.0095
10000	0.0105
10400	0.0114
10800	0.0124
11200	0.0131
11600	0.0142
12000	0.0157
12400	0.0166
12800	0.0181
13200	0.0195
13600	0.0207
14000	0.0216
14400	0.0232
14800	0.0246
15200	0.0262
15600	0.0282
16000	0.0292

Specimen	700B
Fastener	MS-90353 (1/4 in.)
Stress	34 ksi
Test Date	Unknown
Fatigue Life	16000 hrs
Location	Bore

Flight Hrs	Crack Size
3600	0.0021
4000	0.0023
4400	0.0025
4800	0.0027
5200	0.003
5600	0.0033
6000	0.0035
6400	0.0037
6800	0.0039
7200	0.0043
7600	0.0046
8000	0.005
8400	0.0055
8800	0.0059
9200	0.0064
9600	0.007
10000	0.0074
10400	0.0078
10800	0.0083
11200	0.0089
11600	0.0094
12000	0.01
12400	0.0107
12800	0.0113
13200	0.0119
13600	0.0124
14000	0.0132
14400	0.0142
14800	0.0147
15200	0.0153
15600	0.0164
16000	0.018

Table A-19. Fractographic Results for Specimens 467 and 468

Specimen	467A
Fastener	NAS 1580 (1/4 in.)
Stress	38 ksi
Test Date	4/15/1980
Fatigue Life	15550 hrs
Location	Multiple: Bore, C.S.-Bore

Flight Hrs	Crack Size
5200	0.0102
5600	0.012
6000	0.0135
6400	0.0145
6800	0.0163
7200	0.0188
7600	0.0212
8000	0.0237
8400	0.0266
8800	0.0297
9200	0.0334
9600	0.0375
10000	0.0434
10400	0.0498
10800	0.0562
11200	0.0651
11600	0.075
12000	0.0877
12400	0.1045
12800	0.123
13200	0.1437
13600	0.1752
14000	0.1986
14400	0.2351
14800	0.2905
15200	0.3738
15550	0.4251

Specimen	468A
Fastener	NAS 1580 (1/4 in.)
Stress	38 ksi
Test Date	4/16/1980
Fatigue Life	11879 hrs
Location	Multiple: Bore, C.S.-Bore

Flight Hrs	Crack Size
4800	0.018
5200	0.0205
5600	0.0241
6000	0.0278
6400	0.0331
6800	0.0419
7200	0.0504
7600	0.0582
8000	0.0683
8400	0.0816
8800	0.1063
9200	0.1263
9600	0.1477
10000	0.1744
10400	0.2056
10800	0.247
11200	0.3128
11600	0.3921
11879	0.4138

Table A-20. Fractographic Results for Specimens 469 and 470

Specimen	469B
Fastener	NAS 1580 (1/4 in.)
Stress	38 ksi
Test Date	4/15/1980
Fatigue Life	16000 hrs
Location	Multiple: Bore

Flight Hrs	Crack Size
4800	0.0051
5200	0.0063
5600	0.0083
6000	0.0098
6400	0.012
6800	0.0147
7200	0.0173
7600	0.02
8000	0.0224
8400	0.0244
8800	0.0263
9200	0.0292
9600	0.0329
10000	0.0363
10400	0.0397
10800	0.0444
11200	0.0493
11600	0.053
12000	0.059
12400	0.0663
12800	0.0731
13200	0.0808
13600	0.0891
14000	0.1002
14400	0.1087
14800	0.1204
15200	0.1342
15600	0.1498
16000	0.166

Specimen	470B
Fastener	NAS 1580 (1/4 in.)
Stress	38 ksi
Test Date	4/16/1980
Fatigue Life	13959 hrs
Location	Multiple: Bore

Flight Hrs	Crack Size
5200	0.0125
5600	0.0147
6000	0.017
6400	0.0192
6800	0.0215
7200	0.0236
7600	0.0271
8000	0.0316
8400	0.0365
8800	0.0435
9200	0.051
9600	0.0585
10000	0.0652
10400	0.0765
10800	0.0849
11200	0.0965
11600	0.1106
12000	0.1289
12400	0.1572
12800	0.1972
13200	0.251
13600	0.3306
13959	0.3559

Table A-21. Fractographic Results for Specimens 471 and 472

Specimen	471B
Fastener	NAS 1580 (1/4 in.)
Stress	38 ksi
Test Date	4/16/1980
Fatigue Life	16000 hrs
Location	Multiple: Bore

Flight Hrs	Crack Size
8800	0.0089
9200	0.01
9600	0.0114
10000	0.0131
10400	0.0148
10800	0.0166
11200	0.0188
11600	0.0216
12000	0.0241
12400	0.0266
12800	0.0291
13200	0.0328
13600	0.0364
14000	0.0389
14400	0.0434
14800	0.0471
15200	0.0521
15600	0.0566
16000	0.061

Specimen	472A
Fastener	NAS 1580 (1/4 in.)
Stress	38 ksi
Test Date	4/16/1980
Fatigue Life	16000 hrs
Location	Multiple: Bore

Flight Hrs	Crack Size
11200	0.0086
11600	0.0104
12000	0.0121
12400	0.0146
12800	0.0167
13200	0.0197
13600	0.0229
14000	0.0256
14400	0.0291
14800	0.0341
15200	0.039
15600	0.0452
16000	0.0511

Table A-22. Fractographic Results for Specimens 473 and 474

Specimen	473A
Fastener	NAS 1580 (1/4 in.)
Stress	38 ksi
Test Date	4/16/1980
Fatigue Life	16000 hrs
Location	Multiple: Bore

Flight Hrs	Crack Size
5600	0.0117
6000	0.0134
6400	0.0154
6800	0.0176
7200	0.0195
7600	0.0224
8000	0.0251
8400	0.0276
8800	0.0305
9200	0.0343
9600	0.0379
10000	0.0415
10400	0.0458
10800	0.0514
11200	0.0567
11600	0.0622
12000	0.0669
12400	0.0731
12800	0.0784
13200	0.087
13600	0.0949
14000	0.1032
14400	0.1126
14800	0.1238
15200	0.1383
15600	0.1554
16000	0.1769

Specimen	474A
Fastener	NAS 1580 (1/4 in.)
Stress	38 ksi
Test Date	4/16/1980
Fatigue Life	16000 hrs
Location	Multiple: Bore

Flight Hrs	Crack Size
10000	0.0065
10400	0.0079
10800	0.0097
11200	0.0108
11600	0.0123
12000	0.0137
12400	0.0157
12800	0.0184
13200	0.021
13600	0.0248
14000	0.0282
14400	0.0308
14800	0.035
15200	0.0404
15600	0.0446
16000	0.0488

Table A-23. Fractographic Results for Specimens 475 and 476

Specimen	475A
Fastener	NAS 1580 (1/4 in.)
Stress	38 ksi
Test Date	4/16/1980
Fatigue Life	15708 hrs
Location	Multiple: Bore

Flight Hrs	Crack Size
4800	0.0181
5200	0.0205
5600	0.0239
6000	0.0271
6400	0.03
6800	0.0345
7200	0.0394
7600	0.0428
8000	0.0474
8400	0.0527
8800	0.0592
9200	0.066
9600	0.0734
10000	0.0819
10400	0.0896
10800	0.0987
11200	0.1112
11600	0.1239
12000	0.1399
12400	0.1564
12800	0.1765
13200	0.1994
13600	0.2285
14000	0.2633
14400	0.3145
14800	0.3528
15708	0.3961

Specimen	476B
Fastener	NAS 1580 (1/4 in.)
Stress	38 ksi
Test Date	4/16/1980
Fatigue Life	16000 hrs
Location	Multiple: Bore

Flight Hrs	Crack Size
10800	0.0207
11200	0.0243
11600	0.0293
12000	0.0334
12400	0.0381
12800	0.0435
13200	0.048
13600	0.0554
14000	0.0633
14400	0.0721
14800	0.08
15200	0.0913
15600	0.1009
16000	0.1082

Table A-24. Fractographic Results for Specimens 383 and 384

Specimen	383A
Fastener	MS-90353 (1/4 in.)
Stress	38 ksi
Test Date	2/9/1981
Fatigue Life	16000 hrs
Location	Multiple: Bore
Flight Hrs	**Crack Size**
6800	0.0091
7200	0.0102
7600	0.0116
8000	0.0128
8400	0.0137
8800	0.0156
9200	0.0175
9600	0.0192
10000	0.0215
10400	0.024
10800	0.027
11200	0.0298
11600	0.0326
12000	0.036
12400	0.0397
12800	0.0429
13200	0.0463
13600	0.0515
14000	0.057
14400	0.0622
14800	0.0685
15200	0.0766
15600	0.0872
16000	0.0949

Specimen	384A
Fastener	MS-90353 (1/4 in.)
Stress	38 ksi
Test Date	2/12/1981
Fatigue Life	16000 hrs
Location	Multiple: Bore
Flight Hrs	**Crack Size**
7200	0.0094
7600	0.0105
8000	0.0118
8400	0.0134
8800	0.0149
9200	0.0165
9600	0.0182
10000	0.0208
10400	0.0232
10800	0.0258
11200	0.0288
11600	0.0328
12000	0.0371
12400	0.0402
12800	0.0455
13200	0.0514
13600	0.0575
14000	0.0649
14400	0.0742
14800	0.0858
15200	0.1
15600	0.1185
16000	0.1351

Table A-25. Fractographic Results for Specimens 385 and 386

Specimen	385B
Fastener	MS-90353 (1/4 in.)
Stress	38 ksi
Test Date	2/12/1981
Fatigue Life	16000 hrs
Location	Multiple: Bore
Flight Hrs	**Crack Size**
7600	0.0055
8000	0.0061
8400	0.0066
8800	0.0072
9200	0.0078
9600	0.0088
10000	0.0096
10400	0.0108
10800	0.0119
11200	0.0131
11600	0.0147
12000	0.0162
12400	0.018
12800	0.0197
13200	0.0215
13600	0.0235
14000	0.0256
14400	0.0282
14800	0.0305
15200	0.0327
15600	0.0359
16000	0.0384

Specimen	386B
Fastener	MS-90353 (1/4 in.)
Stress	38 ksi
Test Date	2/12/1981
Fatigue Life	16000 hrs
Location	Bore
Flight Hrs	**Crack Size**
7600	0.0077
8000	0.0084
8400	0.0095
8800	0.0105
9200	0.0123
9600	0.0134
10000	0.0149
10400	0.0167
10800	0.0185
11200	0.0207
11600	0.023
12000	0.0247
12400	0.0272
12800	0.0297
13200	0.0325
13600	0.0355
14000	0.0391
14400	0.0431
14800	0.0481
15200	0.0531
15600	0.0596
16000	0.0659

Table A-26. Fractographic Results for Specimens 387 and 581

Specimen	387A
Fastener	MS-90353 (1/4 in.)
Stress	38 ksi
Test Date	2/12/1981
Fatigue Life	16000 hrs
Location	Multiple: Bore
Flight Hrs	**Crack Size**
9600	0.0066
10000	0.0076
10400	0.0087
10800	0.0099
11200	0.0112
11600	0.0125
12000	0.0135
12400	0.0151
12800	0.0166
13200	0.0178
13600	0.0192
14000	0.0216
14400	0.0237
14800	0.026
15200	0.0283
15600	0.0304
16000	0.0323

Specimen	581A
Fastener	MS-90353 (1/4 in.)
Stress	38 ksi
Test Date	
Fatigue Life	10000 hrs
Location	Multiple: Bore
Flight Hrs	**Crack Size**
3200	0.0241
3600	0.0255
4000	0.0281
4400	0.0312
4800	0.0356
5200	0.0418
5600	0.0487
6000	0.0557
6400	0.0635
6800	0.0727
7200	0.0875
7600	0.103
8000	0.1238
8400	0.1489
8800	0.1801
9200	0.1988
9600	0.23
10000	0.3206

Table A-27. Fractographic Results for Specimens 582 and 583

Specimen	582B
Fastener	MS-90353 (1/4 in.)
Stress	38 ksi
Test Date	
Fatigue Life	7206 hrs
Location	Multiple: Bore, C.S.-Bore

Flight Hrs	Crack Size
2000	0.0145
2400	0.025
2800	0.035
3200	0.0442
3600	0.0546
4000	0.0643
4400	0.0753
4800	0.0858
5200	0.1012
5600	0.12
6000	0.1444
6400	0.1772
6800	0.236
7206	0.3402

Specimen	583B
Fastener	MS-90353 (1/4 in.)
Stress	38 ksi
Test Date	
Fatigue Life	10007 hrs
Location	Multiple: Bore

Flight Hrs	Crack Size
3600	0.0188
4000	0.0231
4400	0.0269
4800	0.0299
5200	0.0354
5600	0.0398
6000	0.0457
6400	0.0534
6800	0.064
7200	0.0742
7600	0.0883
8000	0.1047
8400	0.1258
8800	0.1526
9200	0.1861
9600	0.2383
10007	0.3301

Table A-28. Fractographic Results for Specimens 584 and 585

Specimen	584B
Fastener	MS-90353 (1/4 in.)
Stress	38 ksi
Test Date	
Fatigue Life	16000 hrs
Location	Multiple: Bore
Flight Hrs	**Crack Size**
8400	0.0112
8800	0.0132
9200	0.0152
9600	0.0177
10000	0.0188
10400	0.0211
10800	0.0233
11200	0.0266
11600	0.0289
12000	0.0316
12400	0.0347
12800	0.0384
13200	0.042
13600	0.0463
14000	0.0511
14400	0.0571
14800	0.0646
15200	0.0719
15600	0.0799
16000	0.0887

Specimen	585B
Fastener	MS-90353 (1/4 in.)
Stress	38 ksi
Test Date	
Fatigue Life	10678 hrs
Location	Multiple: Bore
Flight Hrs	**Crack Size**
2800	0.0107
3200	0.0127
3600	0.0148
4000	0.0179
4400	0.0228
4800	0.0282
5200	0.0333
5600	0.0386
6000	0.0455
6400	0.0521
6800	0.0595
7200	0.0679
7600	0.0774
8000	0.0896
8400	0.1053
8800	0.1229
9200	0.1471
9600	0.1749
10000	0.2121
10400	0.2691
10678	0.3905

Table A-29. Fractographic Results for Specimens 654 and 655

Specimen	654B
Fastener	MS-90353 (1/4 in.)
Stress	38 ksi
Test Date	
Fatigue Life	
Location	Bore
Flight Hrs	**Crack Size**
10000	0.0148
10400	0.0162
10800	0.0173
11200	0.0186
11600	0.02
12000	0.0214
12400	0.0228
12800	0.0243
13200	0.026
13600	0.0272
14000	0.0289
14400	0.0307
14800	0.0327
15200	0.0343
15600	0.0361
16000	0.0384

Specimen	655A
Fastener	MS-90353 (1/4 in.)
Stress	38 ksi
Test Date	
Fatigue Life	
Location	C.S.-Bore Intersect
Flight Hrs	**Crack Size**
5200	0.0115
5600	0.0141
6000	0.0163
6400	0.0192
6800	0.0225
7200	0.0251
7600	0.0283
8000	0.0315
8400	0.0351
8800	0.0382
9200	0.0408
9600	0.044
10000	0.0472
10400	0.0498
10800	0.0541
11200	0.058
11600	0.0616
12000	0.0651
12400	0.0695
12800	0.0746
13200	0.0797
13600	0.0863
14000	0.0932
14400	0.102
14800	0.1114
15200	0.1212
15600	0.1319
16000	0.1455

Table A-30. Fractographic Results for Specimens 656 and 657

Specimen	656A
Fastener	MS-90353 (1/4 in.)
Stress	38 ksi
Test Date	
Fatigue Life	
Location	C.S.-Bore Intersect

Flight Hrs	Crack Size
10400	0.0173
10800	0.0185
11200	0.0198
11600	0.0211
12000	0.0222
12400	0.0236
12800	0.0253
13200	0.0267
13600	0.0281
14000	0.0299
14400	0.0313
14800	0.0328
15200	0.0346
15600	0.036
16000	0.0376

Specimen	657A
Fastener	MS-90353 (1/4 in.)
Stress	38 ksi
Test Date	
Fatigue Life	
Location	Bore

Flight Hrs	Crack Size
13200	0.0119
13600	0.0127
14000	0.0136
14400	0.0144
14800	0.0152
15200	0.0158
15600	0.0166
16000	0.0172

Table A-31. Fractographic Results for Specimens 658 and 660

Specimen	658B
Fastener	MS-90353 (1/4 in.)
Stress	38 ksi
Test Date	
Fatigue Life	
Location	Bore
Flight Hrs	**Crack Size**
8800	0.0098
9200	0.0118
9600	0.0135
10000	0.0153
10400	0.0177
10800	0.0197
11200	0.0219
11600	0.0243
12000	0.0269
12400	0.0297
12800	0.0321
13200	0.0348
13600	0.0375
14000	0.0401
14400	0.0426
14800	0.046
15200	0.0495
15600	0.0532
16000	0.0588

Specimen	660B
Fastener	MS-90353 (1/4 in.)
Stress	38 ksi
Test Date	
Fatigue Life	
Location	Bore
Flight Hrs	**Crack Size**
15200	0.023
15600	0.026
16000	0.0292

Specimen 659 did not have any crack measurements less than 0.039 inch. No EIDS could be calculated for it with this approach.

Table A-32. Fractographic Results for Specimens 661 and 662

Specimen	661B
Fastener	MS-90353 (1/4 in.)
Stress	38 ksi
Test Date	
Fatigue Life	
Location	Bore
Flight Hrs	**Crack Size**
9600	0.032
10000	0.0349
10400	0.0377
10800	0.0419
11200	0.0453
11600	0.0499
12000	0.0541
12400	0.0587
12800	0.0633
13200	0.0686
13600	0.0739
14000	0.0793
14400	0.0862
14800	0.0933
15200	0.1019
15600	0.1123
16000	0.1246

Specimen	662B
Fastener	MS-90353 (1/4 in.)
Stress	38 ksi
Test Date	
Fatigue Life	
Location	CS-Bore Intersect
Flight Hrs	**Crack Size**
8400	0.0082
8800	0.0092
9200	0.0104
9600	0.0115
10000	0.0126
10400	0.0137
10800	0.0153
11200	0.016
11600	0.0172
12000	0.0185
12400	0.0198
12800	0.0208
13200	0.0224
13600	0.0235
14000	0.0245
14400	0.0263
14800	0.0278
15200	0.0294
15600	0.0309
16000	0.0328

A.3 Equivalent Initial Damage Size Determination

Plots of crack size versus flight hours for all cracks less than 0.0393 inch (1 mm) along with the exponential curve fit to the data are shown in Figure A-3 to Figure A-34.

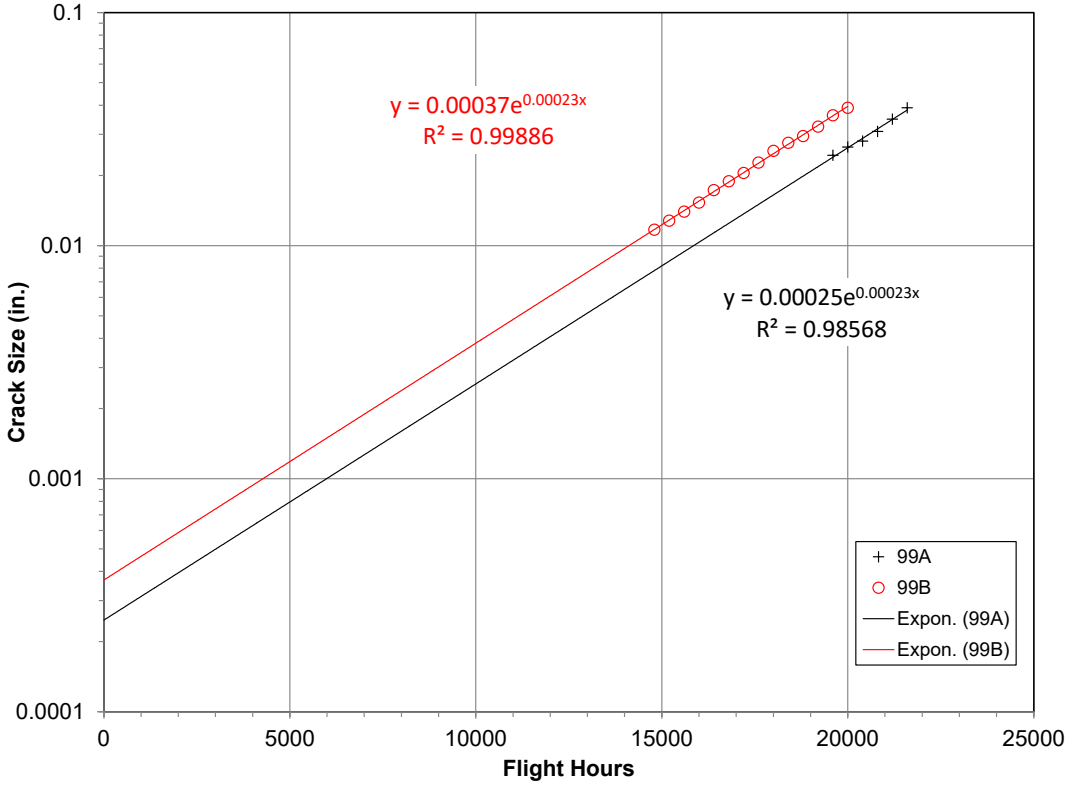

Figure A-3. EIDS Determination for Specimen 99

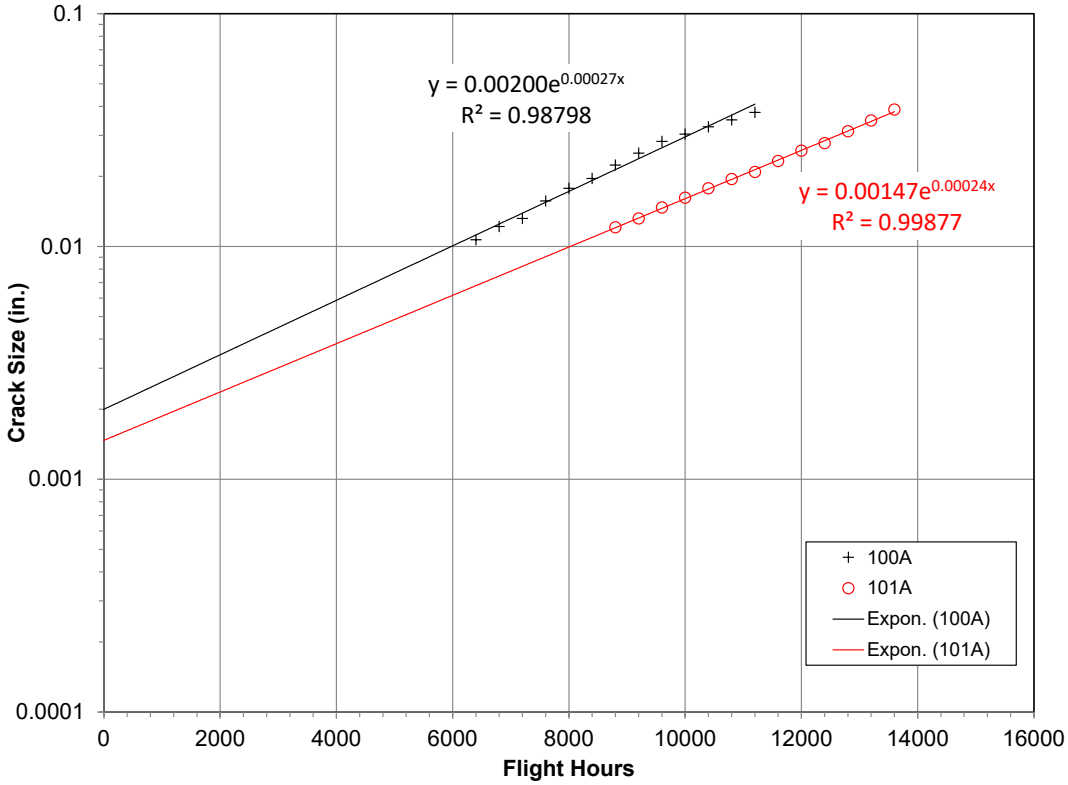

Figure A-4. EIDS Determination for Specimens 100 and 101

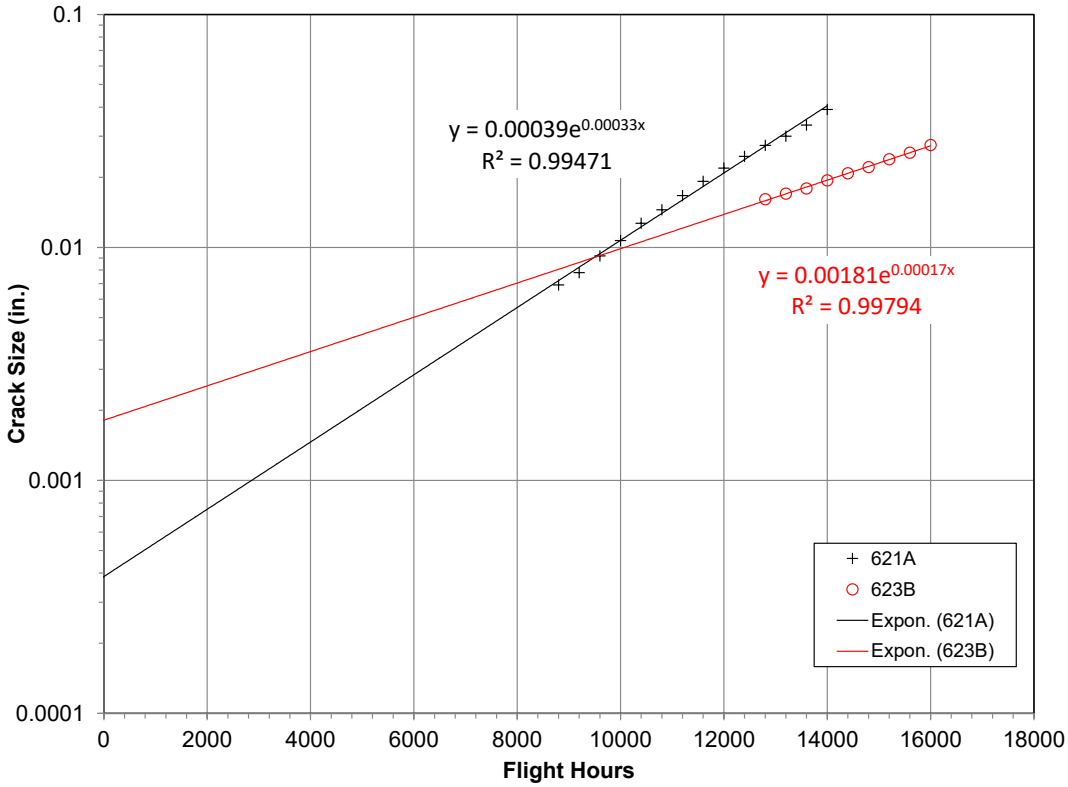

Figure A-5. EIDS Determination for Specimens 621 and 623

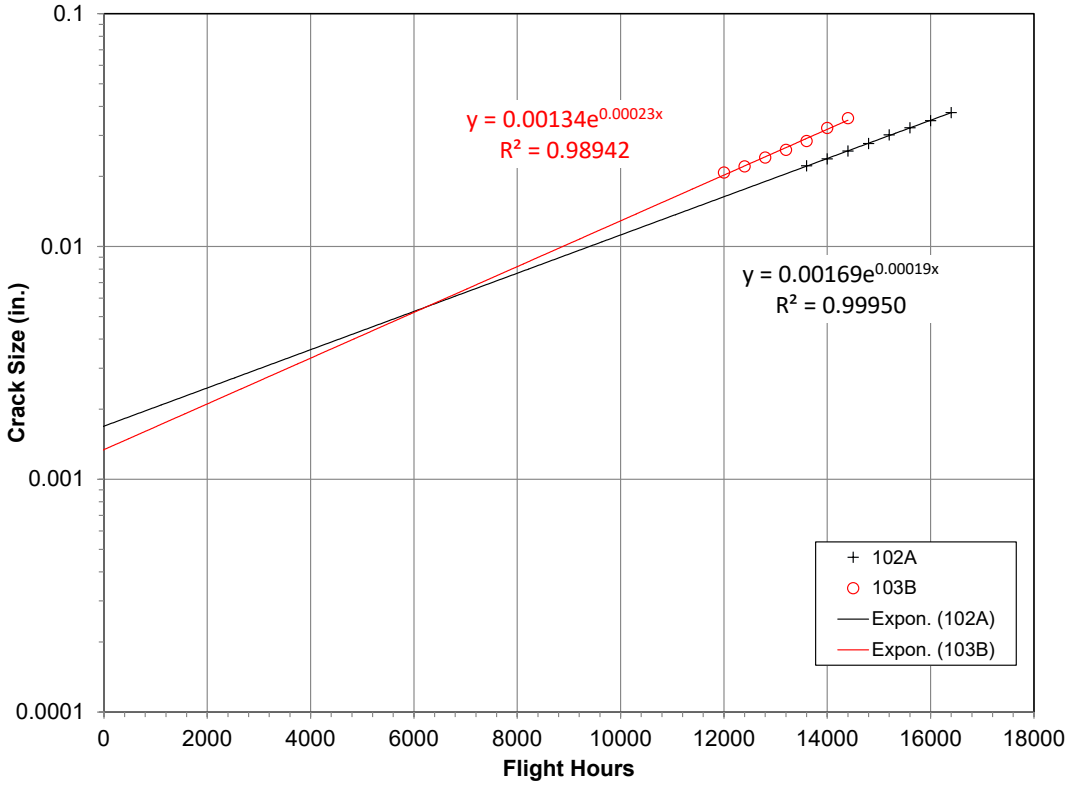

Figure A-6. EIDS Determination for Specimens 102 and 103

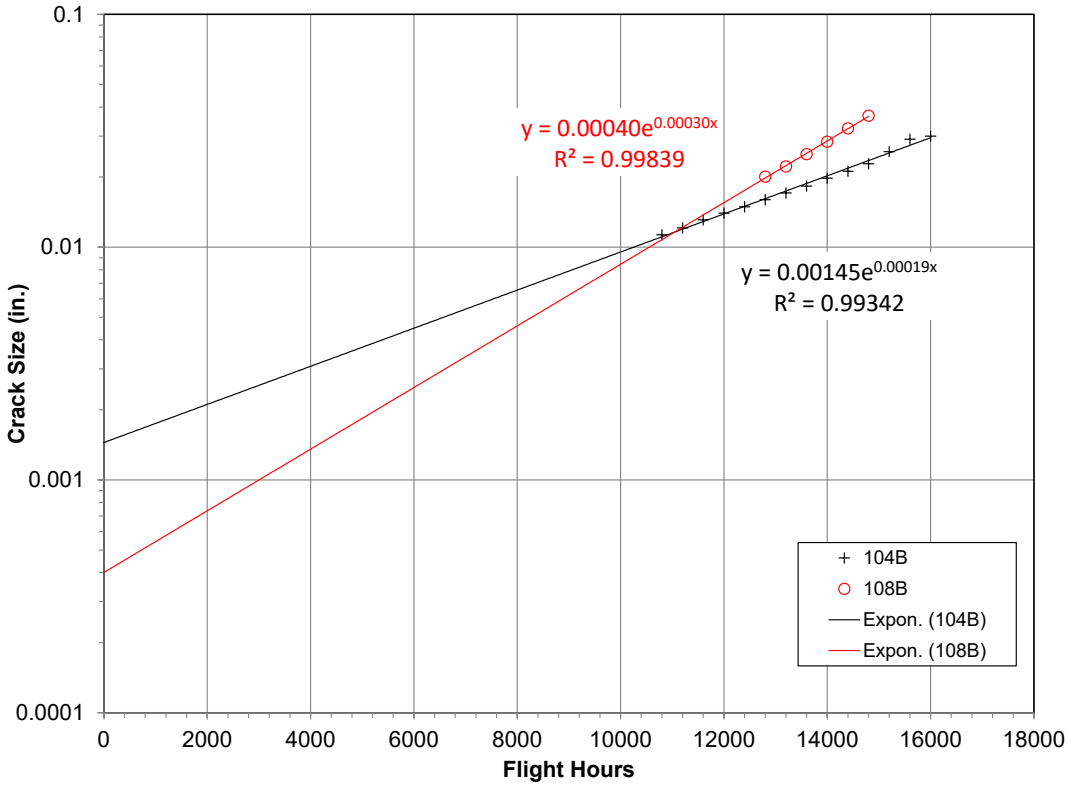

Figure A-7. EIDS Determination for Specimens 104 and 108

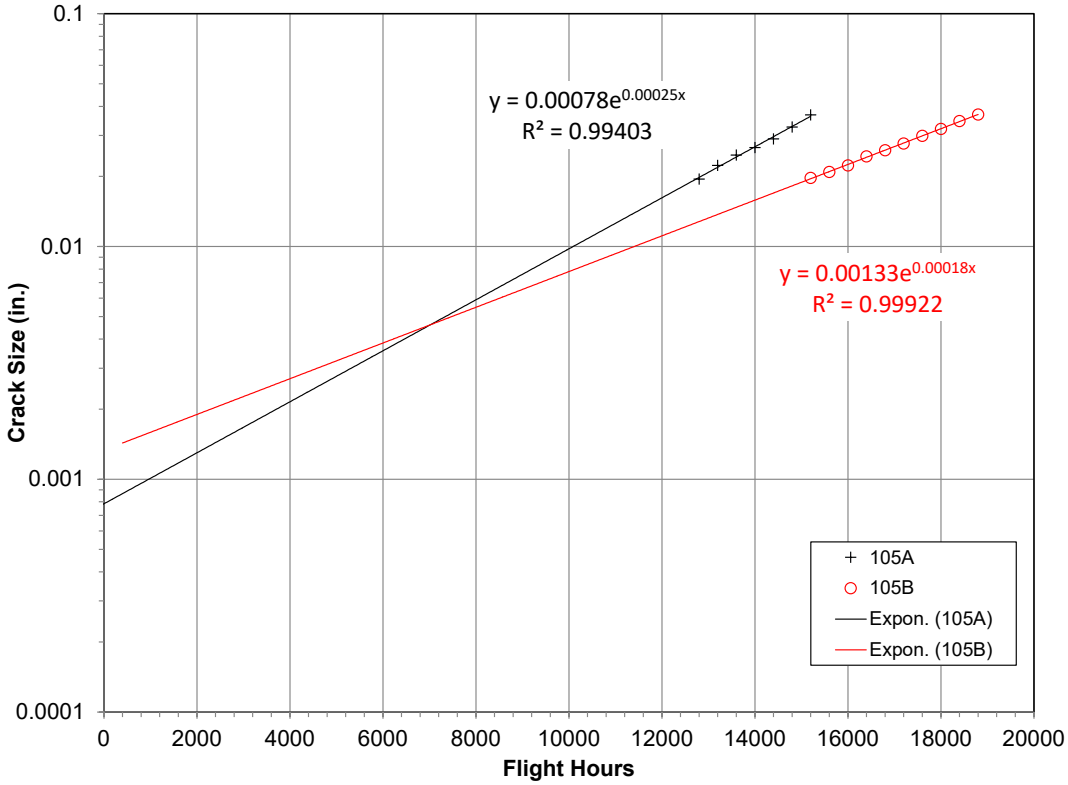

Figure A-8. EIDS Determination for Specimen 105

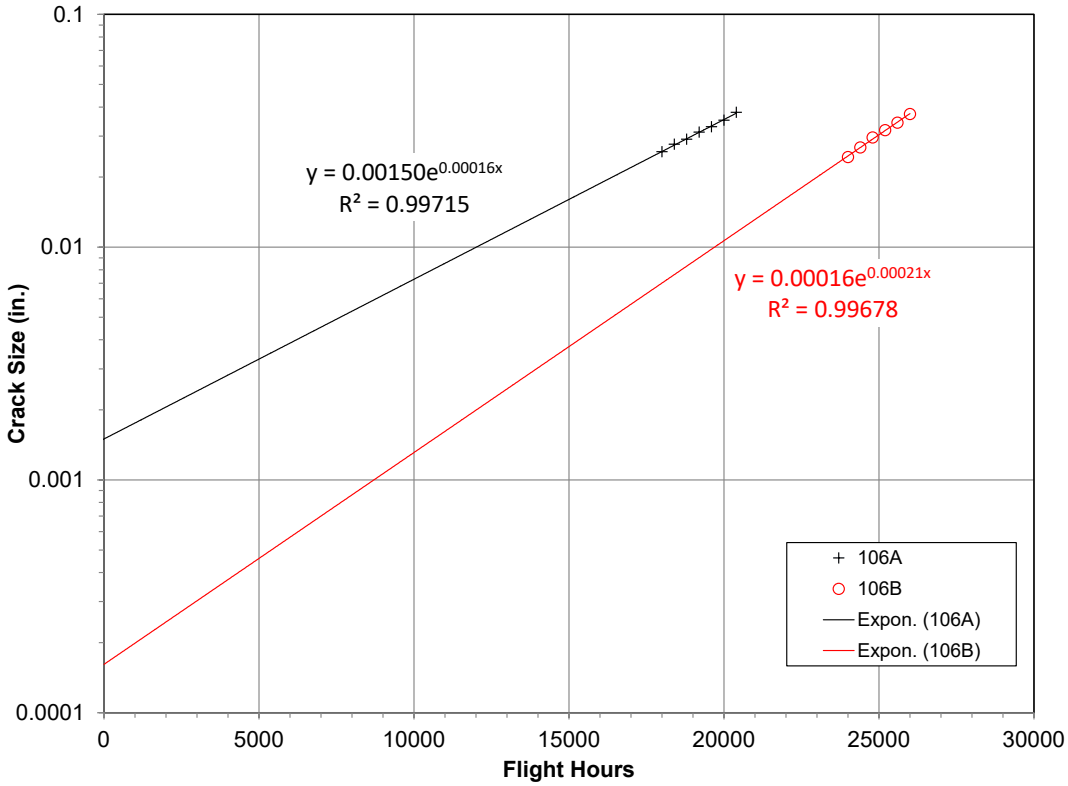

Figure A-9. EIDS Determination for Specimen 106

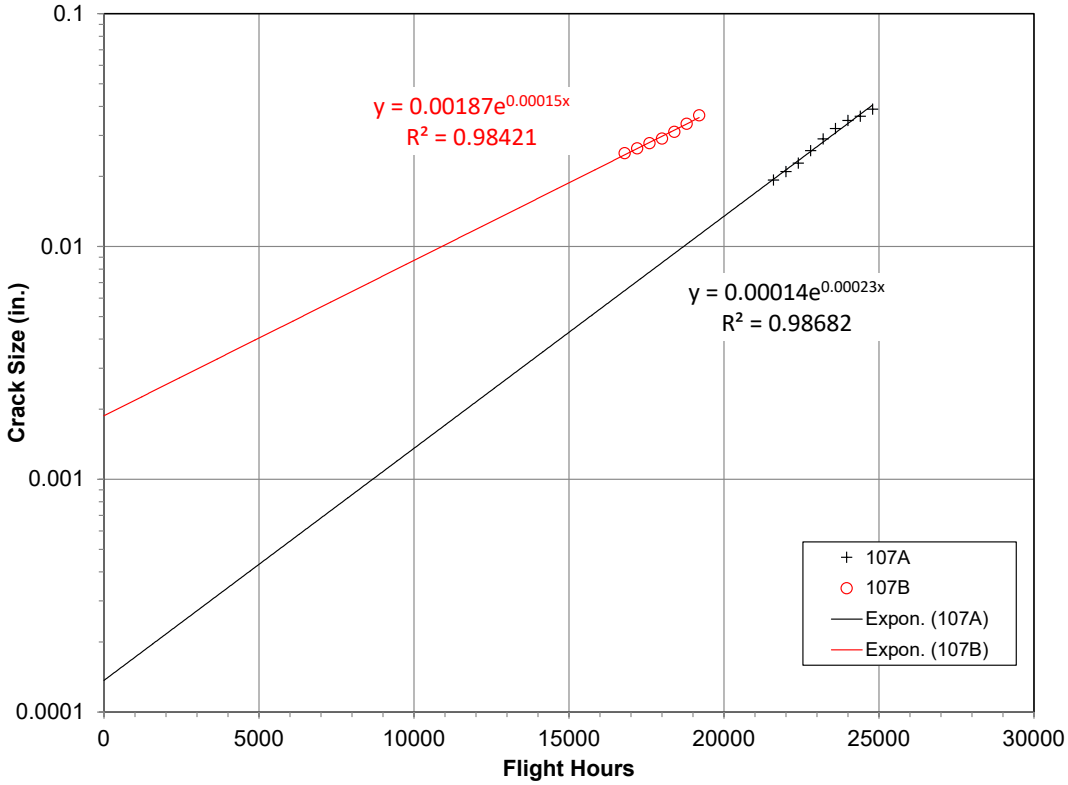

Figure A-10. EIDS Determination for Specimen 107

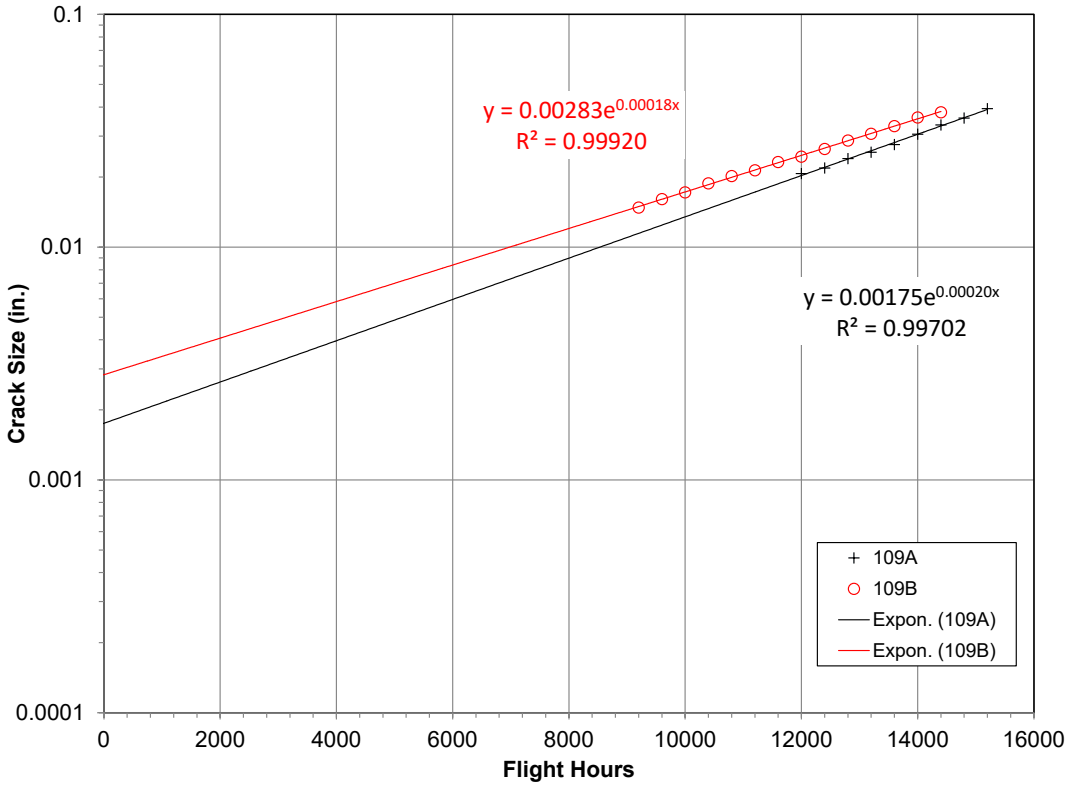

Figure A-11. EIDS Determination for Specimen 109

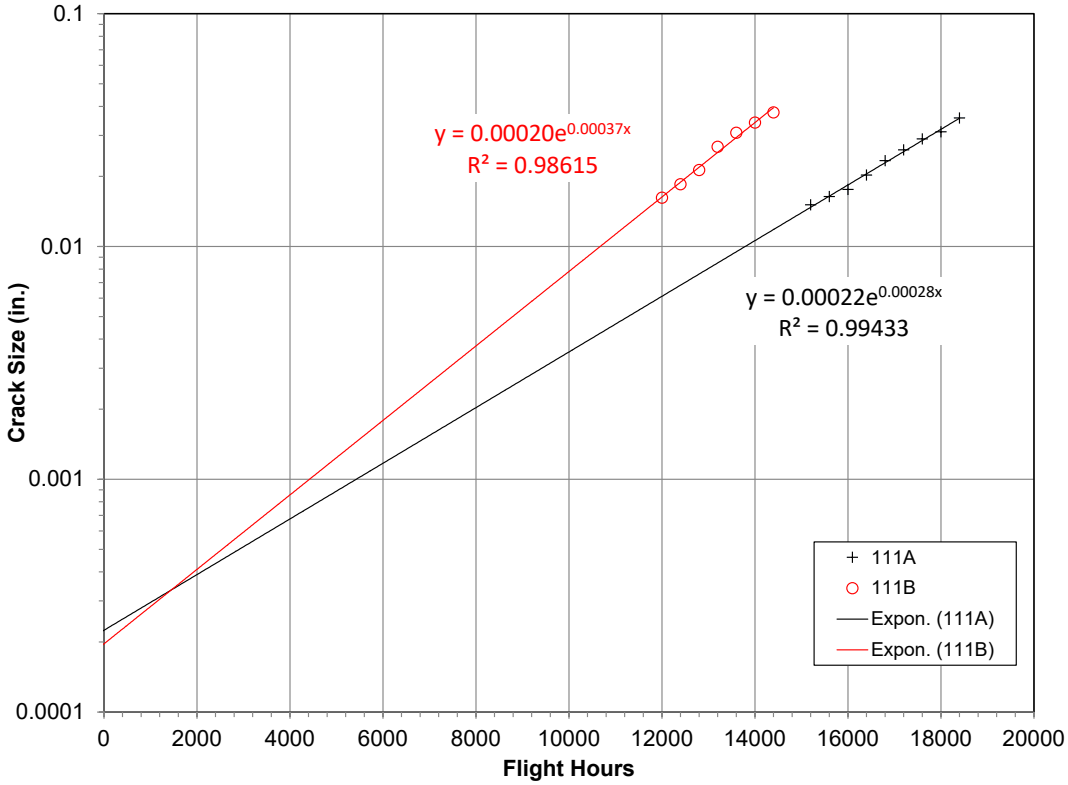

Figure A-12. EIDS Determination for Specimen 111

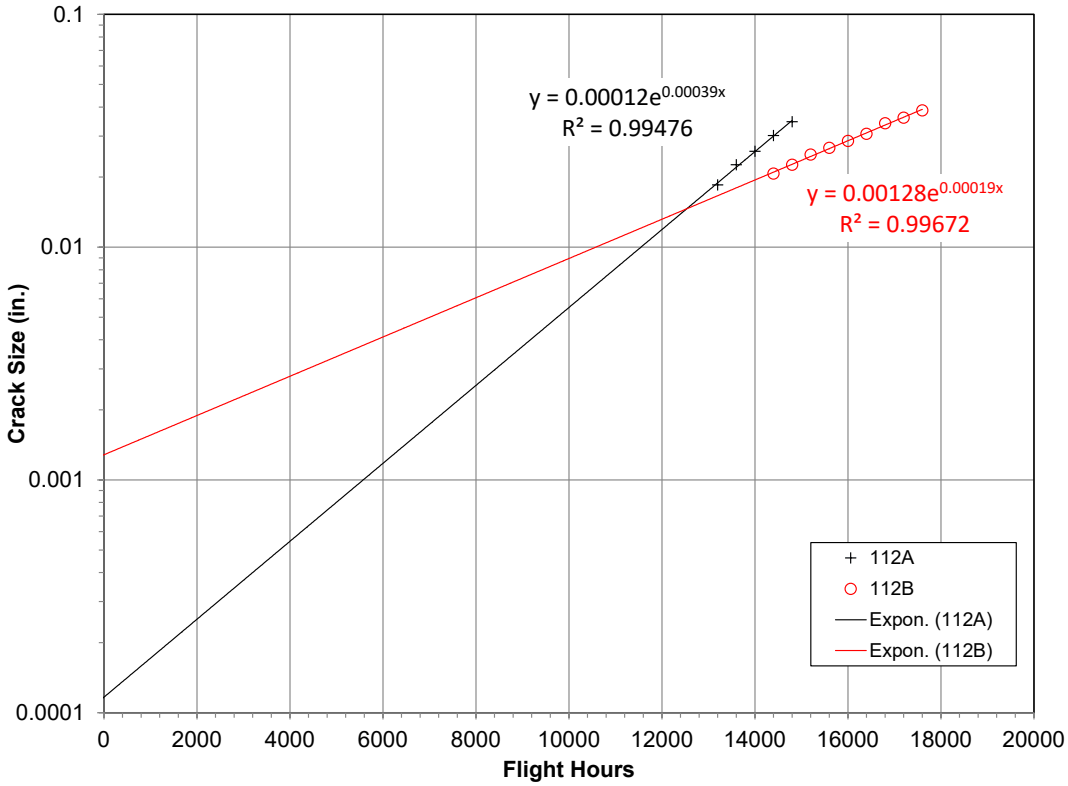

Figure A-13. EIDS Determination for Specimen 112

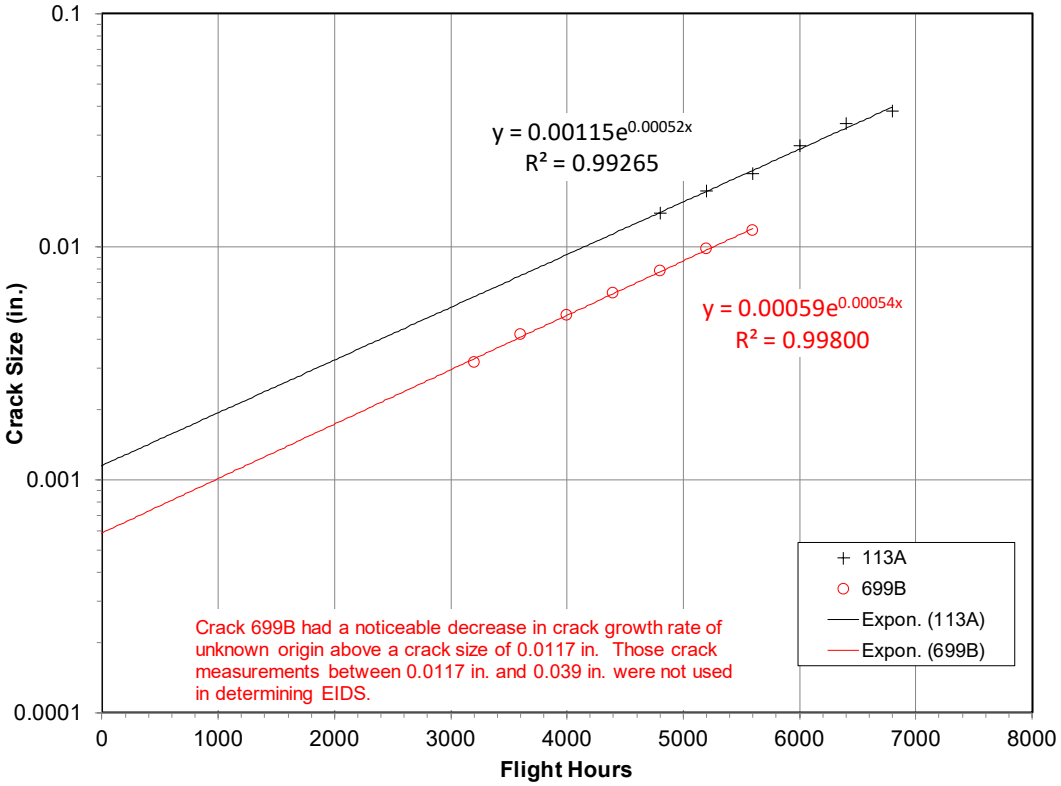

Figure A-14. EIDS Determination for Specimen 113 and 699

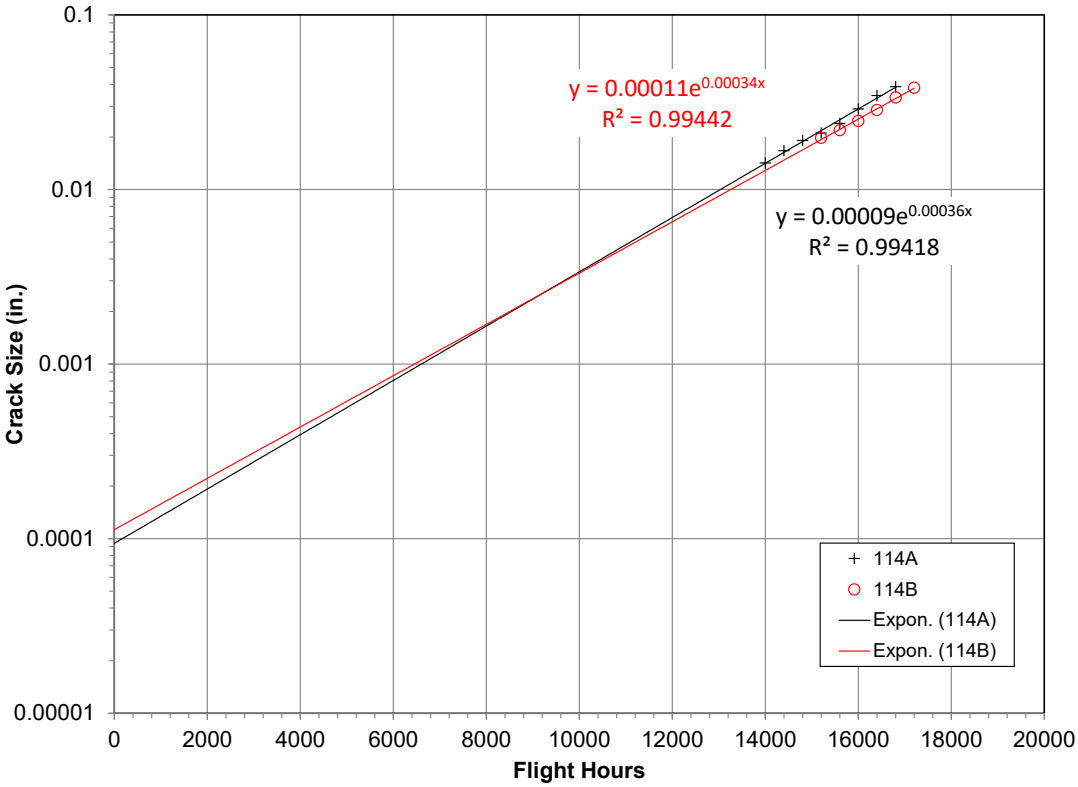

Figure A-15. EIDS Determination for Specimen 114

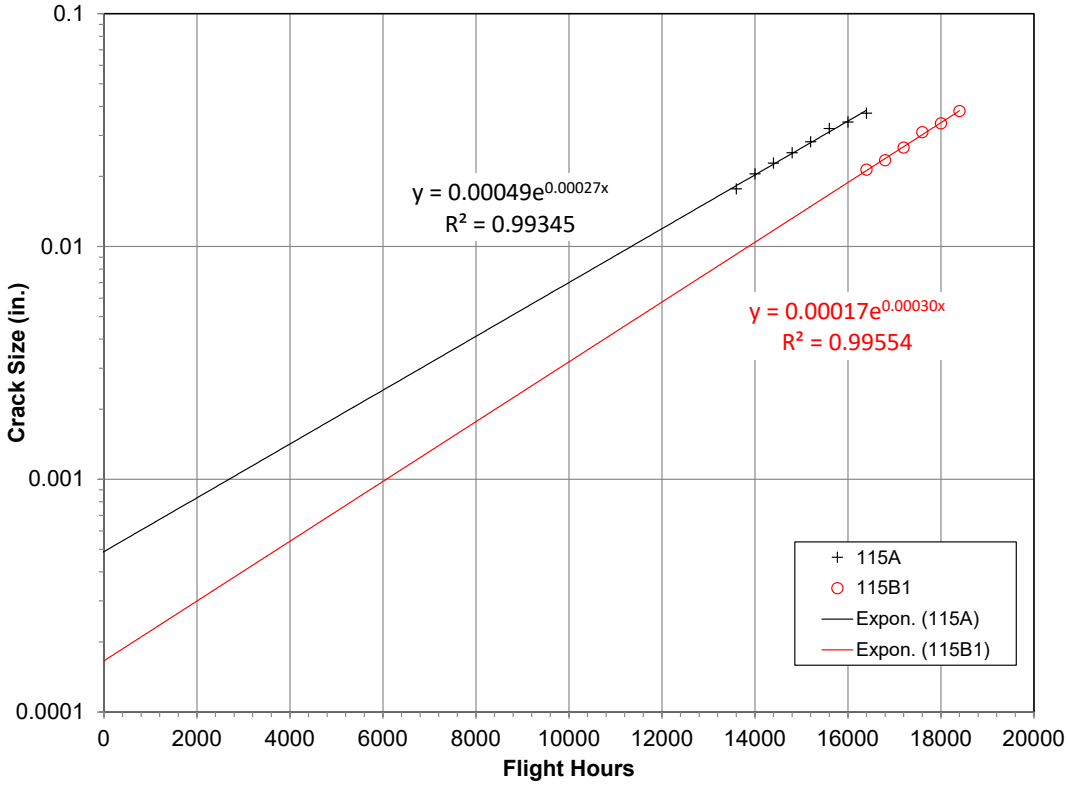

Figure A-16. EIDS Determination for Specimen 115

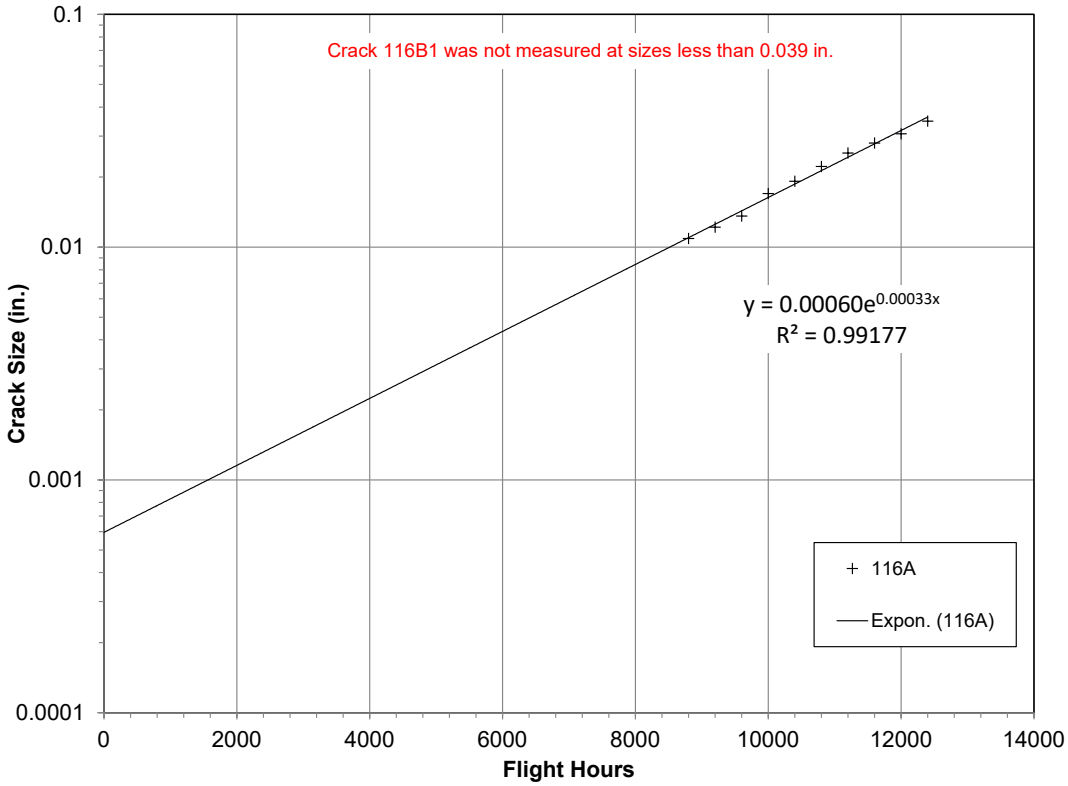

Figure A-17. EIDS Determination for Specimen 116

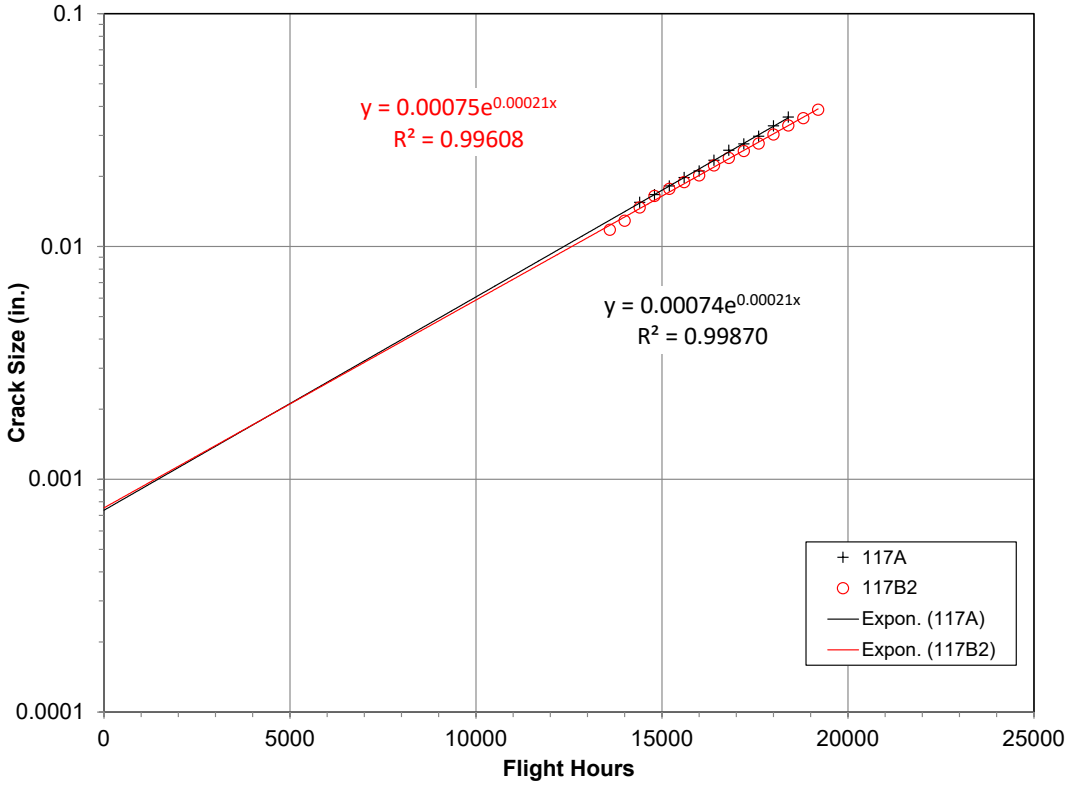

Figure A-18. EIDS Determination for Specimen 117

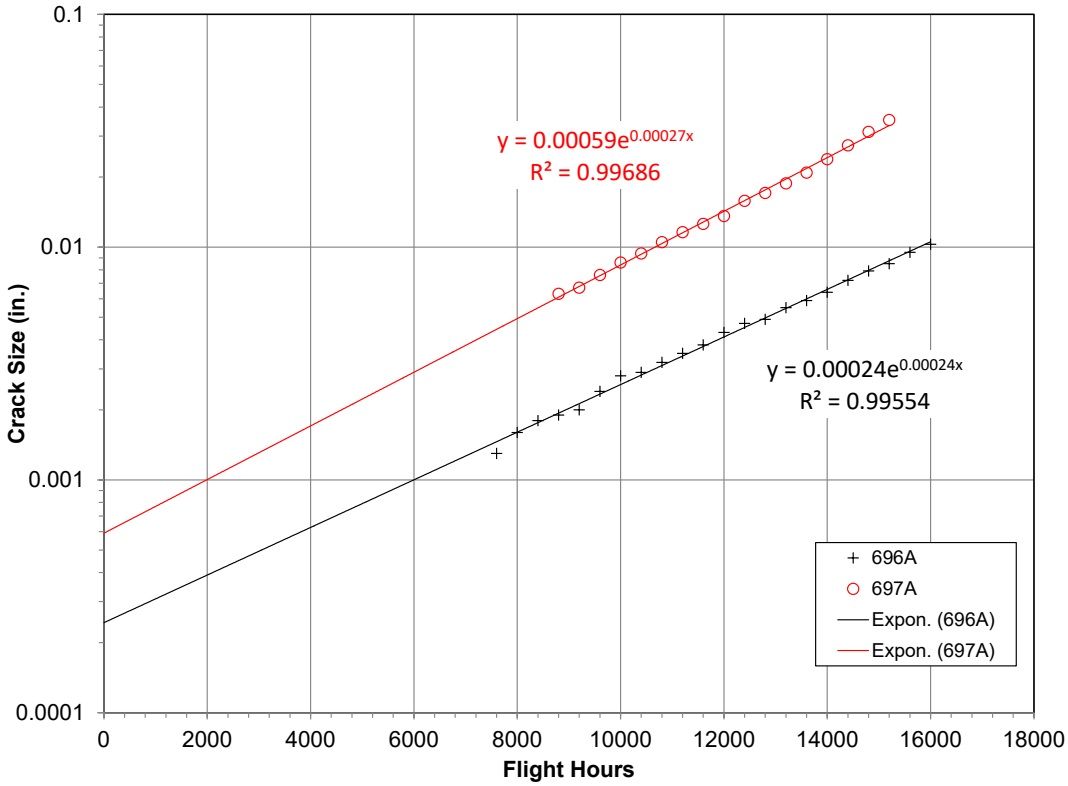

Figure A-19. EIDS Determination for Specimen 696 and 697

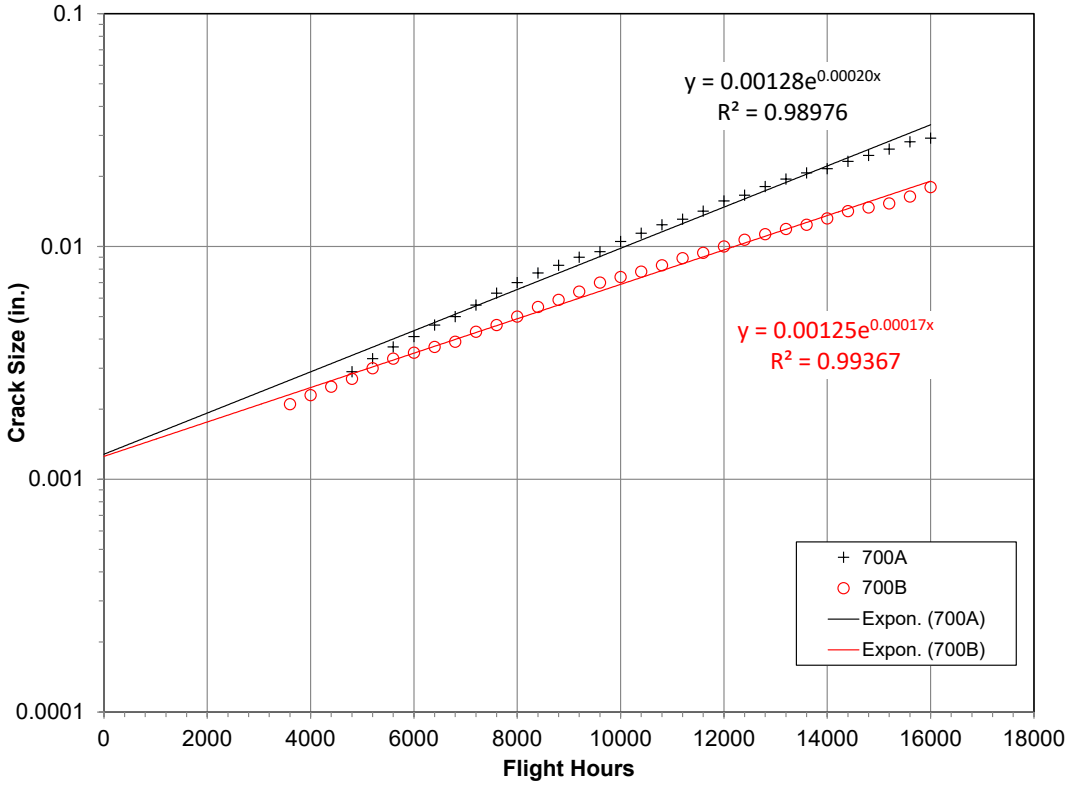

Figure A-20. EIDS Determination for Specimen 700

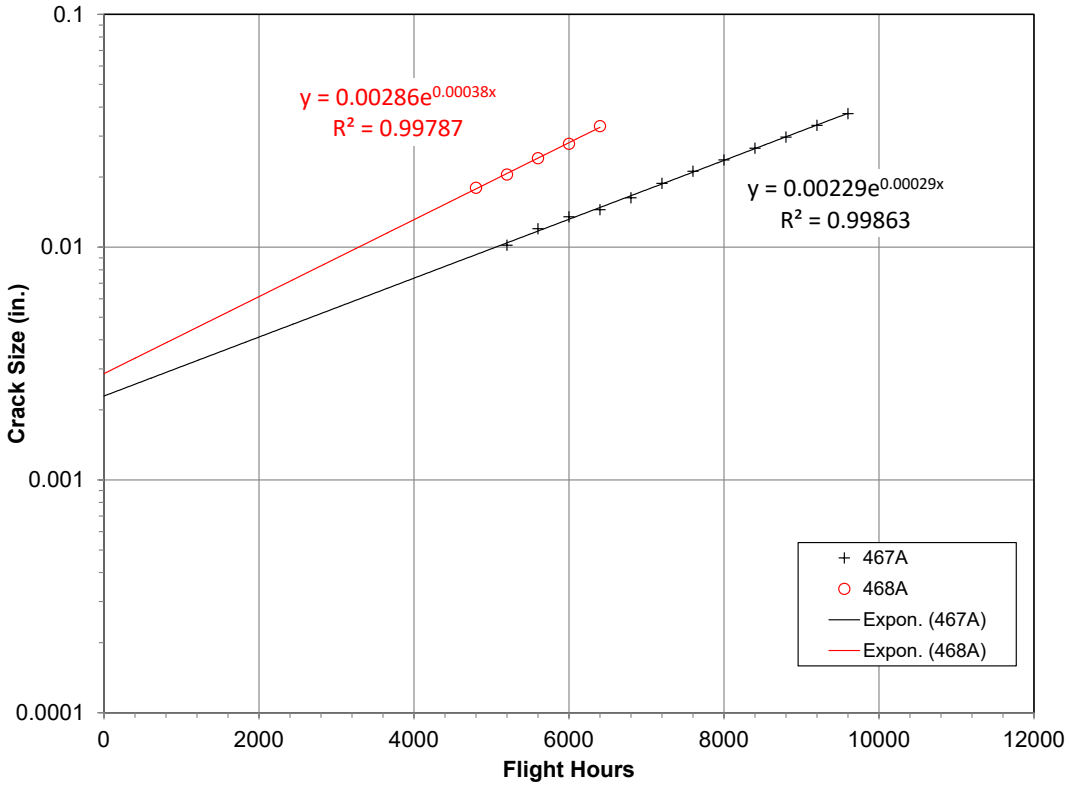

Figure A-21. EIDS Determination for Specimens 467 and 468

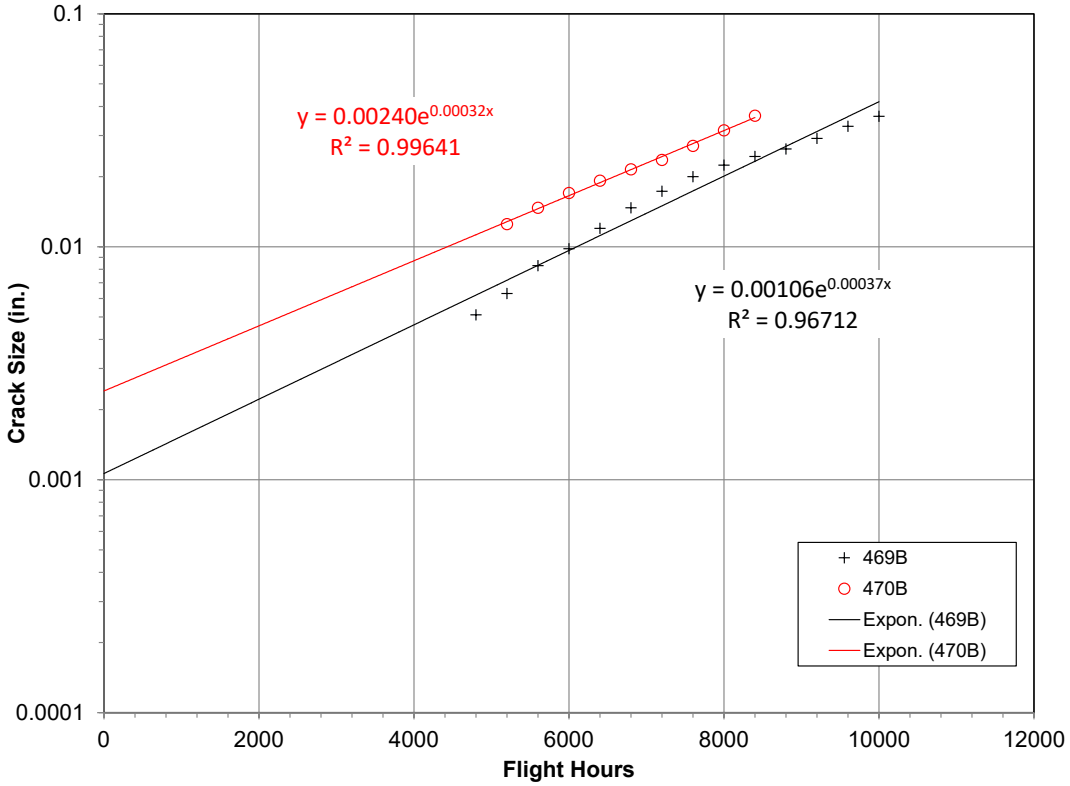

Figure A-22. EIDS Determination for Specimens 469 and 470

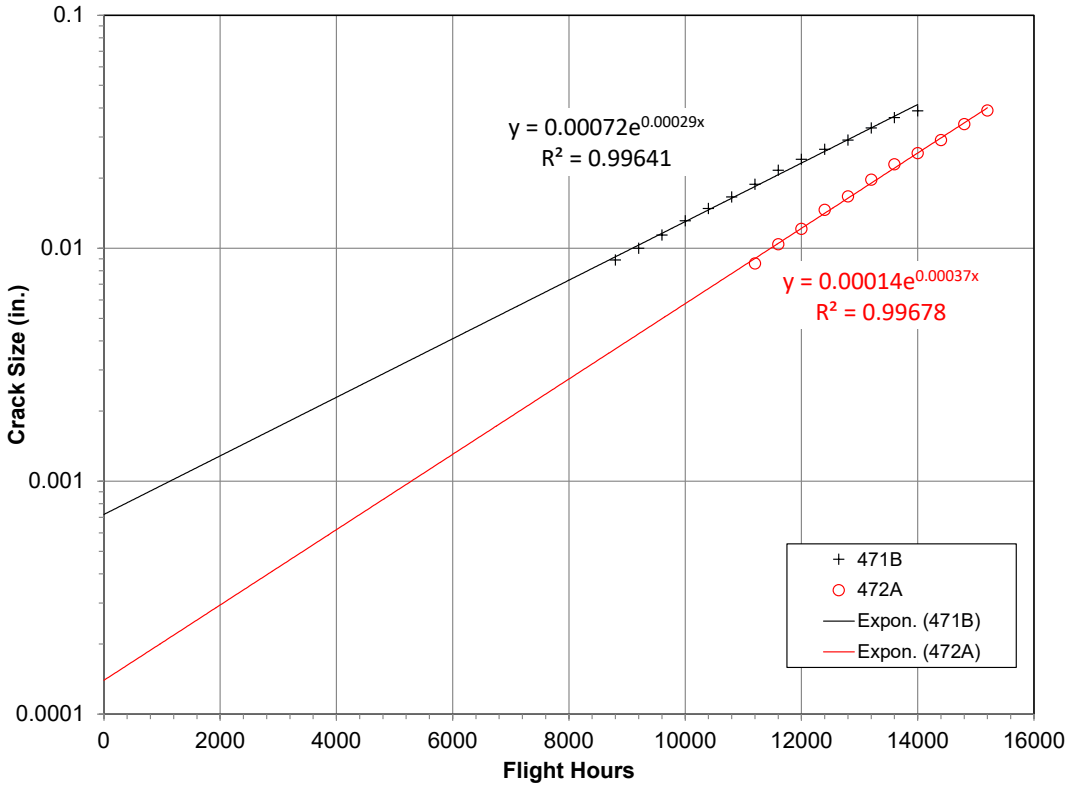

Figure A-23. EIDS Determination for Specimens 471 and 472

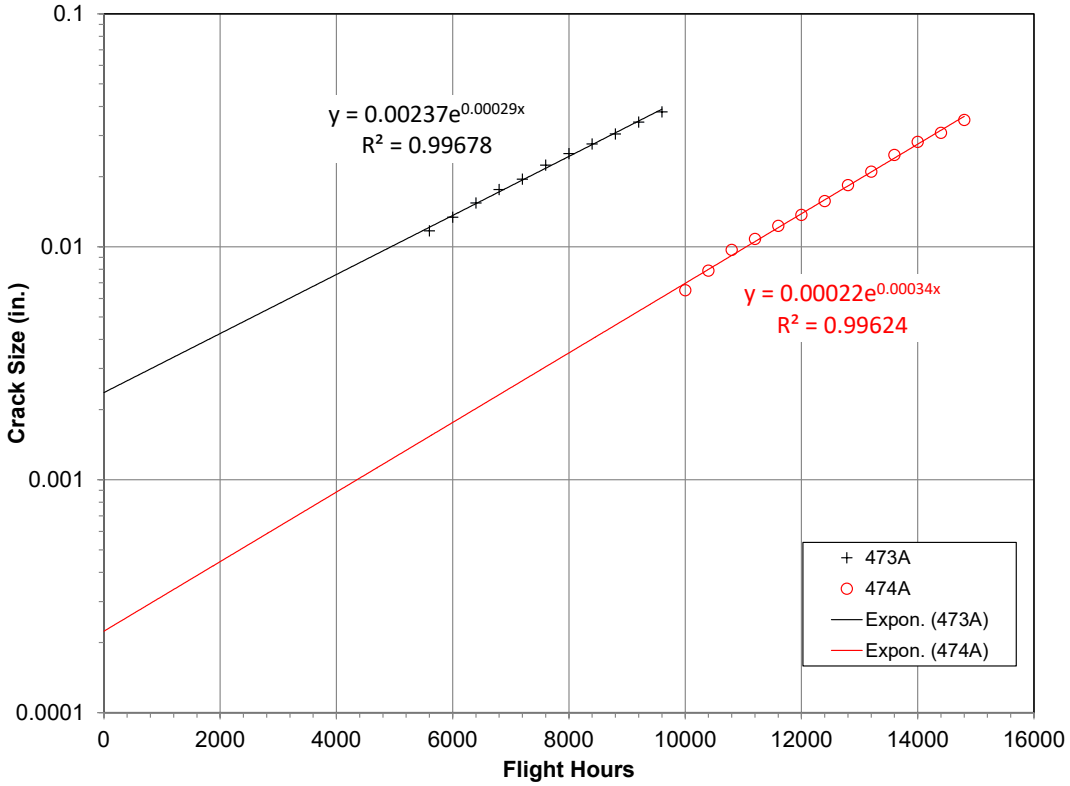

Figure A-24. EIDS Determination for Specimens 473 and 474

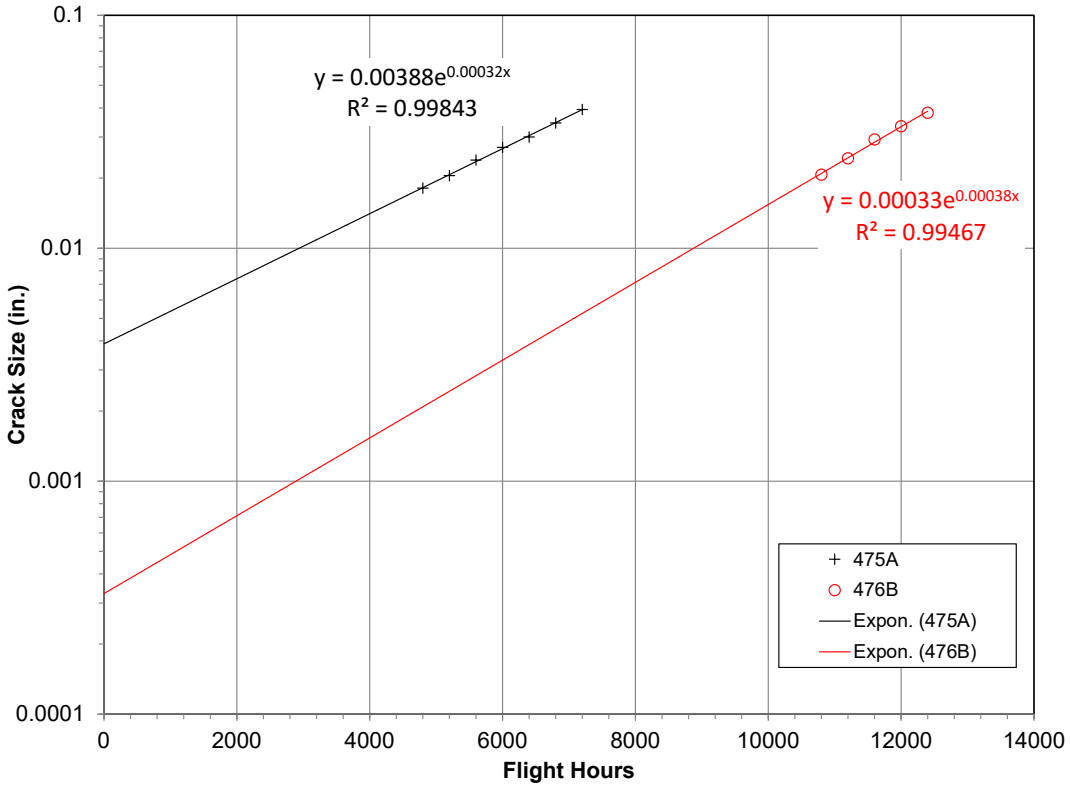

Figure A-25. EIDS Determination for Specimens 475 and 476

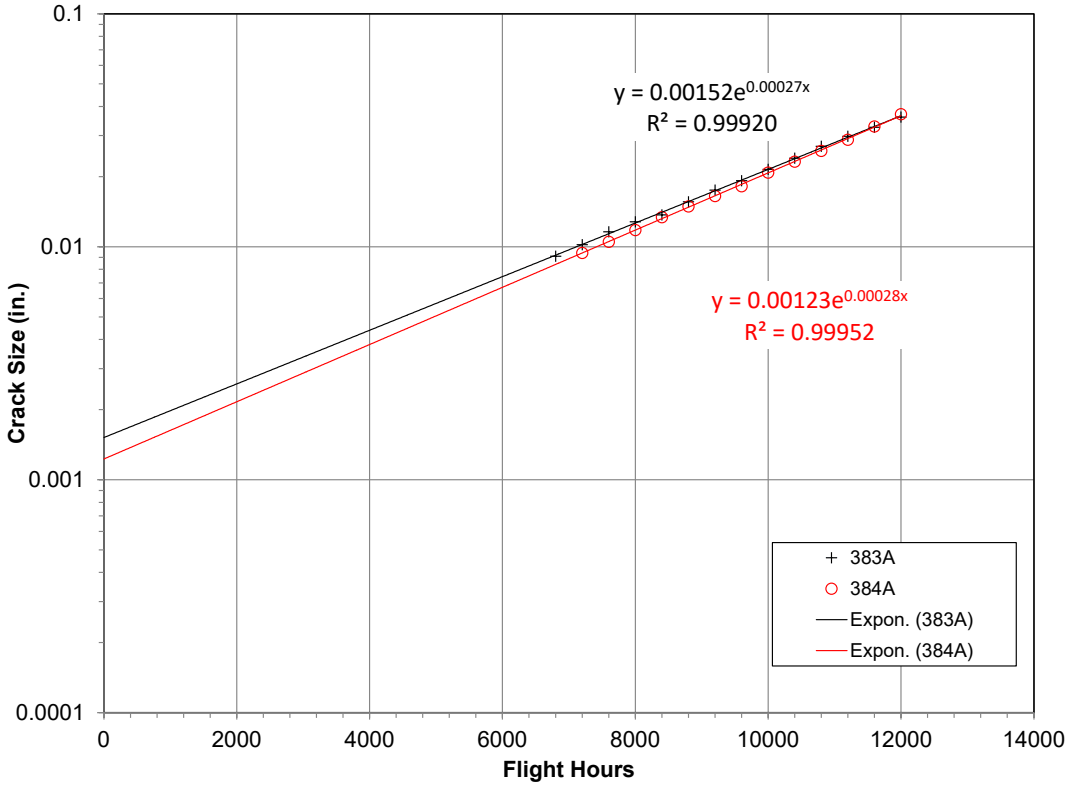

Figure A-26. EIDS Determination for Specimens 383 and 384

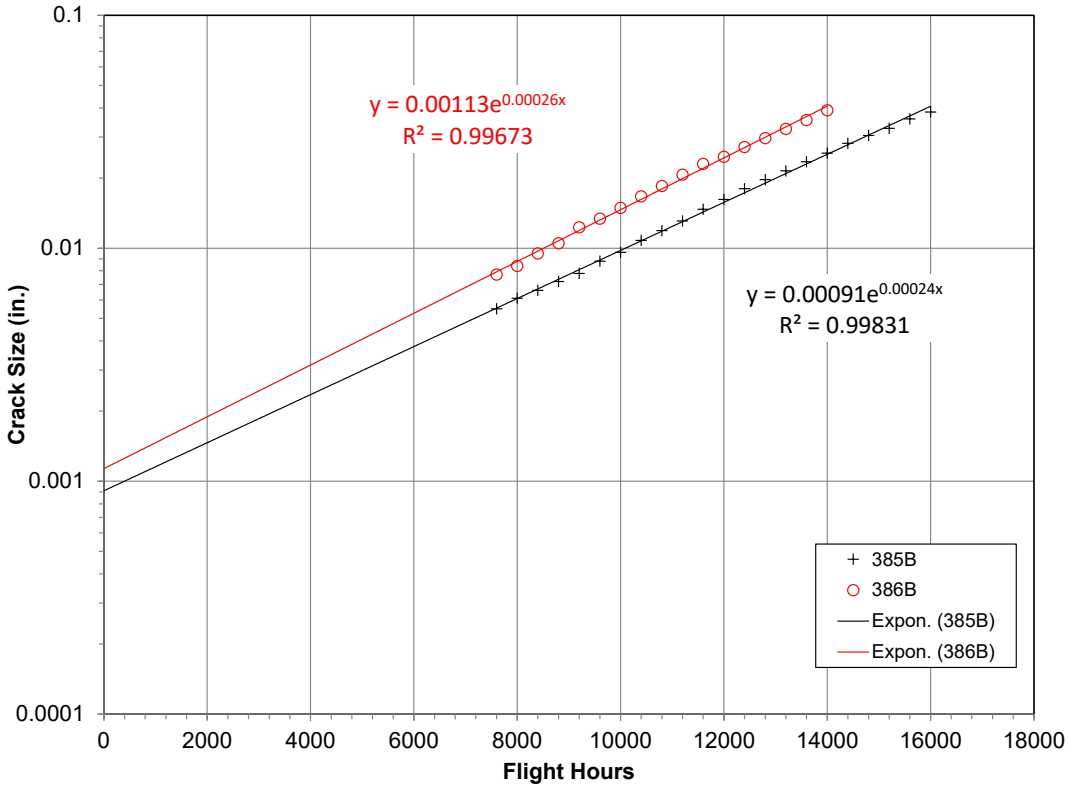

Figure A-27. EIDS Determination for Specimens 385 and 386

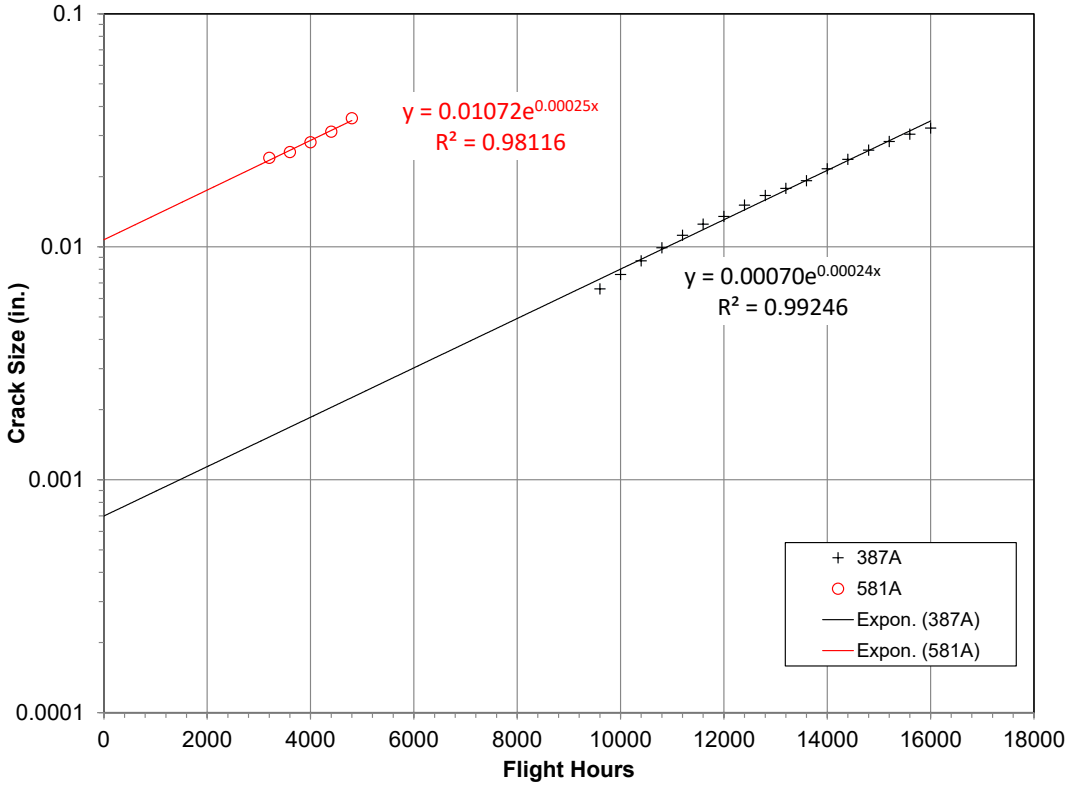

Figure A-28. EIDS Determination for Specimens 387 and 581

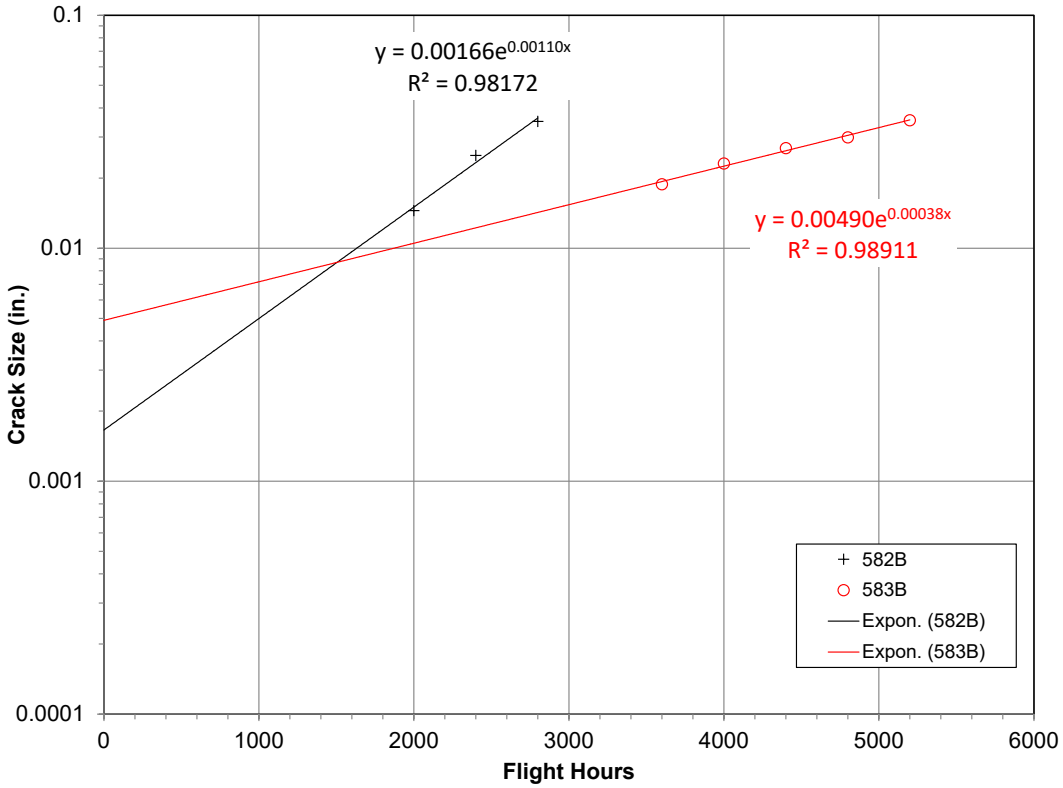

Figure A-29. EIDS Determination for Specimens 582 and 583

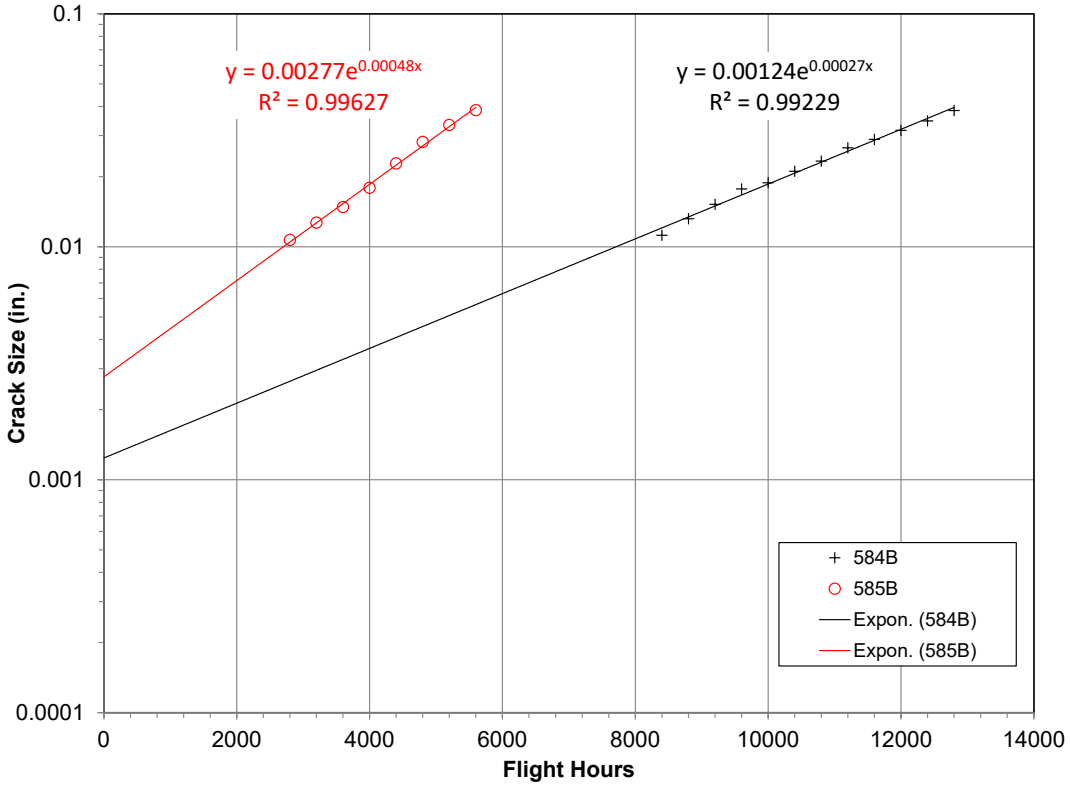

Figure A-30. EIDS Determination for Specimens 584 and 585

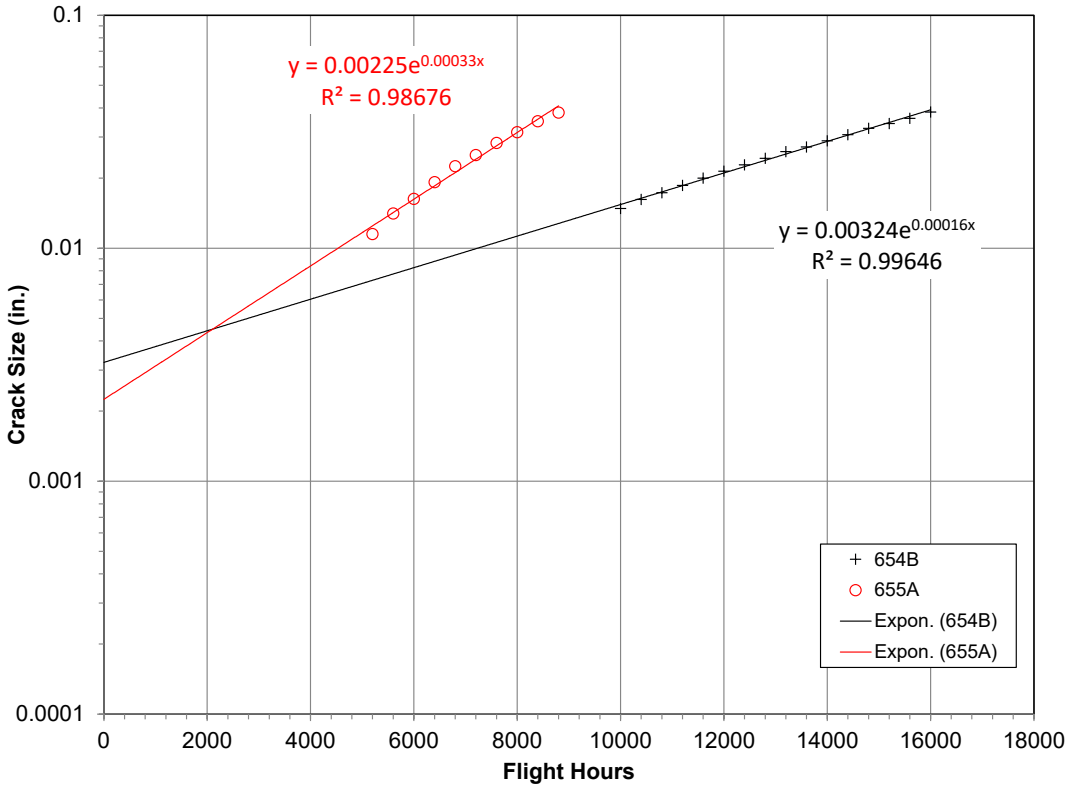

Figure A-31. EIDS Determination for Specimens 654 and 655

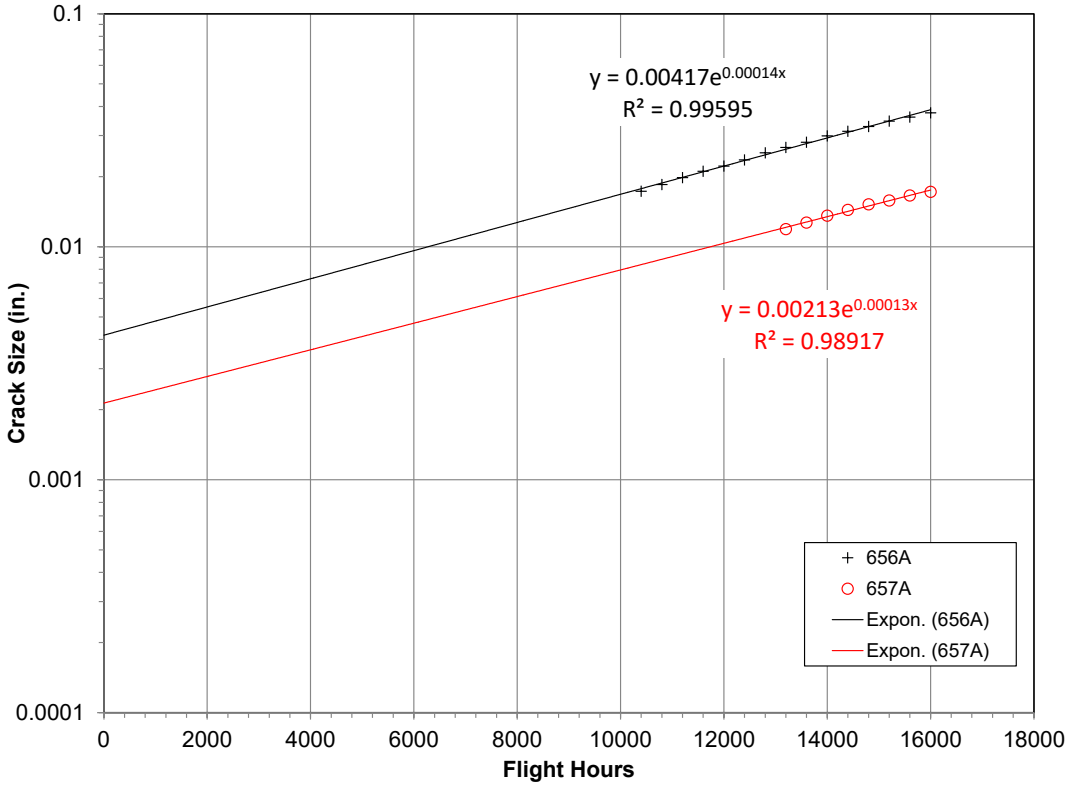

Figure A-32. EIDS Determination for Specimens 656 and 657

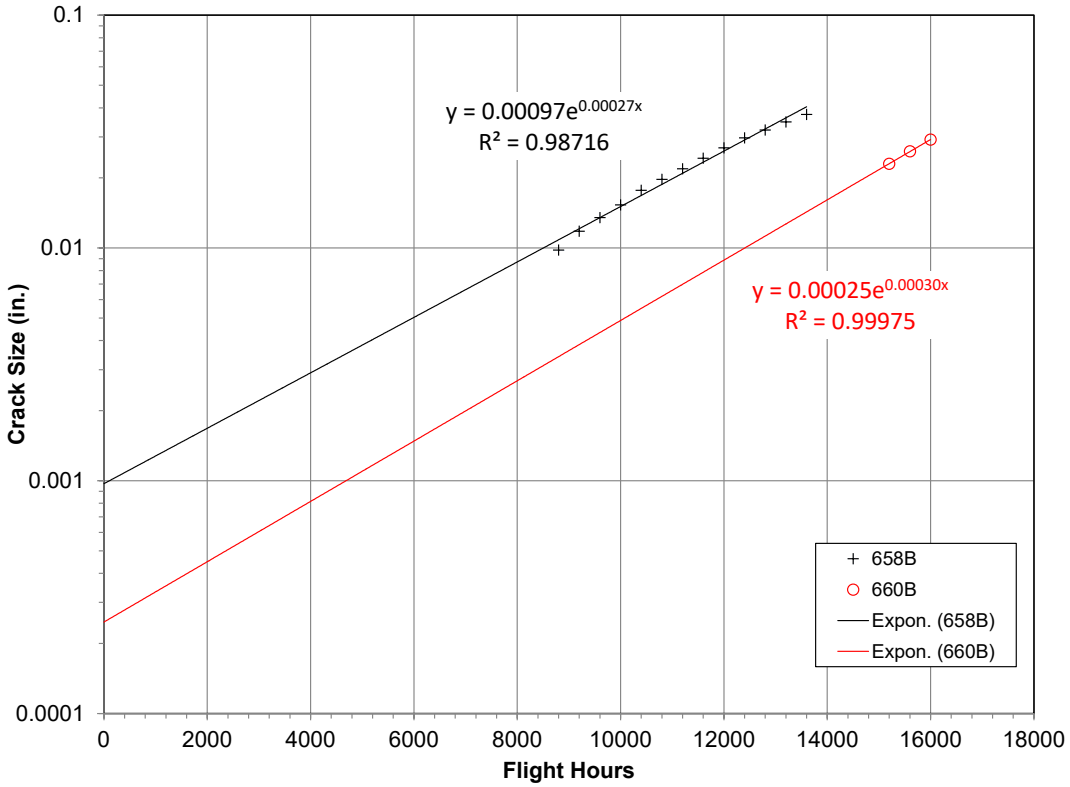

Figure A-33. EIDS Determination for Specimens 658 and 660

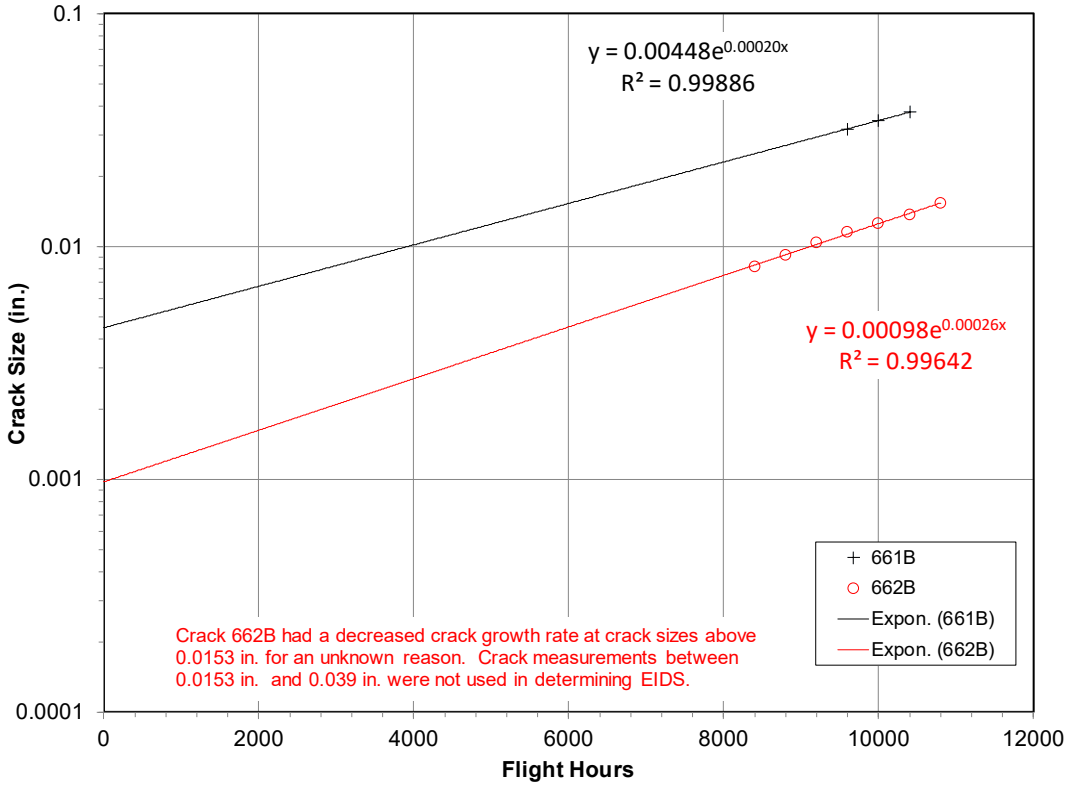

Figure A-34. EIDS Determination for Specimens 661 and 662

APPENDIX B. MONTE CARLO SIMULATION ROUTINES

B.1 Introduction

This appendix provides a listing of the major VBA subroutines used in the MCS of Sections 3.2, 3.3 and 4 of this handbook. Most of the subroutines utilize a Microsoft Excel® worksheet to store intermediate calculations and results. The routines listed here were not written to be fast or efficient, but to illustrate the algorithms and provide intermediate values for the reader to check their understanding. The reader is encouraged create faster, more efficient routines that meet their personal needs.

B.2 Generating Fracture Toughness and Initial Crack Size Samples

The first step in calculating POF with MCS was to generate samples of paired fracture toughness and initial crack size (or EIDS) values. This was done using the VBA subroutine MakeSamples listed in this section. The fracture toughness and initial crack size values were stored in an Excel worksheet part of which is shown in Table B-1.

```
**********************************************

Sub MakeSamples()

' Routine to create a number of sample pairs of fracture toughness and initial crack size
' based upon prescribed distribution parameters

TotSamps = 12000      ' Total number of samples/trials to generate
FTShape = 12.49   ' Shape parameter for fracture toughness Weibull distribution
FTScale = 88.89   ' Scale parameter for fracture toughness Weibull distribution
CrkShape = 0.374  ' Shape parameter for EIDS Weibull distribution
CrkScale = 0.00054 ' Scale parameter for EIDS Weibull distribution

For i = 1 To TotSamps

  ActiveCell.Value = i  'Trial/Sample number in first column (Trial #)

  ' Generate random number for fracture toughness
  Randomize
  FTRndNo = Rnd
  ' Calculate fracture toughness value with inverse Weibull function
  ' Store value in second column (Fracture Toughness)
  ActiveCell.Offset(0, 1).Value = FTScale * (Ln(1 / (1 - FTRndNo))) ^ (1 / FTShape)


  'Generate random number for EIDS
  Randomize
  CrkRndNo = Rnd
  ' Calculate initial crack size value with inverse Weibull function
  ' Store value in third column (Initial Crack Size)
  ActiveCell.Offset(0, 2).Value = CrkScale * (Ln(1 / (1 - CrkRndNo))) ^ (1 / CrkShape)

  'Move down one row for next trial/sample
  ActiveCell.Offset(1, 0).Select

Next i
```

End Sub

****

Table B-1. Worksheet for MCS

Trial #	Fracture Toughness	Initial Crack Size (in.)	Flight Count, f	c(f) @ start of Flight	Peak Stress (f)	beta	Kmax(f)	Δc during flight	c(f) @ end of Flight
1	96.01	0.005427765	22088	2.65171	17.20	2.274840	112.92	1.78E-02	2.66948
2	94.46	2.66785E-05	23127371	2.71529	13.62	2.823115	112.28	2.65E-02	2.74177
3	89.40	0.000174529	16732768	2.71428	11.92	2.812821	97.87	2.63E-02	2.74060
4	82.78	0.000266015	13697476	2.67064	12.22	2.418564	85.61	2.01E-02	2.69071
5	79.44	1.1517E-05	23908050	2.67810	15.98	2.479447	114.91	2.10E-02	2.69914
6	85.71	1.08303E-05	23944030	2.66742	13.14	2.393031	90.99	1.97E-02	2.68709
7	79.80	0.000654849	5858831	2.62659	13.47	2.106330	81.47	1.51E-02	2.64165
8	97.65	1.60943E-05	23669622	2.70936	14.00	2.763632	112.89	2.56E-02	2.73491
9	78.71	0.000258134	13935646	2.61758	15.93	2.051575	93.69	1.42E-02	2.63176
10	87.49	0.000565666	7116843	2.72146	11.51	2.887052	97.11	2.75E-02	2.74894
11	87.63	5.08976E-05	21932913	2.69243	12.91	2.603748	97.74	2.30E-02	2.71545
12	92.07	0.000713033	5161200	2.70165	12.95	2.688970	101.43	2.44E-02	2.72602
13	91.30	0.000854862	3790927	2.71413	11.29	2.811325	92.69	2.63E-02	2.74043
14	72.12	0.00018973	16185348	2.61835	12.50	2.056134	73.67	1.43E-02	2.63260
15	93.21	0.001427376	1105129	2.72079	12.52	2.880002	105.39	2.74E-02	2.74816
16	100.44	1.20366E-05	23880867	2.74437	10.98	3.143624	101.32	3.15E-02	2.77584
17	91.77	2.97344E-07	24502709	2.69451	13.25	2.622616	101.09	2.33E-02	2.71783
18	77.27	8.08029E-06	24088649	2.66314	12.25	2.359736	83.59	1.91E-02	2.68226
19	92.60	3.66128E-07	24499017	2.66297	13.89	2.358445	94.74	1.91E-02	2.68208
20	86.79	9.78383E-07	24466196	2.73301	11.70	3.012644	103.29	2.94E-02	2.76246

B.3 Crack Growth and Fracture Calculation

Fatigue crack growth calculations and determination of fracture occurs were done with the VBA subroutine MonteCarlo listed in this section. This routine used the same worksheet used in the previous section. A section of which is shown in Table B-1.

****

Sub MonteCarlo()

```
' MonteCarlo Macro
' Performs Monte Carlo simulation for crack growth to fracture
' Variables:
'  CatStart - crack size at the start of a flight
'  CatEnd - crack size at the end of a flight
'  deltaCdF - crack extension during a flight
'  PeakStress - Peak stress during a flight
'  PSRndNo - Random number used to generate the peak stress during a flight
'  SIGeoFact - Geometry factor for calculating the max applied Stress Intensity during a flight
                (aka beta)
'  Kmax - max applied stress intensity during a flight
'  Kcrit - Fracture toughness for this sample
'  Cmax - maximum crack size before crack breaks to the free end
'  FlightNo - number of flights flown
'  RefStress - reference stress for normalized load spectrum (multiply spectrum endpoint by this
                value)
'  InspectTime - Flight after which inspection occurs; to run each sample to failure set to a very
                 large values
```

```
Cmax = 2.75
RefStress = 16#
InspectTime = 100000000#
PSCharact = 0.699  ' Characteristic values of Gumbel Distribution for Peak Stress
PSDispersion = 0.06 ' Value of dispersion (shape) of Gumbel Distribution for Peak Stress

For i = 1 To 12000

   'If this is the first flight, not a restart after inspection, the ActiveCell
   '(column labeled 'c(f) at start of Flight') will be empty
 'If this is not the first flight, set CatEnd to Initial Crack Size
 If IsEmpty(ActiveCell) Then
   CatEnd = ActiveCell.Offset(0, -2).Value    'Move into CatStart at start of loop
   FlightNo = 0                'Initialize Flight Count
 Else
   CatEnd = ActiveCell.Offset(0, 5).Value     'Else use values from end of previous interval
   FlightNo = ActiveCell.Offset(0, -1).Value
 End If

 'Read fracture toughness for sample from spreadsheet
 Kcrit = ActiveCell.Offset(0, -3).Value

 ' Loop until Cmax exceeded or Kcrit exceeded
 Do
    FlightNo = FlightNo + 1       'Increment Flight Count
   CatStart = CatEnd          'Move CatEnd from previous flight to CatStart for this flight

   'Determine crack extension during this flight
   If CatStart < 0.00327 Then
     deltaCdF = 1.86251E-11 * Exp(2192.92 * CatStart)
   Else

     If CatStart < 0.01292 Then
       deltaCdF = -34.0272 * CatStart ^ 4 + 0.748415 * CatStart ^ 3 +
                           0.0207707 * CatStart ^ 2 - 0.000121929 * CatStart + 0.000000178475
     Else

       If CatStart < 0.06819 Then
         deltaCdF = 0.0336049 * CatStart ^ 3 + 0.0151617 * CatStart ^ 2 –
                             0.000099355 * CatStart + 0.00000141646
       Else

         If CatStart < 1.49725 Then
           deltaCdF = -0.000264012 * CatStart ^ 6 + 0.00148501 * CatStart ^ 5 –
                               0.00336236 * CatStart ^ 4 + 0.00379001 * CatStart ^ 3 –
                               0.0020336 * CatStart ^ 2 + 0.000642407 * CatStart + 0.0000403256
         Else

           If CatStart <= 2.23841 Then
             deltaCdF = -0.0101093 * CatStart ^ 6 + 0.126576 * CatStart ^ 5 –
```

```
                                0.65644 * CatStart ^ 4 + 1.804418 * CatStart ^ 3 –
                                2.770745 * CatStart ^ 2 + 2.252744 * CatStart - 0.75719
        Else
          deltaCdF = 0.3278 * CatStart ^ 3 - 2.287688 * CatStart ^ 2 +
                              5.333224 * CatStart - 4.150421
        End If
      End If
    End If
  End If
End If


  CatEnd = CatStart + deltaCdF    'Calculate crack size at the end of the flight
'Determine geometry factor for stress intensity calculation based on crack size at start of flight
  If CatStart <= 0.025 Then
    SIGeoFact = -3872710000# * CatStart ^ 6 + 383561000 * CatStart ^ 5 –
                15222900 * CatStart ^ 4 + 310325 * CatStart ^ 3 - 3308.15 * CatStart ^ 2 +
                12.952 * CatStart + 1.99237
  Else
    If CatStart <= 0.059 Then
      SIGeoFact = 481870000 * CatStart ^ 6 - 112480000 * CatStart ^ 5 +
                          10737700 * CatStart ^ 4 - 538394 * CatStart ^ 3 +
                          15108.6 * CatStart ^ 2 - 225.62 * CatStart + 3.34709
    Else
      If CatStart <= 1.2 Then
        SIGeoFact = 12.7731 * CatStart ^ 6 - 57.1413 * CatStart ^ 5 +
                            103.053 * CatStart ^ 4 - 96.2646 * CatStart ^ 3 +
                            49.9938 * CatStart ^ 2 - 14.4465 * CatStart + 2.97336
      Else
        SIGeoFact = 2.37816 * CatStart ^ 6 - 24.848 * CatStart ^ 5 +
                            107.159 * CatStart ^ 4 - 243.928 * CatStart ^ 3 +
                            309.117 * CatStart ^ 2 - 206.791 * CatStart + 57.9809
      End If
    End If
  End If
  ' Pick random number for the Peak Stress during this flight
  Randomize
  PSRndNo = Rnd
  ' Calculate Peak Stress during Flight using inverse Gumbel distribution
  If PSRndNo > 0 Then
    PeakStress = RefStress * (PSCharact - Ln(Ln(1 / PSRndNo)) * PSDispersion)
  Else
    PeakStress = 1   'If PSRndNo is zero (rare instance), set PeakStress to 1.0 ksi
```

```
    End If

    ' Calculate max applied Stress Intensity during Flight based on crack size at start of flight
    Kmax = SIGeoFact * PeakStress * (3.14 * CatStart) ^ 0.5

    'Censor sample for little or no crack growth
    If deltaCdF < 0.0000000000001 Then Exit Do

  Loop Until CatEnd >= 2.75 Or Kmax >= Kcrit Or FlightNo >= InspectTime

  ' Write results for sample to the worksheet
  ActiveCell.Offset(0, -1).Value = FlightNo            ' Store FlightNo in column Flight Count, f
  ActiveCell.Value = CatStart ' Store CatStart in column c(f) @ Start of Flight
  ActiveCell.Offset(0, 1).Value = PeakStress ' Store PeakStress in column Peak Stress(f)
  ActiveCell.Offset(0, 2).Value = SIGeoFact ' Store SIGeoFact in column beta
  ActiveCell.Offset(0, 3).Value = Kmax       ' Store Kmax in column Kmax(f)
  ActiveCell.Offset(0, 4).Value = deltaCdF   ' Store deltaCdF in column Δc during flight
  ActiveCell.Offset(0, 5).Value = CatEnd     ' Store CatEnd in column c @ end of flight

  ActiveWorkbook.Save        ' Save the workbook

  ActiveCell.Offset(1, 0).Select   ' Move down one row for the next sample

Next i

End Sub
**********************************************
```

B.4 Inspection Simulation

Relevant columns from the MCS worksheet are shown in Table B-2: trial number, flight number, crack size at start of the flight, crack size increment during flight, crack size at end of the flight, inspection results (crack detected or not detected), and crack size after the inspection and repair. The inspection was performed after the 5,000 flight. InspectTime in the MonteCarlo subroutine in Section B.3 was set to 5,000. The crack size for the start of flight 5,001 is the crack size after the inspection and repair.

Notice that the cracks in Trial #27 and #40 were detected by the inspection and repaired. The crack sizes after inspection for these two trials is significantly smaller than the crack sizes after flight 5,000. The cracks for all the other trials shown in Table B-2 were not detected. The crack sizes after inspection are the same as the crack sizes after flight 5,000. The VBA subroutine for simulating inspection and repair is listed after Table B-2.

Table B-2. Sample of Worksheet used for Inspection Simulation

Trial #	Flight Count, f	c(f) @ start of Flight	Δc during flight	c(f) @ end of Flight	Inspection (D or N)	c(f) after inspection
1	5000	0.00717	5.58E-07	0.00717	N	0.00717
2	5000	0.00003	1.98E-11	0.00003	N	0.00003
3	5000	0.00017	2.73E-11	0.00017	N	0.00017
4	5000	0.00027	3.34E-11	0.00027	N	0.00027
5	5000	0.00001	1.91E-11	0.00001	N	0.00001
6	5000	0.00001	1.91E-11	0.00001	N	0.00001
7	5000	0.00066	7.84E-11	0.00066	N	0.00066
8	5000	0.00002	1.93E-11	0.00002	N	0.00002
9	5000	0.00026	3.28E-11	0.00026	N	0.00026
10	5000	0.00057	6.44E-11	0.00057	N	0.00057
11	5000	0.00005	2.08E-11	0.00005	N	0.00005
12	5000	0.00071	8.90E-11	0.00071	N	0.00071
13	5000	0.00086	1.22E-10	0.00086	N	0.00086
14	5000	0.00019	2.82E-11	0.00019	N	0.00019
15	5000	0.00143	4.28E-10	0.00143	N	0.00143
16	5000	0.00001	1.91E-11	0.00001	N	0.00001
17	5000	3.91E-07	1.86E-11	3.91E-07	N	3.91E-07
18	5000	0.00001	1.90E-11	0.00001	N	0.00001
19	5000	4.59E-07	1.86E-11	4.59E-07	N	4.59E-07
20	5000	1.07E-06	1.87E-11	1.07E-06	N	1.07E-06
21	5000	0.00008	2.24E-11	0.00008	N	0.00008
22	5000	0.00061	7.07E-11	0.00061	N	0.00061
23	5000	0.00283	9.23E-09	0.00283	N	0.00283
24	5000	0.14055	9.97E-05	0.14065	N	0.14065
25	5000	0.00009	2.26E-11	0.00009	N	0.00009
26	5000	0.00256	5.08E-09	0.00256	N	0.00256
27	5000	0.33798	1.34E-04	0.33812	D	0.00125
28	5000	3.35E-06	1.88E-11	3.35E-06	N	3.35E-06
29	5000	3.90E-07	1.86E-11	3.90E-07	N	3.90E-07
30	5000	0.00123	2.78E-10	0.00123	N	0.00123
31	5000	0.00265	6.22E-09	0.00265	N	0.00265
32	5000	0.00008	2.20E-11	0.00008	N	0.00008
33	5000	0.00006	2.12E-11	0.00006	N	0.00006
34	5000	0.00081	1.10E-10	0.00081	N	0.00081
35	5000	0.00003	1.97E-11	0.00003	N	0.00003
36	5000	1.69E-07	1.86E-11	1.69E-07	N	1.69E-07
37	5000	0.00040	4.44E-11	0.00040	N	0.00040
38	5000	0.00168	7.42E-10	0.00168	N	0.00168
39	5000	0.00017	2.68E-11	0.00017	N	0.00017
40	5000	0.24883	1.21E-04	0.24895	D	0.00006
41	5000	0.00249	4.34E-09	0.00249	N	0.00249
42	5000	0.00011	2.38E-11	0.00011	N	0.00011
43	5000	0.00000	1.86E-11	0.00000	N	0.00000
44	5000	0.00166	7.16E-10	0.00166	N	0.00166
45	5000	0.00031	3.69E-11	0.00031	N	0.00031
46	5000	4.42E-06	1.88E-11	4.42E-06	N	4.42E-06
47	5000	1.24E-06	1.87E-11	1.24E-06	N	1.24E-06
48	5000	0.00208	1.78E-09	0.00208	N	0.00208
49	5000	0.00013	2.49E-11	0.00013	N	0.00013
50	5000	0.00002	1.95E-11	0.00002	N	0.00002

```
**********************************************

Sub Inspect()

'Routine to simulate NDI at location
'Determines a probability of detection for the crack size of each MC sample
'Draws a random number between 0 and 1 - if RN is greater than POD, crack is not detected
'If the crack is detected, another random number is drawn to obtain a repair damage size from the
ERDS distribution
'Crack sizes after the inspection are used for subsequent life prediction

'POD parameters: POD = coeff * (cracksize^expo)/(1 + coeff *(cracksize^expo))
‘These POD parameters are not known to be correct for any NDI method
coeff = 13000
expo = 5

'Equivalent Repair Damage Size Distribution, ERDS (Weibull)
ERDshape = 0.35
ERDscale = 0.00075

'Active Cell should be in Inspection column

For i = 1 To 12000

  cracksize = ActiveCell.Offset(0, -1).Value 'Get cracksize at the end of the last flight
  POD = coeff * (cracksize ^ expo) / (1 + coeff * (cracksize ^ expo)) 'Calculate the POD

  Randomize      'Pick random number for detecting crack
  Detect = Rnd

  'Compare Detect to POD. If Detect is greater than or equal to POD, the crack is not detected

  If Detect >= POD Then

    ActiveCell.Value = "N"    'crack was not detected

    'cracksize remains what it was at end of last flight
    ActiveCell.Offset(0, 1).Value = ActiveCell.Offset(0, -1).Value

  Else

    ActiveCell.Value = "D"    'crack was detected

    'Determine damage/crack size after repair
    Randomize      'Pick random number for repaired crack
    Repair = Rnd

    'Determine crack size from inverse Weibull function, put in column for crack size after
     inspection
    ActiveCell.Offset(0, 1).Value = ERDscale * (Log(1 / (1 - Repair))) ^ (1 / ERDshape)

   End If

  'Move down to the next row for the next sample
  ActiveCell.Offset(1, 0).Select

Next i
```

End Sub

****

B.5 Calculating the POF prior to an Inspection and after an Inspection

The MCS routine for calculating the POF at a single flight based upon the crack size distribution at that flight is listed below. The POF of at a single flight is calculated with the Excel worksheet in Table B-3. The *Sum of POFs* and the *Sum of Squares for POFs* are calculated using the VBA subroutine POFMCS which is listed below. The *Expected Value of POF* is calculated as the *Sum of POFs* divided by *# of Samples*. The *Expected Std. Error* is calculated as the *Sum of Squares for POFs* divided by *# of Samples*. The *Variance* is equal to the *Expected Std. Error* minus the square of the *Expected Value of POF*.

Table B-3. POF Calculation Worksheet

	# of Samples	Sum of POFs	Expected Value of POF	Sum of Squares for POFs	Expected Std. Error	Variance
start of flight 5,000	12000	8.02E-05	6.68E-09	6.3187E-11	5.27E-15	5.22E-15
end of flight 5,000	12000	8.06E-05	6.71E-09	6.2914E-11	5.24E-15	5.20E-15

****

```
Sub POFMCS()
' POFMCS Macro
' Performs Monte Carlo integration of POF equation
' Uses Importance Sampling on all three random variables -
'  fracture toughness, crack size, and peak stress
' Variables:
'  CrackSize - crack size
'  PeakStress - Peak stress during a flight
'  PSRndNo - Random number used to generate the peak stress during a flight
'  SIGeoFact - Geometry factor for calculating the max applied Stress Intensity during a flight
(aka beta)
'  Kmax - max applied stress intensity during a flight
'  Kcrit - Fracture toughness for this sample
'  Cmax - maximum crack size before crack breaks to the free end
'  TotSamps - total number of MC samples to generate
'  FTShape - Shape parameter for fracture toughness Weibull distribution
'  FTScale - Scale parameter for fracture toughness Weibull distribution
'  CrkShape - Shape parameter for crack size Weibull distribution
'  CrkScale - Scale parameter for crack size Weibull distribution
'  PSDisp - Dispersion parameter for peak stress Gumbel distribution, alpha
'  PSChar - Characteristic value for peak stress Gumbel distribution, mu
'  RefStress – Reference stress for the normalized loading spectrum
'  Cmax – Maximum physical crack size before reaching the edge of the part
```

```
TotSamps = 12000
FTShape = 12.49
FTScale = 93.9
PSDisp = 0.06
PSChar = 0.699
RefStress = 16#
Cmax = 2.75

' Use uniform distributions for sampling
' Variables:
'  Kup - upper bound of uniform sampling distribution for fracture toughness
'  Klo - lower bound of uniform samplng distribution for fracture toughness
'  Cup - upper bound of uniform sampling distribution for crack size
'  Clo - lower bound of uniform sampling distribution for crack size
'  PSup - upper bound of uniform sampling distribution for peak stress
'  PSlo - lower bound of uniform sampling distribution for peak stress
'  gK - pdf value for fracture toughness sampling distribution
'  gC - pdf value for crack size sampling distribution
'  gPS - pdf value for peak stress sampling distribution


Kup = 85  ' Failure more likely for low tail of fracture toughness distribution
Klo = 25  ' Limit importance sampling (IS) to low tail
gk = 1 / (Kup - Klo)

Cup = Cmax  ' Failure more likely for large crack size tail, IS from large tail
Clo = 0.07
gC = 1 / (Cup - Clo)

PSup = RefStress * 1.4 ' Failure more likely for large Peak Stresses, sample from these
PSlo = RefStress * 0.7
gPS = 1 / (PSup - PSlo)

For i = 1 To TotSamps

 'Fracture Toughness calculations
 ' Pick random number for the Fracture Toughness
 Randomize
 KcritRndNo = Rnd
 Kcrit = Klo + KcritRndNo / gk
 pdfKcrit = (FTShape / FTScale) * (Kcrit / FTScale) ^ (FTShape - 1) * Exp(-(Kcrit / FTScale) ^
                FTShape)

 ' Pick random number for the Peak Stress
 Randomize
 PSRndNo = Rnd
 ' Calc Peak Stress based on uniform sampling distribution
 PeakStress = PSlo + PSRndNo / gPS
 pdfPS = PSDisp * Exp(-PSDisp * (PeakStress/RefStress - PSChar) + Exp(-PSDisp *
           (PeakStress/RefStress - PSChar)))
```

```
' Pick random number for Crack Size
Randomize
CSRndNo = Rnd
CrackSize = Clo + CSRndNo / gC

' Determine pdf value for Crack Size (start of flight 5,000)
'If CrackSize > 0.4492 Then
'  pdfCS = (0.96584 / 0.11201) * (CrackSize / 0.11201) ^ (0.96584 - 1) * Exp(-((CrackSize / '
  0.11201) ^ 0.96584))
'Else
'  pdfCS = (0.11374 / 0.0000033945) * (CrackSize / 0.0000033945) ^ (0.11374 - 1) * Exp(-   '
  ((CrackSize / 0.0000033945) ^ 0.11374))
'End If

'Determine pdf value for Crack Size (end of flight 5,000)
If CrackSize > 0.449 Then
  pdfCS = (0.96586 / 0.11205) * (CrackSize / 0.11205) ^ (0.96586 - 1) * Exp(-((CrackSize /
            0.11205) ^ 0.96586))
Else
  pdfCS = (0.11378 / 0.0000034098) * (CrackSize / 0.0000034098) ^ (0.11378 - 1) * Exp(-
          ((CrackSize / 0.0000034098) ^ 0.11378))
End If

'Determine geometry factor for stress intensity calculation based on crack size at start of flight
If CrackSize <= 0.025 Then
  SIGeoFact = -3872710000# * CrackSize ^ 6 + 383561000 * CrackSize ^ 5 - 15222900 *
CrackSize ^ 4 + 310325 * CrackSize ^ 3 - 3308.15 * CrackSize ^ 2 + 12.952 * CrackSize +
1.99237
Else
  If CrackSize <= 0.059 Then
    SIGeoFact = 481870000 * CrackSize ^ 6 - 112480000 * CrackSize ^ 5 + 10737700 *
CrackSize ^ 4 - 538394 * CrackSize ^ 3 + 15108.6 * CrackSize ^ 2 - 225.62 * CrackSize +
3.34709
  Else
    If CrackSize <= 1.2 Then
      SIGeoFact = 12.7731 * CrackSize ^ 6 - 57.1413 * CrackSize ^ 5 + 103.053 * CrackSize ^ 4
- 96.2646 * CrackSize ^ 3 + 49.9938 * CrackSize ^ 2 - 14.4465 * CrackSize + 2.97336
    Else
      SIGeoFact = 2.37816 * CrackSize ^ 6 - 24.848 * CrackSize ^ 5 + 107.159 * CrackSize ^ 4 -
243.928 * CrackSize ^ 3 + 309.117 * CrackSize ^ 2 - 206.791 * CrackSize + 57.9809
    End If
  End If
End If
```

```
  'Calculate maximum Stress Intensity
  Kmax = SIGeoFact * PeakStress * (CrackSize * 3.14159) ^ 0.5

  If Kmax >= Kcrit Then
    h = 1                    ' Sample fractured
  Else
    h = 0                    ' Sample survived
  End If

   ' Probability density for sample
  Addend = h * pdfKcrit * pdfPS * pdfCS / gk / gPS / gC

  ActiveCell.Value = ActiveCell.Value + 1              ' Column # of Samples
  ' Column Sum of POFs
  ActiveCell.Offset(0, 1).Value = ActiveCell.Offset(0, 1).Value + Addend
  ' Column Sum of Squares for POFs
  ActiveCell.Offset(0, 3).Value = ActiveCell.Offset(0, 3).Value + Addend ^ 2

  ActiveWorkbook.Save        ' Save the workbook

Next i

End Sub
**********************************************
```

B.6 Determining the Probability Distribution for the Maximum Stress in a Flight

The probability distribution for the maximum stress in a flight was found from a load spectrum as follows. First, develop the CDF for the occurrence of stress peaks in the spectrum as in Table B-4. This is one minus the exceedances from the exceedance curve. Next, determine the average number of stress peaks that occur during a single flight. For the FALSTAFF spectrum, there were 90 stress peaks on average during a single flight.

The CDF was used in the VBA subroutine GenFlight to generate 1,000 random sets of 90 stress peaks representing 1,000 flights. The stress peaks for a flight were written in a row of an Excel spreadsheet.

Table B-4. CDF of Stress Peak Occurrences in FALSTAFF Spectrum

Normalized Peak	Probability Distribution
-0.0214	0
-0.0215	0.00862
0.0193	0.03336
0.1419	0.03576
0.1828	0.06317
0.2236	0.28883
0.2645	0.51932
0.3054	0.63048
0.3462	0.70177
0.3871	0.76578
0.4279	0.82066
0.4688	0.87371
0.5097	0.90930
0.5505	0.93894
0.5914	0.96141
0.6322	0.97436
0.6731	0.98510
0.714	0.99088
0.7548	0.99511
0.7957	0.99761
0.8366	0.99894
0.8774	0.99950
0.9183	0.99989
1	1

```
**********************************************

Sub GenFlight()

' Generate 90 peak loads for 1,000 flights

' Outer loop of 1,000 flights
For i = 1 To 1000
  ActiveCell.Offset(1, 0).Select ' Move active cell down one row for each flight

  ' Generate 90 peaks for this flight
  For j = 0 To 89

    Randomize      'Initialize random number generator
    x = Rnd     ' Random number for cum probability of peak load distribution

    ' Determine peak load from cum probability distribution
    ' CDF value halfway between adjacent points used as dividing line
    If (x < 0.00432) Then
      p = -0.0214
    Else
```

```
If (x < 0.02099) Then
  p = -0.0215
Else
  If (x < 0.03456) Then
    p = 0.0193
  Else
    If (x < 0.04946) Then
      p = 0.1419
    Else
      If (x < 0.176) Then
        p = 0.1828
      Else
        If (x < 0.40408) Then
          p = 0.2236
        Else
          If (x < 0.5749) Then
            p = 0.2645
          Else
            If (x < 0.66613) Then
              p = 0.3054
            Else
              If (x < 0.73378) Then
                p = 0.3462
              Else
                If (x < 0.79322) Then
                  p = 0.3871
                Else
                  If (x < 0.84719) Then
                    p = 0.4279
                  Else
                    If (x < 0.89151) Then
                      p = 0.4688
                    Else
                      If (x < 0.92412) Then
                        p = 0.5097
                      Else
                        If (x < 0.95018) Then
                          p = 0.5505
                        Else
                          If (x < 0.96789) Then
                            p = 0.5914
                          Else
                            If (x < 0.97973) Then
                              p = 0.6322
                            Else
                              If (x < 0.98799) Then
```

```
                p = 0.6731
              Else
                If (x < 0.99299) Then
                  p = 0.714
                Else
                  If (x < 0.99636) Then
                    p = 0.7548
                  Else
                    If (x < 0.99828) Then
                      p = 0.7957
                    Else
                      If (x < 0.99922) Then
                        p = 0.8366
                      Else
                        If (x < 0.99969) Then
                          p = 0.8774
                        Else
                          If (x < 0.99994) Then
                            p = 0.9183
                          Else
                            p = 1
                          End If
                        End If
                      End If
                    End If
                  End If
                End If
              End If
            End If
          End If
        End If
      End If
    End If
  End If
End If
'Assign value to next peak in the flight, index for peak is column index for value
ActiveCell.Offset(0, j).Value = p
```

```
  Next j   ' Increment to next peak in the flight
Next i     ' Increment flight
End Sub
**********************************************
```

The maximum peak in each row was found using the worksheet function MAX. This resulted in 1,000 samples for the maximum stress during a flight. The first 25 samples are shown in Table B-5.

The 1,000 samples were rank ordered using mean rank: rank number, r, divided by 1,001. A probability distribution was then fit to these 1,000 points. In this case, a Gumbel distribution was used. From equation (20),

$$MaxStress = \alpha + \beta\{-ln[-ln(rank)]\} \qquad (100)$$

Then, LSE was used to find α and β, the location and scale parameters for the distribution.

Table B-5. Some of the Maximum Stress in a Flight Values

Sample Flight #	Max Stress
1	0.9183
2	0.7957
3	0.5914
4	0.8366
5	0.714
6	0.6731
7	0.7548
8	0.7957
9	0.6322
10	0.6322
11	0.6731
12	0.6322
13	0.714
14	0.6322
15	0.6731
16	0.5914
17	0.7548
18	0.6731
19	0.714
20	0.6322
21	0.7548
22	0.714
23	0.714
24	0.714
25	0.5914

APPENDIX C. CRACK EXTENSION PER FLIGHT CALCULATION

C.1 Introduction

This appendix discusses the details of the calculation of *dc/d(flight)* in Section 3.3.5.1.

The full range master crack growth curve developed for this example is repeated in Figure C-1. The master crack growth curve starts at a crack size of 0.0015 inch, the smallest crack size at which AFGROW calculated any crack extension. The master crack growth curve extends all the way to failure in order to cover all possible samples in the MCS.

The assumed cracking scenario is a corner crack from a centered hole in a plate. The classical model for this scenario in AFGROW was used to calculate the stress intensities. Since this problem does not involve a fastened joint, the through stress fraction was 1.0 and the bearing and bending fractions were 0. The analysis here started with a semi-circular crack of radius 0.0015 inch. The aspect ratio of the crack was constrained to be 1.

The crack growth rate data for aluminum 7475-T761 plate in the L-T orientation from the NASGRO database contained in AFGROW was used. The loading was the FALSTAFF spectrum with a stress multiplication factor of 16 ksi.

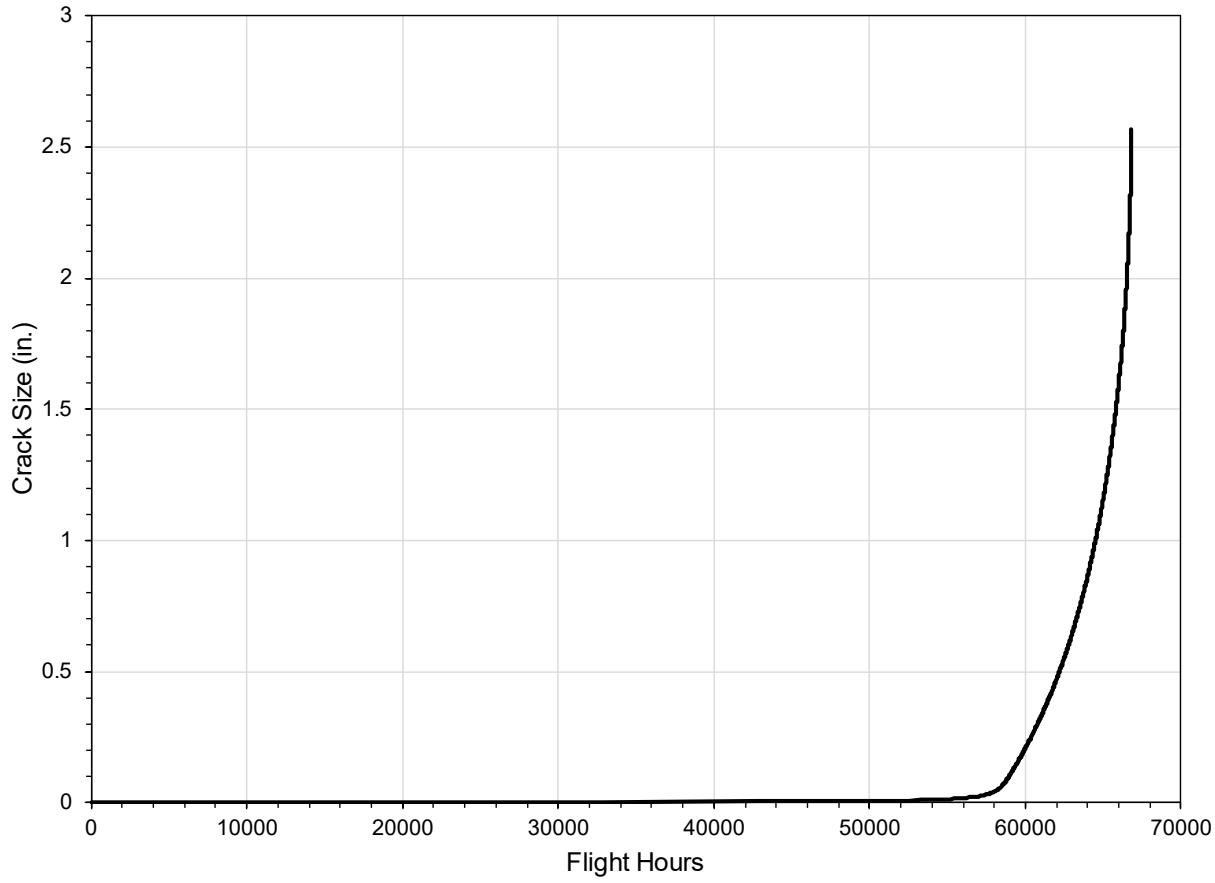

Figure C-1. Fatigue Crack Growth Curve

C.2 Piecewise Curve Fits to the Master Crack Growth Curve

Cycles were first converted to flights by multiplying the cycle count by (200 flights/17,983 cycles). Then, polynomials were fit piecewise to segments of the crack growth curve as in Figure C-2 to Figure C-9. The polynomial for each segment is provided in the figure. When the number of flights got large, it was necessary to adjust the flight count in a segment by setting the flight number for the first point in the segment to zero and adjusting the number for flights for all subsequent points accordingly. For some segments of the crack growth curve, it was necessary to include points from the previous segment at the low end of the curve in order to control the slope of the polynomial as it went through the first point of the segment. These polynomials give the crack size as a function of flights.

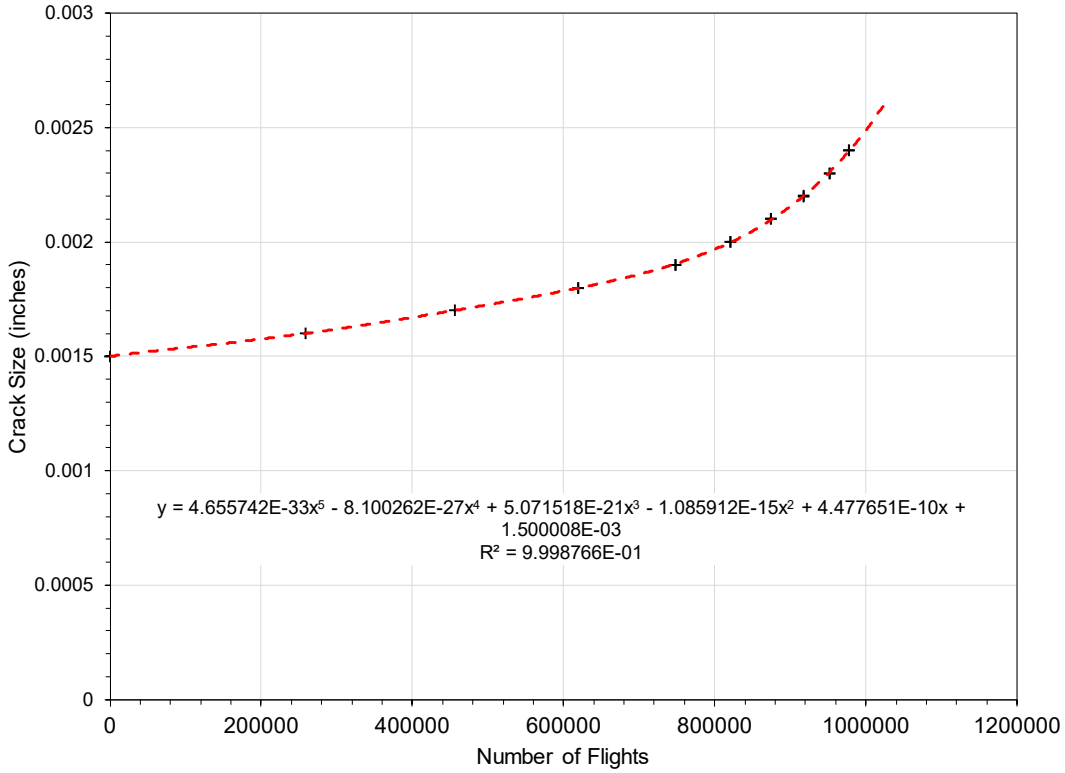

Figure C-2. Fit to Crack Growth Curve for 0.0015 ≤ c ≤ 0.0024 Inch

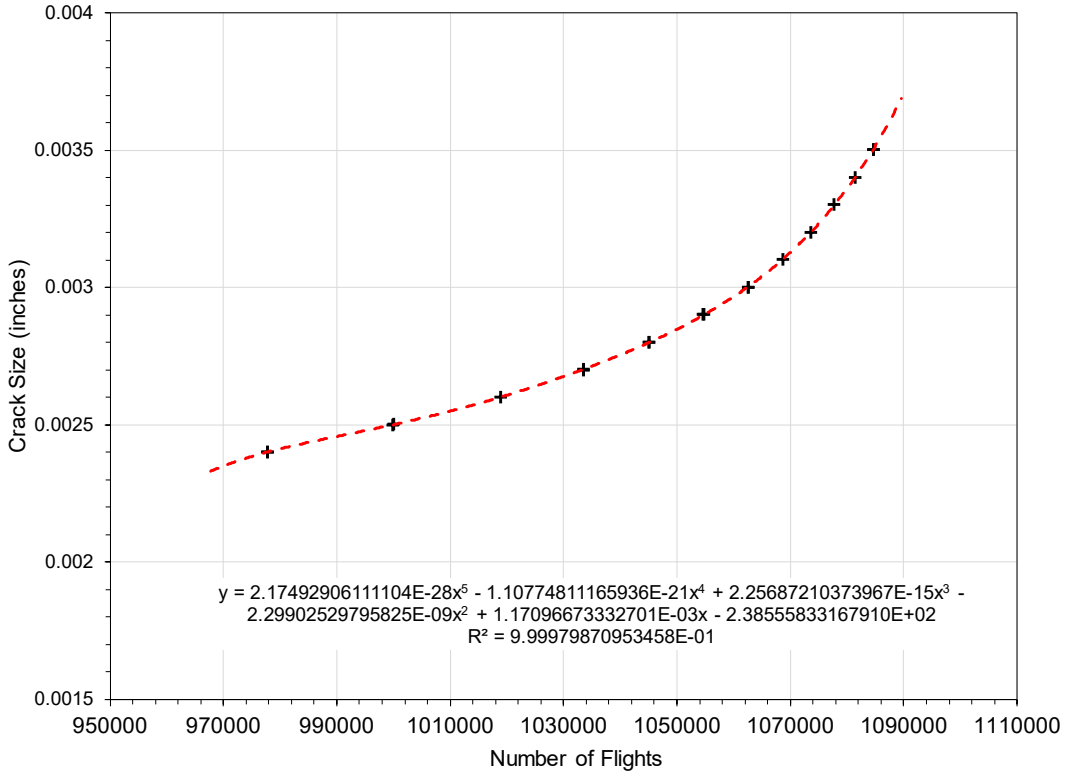

Figure C-3. Fit to Crack Growth Curve for 0.0024 < c < 0.0036 Inch

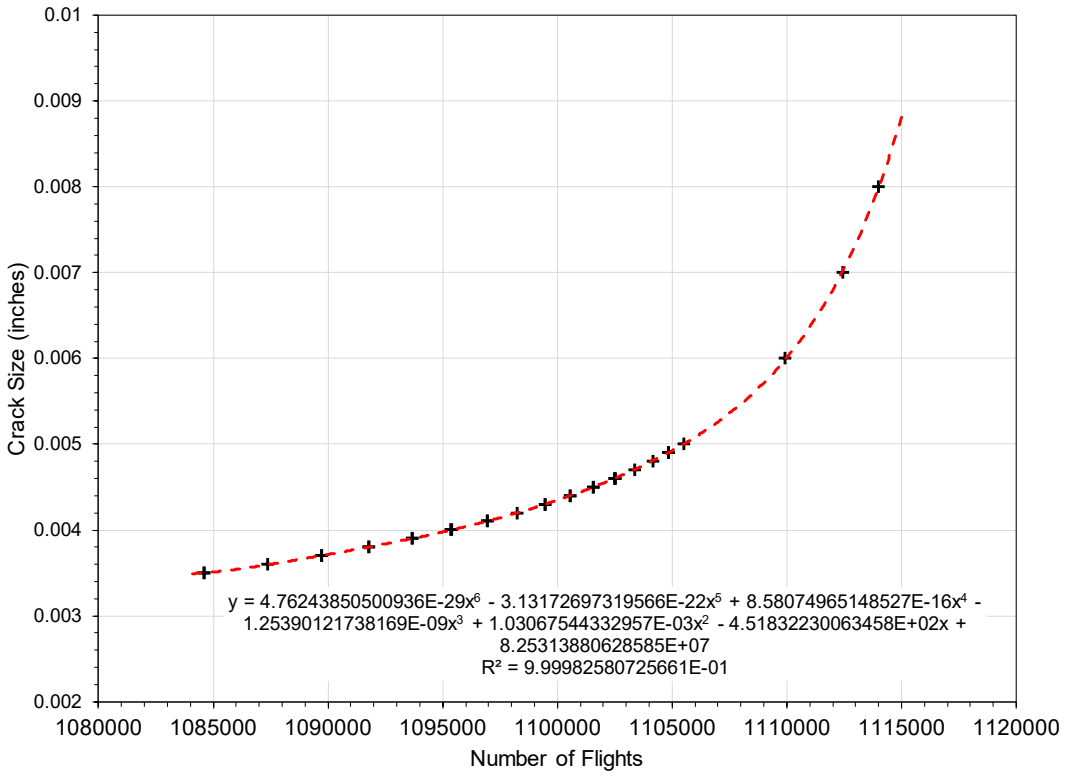

Figure C-4. Fit to Crack Growth Curve for 0.0036 ≤ c ≤ 0.008 Inch

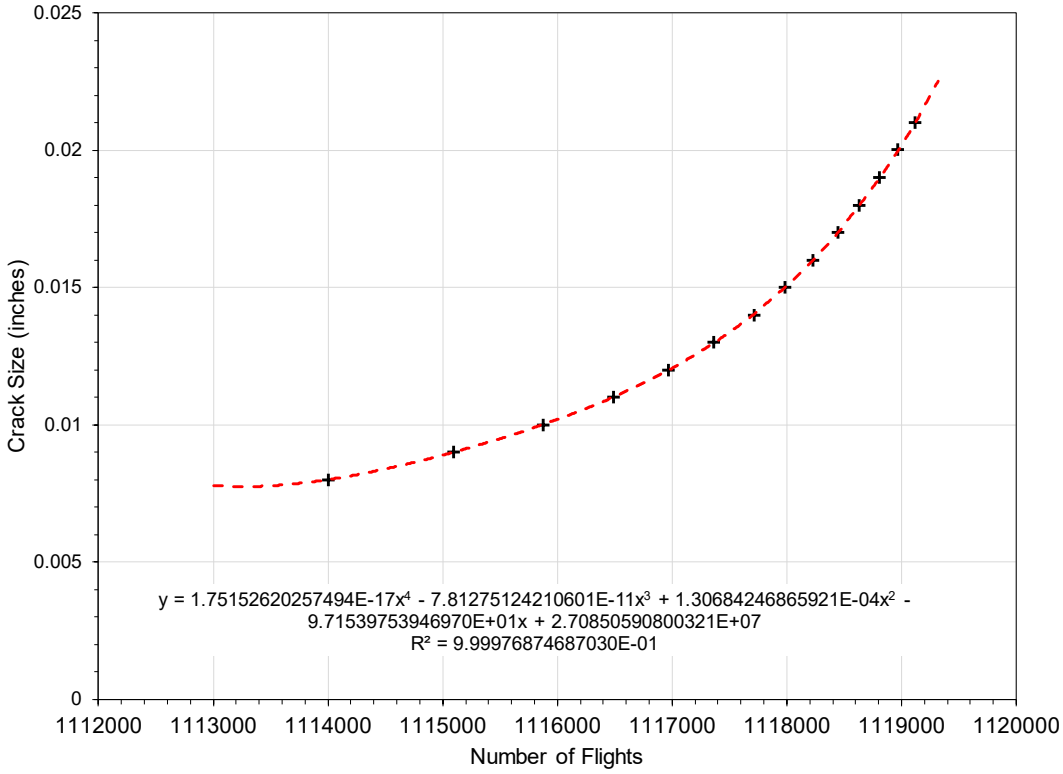

Figure C-5. Fit to Crack Growth Curve for 0.008 < c < 0.022 Inch

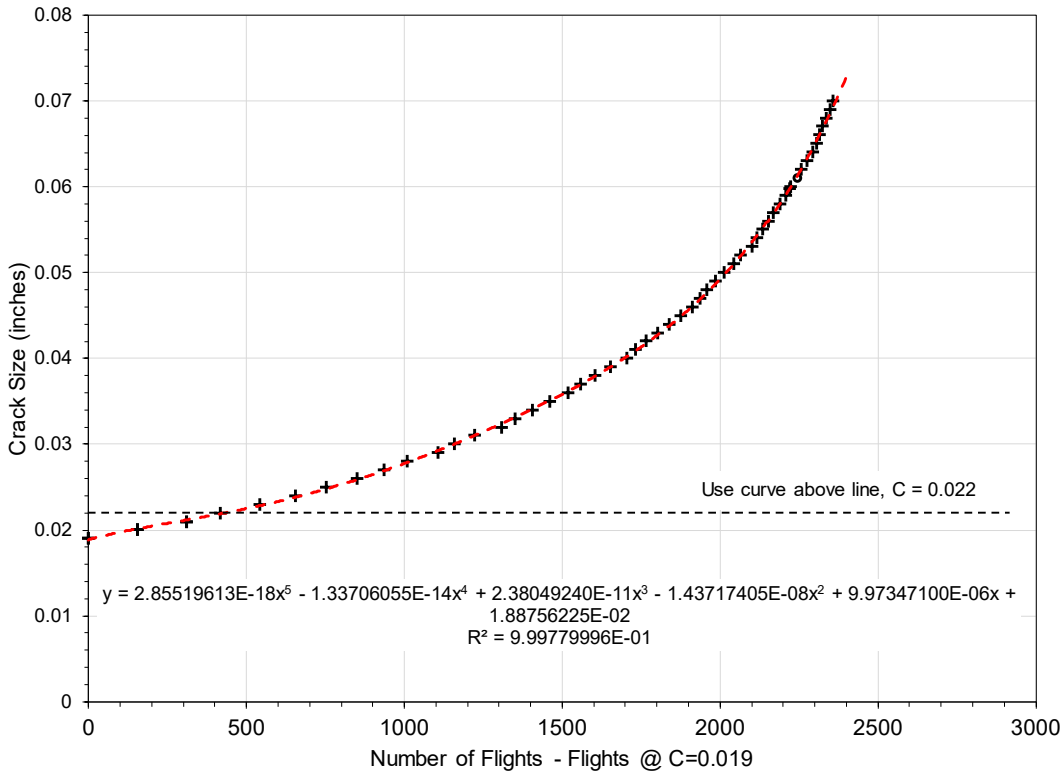

Figure C-6. Fit to Crack Growth Curve for 0.022 ≤ c < 0.07 Inch

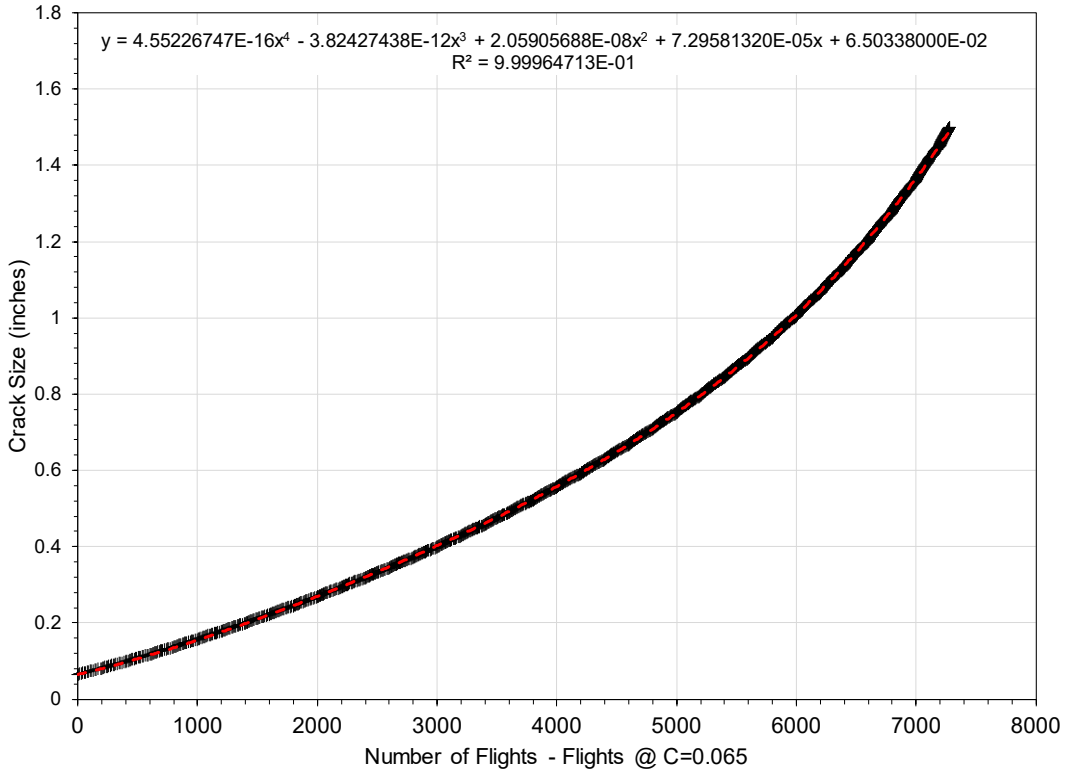

Figure C-7. Fit to Crack Growth Curve for 0.07 ≤ c < 1.5 Inch

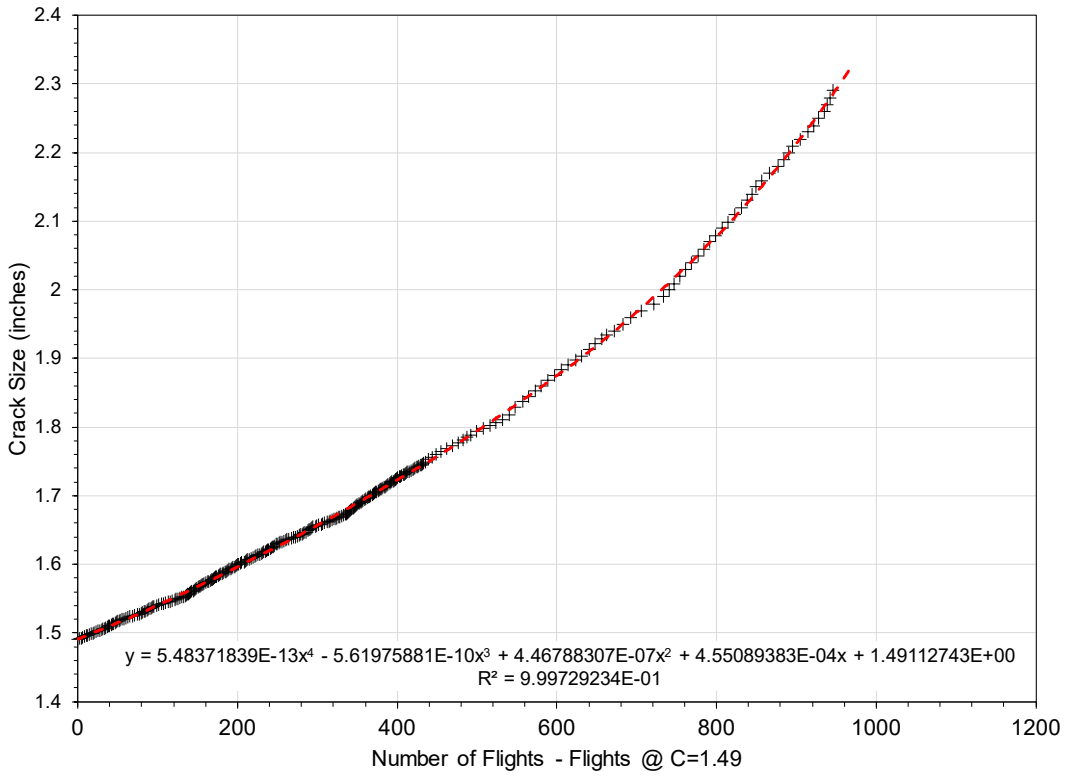

Figure C-8. Fit to Crack Growth Curve for 1.5 ≤ c ≤ 2.29 Inch

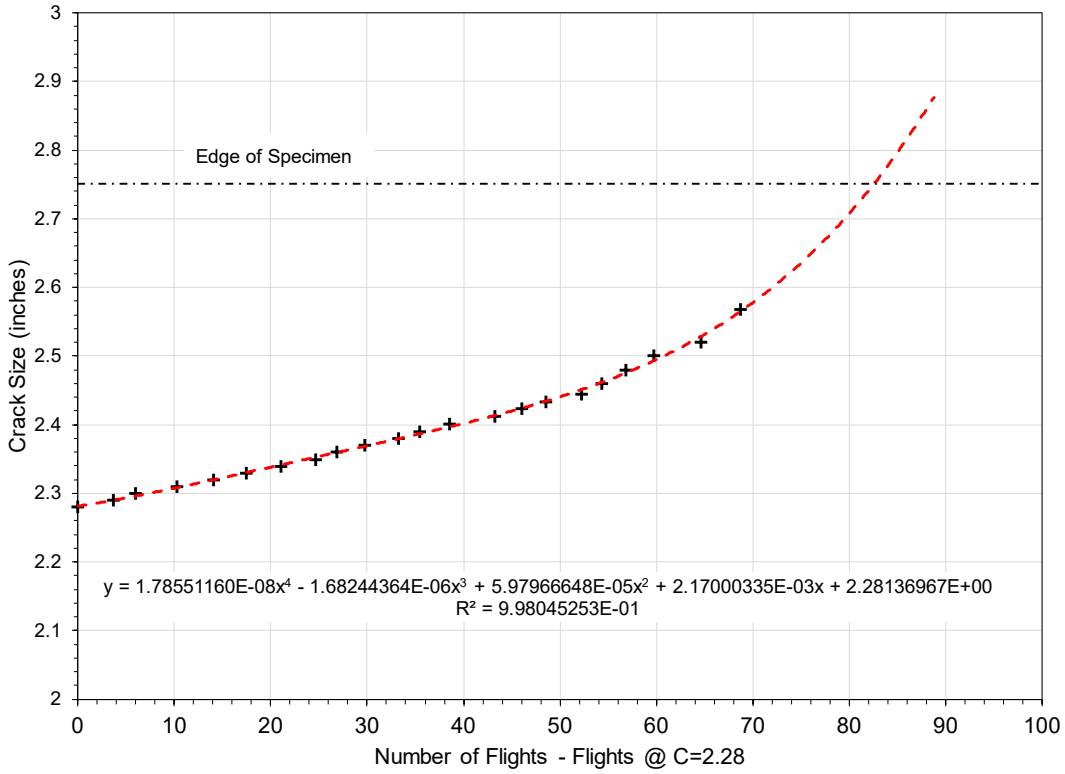

Figure C-9. Fit to Crack Growth Curve for c > 2.29 Inch

C.3 Calculation of *dC/d(flight)*

The equations for *c* as a function of *flights* in Section C.2 were differentiated to obtain *dc/d(flight)* at each crack size in the AFGROW output. *dc/d(flight)* was plotted versus crack size and equations were fit piecewise using the trendline option in Excel as in Figure C-10 to Figure C-15. Polynomials were fit to *dc/d(flight)* versus crack size for crack sizes greater than 0.00327 inches and are given in each figure. An exponential function was fit to the crack sizes less than 0.00327 inch and extrapolated back to a crack size of zero. The curve fits to the crack growth curve (Figure C-2 through Figure C-9) did not produce smooth curves for *dc/d(flight)* vs. crack size, especially across the segment boundaries. The curve fits to *dc/d(flight)* vs. crack size smoothed out the transitions between segments. In order to obtain smooth transitions in *dc/d(flight)*, the crack size where transition between segments occurred was chosen to be where *dc/d(flight)* was approximately equal between two adjoining segments.

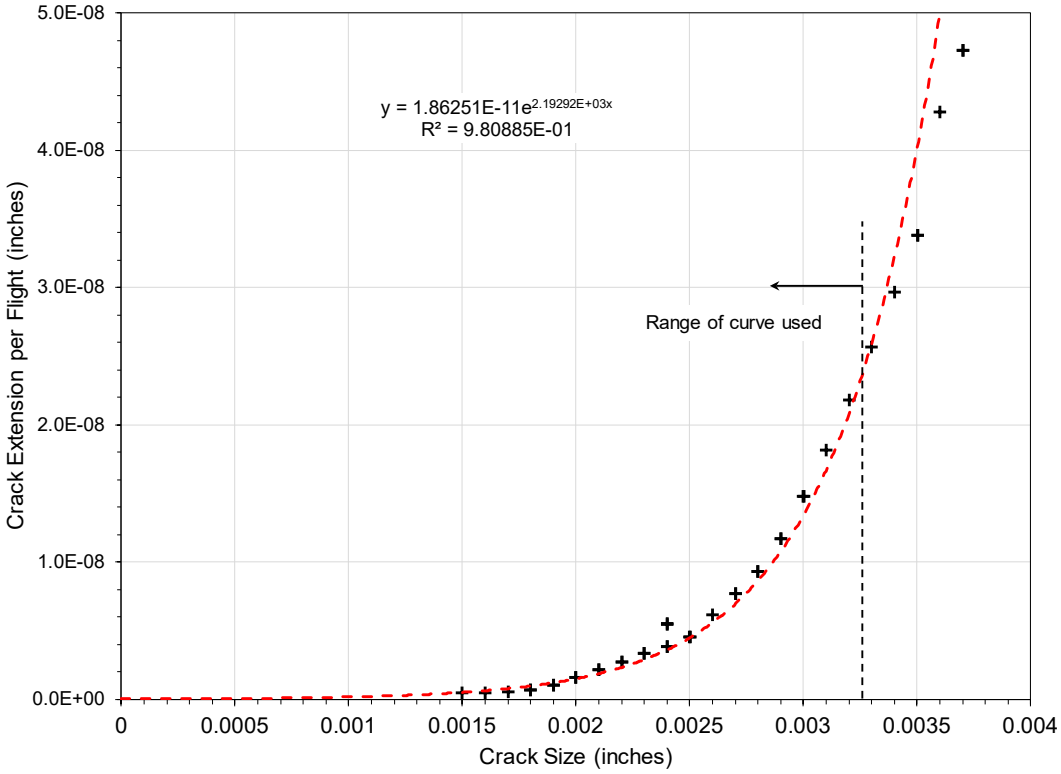

Figure C-10. *dc/d(flight)* for c < 0.00327 Inch

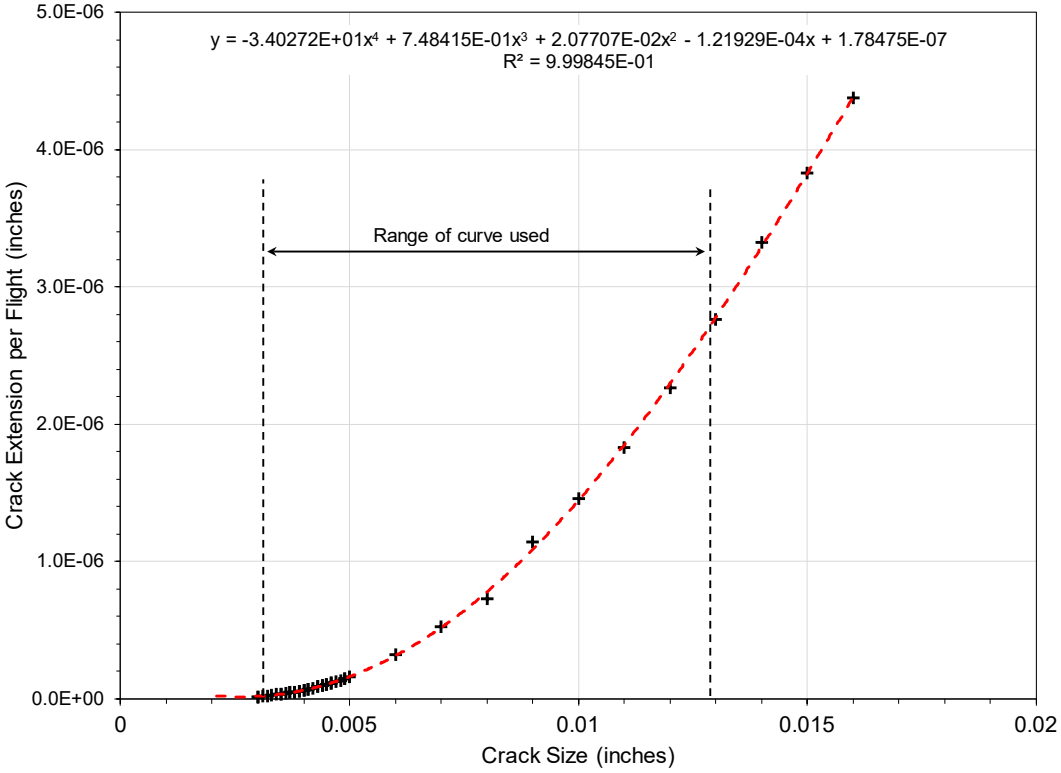

Figure C-11. *dc/d(flight)* for 0.00327 ≤ c ≤ 0.01292 Inch

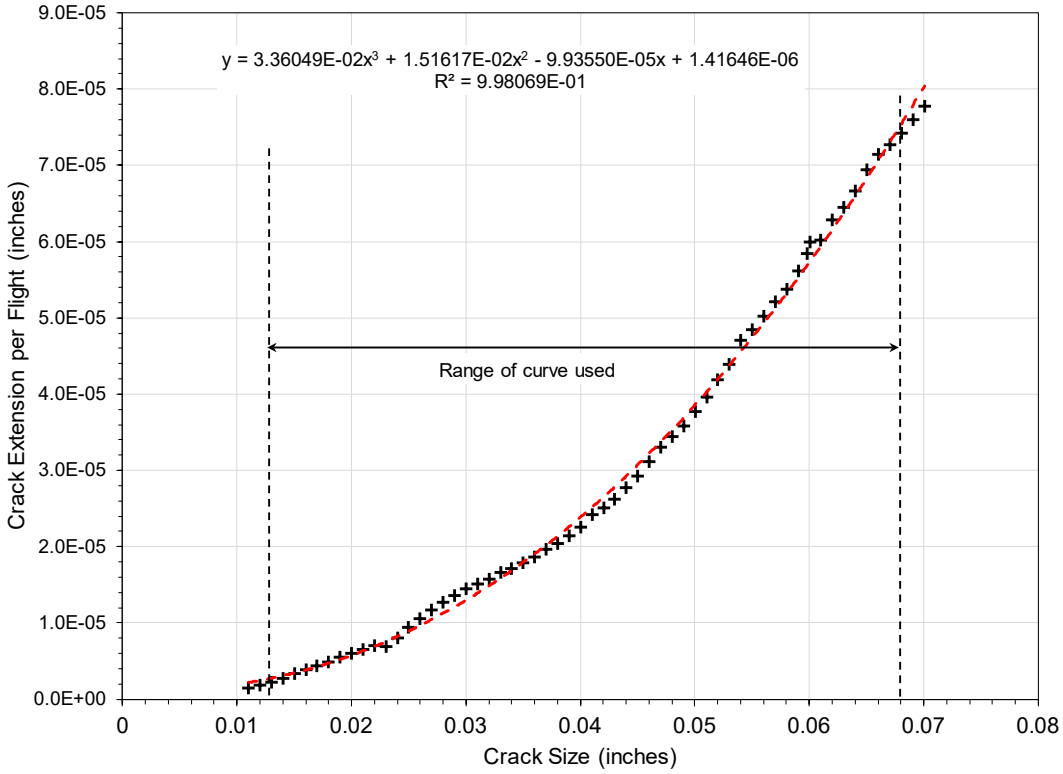

Figure C-12. *dc/d(flight)* for 0.01292 < c < 0.0682 Inch

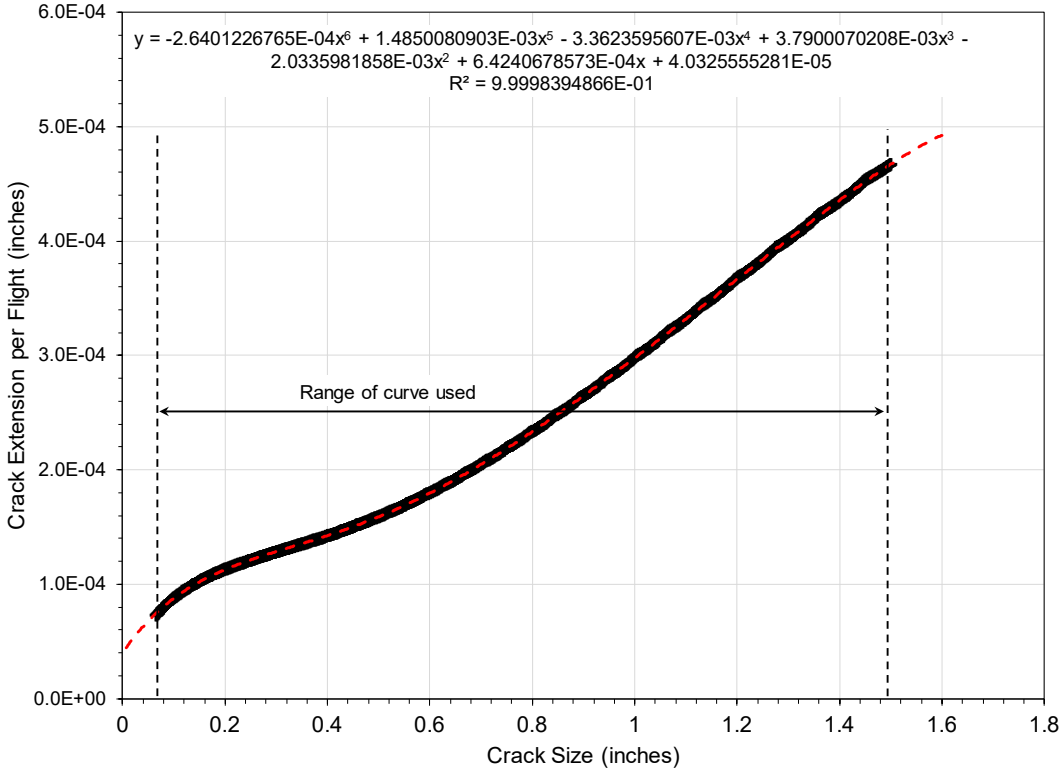

Figure C-13. *dc/d(flight)* for 0.0682 ≤ c < 1.4973 Inch

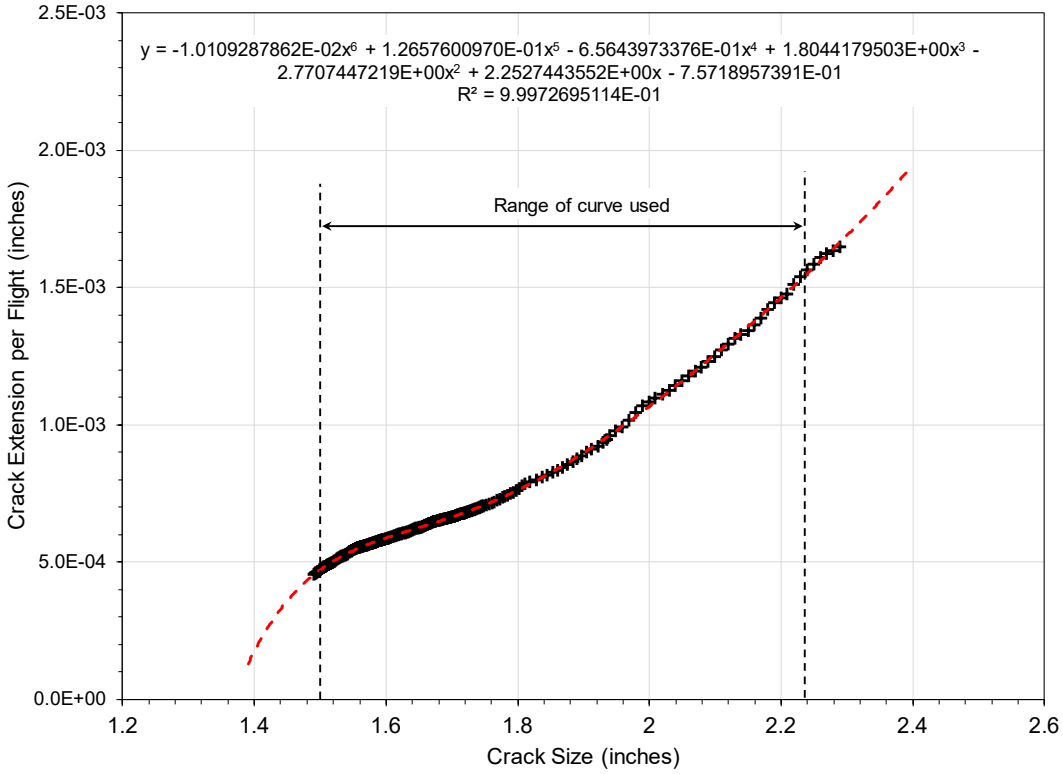

Figure C-14. *dc/d(flight)* for 1.4973 ≤ c ≤ 2.2384 Inch

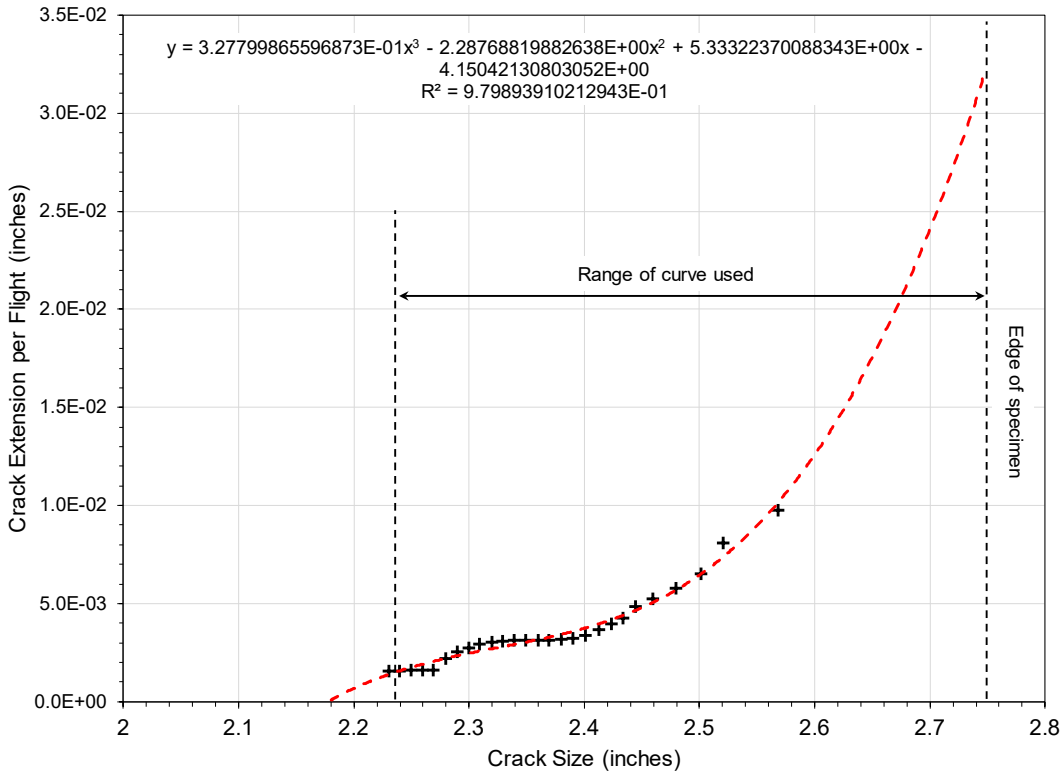

Figure C-15. *dc/d(flight)* for c > 2.2384 Inch